

**Development of *E*-and *Z*-Selective Base-Catalyzed Redox Isomerizations and Ene-Diene  
Cross Metathesis**

by

**John P. Sonye**

B.A., Rutgers University, 2003

Submitted to the Graduate Faculty of  
Arts and Sciences in partial fulfillment  
of the requirements for the degree of  
Master in Science

University of Pittsburgh

2006

UNIVERSITY OF PITTSBURGH  
FACULTY OF ARTS AND SCIENCES

This thesis was presented

By  
John P. Sonye

It was defended on

April 27, 2006

and approved by

Paul E. Floreancig, Associate Professor, Department of Chemistry

Christian E. Schafmeister, Assistant Professor, Department of Chemistry

Thesis Director: Kazunori Koide, Assistant Professor, Department of Chemistry

**The Development of *E*-and *Z*-Selective Base-Catalyzed Redox Isomerizations  
and Ene-Diene Cross Metathesis**

John P. Sonye, B.A.

University of Pittsburgh, 2006

$\gamma$ -Oxo- $\alpha,\beta$ -alkenoates are found in several natural products and are versatile synthetic intermediates. We have developed methods to selectively prepare *E* and *Z*-alkenoates from  $\gamma$ -hydroxy- $\alpha,\beta$ -alkynoates wherein the optimization, mechanism, and scope of the reactions are described. Biological testing of  $\gamma$ -oxo- $\alpha,\beta$ -alkenoates and their derivatives in zebrafish embryos also are discussed.

Since the development of ruthenium alkylidene catalysts, olefin metathesis has become a useful method in synthetic organic chemistry. However, certain areas of metathesis have remained under-researched; in particular, the cross metathesis of a 1,3-diene with a terminal olefin known as ene-diene cross metathesis (EDCM). The attempt at optimization of EDCM reactions using a general model is also discussed.

## TABLE OF CONTENTS

ACKNOWLEDGEMENTS .....	XIV
1.0 INTRODUCTION.....	1
1.1 $\gamma$ -OXO- $\alpha,\beta$ -UNSATURATED ESTERS AS BIOLOGICALLY ACTIVE SMALL MOLECULES .....	1
1.2 PREPARATION OF $\gamma$ -OXO- $\alpha,\beta$ -UNSATURATED ESTERS .....	3
1.3 REDOX ISOMERIZATION OF $\gamma$ -HYDROXY- $\alpha,\beta$ -ALKYNOATES TO $\gamma$ -OXO- $\alpha,\beta$ -ALKENOATES .....	6
1.4 RESEARCH AIMS.....	10
2.0 RESULTS AND DISCUSSION .....	11
2.1 BACKGROUND .....	11
2.2 <i>E</i> -SELECTIVE REDOX ISOMERIZATION .....	15
2.2.1 Reaction Optimization and Mechanistic Studies .....	15
2.2.2 Reaction Scope of DABCO-Catalyzed Redox Isomerization.....	28
2.3 <i>Z</i> -SELECTIVE REDOX ISOMERIZATION.....	33
2.3.1 Reaction Optimization and Mechanistic Studies .....	33
2.3.2 Reaction Scope of NaHCO <sub>3</sub> -Catalyzed Redox Isomerization.....	48
2.4 SYNTHETIC APPLICATIONS OF $\gamma$ -OXO- $\alpha,\beta$ -ALKENOATES.....	52
2.5 BIOLOGICAL STUDIES OF LIBRARY COMPOUNDS IN ZEBRAFISH EMBRYOS.....	54
3.0 CONCLUSION.....	58
4.0 EXPERIMENTAL .....	59
5.0 <sup>1</sup> H AND <sup>13</sup> C NMR SPECTRA.....	72
6.0 ENE-DIENE CROSS METATHESIS.....	139
6.1 INTRODUCTION .....	139

6.2	RESULTS AND DISCUSSION .....	142
6.3	CONCLUSION .....	154
7.0	EXPERIMENTAL AND $^1\text{H}$ AND $^{13}\text{C}$ NMR SPECTRA.....	155
	BIBLIOGRAPHY.....	164

## LIST OF TABLES

Table 1. Attempts at structural diversity using acid. ....	12
Table 2. Initial base and solvent effect studies. ....	13
Table 3. Attempts at phosphine-catalyzed redox isomerization. ....	23
Table 4. DABCO-catalyzed redox isomerization: alkynoate concentration studies.....	27
Table 5. DABCO-catalyzed redox isomerization: aromatic and vinylogous alkynoates. ....	28
Table 6. DABCO-catalyzed redox isomerization: aliphatic alkynoates. ....	29
Table 7. DABCO-catalyzed redox isomerization: other electron withdrawing groups. ....	30
Table 8. Phosphonate 115 optimization.....	32
Table 9. <i>E</i> -selective redox isomerization: base conditions revisited. ....	32
Table 10. <i>Z</i> -selective redox isomerization found.....	34
Table 11. <i>i</i> Pr <sub>2</sub> NEt-catalyzed redox isomerization: proton source studies.....	36
Table 12. <i>Z</i> -selective redox isomerization: base studies.....	37
Table 13. <i>i</i> Pr <sub>2</sub> NEt-catalyzed redox isomerization: DMSO/water ratio studies.....	38
Table 14. <i>i</i> Pr <sub>2</sub> NEt-catalyzed redox isomerization: different metal cations.....	38
Table 15. <i>i</i> Pr <sub>2</sub> NEt-catalyzed redox isomerization: different solvents.....	39
Table 16. NaHCO <sub>3</sub> -catalyzed redox isomerization: hydroquinone studies. ....	42
Table 17. NaHCO <sub>3</sub> -catalyzed redox isomerization: DMSO/water ratios revisited. ....	43
Table 18. NaHCO <sub>3</sub> isomerization: aromatic and vinylogous substrates.....	48
Table 19. NaHCO <sub>3</sub> isomerization: aliphatic substrates.....	50
Table 20. NaHCO <sub>3</sub> isomerization: other electron withdrawing groups.....	50
Table 21. NaHCO <sub>3</sub> isomerization: phosphonate studies.....	51
Table 22. NaHCO <sub>3</sub> isomerization: amide studies. ....	52
Table 23. Olefin classes in cross-metathesis.....	140
Table 24. Different solvents in EDCM.....	146

Table 25. EDCM: substrate concentration studies.....	147
Table 26. EDCM: temperature studies.....	147
Table 27. EDCM: solvent studies using Grela-Hoyveda-Grubbs 203.....	148
Table 28. EDCM: different catalyst studies.....	149
Table 29. EDCM: catalyst amount studies using Grubbs II. ....	150
Table 30. EDCM: catalyst amount studies using Grubbs II and benzoquinone. ....	150
Table 31. EDCM: ene/diene ratio studies using Grubbs II.....	151
Table 32. EDCM: ene/diene ratio studies using catalyst 202. ....	152

## LIST OF FIGURES

Figure 1. Electrophilic natural products.....	1
Figure 2. Natural products containing $\gamma$ -oxo- $\alpha,\beta$ -unsaturated esters. ....	2
Figure 3. Systematic biological studies of $\gamma$ -oxo- $\alpha,\beta$ -unsaturated esters and acids.....	3
Figure 4. Et <sub>3</sub> N-catalyzed redox isomerization: solvent effects.....	14
Figure 5. iPr <sub>2</sub> NEt-catalyzed redox isomerization: solvent effects. ....	14
Figure 6. Cyclobutyl-alkynoates that elude to mechanisms B or C.....	17
Figure 7. DABCO amount studies. ....	19
Figure 8. Initial reaction rate versus [DABCO].....	20
Figure 9. Key HMBC coupling for <i>E</i> 43.....	23
Figure 10. Key HMBC coupling for <i>Z</i> 43.....	33
Figure 11. NaHCO <sub>3</sub> -catalyzed redox isomerization is second order overall. ....	44
Figure 12. Natural products containing syn- $\beta$ -hydroxy esters.....	53
Figure 13. Ruthenium catalysts for olefin metatheses. ....	139

## LIST OF SCHEMES

Scheme 1. Cysteine reactivity toward <i>E</i> and <i>Z</i> -alkenoates. ....	3
Scheme 2. Sulfoxide elimination to yield <i>E</i> -alkenoates. ....	4
Scheme 3. Aldol condensation, epoxidation to yield <i>E</i> -alkenoates. ....	4
Scheme 4. Phosphine elimination to yield <i>E</i> -alkenoates. ....	5
Scheme 5. Hydrolysis of nitro group to yield <i>E</i> -alkenoates. ....	5
Scheme 6. Preparation of <i>Z</i> -alkenoates via a furan oxidation. ....	5
Scheme 7. General redox isomerization conditions from others. ....	6
Scheme 8. Convergent preparations of $\gamma$ -hydroxy- $\alpha,\beta$ -alkynoates. ....	6
Scheme 9. Raphael's conditions for Et <sub>3</sub> N-catalyzed redox isomerization. ....	7
Scheme 10. Et <sub>3</sub> N-catalyzed redox isomerization: proposed allenol intermediate. ....	7
Scheme 11. Et <sub>2</sub> NH-facilitated lactonization of $\gamma$ -hydroxy- $\alpha,\beta$ -alkynoates. ....	7
Scheme 12. Et <sub>3</sub> N-catalyzed redox isomerization of a thiophene derivative. ....	8
Scheme 13. Et <sub>3</sub> N-catalyzed redox isomerization using pyridazinone derivatives. ....	8
Scheme 14. Proposed mechanism for Et <sub>3</sub> N-catalyzed redox isomerization. ....	8
Scheme 15. Combined Sonagashira coupling and redox isomerization. ....	9
Scheme 16. Preparation of aryl piperazines using Et <sub>3</sub> N-catalyzed redox isomerization. ....	9
Scheme 17. <i>n</i> -Bu <sub>3</sub> N-catalyzed redox isomerization . ....	9
Scheme 18. [P(Ph <sub>3</sub> ) <sub>3</sub> RhCl] catalyzed redox isomerization. ....	10
Scheme 19. DABCO-catalyzed <i>E</i> -selective redox isomerization using THF. ....	11
Scheme 20. Formation of <i>Z</i> <sub>2</sub> by-product from O-allylation. ....	11
Scheme 21. Mechanism A: methine deprotonation mechanism. ....	15
Scheme 22. Mechanism B: 1,2-hydride shift mechanism. ....	15
Scheme 23. Mechanism C: conjugate addition / 1,2-hydride shift mechanism. ....	16
Scheme 24. Mechanism D: conjugate addition / methine deprotonation mechanism. ....	17

Scheme 25. Mechanism for DABCO-catalyzed redox isomerization and ring expansion.....	18
Scheme 26. Failed ring expansion on bicyclic alkynoate using DABCO. ....	18
Scheme 27. Failed ring expansion on cyclobutyl alkynoate using DABCO. ....	18
Scheme 28. DABCO-catalyzed Z43-to-E43 isomerization. ....	20
Scheme 29. DABCO-catalyzed Z43-to-E43 isomerization: deuterium experiment.....	21
Scheme 30. DABCO-catalyzed Z-to-E isomerization mechanism. ....	21
Scheme 31. One possible trapping mechanism using TESC1. ....	22
Scheme 32. Failed TESC1 trapping of DABCO-catalyzed redox isomerization intermediate. ....	22
Scheme 33. Location of deuterium incorporation for mechanism B. ....	23
Scheme 34. Location of deuterium incorporation for mechanism C. ....	24
Scheme 35. D <sub>2</sub> O-incorporation experiment using DABCO. ....	24
Scheme 36. Mechanism for DABCO-catalyzed redox isomerization. ....	25
Scheme 37. DABCO-catalyzed redox isomerization: deuterium isotope effect.....	25
Scheme 38. DABCO-catalyzed redox isomerization: crossover experiment. ....	26
Scheme 39. DABCO-catalyzed redox isomerization: residual water removal.....	27
Scheme 40. Preparation of phosphonate 115.....	31
Scheme 41. Failed semi hydrogenation to yield Z43. ....	33
Scheme 42. D <sub>2</sub> O incorporation experiments using iPr <sub>2</sub> NEt and DABCO.....	34
Scheme 43. E-alkenoate stability towards iPr <sub>2</sub> NEt-catalyzed redox isomerization. ....	35
Scheme 44. Possible mechanism for Z-selective redox isomerization. ....	35
Scheme 45. DABCO and iPr <sub>2</sub> NEt yielding same results with bicyclic alkynoate 76.....	36
Scheme 46. One possible polymerization mechanism catalyzed by NaHCO <sub>3</sub> . ....	40
Scheme 47. Failed attempt to stop polymerization in NaHCO <sub>3</sub> -catalyzed redox isomerization. ....	40
Scheme 48. NaHCO <sub>3</sub> -catalyzed redox isomerization: radical polymerization mechanism.....	41
Scheme 49. Z43 stability with hydroquinone alone.....	42
Scheme 50. DABCO-catalyzed redox isomerization: hydroquinone experiment. ....	42
Scheme 51. Z-selective redox isomerization is optimized.....	43
Scheme 52. D <sub>2</sub> O incorporation experiments using DABCO, iPr <sub>2</sub> NEt, and NaHCO <sub>3</sub> . ....	44
Scheme 53. NaHCO <sub>3</sub> -catalyzed redox isomerization: E-alkenoate stability experiment. ....	45
Scheme 54. NaHCO <sub>3</sub> -catalyzed redox isomerization: slow Z-to-E isomerization. ....	45
Scheme 55. E:Z isomerization selectivity for DABCO and NaHCO <sub>3</sub> reactions.....	45

Scheme 56. Cyclobutyl alkynoate 77 giving different results for DABCO and NaHCO <sub>3</sub> . .....	46
Scheme 57. NaHCO <sub>3</sub> -catalyzed redox isomerization: D <sub>2</sub> O incorporation experiment. ....	46
Scheme 58. NaHCO <sub>3</sub> -catalyzed redox isomerization: deuterium isotope effect. ....	47
Scheme 59. Mechanism for NaHCO <sub>3</sub> -catalyzed redox isomerization. ....	47
Scheme 60. Preparation of syn-β-hydroxy ester precursor. ....	53
Scheme 61. Formation of cyclohexyl esters from the <i>E</i> -alkenoates. ....	53
Scheme 62. Formation of γ-lactone from <i>Z</i> -alkenoates. ....	54
Scheme 63. DOS library derived from γ-hydroxy-α,β-alkynoates. ....	55
Scheme 64. Biological effects of Pauson-Khand product 147. ....	56
Scheme 65. Biological activity of Diels-Alder products. ....	56
Scheme 66. Summary of <i>E</i> -selective redox isomerization. ....	58
Scheme 67. Summary of <i>Z</i> -selective redox isomerization. ....	58
Scheme 68. Classes of olefin metathesis. ....	140
Scheme 69. Ideal catalytic cycle for EDCM. ....	141
Scheme 70. Anticipated products from EDCM. ....	142
Scheme 71. Preliminary EDCM. ....	143
Scheme 72. Reason for complex mixture in EDCM. ....	144
Scheme 73. Diene 227 minimizing unwanted by-products. ....	144
Scheme 74. Preparation of diene 235. ....	145
Scheme 75. EDCM: CM-product stability. ....	152
Scheme 76. EDCM: re-metathesis experiment. ....	153
Scheme 77. EDCM: Ene-dimer reaction. ....	153
Scheme 78. Most promising conditions from EDCM. ....	154

## LIST OF ABBREVIATIONS

%	percent
°C	Celsius
$\alpha$	alpha
$\beta$	beta
$\gamma$	gamma
$\delta$	delta
$\mu\text{L}$	microliter
Ac	acetyl
aq	aqueous
BORSM	based on recovered starting material
Bz	benzoyl
CM	cross metathesis
Cy	cyclohexyl
DABCO	1,4-diazabicyclo[2.2.2]octane
DBU	1,8-diazabicyclo[5.4.0]undec-7-ene
DIBAL-H	diisobutylaluminum hydride
DMAP	4-dimethylaminopyridine
DMF	dimethylformamide
DMSO	dimethyl sulfoxide
EDCM	ene-diene cross metathesis
EI <sup>+</sup>	electron impact ionization
mol%	mole percent
ES <sup>+</sup>	electrospray ionization
Et	ethyl

EWG	electron withdrawing group
h	hour
hex	hexanes, hexyl
HMBC	heteronuclear multiple bond correlation
HMQC	heteronuclear multiple quantum coherence
IR	infrared
K	Kelvin
L	liter
M	molar
Me	methyl
Mes	mesityl
MHz	megahertz
min	minutes
mL	milliliter
MS	mass spectroscopy
n.d.	not determined
NMR	nuclear magnetic resonance
<i>n</i> -Pr	normal propyl
PCC	pyridinium chlorochromate
Ph	phenyl
PPTS	pyridinium <i>p</i> -toluenesulfonate
<i>p</i> TsOH	<i>p</i> -toluenesulfonic acid
TES	triethylsilyl
THF	tetrahydrofuran
TLC	thin-layer chromatography
Trt	triphenylmethyl or trityl

## ACKNOWLEDGEMENTS

I would like to thank the members of the Koide group, both past and present. Also I would like to thank the Schafmeister group for answering my NMR queries as well as the use of their facilities. I would also like to thank the Nelson and Floreancig groups for their resources, the chemistry department, the University of Pittsburgh, Dr. Achary for the NMR facilities, and Dr. Somyajula and Dr. Williams for MS analyses. I also want to thank my committee, Professor's Floreancig and Schafmeister. Most importantly I want to thank my advisor, Professor Koide for his guidance and knowledge. Finally, I would like to thank my family, friends and God for their patience and understanding.

## 1.0 INTRODUCTION

### 1.1 $\gamma$ -OXO- $\alpha,\beta$ -UNSATURATED ESTERS AS BIOLOGICALLY ACTIVE SMALL MOLECULES

Electrophilic natural products exhibit useful biological activities.<sup>1</sup> Fumagillin (Figure 1, **1**) and epoxomicin (**2**) both use epoxide functionalities to covalently trap proteases in which fumagillin inhibits angiogenesis and epoxomicin inhibits protein degradation caused by the proteasome. Epoxides are not the only electrophilic moiety found in natural products.  $\beta$ -lactones are also potent proteasome inhibitors. For example, lactacystin (**3**) contains a masked  $\beta$ -lactone and salinosporamide (**4**) contains an explicit  $\beta$ -lactone.

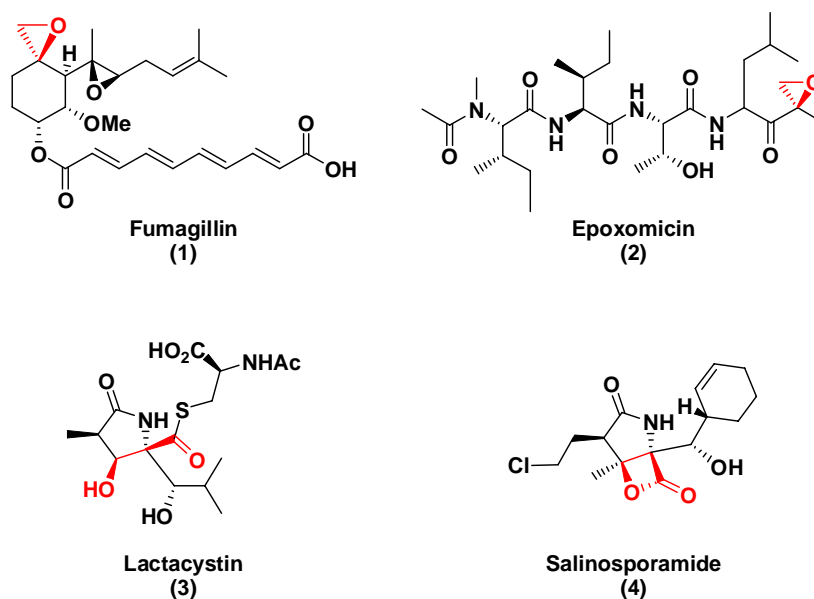
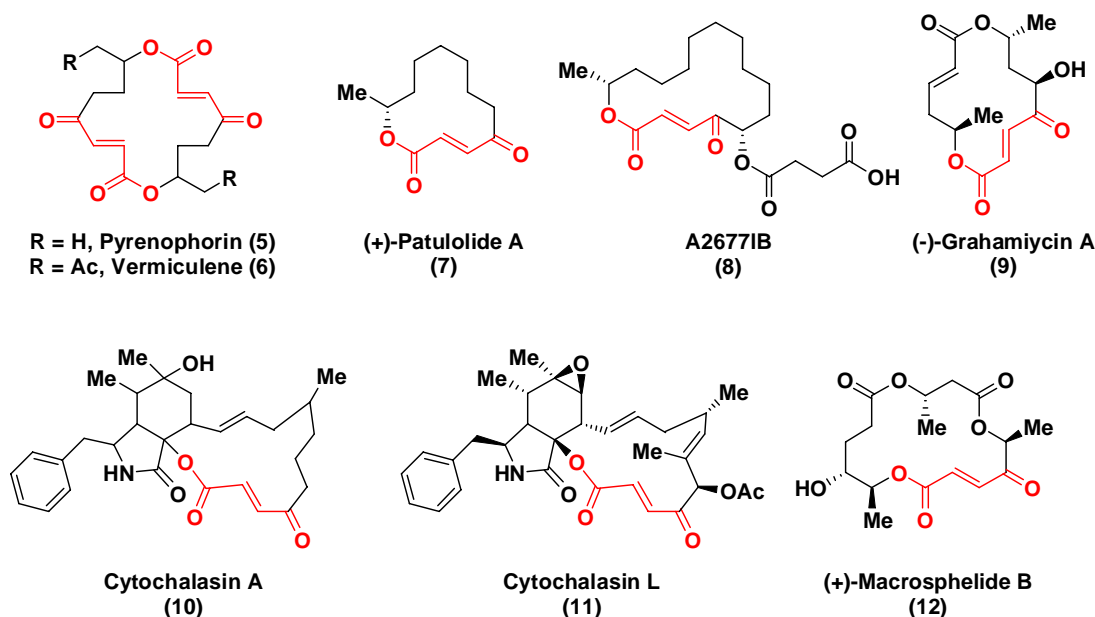


Figure 1. Electrophilic natural products

One class of electrophilic natural products that contain  $\gamma$ -oxo- $\alpha,\beta$ -unsaturated esters also exhibit biological activities (Figure 2). For example, pyrenophorin<sup>2,3</sup> (Figure 2, **5**), vermiculine<sup>4,5</sup> (**6**), (+)-patulolide A<sup>6,7</sup> (**7**), A26771B<sup>8,9</sup> (**8**), and grahamimycin A<sup>10,11</sup> (**9**) exhibit antifungal and/or antibiotic activity. The cytochalasins A<sup>12</sup> and L<sup>13</sup> (**10** and **11**) belong to a unique class of macrocycles that display several activities such as inhibition of the division of the cytoplasm (from which their name originates),<sup>14</sup> reversible inhibition of cell movement,<sup>14</sup> glucose transport,<sup>15</sup> among others. In particular cytochalasin A (**10**) inhibits growth and sugar uptake in a *Saccharomyces* strain.<sup>12,16,17</sup> Finally, (+)-macrospheptide B (**12**) inhibits cell-cell adhesion molecules.<sup>18,19</sup>



**Figure 2.** Natural products containing  $\gamma$ -oxo- $\alpha,\beta$ -unsaturated esters.

For the natural products shown above, except for the cytochalasins,<sup>14</sup> the  $\gamma$ -oxo- $\alpha,\beta$ -unsaturated ester moiety is the most-likely reactive part of the molecule since it is a Michael acceptor. The biological activity of this functionality was important enough to merit a systematic study by Dal Pozzo,<sup>20</sup> who prepared derivatives of the basic structure shown in Figure 3 wherein (1) the substitution on the olefin was varied; (2) the aromatic groups were varied based on electron donating/withdrawing ability; (3) the olefin geometry was varied (*E/Z*); and (4) either a carboxylic acid or methyl ester was used. These molecules' reactivities toward cysteine (which is the functional part of cysteine proteases) were studied by UV spectroscopy. Although the

product was not isolated, they determined that the cysteine addition to the olefin caused the loss of the starting material's UV peak. These kinetic studies made trends apparent: (1) increasing the sterics around the olefin decreased the reactivity of the molecule; (2) the methyl esters were more reactive than the corresponding acid; (3) electron-donating aromatic rings decrease the reactivity towards cysteine due to a decrease in the overall electrophilicity of the molecule; and (4) the *Z*-olefin was less reactive than the *E*-olefin. Concerning the olefin geometry, the *Z*-olefin reacted between 7–500 times slower than the *E*-olefin (Scheme 1). Dal Pozzo hypothesized the *Z*-olefin was not planar due to lone pair repulsion on the carbonyl oxygen that decreased the molecule's overall conjugation and its reactivity towards cysteine. This difference in reactivity merited methods that would produce *E*- and *Z*- $\gamma$ -oxo- $\alpha,\beta$ -unsaturated esters selectively.

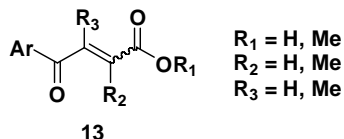
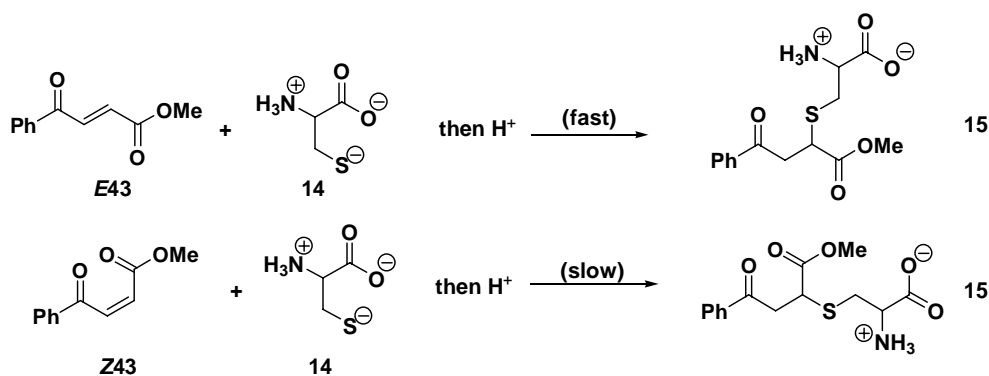


**Figure 3.** Systematic biological studies of  $\gamma$ -oxo- $\alpha,\beta$ -unsaturated esters and acids.

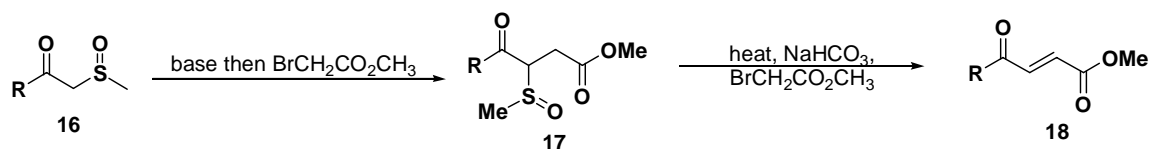


**Scheme 1.** Cysteine reactivity toward *E* and *Z*-alkenoates.

## 1.2 PREPARATION OF $\gamma$ -OXO- $\alpha,\beta$ -UNSATURATED ESTERS

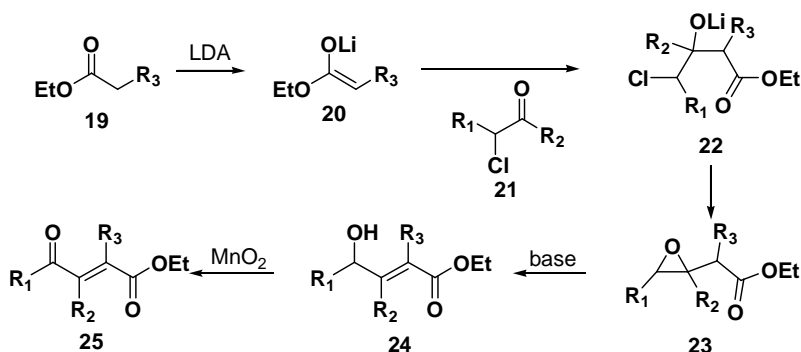
Currently, there are several methods to prepare  $\gamma$ -oxo- $\alpha,\beta$ -unsaturated esters. One of the more efficient methods is shown in Scheme 2.<sup>21</sup> This method uses a base to deprotonate in-between

the C=O and S=O bond of **16** and the resulting enolate is reacted with methylbromoacetate to yield the  $\beta$ -keto sulfoxide **17**. When the intermediate is heated in refluxing dioxane, the elimination of sulfoxide moiety yields the desired  $\gamma$ -oxo- $\alpha,\beta$ -unsaturated ester **18** in 85–99 %. The preparation is efficient; however, the elimination only yields the *E*-olefin.



**Scheme 2.** Sulfoxide elimination to yield *E*-alkenoates.

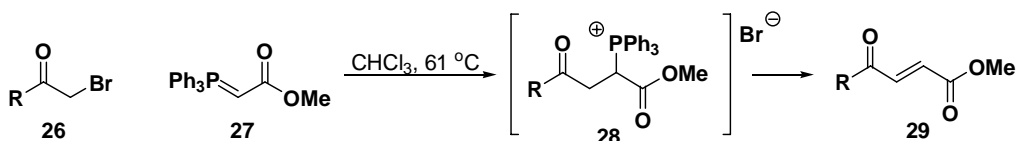
A second method is shown in Scheme 3.<sup>22</sup> The sequence starts similarly to Scheme 2, in which removal of the  $\alpha$ -proton from **19** generates enolate **20**; however, **20** undergoes an aldol condensation with **21** to form alkoxide **22**. This alkoxide then eliminates chloride to generate epoxide **23**, which in turn is opened by the base removal of the  $\alpha$ -proton to yield  $\gamma$ -hydroxy- $\alpha,\beta$ -alkenoate **24** in 40–87 % yield. This  $\gamma$ -hydroxy- $\alpha,\beta$ -alkenoate is oxidized by  $\text{MnO}_2$  to give  $\gamma$ -oxo- $\alpha,\beta$ -alkenoate **25** in 79–87 % yield. Several problems exist with this method, such as the potential for over-chlorination in the preparation of the  $\alpha$ -chloro aldehyde or ketone and the difficulty of the formation of the epoxide intermediate.



**Scheme 3.** Aldol condensation, epoxidation to yield *E*-alkenoates.

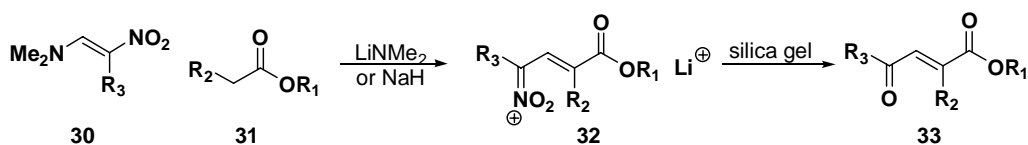
A third method to make these substrates is shown in Scheme 4.<sup>23</sup> This method involves a substitution reaction between  $\alpha$ -bromoketone **26** and phosphonium ylide **27** in which the ylide participates in a substitution reaction instead of a Wittig reaction to give **28**. Refluxing in

chloroform causes the elimination of the triphenylphosphine to yield the desired  $\gamma$ -oxo- $\alpha,\beta$ -(*E*)-unsaturated ester **29** in 58–85 % yield.



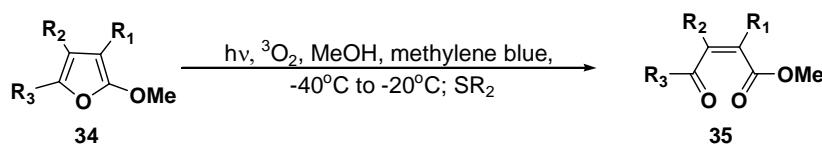
**Scheme 4.** Phosphine elimination to yield *E*-alkenoates.

A fourth method to make  $\gamma$ -oxo- $\alpha,\beta$ -(*E*)-unsaturated esters appears in Scheme 5.<sup>24</sup> This approach involves the initial  $\alpha$ -deprotonation of ester **31**, and the ester enolate subsequently attacks the unsaturated nitro-amine compound **30** to eliminate the amine. Then a second deprotonation occurs to make **32**. Finally, treatment of **32** with silica gel facilitates the hydrolysis to yield the  $\gamma$ -oxo- $\alpha,\beta$ -(*E*)-unsaturated ester **33** in 26–90 % yield.



**Scheme 5.** Hydrolysis of nitro group to yield *E*-alkenoates.

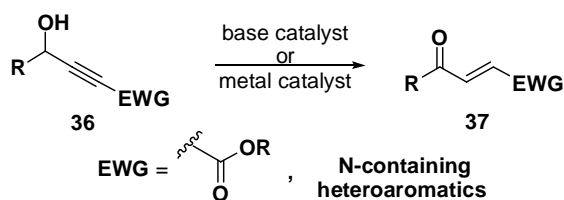
Although there are several approaches to make the *E*-alkenoate, there are limited ways to make the *Z*-alkenoate. Aside from using UV light to isomerize the *E*-alkenoate to the *Z*-alkenoate,<sup>25</sup> the only other known approach is the oxidation of furans. Oxidants such as PCC have been used,<sup>26</sup> but one of the mildest methods is portrayed in Scheme 6.<sup>27</sup> This method uses triplet oxygen and methylene blue in methanol to facilitate the oxidation of furan **34** to *Z*-alkenoate **35** in 75–98 % yield. While this furan oxidation is efficient, the preparation of the furan may take several steps to accomplish.



**Scheme 6.** Preparation of *Z*-alkenoates via a furan oxidation.

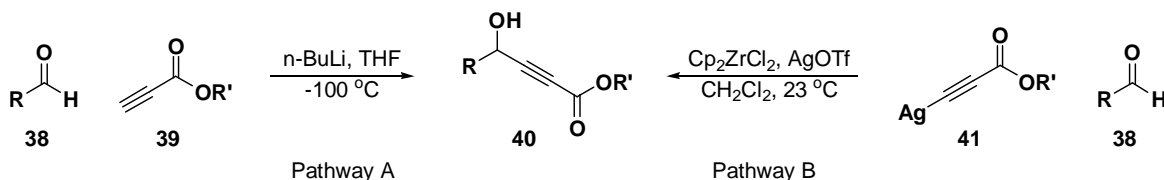
### 1.3 REDOX ISOMERIZATION OF $\gamma$ -HYDROXY- $\alpha,\beta$ -ALKYNOATES TO $\gamma$ -OXO- $\alpha,\beta$ -ALKENOATES

Despite the success of the previously reported methods, a more direct way to prepare  $\gamma$ -oxo- $\alpha,\beta$ -alkenoates **37** involves a redox isomerization using  $\gamma$ -hydroxy- $\alpha,\beta$ -alkynoates **36**. The term redox is applied to this reaction because the hydroxy group is oxidized to the ketone and the alkyne is reduced to the alkene (Scheme 8).



**Scheme 7.** General redox isomerization conditions from others.

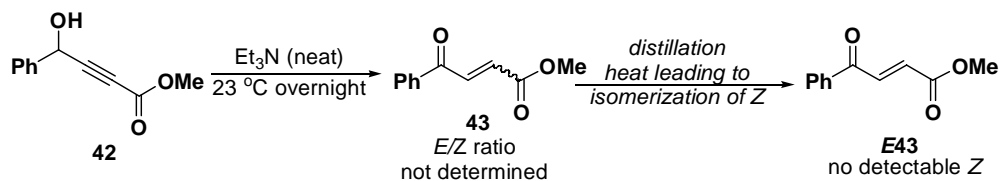
Using this approach,  $\gamma$ -hydroxy- $\alpha,\beta$ -alkynoates **40** can be convergently prepared from aldehydes and electron deficient alkynes in one step using one of two methodologies. Aldehyde **38** and alkyne **39** are united by the action of *n*-butyllithium (Scheme 8, Pathway A).<sup>28</sup> Alternatively, silver acetylide **41** reacts with aldehyde **38** (Pathway B) to yield the desired  $\gamma$ -hydroxy- $\alpha,\beta$ -alkynoate using  $\text{Cp}_2\text{ZrCl}_2$  and  $\text{AgOTf}$ .<sup>29</sup>



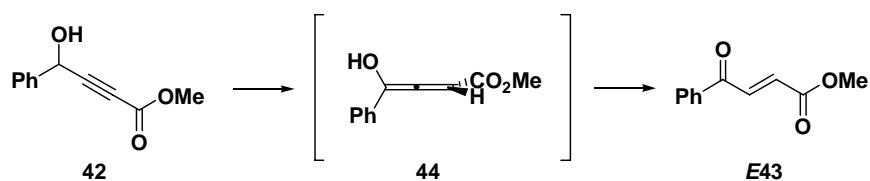
**Scheme 8.** Convergent preparations of  $\gamma$ -hydroxy- $\alpha,\beta$ -alkynoates.

Several groups have reported redox isomerization of  $\gamma$ -hydroxy- $\alpha,\beta$ -alkynoates to  $\gamma$ -oxo- $\alpha,\beta$ -alkenoates. The Raphael group showed in 1949 that the treatment of alkynoate **42** with neat  $\text{Et}_3\text{N}$  overnight at 23 °C yielded *E*-alkenoate **E43**, in 94 %, after distillation of the reaction mixture (Scheme 9) and did not isolate the *Z*-alkenoate.<sup>30</sup> Although the *E*-alkenoate was isolated, the *Z*-alkenoate could be formed and was converted to the *E*-alkenoate by residual amounts of  $\text{Et}_3\text{N}$  in the distillation. The Raphael group (Scheme 10) also proposed that during

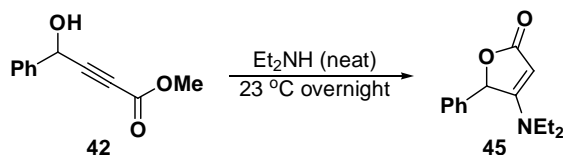
the transformation allenol **44** was formed as an intermediate; however they did not experimentally demonstrate if this was a plausible pathway. Finally, this transformation was unique to only tertiary amines, for the use of a secondary amine (Scheme 11) caused a conjugate addition/lactonization reaction to yield **45** in 70 % yield.<sup>30</sup>



**Scheme 9.** Raphael's conditions for Et<sub>3</sub>N-catalyzed redox isomerization.

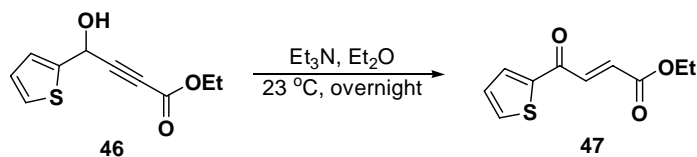


**Scheme 10.** Et<sub>3</sub>N-catalyzed redox isomerization: proposed allenol intermediate.

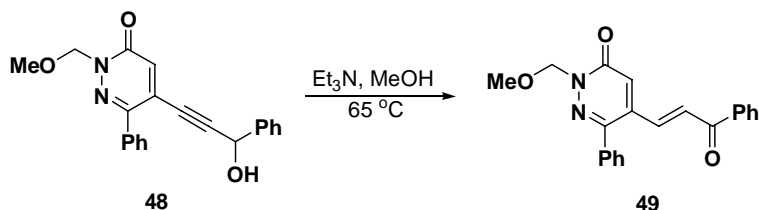


**Scheme 11.** Et<sub>2</sub>NH-facilitated lactonization of  $\gamma$ -hydroxy- $\alpha,\beta$ -alkynoates.

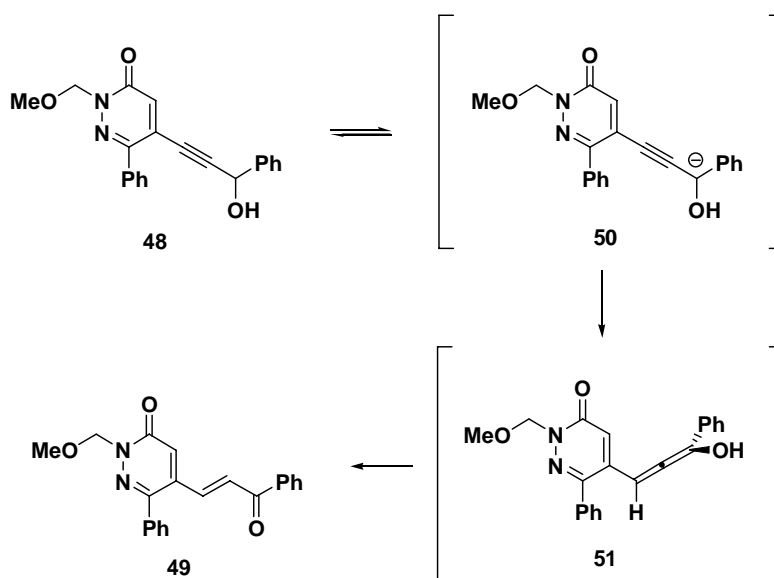
An adaptation of Raphael's conditions was applied to thiophene derivative **46** to yield *E*-alkenoate **47** (Scheme 12) in 84 % yield.<sup>31</sup> Likewise, another modification using a pyridazinone **48** instead of the ester yielded the *E*-oxoalkene derivative **49** (Scheme 13).<sup>32</sup> In this example, the authors propose the following mechanism. Because of the electron withdrawing pyridazinone and phenyl rings, the resulting acidity of the methine proton is increased and can be deprotonated by Et<sub>3</sub>N (Scheme 14) in which the negative charge can be stabilized by the alkyne to give the allenyl anion **50**. The allenyl anion is then immediately protonated by the protonated Et<sub>3</sub>N to give allenol **51**. This allenol tautomerizes to yield the *E*-oxo-alkene **49** in 80 % yield.



**Scheme 12.** Et<sub>3</sub>N-catalyzed redox isomerization of a thiophene derivative.

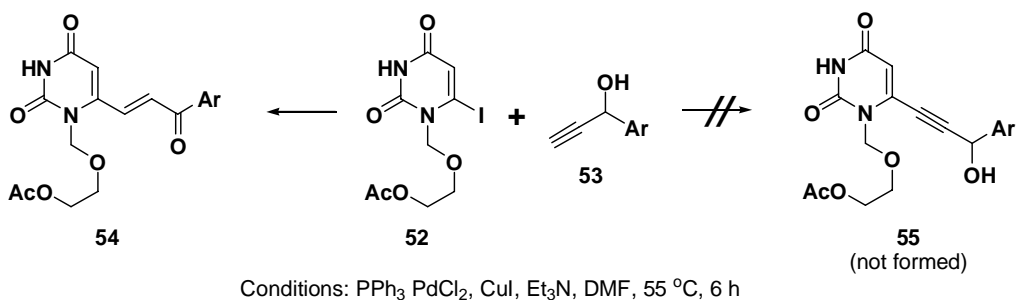


**Scheme 13.** Et<sub>3</sub>N-catalyzed redox isomerization using pyridazinone derivatives.



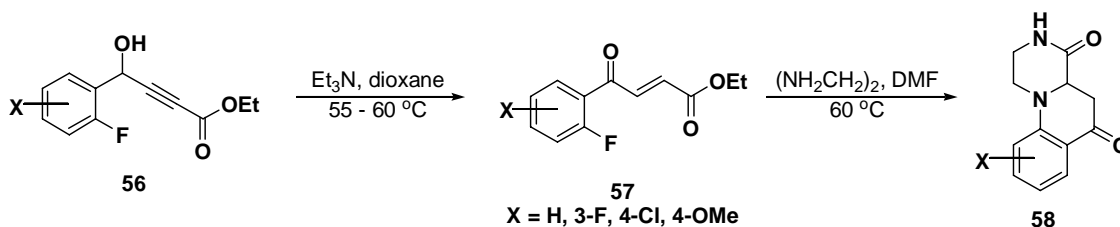
**Scheme 14.** Proposed mechanism for Et<sub>3</sub>N-catalyzed redox isomerization.

The mechanism shown in Scheme 14 was based on previous literature in that similar mechanisms to Scheme 14 were proposed to explain the formation of *E*-oxo-alkene **54** (Scheme 15) instead of **55**.<sup>33-38</sup> One such example was reported by the Kundu group in 1997, in which a Sonagashira coupling was attempted to yield alkynyl uracils; however the *E*-oxo-alkene **54** was isolated instead of alkynol **55** (Scheme 15).<sup>35</sup> The Kundu group also proposed that after the palladium coupling, Et<sub>3</sub>N deprotonated the methine proton in **P36** leading to the allenol and finally to the *E*-oxo-alkene **P35** in 71–92 % yield.



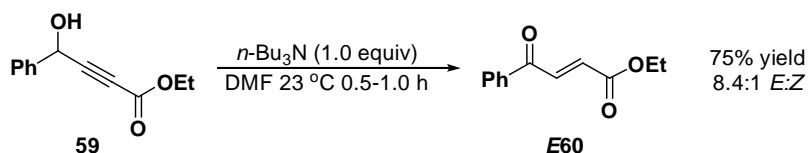
**Scheme 15.** Combined Sonagashira coupling and redox isomerization.

A third use of Raphael's conditions was demonstrated by Bernotas in 2004.<sup>39</sup> Bernotas used the transformation in the preparation of arylpiperazines that are a common motif in G-protein receptor ligands. In the transformation, he treated several *o*-fluorophenyl alkynoate derivatives **56** (Scheme 16) with Et<sub>3</sub>N in dioxane at 55–60 °C for 6–8 h and yielded the corresponding *E*-alkenoate **57** exclusively in 63–95 % yield. This alkenoate was then treated with ethylenediamine in DMF to yield the arylpiperazine **58** in 53–64 % yield.



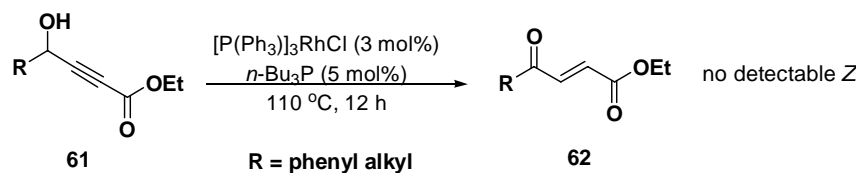
**Scheme 16.** Preparation of aryl piperazines using Et<sub>3</sub>N-catalyzed redox isomerization.

A final modification of the Raphael conditions was demonstrated by the Misiti group.<sup>40</sup> During their studies on palladium-catalyzed hydroarylation and hydrogenation, treatment of aromatic alkynoates **59** (Scheme 17) with tributylamine in DMF at 23 °C for 0.5 to 1 h resulted in a mixture of *E:Z* alkenoates **E60** in 16–98 % yield. Although the redox isomerization occurred rapidly, the *E:Z* selectivity ranged from poor to good with the best *E:Z* selectivity of 8.4:1.



**Scheme 17.** *n*-Bu<sub>3</sub>N-catalyzed redox isomerization.

Although there are several methods to accomplish the redox isomerization using bases, only one example of an intentional redox isomerization using transition metals has been reported. Treatment of an aromatic or alkyl alkynoate **61** (Scheme 18) with  $(\text{PPh}_3)_3\text{RhCl}$  and tributylphosphine at 110 °C for 12 h yielded exclusively the *E*-alkenoate **62** in 56–82 % yield.<sup>41</sup> The high temperature was a necessity for this reaction to proceed with high *E*-selectivity.



**Scheme 18.**  $[\text{P}(\text{Ph}_3)_3\text{RhCl}]$  catalyzed redox isomerization.

## 1.4 RESEARCH AIMS

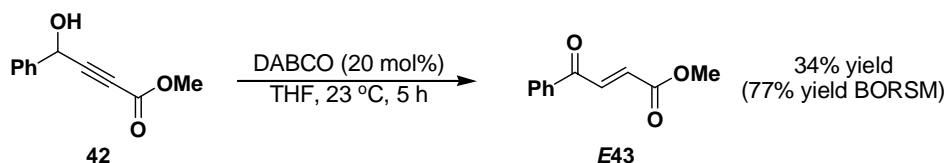
Despite the utility of such redox isomerizations, the mechanisms of these reactions were never studied. Only one hypothesis was proposed but not experimentally elucidated. Raphael proposed an allenol intermediate but no mechanism on how this redox isomerization proceeds. Similar to Raphael's pathway, Kundu and others propose a methine deprotonation by the amine leading to an allenyl anion which can be stabilized by the nitrogen heterocycle, but none attempted to elucidate it.<sup>33-38</sup> One of the objectives of my research was to study the mechanism.

Once the reactions were optimized selectively yielding multiple *E* and *Z*-alkenoates, these alkenoates would then be submitted for biological testing to determine their biological activity. These molecules should be good electrophiles and be biologically active. If a molecule exhibits potent activity, analogues of that molecule would be prepared and tested to gain insight into a possible mode of action.

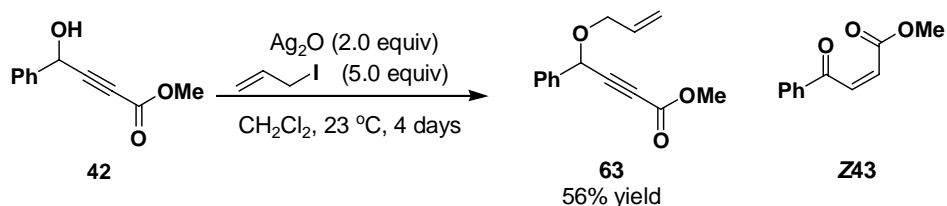
## 2.0 RESULTS AND DISCUSSION

### 2.1 BACKGROUND

A former group member discovered that treatment of **42** with 20 mol% of DABCO in THF for 5 h produced **E43** in 34 % yield (77 % yield BORSM) (Scheme 19). In addition, **Z43** was isolated as a by-product of the O-allylation of **1** (Scheme 20). These reactions suggested that it might be possible to produce **E43** and **Z43** selectively from **42**.



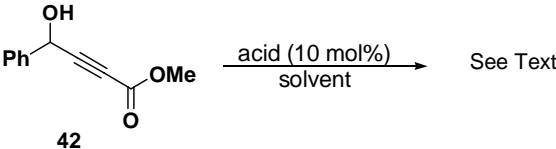
**Scheme 19.** DABCO-catalyzed *E*-selective redox isomerization using THF.



**Scheme 20.** Formation of **Z2** by-product from O-allylation.

Initially we hypothesized that if base promoted the redox isomerization of **42** to **E43**, then acid might promote a skeletal-diversification of **42**. Treatment of **42** with either 10 mol% of acetic acid or *p*TsOH at 23, 50 or 80 °C, however, only resulted in recovery of the starting material (Table 1) showing that **42** is inert to acid.

**Table 1.** Attempts at structural diversity using acid.



42

Acid	Solvent	Temperature (°C)	Time (h)	Result
AcOH	CH <sub>2</sub> Cl <sub>2</sub>	23	0.5	Starting Material
<i>p</i> TsOH	CH <sub>2</sub> Cl <sub>2</sub>	23	1.0	Starting Material
AcOH	(ClCH <sub>2</sub> ) <sub>2</sub>	50	1.3	Starting Material
		80	1.5	
<i>p</i> TsOH	(ClCH <sub>2</sub> ) <sub>2</sub>	50	1.3	Starting Material
		80	1.5	

Since an acid-catalyzed skeletal-diversification was not feasible, we pursued a base-catalyzed redox isomerization instead. In order to elucidate reaction order, kinetics and obtain an accurate *E/Z* selectivity, Alkynoate **42** was treated with 10 mol% of base in CDCl<sub>3</sub> and the reaction was monitored by <sup>1</sup>H NMR spectroscopy until the majority of the starting material was consumed. When alkynoate **42** was treated with DMAP, no desired product was formed after the consumption of the starting material (Table 2, Entry 1) whereas DABCO only gave a trace amount of conversion after 3 days (Entry 2). Treatment of alkynoate **42** with Et<sub>3</sub>N and DBU gave *E:Z* selectivity of 1.9:1 (Entry 3) and 5:1 (Entry 4) respectively. Although DBU gave a good stereoselectivity, a less basic tertiary amine would be more desirable so that base sensitive functionalities can be used. Interestingly, when alkynoate **42** was subjected to 10 mol% of *i*Pr<sub>2</sub>NEt, the reaction gave a modest selectivity in favor of the *Z*-olefin (*E:Z* = 1:1.4, Entry 5). During all these reactions, the *E:Z* selectivity did not change as the reaction progressed, showing that the conversion of one isomer to another did not occur. Although the *E:Z* selectivity remained constant, the reaction times could be improved. Therefore solvent effects were studied to improve reaction time and yield.

Increasing the polarity of the solvent decreased the reaction time, which indicates that the DMSO stabilized some charged intermediates as shown by Et<sub>3</sub>N and *i*Pr<sub>2</sub>NEt (Figures 4 and 5 respectively). The *E:Z* selectivity was not dramatically affected by the solvent (compare Entries

3, 7, 9 and Entries 5, 8, 10). In C<sub>6</sub>D<sub>6</sub>, treatment of alkynoate **42** with DABCO gave only a trace conversion (Entry 6), similar to CDCl<sub>3</sub> (Entry 2), but when the solvent was changed to DMSO-d<sub>6</sub>, alkynoate **42** was easily converted to the alkenoate with an excellent *E:Z* selectivity of 33:1 (Entry 11). In CD<sub>3</sub>CN, the *E:Z* selectivity was 10:1 and intractable by-products were also formed (Entry 12). From the results, we decided to pursue an *E*-selective DABCO-catalyzed redox isomerization as well as a *Z*-selective, iPr<sub>2</sub>NEt-catalyzed redox isomerization.

**Table 2.** Initial base and solvent effect studies.

Entry	Base	Solvent	<i>t</i> <sub>1/2</sub> (h)	% Yield	<i>E:Z</i>
1	DMAP	CDCl <sub>3</sub>	n.d.	n.d.	Not formed
2	DABCO	CDCl <sub>3</sub>	n.d.	n.d.	Trace after 72 h
3	Et <sub>3</sub> N	CDCl <sub>3</sub>	17	56	1.9 : 1
4	DBU	CDCl <sub>3</sub>	<0.3	61	5 : 1
5	iPr <sub>2</sub> NEt	CDCl <sub>3</sub>	60	93	1 : 1.4
6	DABCO	C <sub>6</sub> D <sub>6</sub>	n.d.	n.d.	Trace after 72h
7	Et <sub>3</sub> N	C <sub>6</sub> D <sub>6</sub>	16	n.d.	1.3 : 1
8	iPr <sub>2</sub> NEt	C <sub>6</sub> D <sub>6</sub>	126	n.d.	1 : 1
9	Et <sub>3</sub> N	DMSO-d <sub>6</sub>	1.5	50	1.5 : 1
10	iPr <sub>2</sub> NEt	DMSO-d <sub>6</sub>	12	n.d.	1 : 1.6
11	DABCO	DMSO-d <sub>6</sub>	1.5	70	33 : 1
12	DABCO	CD <sub>3</sub> CN	n.d.	n.d.	>10 : 1

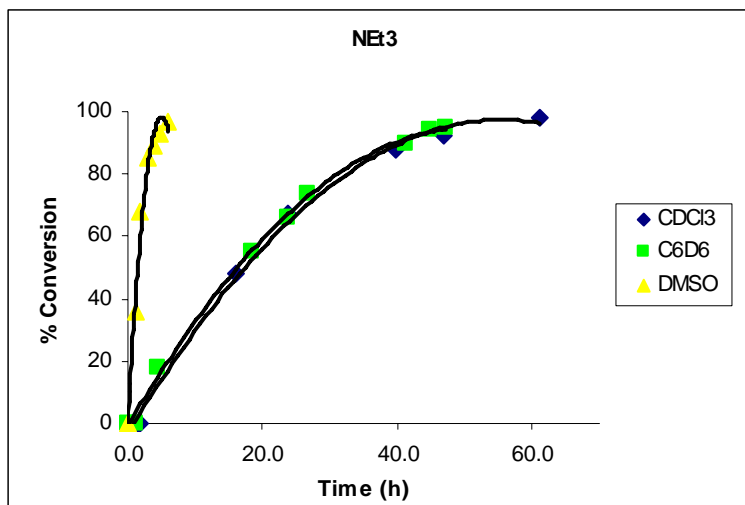


Figure 4. Et<sub>3</sub>N-catalyzed redox isomerization: solvent effects.

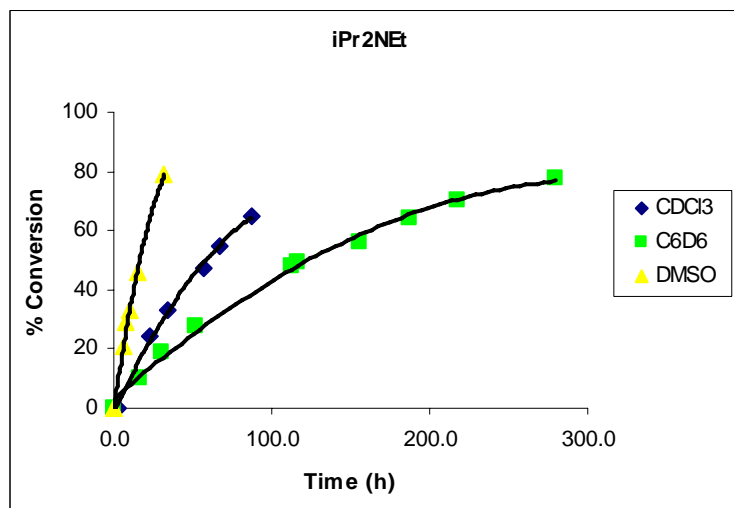
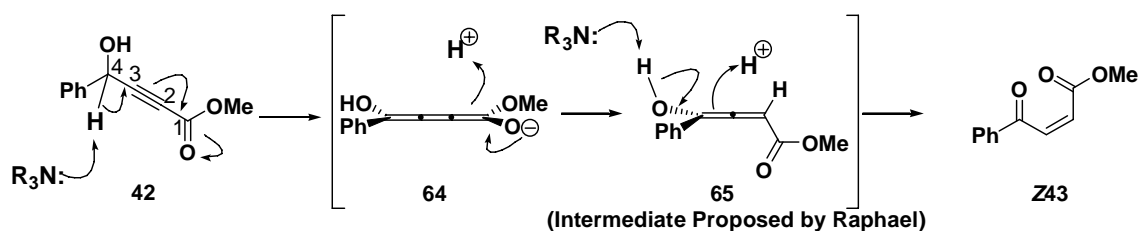


Figure 5. iPr<sub>2</sub>NEt-catalyzed redox isomerization: solvent effects.

## 2.2 E-SELECTIVE REDOX ISOMERIZATION

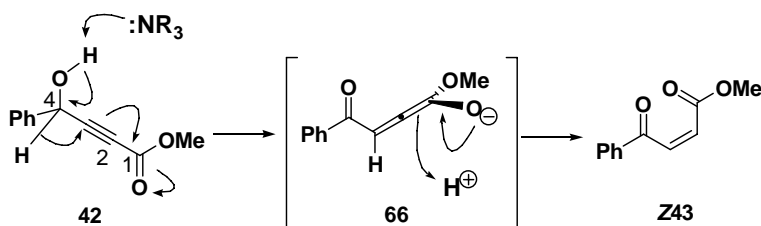
### 2.2.1 Reaction Optimization and Mechanistic Studies

**Mechanisms:** During these NMR studies, four plausible mechanisms were hypothesized. Mechanism A involves the deprotonation of 4-H in alkynoate **42**, wherein the negative charge can be stabilized by the unsaturated ester system to give cummulenate **64** (Scheme 21). Then **64** is protonated by the most acidic proton source in the reaction system to give allenol **65**<sup>30</sup> that in turn tautomerizes to yield Z-alkenoate **43**.<sup>42</sup>



Scheme 21. Mechanism A: methine deprotonation mechanism.

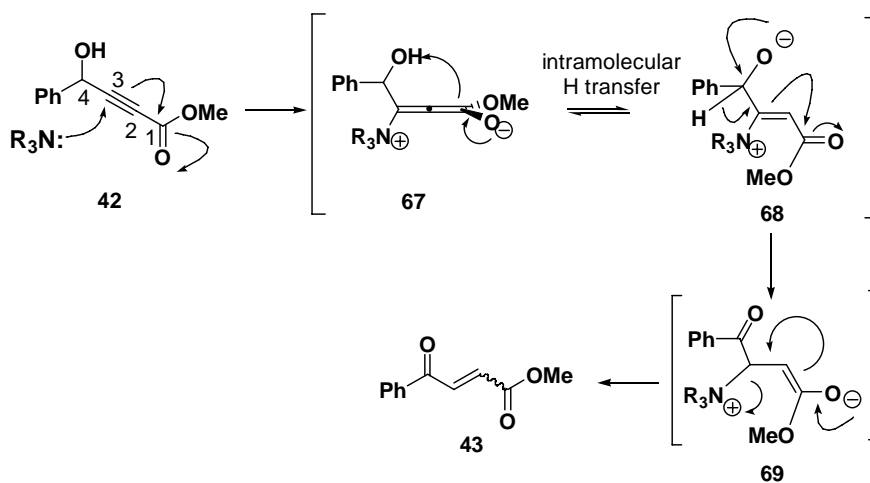
Mechanism B involves the amine deprotonating the hydroxyl group, which in turn causes a 1,2-hydride shift of 4-H to produce allenolate **66** (Scheme 22). This allenolate is then protonated most likely on the less hindered side to yield the Z-alkenoate.



Scheme 22. Mechanism B: 1,2-hydride shift mechanism.

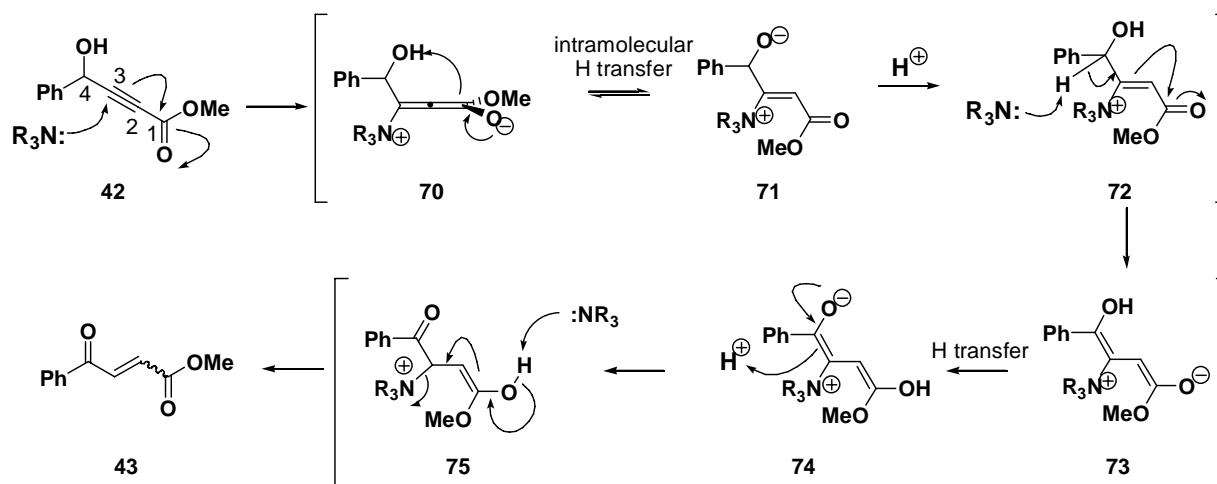
Mechanism C involves the nucleophilic addition of the amine to 3-C of the unsaturated ester system to generate allenolate **67** (Scheme 23). Allenolate **67** then undergoes an intramolecular proton transfer to produce alkoxide **68**. This alkoxide undergoes a 1,2-hydride shift of the hydrogen in the 4-position, which in turn is stabilized by the unsaturated ester system

to give ester enolate **69**. Ester enolate **69** then reforms the ester carbonyl and eliminates the amine to yield an *E:Z*-mixture of alkenoates.



**Scheme 23.** Mechanism C: conjugate addition / 1,2-hydride shift mechanism.

Finally mechanism D starts similarly as mechanism C, in which the amine adds to the 3-position to generate allenolate **70**; this in turn undergoes an intramolecular hydrogen transfer to give alkoxide **71** (Scheme 24). This alkoxide is protonated at the alkoxide oxygen to produce intermediate **72** which is then deprotonated at the 4-position and the negative charge is stabilized by the unsaturated ester system to 3,4-unsaturated ester enolate **73**. This ester enolate undergoes a proton transfer to generate enol-ester enolate **74**. Enol-ester enolate **74** is then protonated at the 3-position to give the 4-oxo-enol ester **75**. This 4-oxo-enol ester is then deprotonated causing the reformation of the ester carbonyl and the amine elimination to yield an *E:Z*-mixture of alkenoates.



**Scheme 24.** Mechanism D: conjugate addition / methine deprotonation mechanism.

**Cyclobutyl alkynoate studies:** To help indicate which mechanism was more plausible, two analogues based on alkynoate **42** were prepared. Alkynoates **76** and **77** (Figure 6) were prepared to aid in indicating if the DABCO-catalyzed redox isomerization was proceeding by mechanism B (1,2-hydride shift) or mechanism C (conjugate addition / 1,2-hydride shift). The premise (as shown compared to mechanism B in Scheme 25) is that DABCO deprotonates the alcohol in alkynoate **76** but instead of the 1,2-hydride shift, alkynoate **76** would undergo a ring expansion to relieve the strain of the 4-membered ring. The reaction should then progress to generate an *E:Z* mixture of **79**. These two substrates can elude to mechanism C as well (not shown).

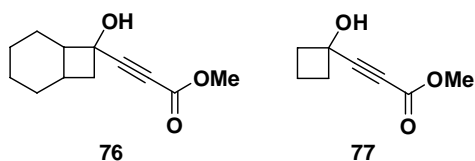
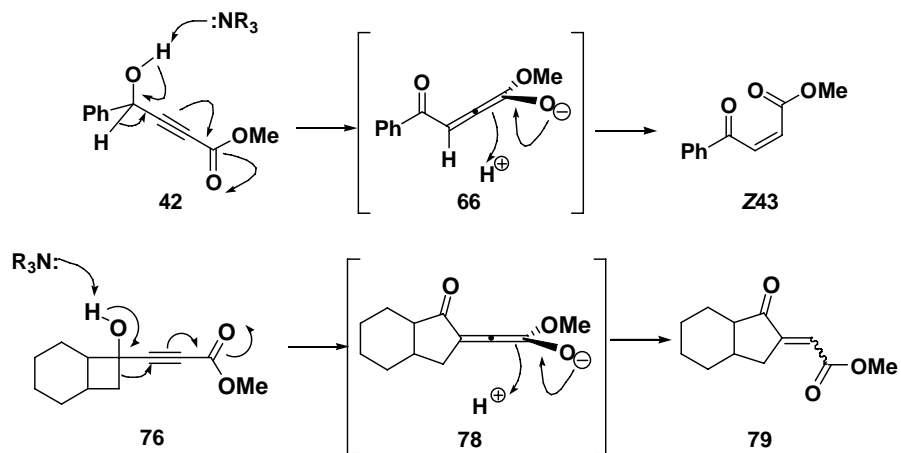
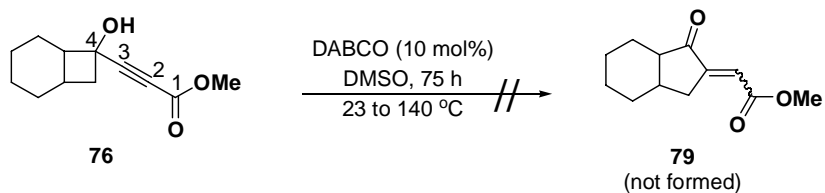


**Figure 6.** Cyclobutyl-alkynoates that elude to mechanisms B or C.

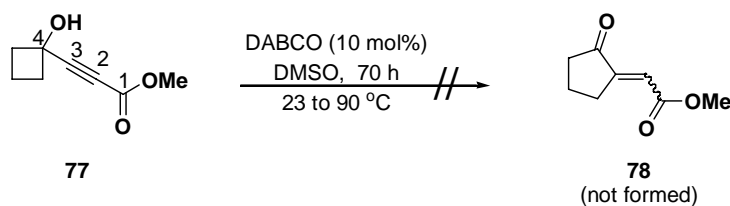


**Scheme 25.** Mechanism for DABCO-catalyzed redox isomerization and ring expansion.

Treatment of alkyne **76** with 10 mol% DABCO in DMSO (Scheme 26) resulted in recovering starting material even when the reaction was heated to 140 °C. The inertness of this substrate could be due to the bicyclic structure causing extra strain as the four-member ring “reached” to bind to 3-C. In an attempt to alleviate the added strain from the bicyclic system, alkyne **77** was prepared. However, exposure of alkyne **77** to similar reaction conditions (Scheme 27) resulted in only isolation of the starting material even when heated to 90 °C. Failure of alkyne **76** and **77** to form any alkenoate indicated that the reaction may not proceed via mechanisms B or C. However, these results did not elucidate the actual mechanism.



**Scheme 26.** Failed ring expansion on bicyclic alkyne using DABCO.



**Scheme 27.** Failed ring expansion on cyclobutyl alkyne using DABCO.

**DABCO amount studies:** To determine which one of these mechanisms is most plausible for the DABCO-catalyzed redox isomerization, kinetic studies were performed. From the NMR study of the DABCO reaction, second order kinetics provided the best fit for the data collected which demonstrated that the reaction is second order overall (Figure 7). We hypothesized that the reaction was first order with respect to DABCO and alkynoate. In order to verify this, the DABCO-catalyzed redox isomerization was repeated using different DABCO amounts and again monitored using  $^1\text{H}$  NMR spectroscopy. By plotting the initial rate of the three reactions versus the base concentration, we determined that the reaction is indeed first order in base (Figure 8). Since the reaction was second order overall, the reaction must be first order in alkynoate. Therefore, the rate determining step must involved one molecule of DABCO and one molecule of alkynoate.

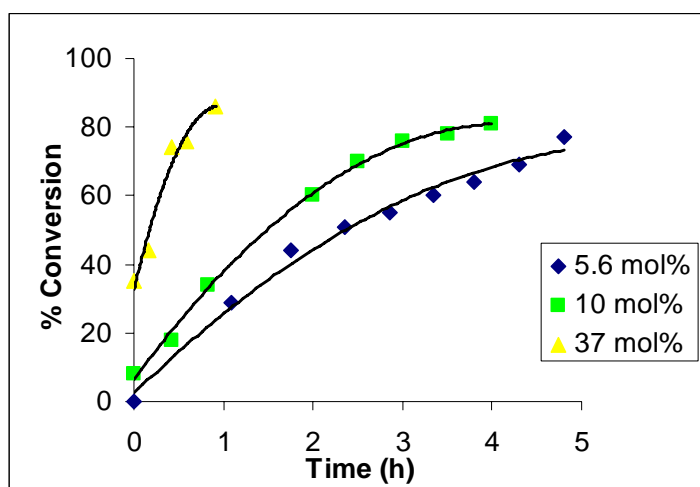


Figure 7. DABCO amount studies.

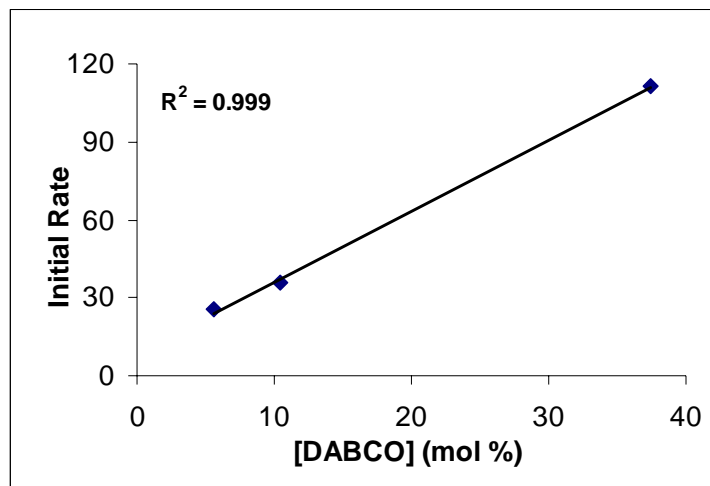
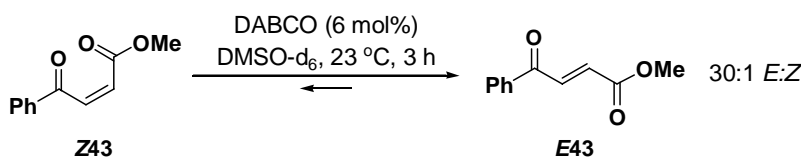


Figure 8. Initial reaction rate versus [DABCO].

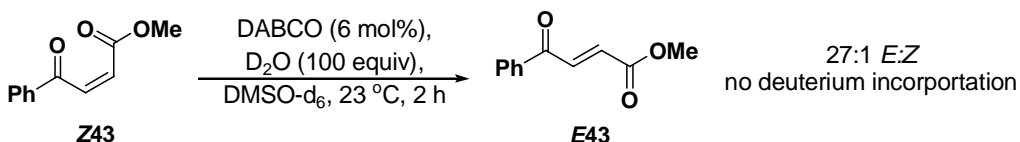
**Z-to-E isomerization studies:** To aid in the elucidation of the DABCO-catalyzed redox isomerization, we investigated product stability toward the reaction conditions. From the  $^1\text{H}$  NMR experiments it was relatively clear that DABCO yielded **E43** selectively; however one remaining question was whether the *E*-selective redox isomerization was thermodynamically controlled. To determine if the reaction is thermodynamically controlled, **Z43** was treated with 6 mol% of DABCO in  $\text{DMSO-d}_6$  and the reaction was monitored by  $^1\text{H}$  NMR. The half-life of the **Z43** to **E43** isomerization (Scheme 28) was less than 5 min, whereas the redox isomerization of alkynoate **42** to alkenoate **E43** was 90 min. After 3 h the same *E:Z* ratio was obtained as when DABCO catalyzed the redox isomerization starting from alkynoate **42**. Although this experiment did not rule out that **E43** was kinetically formed, this experiment explained that **E43** was thermodynamically favored.



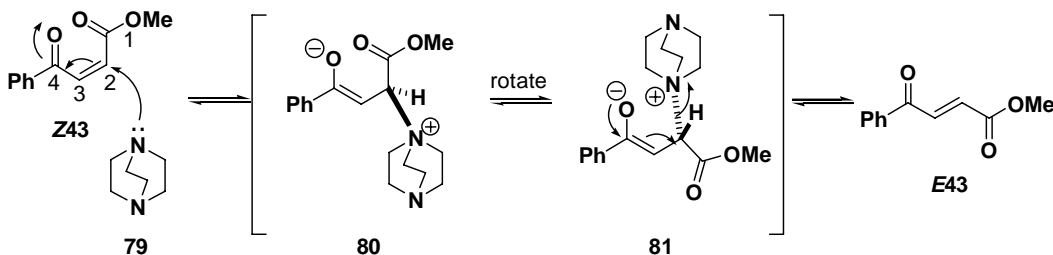
Scheme 28. DABCO-catalyzed **Z43**-to-**E43** isomerization.

In order to elucidate the mechanism of this **Z43**-to-**E43** isomerization, a deuterium incorporation experiment was carried out. Alkenoate **Z43** was treated with 6 mol% of DABCO in 1:2 ratio of  $\text{D}_2\text{O}$  and  $\text{DMSO-d}_6$ , and the reaction was monitored using  $^1\text{H}$  NMR spectroscopy.

After 2 h, **E43** was formed without any deuterium incorporation into the alkenoate (Scheme 29). This showed that the **Z43** to **E43** isomerization occurred at a faster rate than any proton exchange with the solvent. DABCO first inserted itself at the 2-C (Scheme 30). Upon insertion, the 2-C-3-C bond of **80** rotated to minimize lone pair repulsions between enolate and the ester carbonyl oxygen. Finally, the ketone-carbonyl in **81** reformed to eliminate DABCO without any proton exchange with the solvent.

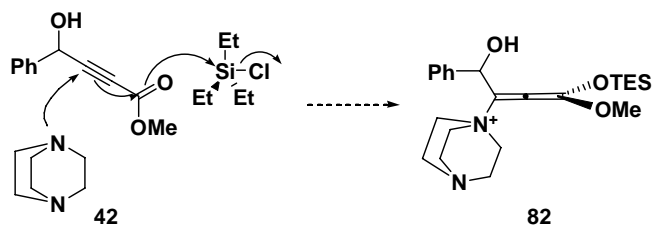


Scheme 29. DABCO-catalyzed **Z43**-to-**E43** isomerization: deuterium experiment.

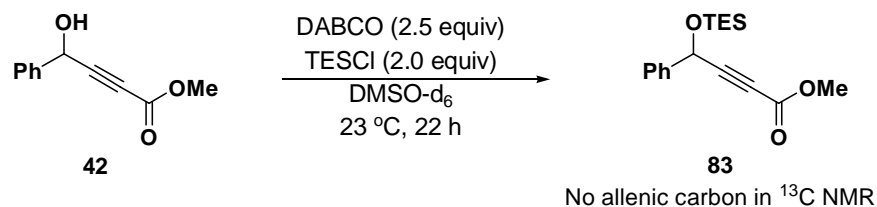


Scheme 30. DABCO-catalyzed *Z*-to-*E* isomerization mechanism.

**Intermediate trapping studies:** Although the **Z43** to **E43** isomerization experiments allude to the *E*-selectivity of the DABCO-catalyzed redox isomerization, they did not elucidate the redox isomerization mechanism. To gain mechanistic insight, we decided to trap the reaction intermediate as a stable compound. For example, if the redox isomerization proceeds under a conjugate addition mechanism, there might be a possibility that TESCl could react with the formed allenolate to make an allenic ether (Scheme 31). To ensure that the intermediate is trapped, 2.0 equiv of TESCl and 2.5 equiv of DABCO were used and the reaction was monitored by  $^1\text{H}$  and  $^{13}\text{C}$  NMR. Despite the excess of TESCl and DABCO, a  $^{13}\text{C}$  NMR spectrum indicated that the experiment did not trap any intermediate complexes. The only reaction that seemed to occur was the TES-protection of the alcohol in the 4 position (Scheme 32).



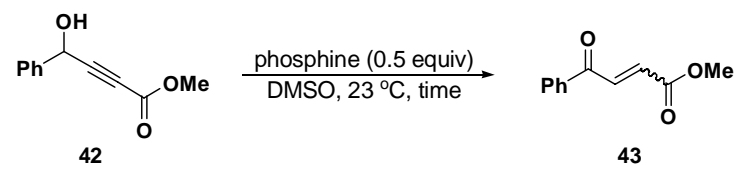
**Scheme 31.** One possible trapping mechanism using TESCl.



**Scheme 32.** Failed TESCl trapping of DABCO-catalyzed redox isomerization intermediate.

**Phosphine Studies:** Another method to deduce a plausible mechanism was to use a catalyst that can only behave in one particular manner. In the DABCO-catalyzed redox isomerization, DABCO can be a base and/or nucleophile. If DABCO was a nucleophile, a stronger nucleophile should expedite the redox isomerization. Using triphenylphosphine in lieu of DABCO would be desirable, for the isomerization could only proceed via mechanisms C or D (Schemes 24 and 25) since phosphines are weaker bases. Alkynoate **42** was subjected to 50 mol% of triphenylphosphine in DMSO (Table 3, Entry 1) and the reaction was stirred for 4 days. However, the reaction was sluggish and resulted in a complex mixture that only contained 20–43 % of alkynoate **Z43**. Although treatment of alkynoate **42** with 50 mol% of more nucleophilic tri-*n*-butylphosphine decreased the reaction time to 16 h, the  $^1\text{H}$  NMR of the crude reaction mixture yielded neither of the desired alkenoates (Table 3, Entry 2). These two experiments indicated that DABCO was more likely acting as a base because the phosphine-catalyzed reaction should yield a higher quantity of the alkenoates.

**Table 3.** Attempts at phosphine-catalyzed redox isomerization.



Entry	Catalyst	Time (h)	Result
1	PPh <sub>3</sub>	96	complex mixture with 20 to 43 % Z43
2	P( <i>n</i> -Bu) <sub>3</sub>	16	no desired product

**Deuterium Studies:** In order to further elucidate the mechanism, a deuterium incorporation experiment using D<sub>2</sub>O was envisioned. However, before that experiment was performed, the 2- and 3-H's of **E43** had to be properly assigned. An HMBC experiment determined 2-H and 3-H to be 6.89 and 7.93 ppm respectively. Depending on where the deuterium incorporated, a number of the mechanisms can be eliminated. For example, if the deuterium was added at 2-C the more likely mechanisms are mechanisms B and C where the deprotonated hydrogen attached to 2-C (Schemes 33 and 34).

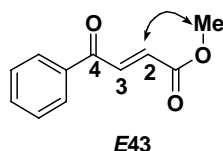
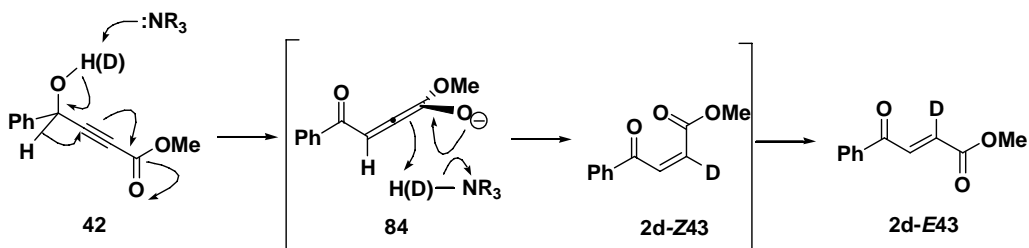
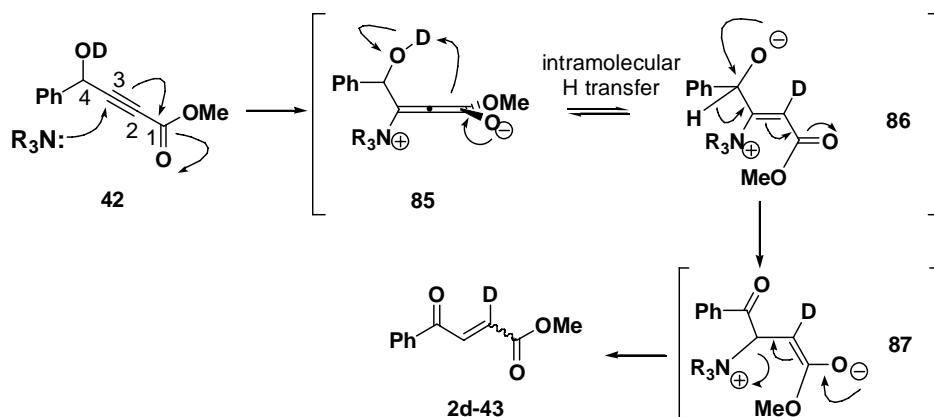


**Figure 9.** Key HMBC coupling for **E43**.

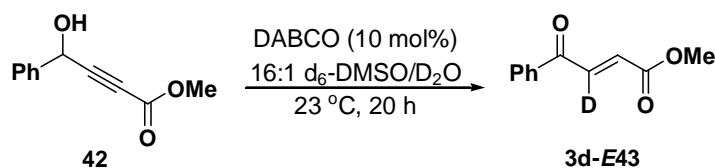


**Scheme 33.** Location of deuterium incorporation for mechanism B.



**Scheme 34.** Location of deuterium incorporation for mechanism C.

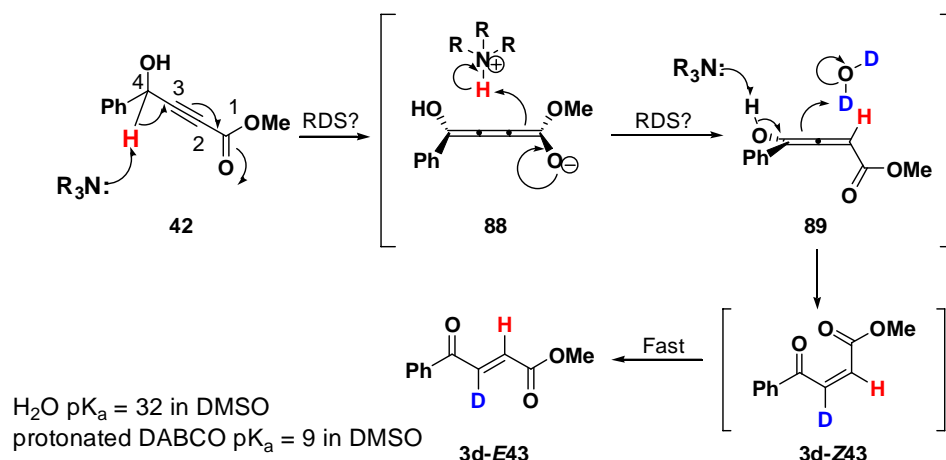
Treatment of alkynoate **42** with 10 mol% of DABCO in solution of 2:1 ratio of DMSO- $d_6$ /D $_2$ O at 23 °C resulted in mostly decomposition indicating that excessive water may be detrimental. This result prompted the reduction in the amount of D $_2$ O. Treatment of alkynoate **42** with 10 mol% of DABCO but changing to a 16:1 ratio of DMSO/D $_2$ O (Scheme 35) resulted in the formation of alkenoate **3d-E43**. Due to the location of the deuterium, this experiment not only eliminated mechanisms B and C (the deuterium incorporation would occur on C-2) (Schemes 33 and 34), but it also determined that the most plausible mechanism was mechanism A.



**Scheme 35.** D $_2$ O-incorporation experiment using DABCO.

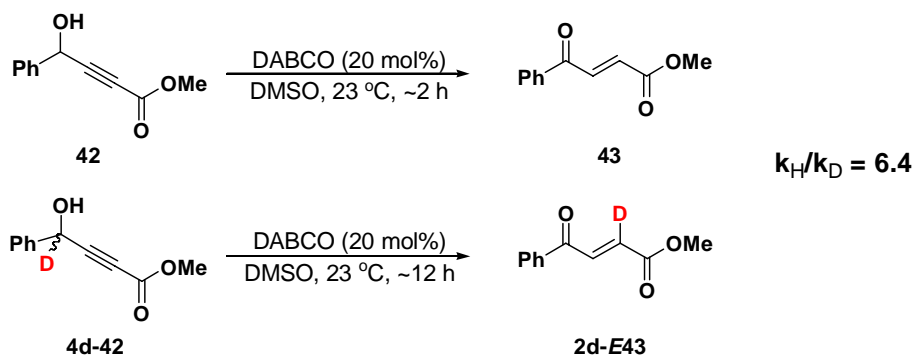
DABCO deprotonates at the 4-H (Scheme 36), and the resulting cummulenolate **88** abstracts a proton from the more acidic protonated DABCO ( $pK_a$  in DMSO = 9) rather than water ( $pK_a$  in DMSO = 32) in the reaction system to give allenol **89**. This allenol tautomerizes with D $_2$ O adding on the less hindered side<sup>42</sup> to give alkenoate **3d-Z43**. From the isomerization studies, the *Z*-alkenoate in the presence of DABCO is then immediately isomerized to yield **3d-E43**. Since one molecule of DABCO and one molecule of substrate have to be involved in the rate determining step, either the 4-H deprotonation or allenol tautomerization is the rate

determining step. Since the reaction smoothly preceded DMSO, a solvent that can stabilize charged species more efficiently, the rate determining step must be the formation of the charged cummulenolate.



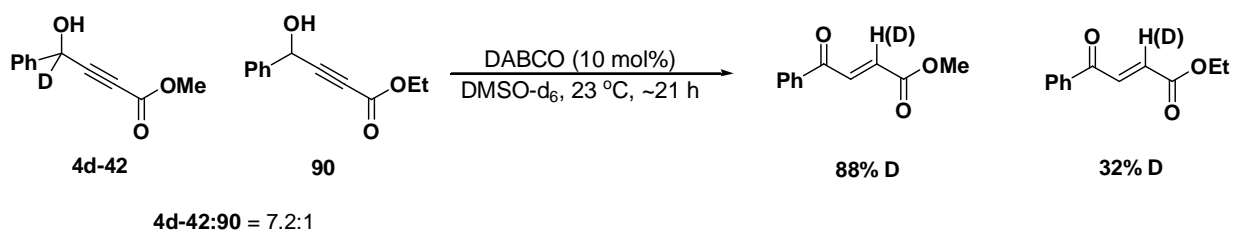
**Scheme 36.** Mechanism for DABCO-catalyzed redox isomerization.

Therefore if the methine proton is switched to a deuterium, a maximum primary isotope effect should be observed as well as the formation of **2d-E43** as the sole product. Alkynoate **4d-42**, prepared from PhCDO, was then subjected to 20 mol% of DABCO in DMSO and the reaction rate was compared to the control alkynoate **42** using <sup>1</sup>H NMR. Alkynoate **4d-42**, gave only **2d-E43** and a maximum primary isotope effect of 6.4 was observed consistent with mechanism A (Scheme 36). Finally, <sup>1</sup>H NMR experiments showed the DABCO-catalyzed isomerization had a nearly quantitative conversion when compared to an internal standard of dibenzyl ether.



**Scheme 37.** DABCO-catalyzed redox isomerization: deuterium isotope effect.

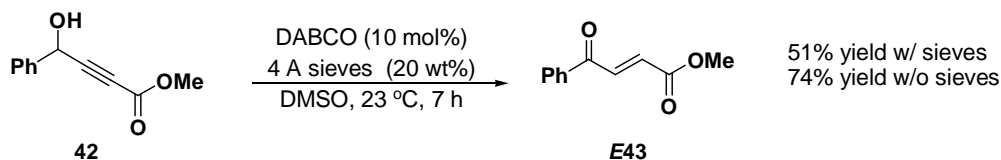
**Crossover Experiment:** One final inquiry about the DABCO-catalyzed redox isomerization was how tight an ion pair was formed when DABCO deprotonated alkynoate **42** forming the cummlenolate **88**. To answer this, a crossover experiment was devised using alkynoate **4d-42** along with the ethyl ester derivative of alkynoate **42** (alkynoate **90**). The two compounds would be combined and subjected to the redox isomerization conditions. If the protonated DABCO formed a tight ion pair with the cummlenolate **88**, then there should be no deuterium enrichment on the ethyl ester derivative. During the reaction, it was important to compensate for the 6.4 times slower reaction with the deuterated alkynoate **4d-42**; otherwise DABCO would solely react with alkynoate **90** before it ever reacted with alkynoate **4d-42**. To alleviate this, alkynoates **4d-42** and **90**, in a 7.2 to 1 ratio respectively, were treated with DABCO in DMSO- $d_6$  and the reaction was monitored. Upon reaction completion and filtration, the methyl ester derivative had 88 % deuterium enrichment and the ethyl ester had 32 % deuterium enrichment at 2-C when compared to a  $^1\text{H}$  NMR spectrum of the non-deuterated alkenoate (Scheme 38). This 32 % enrichment of the ethyl ester showed that the protonated DABCO did not form an intimate ion pair with the cummlenolate **88**.



**Scheme 38.** DABCO-catalyzed redox isomerization: crossover experiment.

**DABCO-Catalyzed Redox Isomerization Optimization:** Upon mechanistic elucidation, the DABCO-catalyzed redox isomerization was also optimized. Desirable reaction conditions include the following: (1) the temperature should be 23 °C, (2) too acidic or basic conditions should be avoided, and (3) the catalyst should be relatively inexpensive and kept to a minimum. Since different DABCO amounts only affected reaction time, we decided to use 10 mol% of DABCO as the optimal quantity. Based on the NMR experiments, the best solvent for the redox isomerization was DMSO. Since residual water may affect the yield, 4 Angstrom sieves were added to the DABCO-catalyzed redox isomerization (Scheme 39). Upon completion of the

reaction, alkenoate **E43** was isolated in 51 % yield which was lower than in the absence of 4 angstrom sieves. Therefore, the removal of residual water was not necessary.



**Scheme 39.** DABCO-catalyzed redox isomerization: residual water removal.

The final condition that could be optimized is the initial concentration of alkynoate **42**. Increasing the concentration of substrate to 1.0 M (Table 4, Entry 1) and 0.5 M (Entry 2) gave yields of 44 % and 47 %. This decrease in yield at higher concentrations (0.25 M gave a 59 % yield, Entry 3) might be due to an intermolecular reaction between two molecules of either alkynoate and alkenoate leading to a polymerization. Decreasing the initial concentration to 0.125 M gave a yield of 63 %. From the results in Table 4, apparently the ideal initial concentration to use in the DABCO-catalyzed redox isomerization was approximately 0.25 M (Entry 3) because in 8.5 h, these conditions gave a similar yield to the highest yielding concentration of 0.125 M.

**Table 4.** DABCO-catalyzed redox isomerization: alkynoate concentration studies.

Entry	Initial Alkynoate Concentration (M)	Time (h)	% Yield of <b>E43</b>
1	1.00	5.5	44
2	0.500	5.8	47
3	0.250	8.5	59
4	0.125	20	63

## 2.2.2 Reaction Scope of DABCO-Catalyzed Redox Isomerization

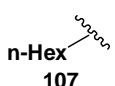
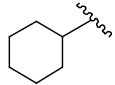
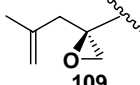
**Table 5.** DABCO-catalyzed redox isomerization: aromatic and vinylogous alkynoates.

Entry	R	Time (h)	% Yield
1		25	<b>E92</b> - 70
2		2.0	<b>E94</b> - 62
3		23	<b>E96</b> - 34
4		20	<b>E98</b> - 60
5		9.0	<b>E100</b> - 78
6		1.0	<b>E102</b> - quantitative
7		24	<b>E104</b> - decomposition

**Aromatic and Vinylogous Substrates:** Upon the optimization of the DABCO-catalyzed redox isomerization (DABCO 20 mol%, DMSO, 23 °C, [alkynoate]<sub>initial</sub> = 0.2 M), several substrates were tested. In agreement with the mechanism of the reaction, the electron rich *p*-methoxyphenyl derivative **91** (Table 5, Entry 1) required a longer reaction time (25 h) than alkynoate **1**, with a 70 % yield. Likewise the electron poor *p*-trifluoromethylphenyl derivative

**93** (Entry 2) exhibited a much shorter reaction time (2.0 h) than alkynoate **42** in 62 % yield. Interestingly, the *o*-bromophenyl derivative **95** gave a longer reaction time (23 h) and 34 % yield (Entry 3), presumably due to the bulkiness of the bromine atom that interfered with the initial 4-H deprotonation by DABCO. Apparently this hypothesis seemed plausible, because when fluorine (**97**) was used, the reaction yielded a higher amount of the desired alkenoate (60 %, Entry 4) in 20 h. In agreement with the phenyl derivatives, heteroaromatics compounds such as the furanyl derivative **99** (Entry 5) gave 78 % yield in 9.0 h. The styrenyl derivative **101** was an interesting example (Entry 6) for the formation the desired alkenoate occurred after 1.0 h and had a quantitative yield. A plausible explanation for the shorter reaction time was that the alkenoate contains an inherent stability from its higher conjugation. Finally, the hexenyl derivative **103** decomposed under the DABCO-catalyzed redox isomerization conditions (Entry 7) because the product may be unstable in the presence of DABCO.

**Table 6.** DABCO-catalyzed redox isomerization: aliphatic alkynoates.

Entry	R	Temperature (°C)	Time (h)	% Yield
1		23 to 95	4.5	no reaction
2		23 to 80	25.5	no reaction
3		23 to 80	26	decomposition

**Aliphatic Substrates:** Although the aromatic and vinylogous derivatives **91**, **93**, **95**, **97**, **99**, **101** gave favorable results, the aliphatic substrates did not result in anything promising (Table 6). Even when **107** (Table 6, Entry 1) and **108** (Entry 2) were heated to 95 °C and 80 °C respectively, only the starting materials were isolated. The inertness of **107** and **108** may be because the 4-H in these substrates was not acidic enough. Also, Misiti et. al. reported that  $n\text{-C}_7\text{H}_{15}\text{CH}(\text{OH})\text{C}\equiv\text{CCO}_2\text{Et}$  was inert to treatment with tributylamine indicating that DABCO

was not basic enough to deprotonate aliphatic substrates.<sup>40</sup> Likewise the decomposition of the epoxide derivative was mostly due to the high temperature and not DABCO (Entry 3). Therefore, a plausible solution would be to use a stronger base, but the use of a stronger base resulted in a complex mixture (not shown) as well as the possible hydrolysis of the methyl ester. This will be further elaborated in the scope for the *E*-selective redox isomerization.

**Table 7.** DABCO-catalyzed redox isomerization: other electron withdrawing groups.

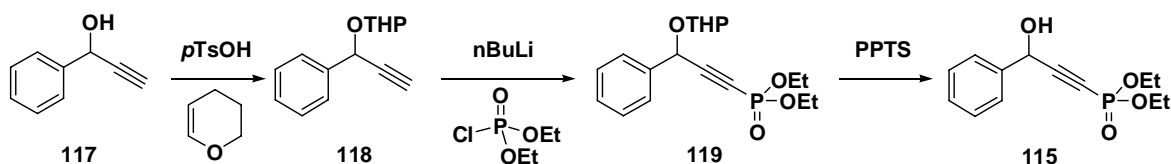
Entry	R	EWG	Temperature (°C)	Time (h)	% Yield	
1			<b>90</b>	23	4.0	<b>E110</b> - 72
2			<b>111</b>	23	22	<b>E112</b> - 76 <sup>a</sup>
3			<b>113</b>	23	25	<b>E114</b> - no reaction
4			<b>115</b>	40	30	<b>116</b> - 95 <b>E:Z</b> = 10:1

a: 20 mol% of NaOAc is also added.

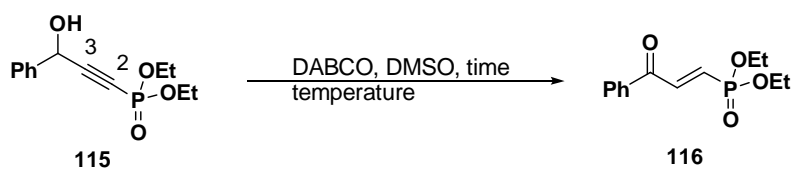
**Different Electron Withdrawing Groups:** Using the ethyl ester **90** in the DABCO-catalyzed redox isomerization resulted in the formation of the desired alkenoate in 72 % yield in 4.0 h (Table 7, Entry 1). This demonstrated that the redox isomerization was amenable to different ester functionalities. While the reaction with the different ester group proceeded smoothly, using an amide in place of the ester presented its own challenges. When the amide derivative **111** (Entry 2) was subjected to the DABCO-catalyzed redox isomerization conditions, the reaction did not yield the desired alkenoate (not shown). This was most likely due to 4-H in

**111** was not as acidic as 4-H in **42**. Since amides are relatively inert, a stronger base should not react with the amide moiety. Therefore, **111** was treated with 20 mol% of NaOAc and 20 mol% of DABCO (Entry 2), and the reaction yielded the desired *E*-alkene-amide in 76 % yield after 23 h. We hypothesized (and later will be shown) that NaOAc deprotonated 4-H to yield an *E:Z* mixture of **112** and this mixture was isomerized by DABCO to yield the *E112* as the sole product. Although alkynoates were converted to alkenoates by other groups, this was the first time that an amide functionality was transformed by a base-catalyzed redox isomerization.

Despite the difficulties with the amide, the phosphonate derivative presented challenges of its own. Treatment of the alkylphosphonate **113** (Entry 3) to the DABCO-catalyzed redox isomerization conditions resulted in the isolation of the starting material. This failure could be because the 4-H is not benzylic. Used in [2+2], [3+2] and [4+2] cycloaddition reactions,<sup>43</sup> a phenyl phosphonate derivative **115** (Entry 4) was prepared in three steps (Scheme 40). This phosphonate was then subjected to the DABCO-catalyzed redox isomerization conditions and slowly gave a 4:1 *E:Z* mixture of **116** with 36 % overall yield. In an attempt to decrease the reaction time and increase yield and selectivity, the amount of base was increased to 40 mol% (Table 8, Entry 2). However, this reaction gave a 5.7:1 *E:Z* mixture with a 50 % overall yield. Gratifyingly, simply heating the DABCO-catalyzed redox isomerization to 40 °C (Entry 3) increased the reaction rate, the *E:Z* selectivity (10:1) and dramatically increased the yield (95 %). Analogous to the amide, this was also the first time that a phosphonate functionality was used in a base catalyzed redox isomerization.

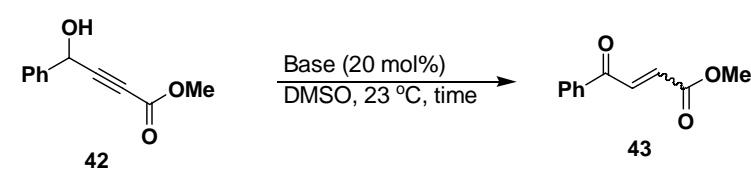


**Scheme 40.** Preparation of phosphonate **115**.

**Table 8.** Phosponate 115 optimization.


Entry	DABCO (mol %)	Temperature (°C)	Time (h)	% Yield	<i>E:Z</i>
1	20	23	49	36	4:1
2	40	23	81	50	5.7:1
3	20	40	30	95	10:1

**E-Selective Redox Isomerization: Different Bases:** Finally, from the results with the amide, we hypothesized that a combination of NaOAc, and DABCO could provide a more expedient *E*-selective redox isomerization. Using the redox isomerization conditions for the amide **111** on alkyne **42**, alkenoate **E43** was formed after 0.8 h with a 62 % yield, (Table 9, Entry 1) which was lower yielding than DABCO alone (Entry 2). To confirm that DABCO is necessary, a control reaction with only NaOAc yielded a 1:2.4 mixture of *E:Z* alkenoates in 0.5 h (Entry 3). Since the reaction gave a poor *E* selectivity, it was not synthetically useful and the alkenoates were not isolated. To conclude, DABCO or a combination of NaOAc and DABCO can catalyze an *E*-selective redox isomerization.

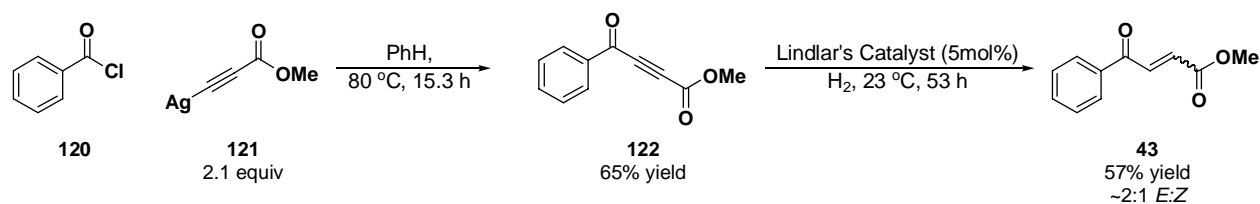
**Table 9.** *E*-selective redox isomerization: base conditions revisited.


Entry	Base	Time (h)	% Yield	<i>E:Z</i>
1	DABCO/NaOAc	0.8	62	30 : 1
2	DABCO	7.0	70	33 : 1
3	NaOAc	0.5	n.d.	1 : 2.4

## 2.3 Z-SELECTIVE REDOX ISOMERIZATION

### 2.3.1 Reaction Optimization and Mechanistic Studies

Originally we thought that the *Z*-alkenoate could be convergently prepared in two steps (Scheme 41). The first step involves silver acetylide **121** coupling with PhCOCl **120**; the subsequent partial reduction using Lindlar's catalyst gave a 2:1 mixture of *E* and *Z*-alkenoates **122** as in 57 % yield. This poor selectivity may be due to the instability of the **Z43** toward the partial reduction conditions.



**Scheme 41.** Failed semi hydrogenation to yield **Z43**.

**Z-Selective Redox Isomerization Conditions Found**: This failure prompted us to investigate the redox isomerization using *i*Pr<sub>2</sub>NEt since our previous results gave a higher *Z*-selectivity (Table 2, Entries 5 and 10). Rather than varying reaction conditions, we decided to investigate the *i*Pr<sub>2</sub>NEt-catalyzed redox isomerization mechanism using a D<sub>2</sub>O incorporation experiment by determining the location of D in **Z43**. To assign D, an HMBC experiment of alkenoate **Z43** was conducted. From the experiment a coupling between the methyl protons and 2-C was observed (Figure 10), allowing for assigning the chemical shifts of 2-H and 3-H as 6.30 and 6.92 ppm, respectively.

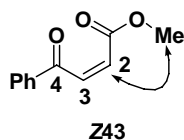


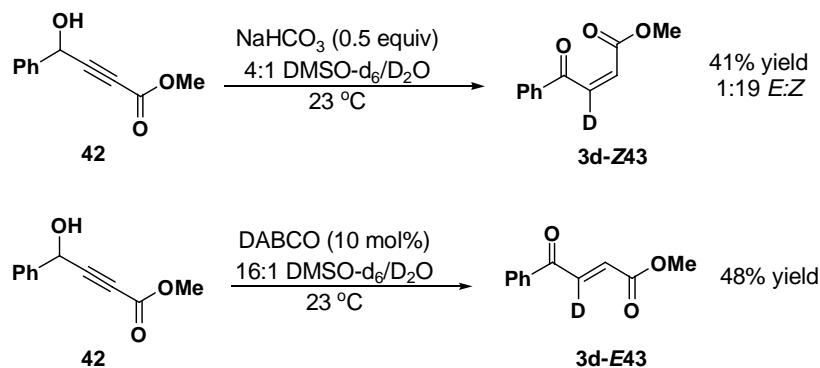
**Figure 10.** Key HMBC coupling for **Z43**.

Treatment of alkynoate **42** with 10 mol% *i*Pr<sub>2</sub>NEt in DMSO gave 1:1.6 *E*:*Z*-selectivity (Table 10, Entry 1). However using a 2:1 ratio of DMSO-*d*<sub>6</sub>/D<sub>2</sub>O yielded alkenoate **3d-Z43** (see

Scheme 36) in 50 % yield with a 1:19 *E*:*Z*-selectivity (Entry 2). This demonstrated that a *Z*-selective redox isomerization was feasible. The placement of the deuterium occurred on 3-C which indicated that the *Z*-selective redox isomerization (Scheme 42) proceeded via the same mechanism as the *E*-selective DABCO-catalyzed redox isomerization. To make certain that this result was not unique to the deuterium isotope, the reaction was repeated using the deuterium-free solvent (Entry 3). The reaction yielded exclusively alkenoate **Z43** without any detectable *E*-alkenoate in a 22 % yield. To increase the yield, treatment of alkynoate **42** with 10 mol% of *i*Pr<sub>2</sub>NEt in 4:1 ratio of DMSO/water (Entry 4) resulted in a 1:10 *E*:*Z* mixture with a 47 % yield. From these experiments, it appeared the *i*Pr<sub>2</sub>NEt-catalyzed redox isomerization can only give either high yield or high *Z*-selectivity.

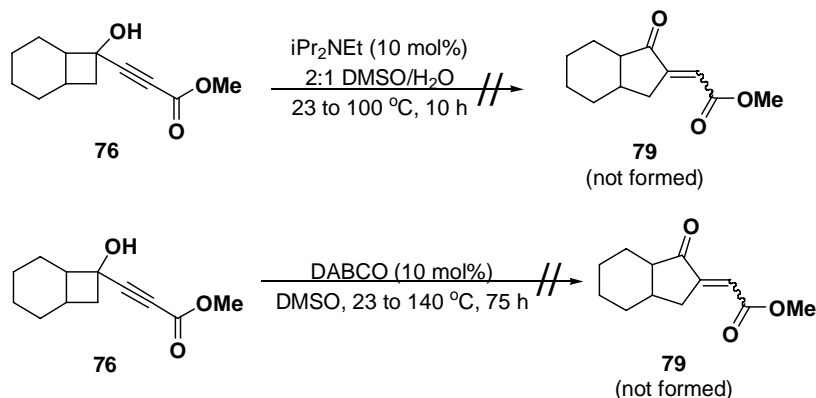
**Table 10.** *Z*-selective redox isomerization found.

Entry	Solvent	Time (h)	% Yield	<i>E</i> : <i>Z</i>
1	DMSO	16	79 % conversion	1 : 1.6
2	2:1 DMSO-d <sub>6</sub> /D <sub>2</sub> O	95	50	1 : 19
3	2:1 DMSO/H <sub>2</sub> O	104	22	no detectable <i>E</i>
4	4:1 DMSO/H <sub>2</sub> O	52	47	1 : 10



**Scheme 42.** D<sub>2</sub>O incorporation experiments using *i*Pr<sub>2</sub>NEt and DABCO.





**Scheme 45.** DABCO and  $\text{iPr}_2\text{NEt}$  yielding same results with bicyclic alkyne **76**.

**Proton Source Studies:** We hypothesized that a stronger proton source than water could increase the reaction polarity and stabilize any charged intermediates leading to a shorter reaction time. The original conditions of 4:1 DMSO/water (Table 11, Entry 1) gave a 47 % yield with an *E:Z*-selectivity of 1:10. Increasing the acidity, by using 5 mol% of HCl (Entry 2), resulted in a 35 % overall yield with a 1:1.2 *E:Z*-selectivity indicating that a low pH was detrimental. Using AcOH instead of water gave a 71 % overall yield and an *E:Z*-selectivity of 3:1 (Entry 3). Finally, using  $\text{CF}_3\text{CH}_2\text{OH}$  instead of water gave a 78 % overall yield with a 1:3.3 *E:Z*-selectivity (Entry 4). To conclude, water was the best co-solvent for the  $\text{iPr}_2\text{NEt}$ -catalyzed redox isomerization.

**Table 11.**  $\text{iPr}_2\text{NEt}$ -catalyzed redox isomerization: proton source studies.

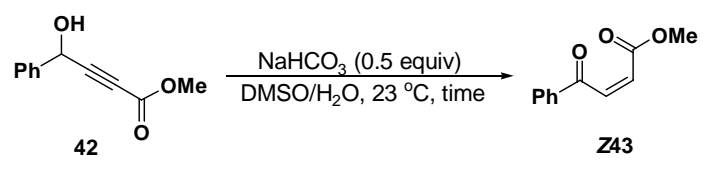
Entry	Proton Source	Quantity	Time (d)	% Yield	<i>E:Z</i>
1	$\text{H}_2\text{O}$	22 equiv	2.0	47	1 : 10
2	HCl in $\text{H}_2\text{O}$	5 mol%	2.0	35	1 : 1.2
3	AcOH	7.0 equiv	3.3	71	3 : 1
4	$\text{CF}_3\text{CH}_2\text{OH}$	5.5 equiv	5.0	78	1 : 3.3

**Base Studies:** Treatment of alkynoate **42** with 10 mol% of Et<sub>3</sub>N using a 4:1 DMSO/water ratio gave a 1:1.2 *E:Z*-selectivity (Table 12, Entry 1). The products were not isolated because of >46 h reaction time in which the long reaction time might be from an insolubility of Et<sub>3</sub>N. Also, the different DMSO/water ratio had no appreciable effect on *E:Z*-selectivity. However, more soluble N(CH<sub>2</sub>CH<sub>2</sub>OH)<sub>3</sub> required >91 h and gave an *E:Z*-selectivity of 1:5.3 (Entry 2). Gratifyingly, treatment of alkynoate **42** with 50 mol% of NaHCO<sub>3</sub> (Entry 3) resulted in a 57 % yield of the desired *Z*-alkenoate after 21 h without any detectable *E*-alkenoate. Treatment of alkynoate **42** with 20 mol% of NaOAc in an 8:1 DMSO/water ratio yielded a 1:2.9 *E:Z*-mixture of alkenoates (Entry 4). Finally switching the base to Na<sub>2</sub>HPO<sub>4</sub> (Entry 5) gave the same *Z*-selectivity as NaHCO<sub>3</sub> but the reaction was not complete even after 51 h. Therefore, NaHCO<sub>3</sub> was the most promising base.

**Table 12.** *Z*-selective redox isomerization: base studies.

Entry	Base	Time (h)	% Yield	<i>E:Z</i>
1	Et <sub>3</sub> N	46	79 % conversion	1 : 1.2
2	N(CH <sub>2</sub> CH <sub>2</sub> OH) <sub>3</sub>	91	28 % conversion	1 : 5.3
3	NaHCO <sub>3</sub>	21	57	no detectable E
4	NaOAc	4.0	n.d.	1 : 2.9
5	Na <sub>2</sub> HPO <sub>4</sub>	51	n.d.	no detectable E

**Table 13.**  $i\text{Pr}_2\text{NEt}$ -catalyzed redox isomerization: DMSO/water ratio studies.

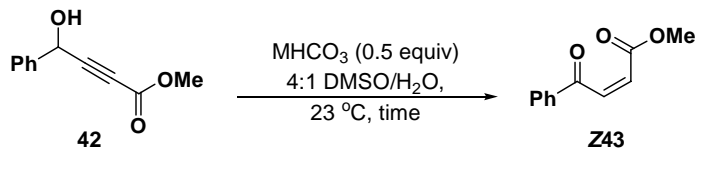


Reaction scheme showing the redox isomerization of compound **42** (a propargyl alcohol derivative) to compound **Z43** (a 2-phenyl-5-methoxy-2H-pyridin-3(1H)-one derivative) using  $\text{NaHCO}_3$  (0.5 equiv) in a DMSO/ $\text{H}_2\text{O}$  mixture at 23 °C for a certain time.

Entry	DMSO/ $\text{H}_2\text{O}$ ratio	Time (h)	% Yield	<i>E:Z</i>
1	1 : 1	28	13	no detectable <i>E</i>
2	2 : 1	29	17	no detectable <i>E</i>
3	4 : 1	21	57	no detectable <i>E</i>

**DMSO/Water Ratio Studies:** Although  $\text{NaHCO}_3$  gave better results than  $i\text{Pr}_2\text{NEt}$ , the conditions were far from optimized. Because  $\text{NaHCO}_3$  was not completely soluble in DMSO, DMSO/water ratios of 1:1 and 2:1 were pursued. Unlike  $i\text{Pr}_2\text{NEt}$ ,  $\text{NaHCO}_3$  showed no decrease in *Z*-selectivity when 1:1 and 2:1 DMSO/water ratios were used (Table 13, Entries 1, 2). However, using 1:1 and 2:1 DMSO/water ratios gave 13 % and 17 % yields respectively. One reason for the yield decrease is that the alkynoate was not entirely soluble in the decreased amount of DMSO leading to an incomplete reaction. Therefore, a desirable DMSO/water ratio was determined to be 4:1 (Entry 3).

**Table 14.**  $i\text{Pr}_2\text{NEt}$ -catalyzed redox isomerization: different metal cations.



Reaction scheme showing the redox isomerization of compound **42** (a propargyl alcohol derivative) to compound **Z43** (a 2-phenyl-5-methoxy-2H-pyridin-3(1H)-one derivative) using  $\text{MHCO}_3$  (0.5 equiv) in a 4:1 DMSO/ $\text{H}_2\text{O}$  mixture at 23 °C for a certain time.

Entry	Metal	Time (h)	% Yield	<i>E:Z</i>
1	Li (LiBr 60 mol%)	13	54	no detectable <i>E</i>
2	Na	21	57	no detectable <i>E</i>
3	Cs	24	28	1 : 6.5

**Metal Cation Studies:** Since NaHCO<sub>3</sub> was not entirely soluble, changing the metal cation to lithium might help with the solubility in DMSO. Although LiHCO<sub>3</sub> was not commercially available, it was generated by mixing NaHCO<sub>3</sub> and LiBr in which the lithium cation would form tighter ion pair with the carbonate anion than sodium. In effect, treatment of alkynoate **42** with 60 mol% of LiBr and 50 mol% of NaHCO<sub>3</sub> formed **Z43** after 13 h (Table 14, Entry 1) in 54 % yield similarly to NaHCO<sub>3</sub> alone (57 %, Entry 2). Unfortunately using the more organic solvent soluble CsHCO<sub>3</sub> (Entry 3) yielded a 1:6.5 *E:Z* mixture of alkenoates with a 28 % yield. From these experiments, the use of either NaHCO<sub>3</sub> or LiHCO<sub>3</sub> gave good results.

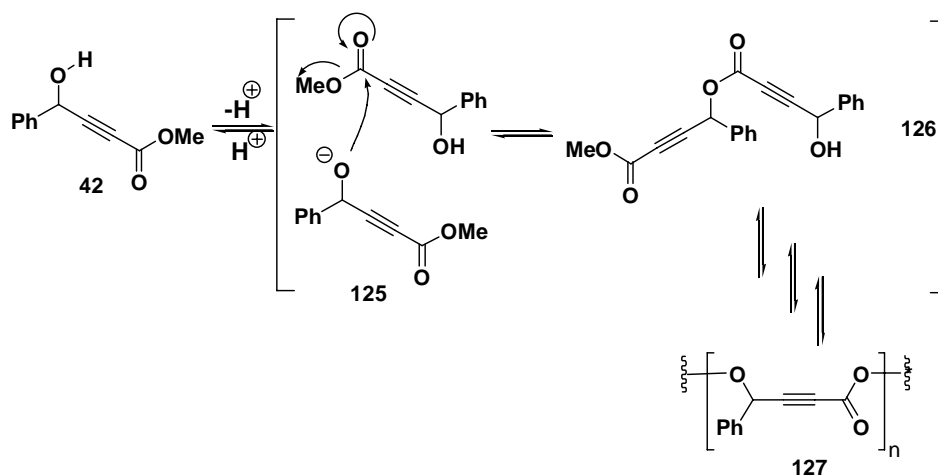
**Table 15.** iPr<sub>2</sub>NEt-catalyzed redox isomerization: different solvents.

Entry	X	Y	60 mol% LiBr	Time (h)	% Yield	<i>E:Z</i>
1	tBuOH	DMSO	yes	45	72	1 : 6
2	H <sub>2</sub> O	Et <sub>2</sub> O	no	28	n.d.	n.d.
3	H <sub>2</sub> O	acetone	no	120	n.d.	n.d.
4	H <sub>2</sub> O	DMSO	yes	13	54	no detectable <i>E</i>

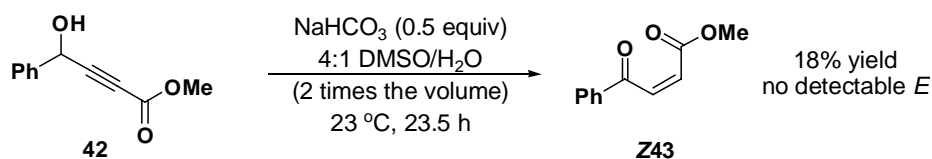
**Solvent Effect Studies:** Besides metal effects, solvent effects were studied. tBuOH might be able to stabilize a reaction intermediate to increase the yield. However, this hypothesis was not sound. Treatment of alkynoate **42** with 50 mol% of NaHCO<sub>3</sub> and 60 mol% of LiBr in 4:1 DMSO/tBuOH (Table 15, Entry 1) gave a 72 % yield but an *E:Z*-selectivity of 1:6. We hypothesized that the biphasic conditions (using Et<sub>2</sub>O instead of DMSO, Entry 3) would improve both the base and alkynoate solubilities. After one day of stirring, only alkynoate **42** was observed. Finally we hypothesized that acetone could be used to simplify reaction workup (Entry 4), but this reaction was not complete even after five days. We hypothesized that acetone's lower polarity was unable to stabilize a charged transition state. Therefore, the best

solvent conditions were obtained from using the original conditions of 4:1 DMSO/water (Entry 4).

**Polymerization Prevention:** During these reaction optimizations, a polymeric by-product was possibly produced. Although several attempts to characterize the polymer using  $^1\text{H}$  NMR were inconclusive, several polymerization mechanisms could be deduced. One such pathway could involve a deprotonation of the alkynoate's hydroxy group to give alkoxide **125** (Scheme 46). This alkoxide can attack a second alkynoate molecule to give transesterification product **126**. This could repeat for n-times to yield polymer **127**. For this polymerization to occur, the alkynoate molecules must be in close proximity to each other. Therefore, diluted the reaction mixture might reduce this side polymerization. However, treatment of alkynoate **42**, in which the initial concentration was diluted to 0.125 M instead of 0.25 M (Scheme 47) with  $\text{NaHCO}_3$  gave an 18 % yield.



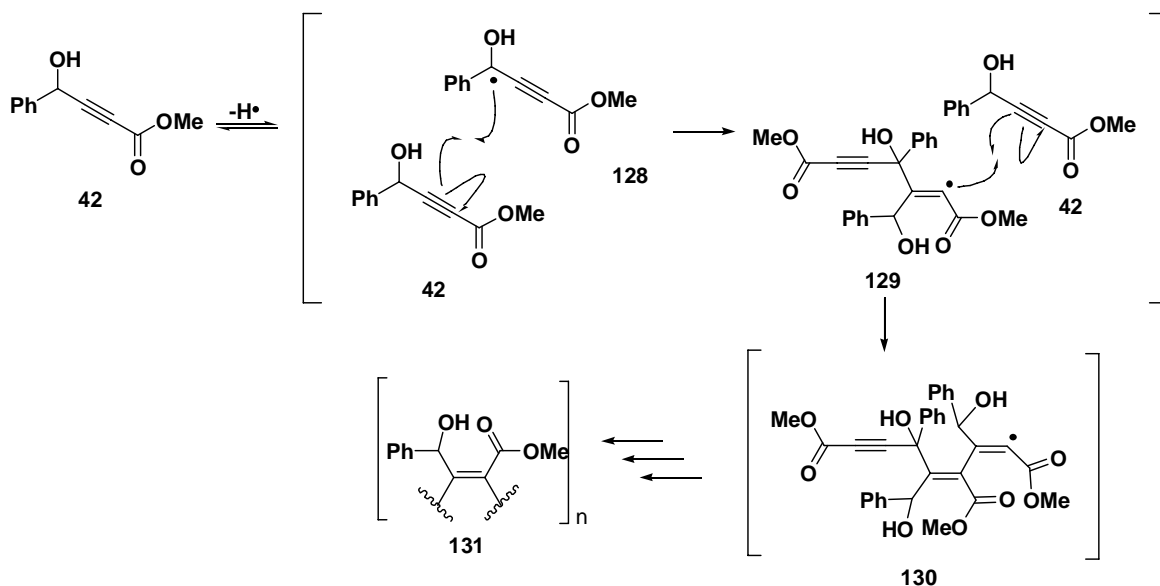
**Scheme 46.** One possible polymerization mechanism catalyzed by  $\text{NaHCO}_3$ .



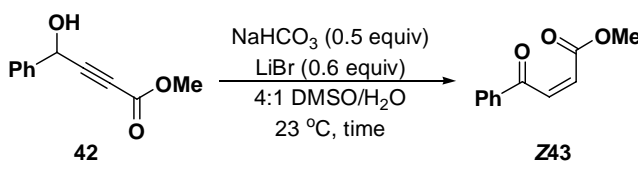
**Scheme 47.** Failed attempt to stop polymerization in  $\text{NaHCO}_3$ -catalyzed redox isomerization.

Since dilution did not prevent a possible side polymerization, the polymerization might proceed via a radical pathway (Scheme 48). Therefore, we deduced the use of a radical quencher such as hydroquinone should increase the yield. A 54 % yield was obtained (Table 16, Entry 1)

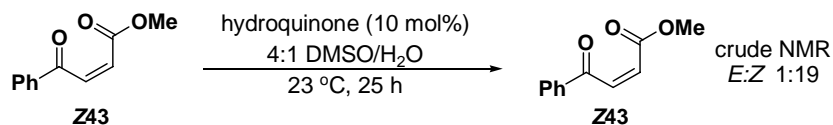
in hydroquinone's absence, while the addition of 0.1 mol% of hydroquinone (Entry 2) gave the Z-alkenoate in 64 %. The addition of 1.0 mol% hydroquinone to the LiHCO<sub>3</sub>-catalyzed redox isomerization (Entry 3) gave 63 % yield of the Z-alkenoate. Due to the similar yields between 0.1 mol% and 1.0 mol% experiments, we decided that 0.1 mol% is the effective amount of hydroquinone to minimize radical polymerization. Next two control experiments were conducted to confirm that hydroquinone does not affect the alkynoate or alkenoate. Treatment of alkynoate **42** with 10 mol% of hydroquinone in 4:1 DMSO/water ratio only exhibited starting material after 26 h (Entry 4). This demonstrated that hydroquinone did not catalyze redox isomerization and more importantly did not harm the alkynoate.



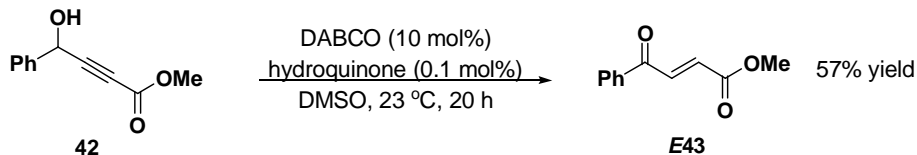
**Scheme 48.** NaHCO<sub>3</sub>-catalyzed redox isomerization: radical polymerization mechanism.

**Table 16.** NaHCO<sub>3</sub>-catalyzed redox isomerization: hydroquinone studies.

Entry	LiBr/NaHCO <sub>3</sub>	Hydroquinone	Time (h)	% Yield	<i>E:Z</i>
1	yes	no	13	54	no detectable <i>E</i>
2	yes	0.1 mol%	49	64	1 : 35
3	yes	1.0 mol%	23	63	1 :19
4	no	10 mol%	26	n.d.	n.d.

**Scheme 49.** Z43 stability with hydroquinone alone.

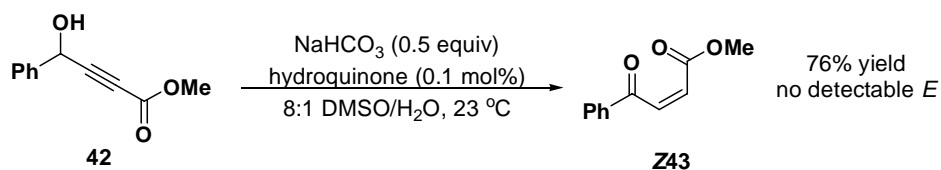
Since the hydroquinone was effective, it might be able to increase the yield of the DABCO-catalyzed redox isomerization. However, when 0.1 mol% hydroquinone was added to the DABCO isomerization (Scheme 50), a 57 % yield of *E*-alkenoate was obtained. This result suggested a radical polymerization did not decrease yield.

**Scheme 50.** DABCO-catalyzed redox isomerization: hydroquinone experiment.

**DMSO/Water Ratios:** Finally, we varied the DMSO/water ratio to improve the yield. In the 2:1 DMSO/water ratio (Table 17, Entry 1) the starting material was insoluble, while a 4:1 ratio (Entry 2) gave 65% yield of the *Z*-alkenoate. Using an 8:1 DMSO/water (Entry 3) yielded the *Z*-alkenoate in 76 % yield while using a 16:1 DMSO/water ratio (Entry 4) gave a 62 % yield of the *Z*-alkenoate,. Therefore, the best DMSO/water ratio for the NaHCO<sub>3</sub>-catalyzed redox isomerization was 8:1

**Table 17.** NaHCO<sub>3</sub>-catalyzed redox isomerization: DMSO/water ratios revisited.

Entry	DMSO/H <sub>2</sub> O ratio	Time (h)	% Yield	<i>E</i> : <i>Z</i>
1	2 : 1	22	n.d.	n.d.
2	4 : 1	23	65	no detectable <i>E</i>
3	8 : 1	25	76	no detectable <i>E</i>
4	16 : 1	23	62	no detectable <i>E</i>



**Scheme 51.** *Z*-selective redox isomerization is optimized.

From these final DMSO/water ratio studies, the NaHCO<sub>3</sub>-catalyzed redox isomerization was optimized (Scheme 51). Even though the reaction conditions were optimized, the redox isomerization mechanism was still unknown. In order to obtain insight to the kinetics, alkynoate **42** was treated with 50 mol% of NaHCO<sub>3</sub> in a 4:1 DMSO-d<sub>6</sub>/D<sub>2</sub>O ratio and the reaction was monitored using <sup>1</sup>H NMR. From the experiment, we found the NaHCO<sub>3</sub>-catalyzed redox isomerization was second order overall (Figure 11). Also the *E*:*Z* selectivity for this reaction was 1:19.

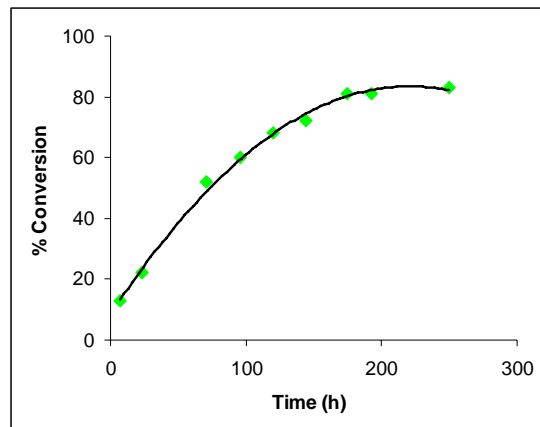
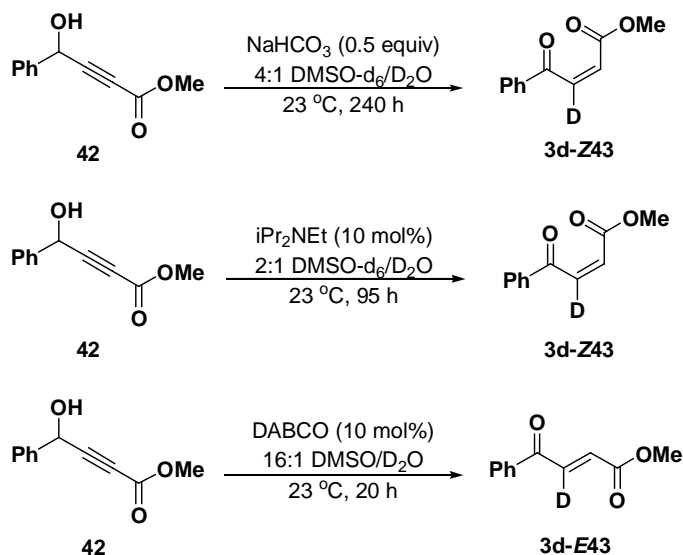


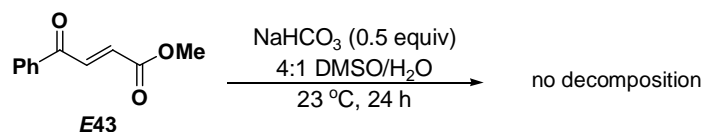
**Figure 11.** NaHCO<sub>3</sub>-catalyzed redox isomerization is second order overall.



**Scheme 52.** D<sub>2</sub>O incorporation experiments using DABCO, iPr<sub>2</sub>NEt, and NaHCO<sub>3</sub>.

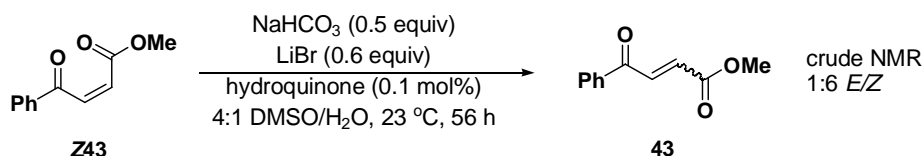
In addition to determining the reaction order, <sup>1</sup>H NMR analysis determined that a deuterium incorporation occurred at the 3-position. This result suggested that the NaHCO<sub>3</sub>-catalyzed redox isomerization (Scheme 52) proceeded by the same mechanism as the iPr<sub>2</sub>NEt-catalyzed redox isomerization and similarly to the DABCO-catalyzed redox isomerization.

**E:Z Isomerization:** Another aspect we examined was the product stability toward the reaction conditions. NaHCO<sub>3</sub>-catalyzed redox isomerization's high Z-selectivity might be due to the decomposition of the *E*-alkenoate by NaHCO<sub>3</sub>. Treatment of alkenoate **E43** with 50 mol% of NaHCO<sub>3</sub> in a 4:1 mixture of DMSO/H<sub>2</sub>O (Scheme 53) resulted in isolation of **E43** after 24 h. This experiment demonstrated that this reaction did not destroy the *E*-alkenoate.

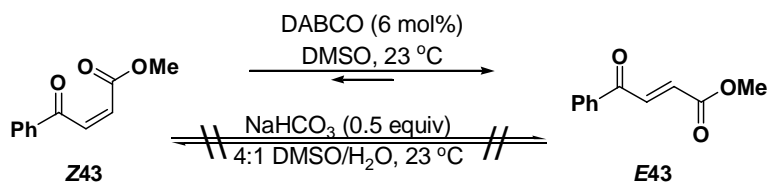


**Scheme 53.** NaHCO<sub>3</sub>-catalyzed redox isomerization: *E*-alkenoate stability experiment.

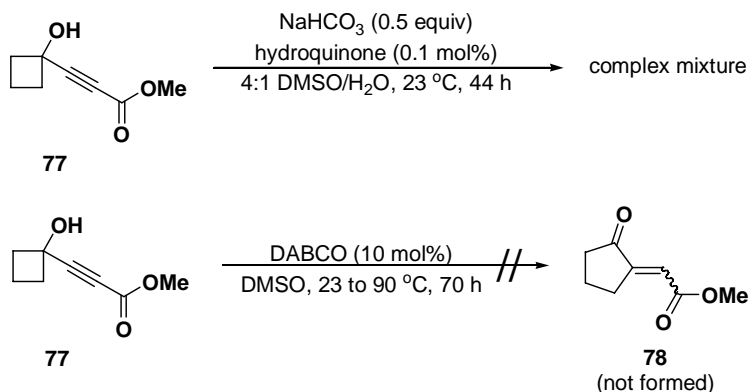
Alkenoate **Z43** was tested for stability. Treatment of alkenoate **Z43** with 0.1 mol% of hydroquinone, 60 mol% of LiBr, and 50 mol% of NaHCO<sub>3</sub> in 4:1 mixture of DMSO/H<sub>2</sub>O (Scheme 54) gave an *E*:*Z*-selectivity of 1:6 after 56 h. Typically, the NaHCO<sub>3</sub>-catalyzed redox isomerization was complete after 24 h. Therefore, the NaHCO<sub>3</sub>-catalyzed redox isomerization was faster than the *Z* to *E* alkenoate isomerization. Thus, this *Z*-to-*E*-alkenoate isomerization did not occur in an appreciable manner during the redox isomerization, which explains why the NaHCO<sub>3</sub> catalyzed reaction was *Z*-selective. To summarize the isomerization studies, DABCO favored the formation of predominately the *E*-alkenoate (Scheme 55), while NaHCO<sub>3</sub> did not cause any appreciable *Z* to *E* or *E* to *Z* isomerization.



**Scheme 54.** NaHCO<sub>3</sub>-catalyzed redox isomerization: slow *Z*-to-*E* isomerization.



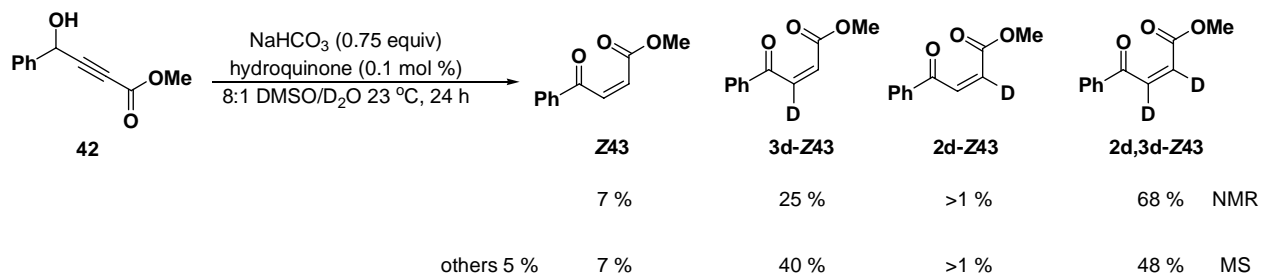
**Scheme 55.** *E*:*Z* isomerization selectivity for DABCO and NaHCO<sub>3</sub> reactions.



**Scheme 56.** Cyclobutyl alkynoate **77** giving different results for DABCO and NaHCO<sub>3</sub>.

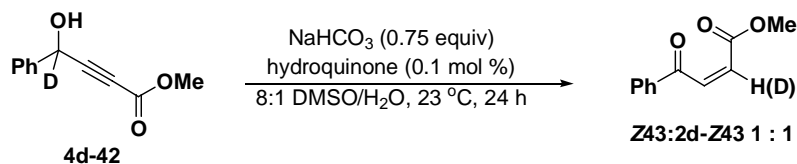
Although these isomerization and kinetic studies helped elucidate a mechanism, their results were not conclusive. Therefore alkynoate **77**, which can allude to mechanism B or C, was treated with 50 mol% of NaHCO<sub>3</sub>, 0.1 mol% of hydroquinone in a 4:1 DMSO/water mixture (Scheme 56) yielded a complex mixture without any sign of the desired product. This was different than the DABCO-catalyzed redox isomerization where the alkynoate was inert to the reaction conditions (Scheme 56). Although the NaHCO<sub>3</sub> reaction did not yield any of the desired substrate, no mechanism could be deduced from these studies.

**Deuterium Studies:** We then deduced that a deuterium incorporation experiment with D<sub>2</sub>O would present more concrete results. However, repeating the D<sub>2</sub>O experiment with the optimized NaHCO<sub>3</sub> redox isomerization conditions (Scheme 57) yielded many products. The 7 % of the non-deuterated product (7 % by MS) was reasonable. The formation of the **3d-Z43** alkenoate (25 % by NMR or 40 % by MS) and the lack of formation of alkenoate **2d-Z43** alluded to mechanism A. However, the formation of **2d,3d-Z43** (68 % by NMR or 48 % by MS) was reasonable. We hypothesized that this product was a result from NaHCO<sub>3</sub> participating in a proton exchange with D<sub>2</sub>O. These results merited a final examination of the mechanism.

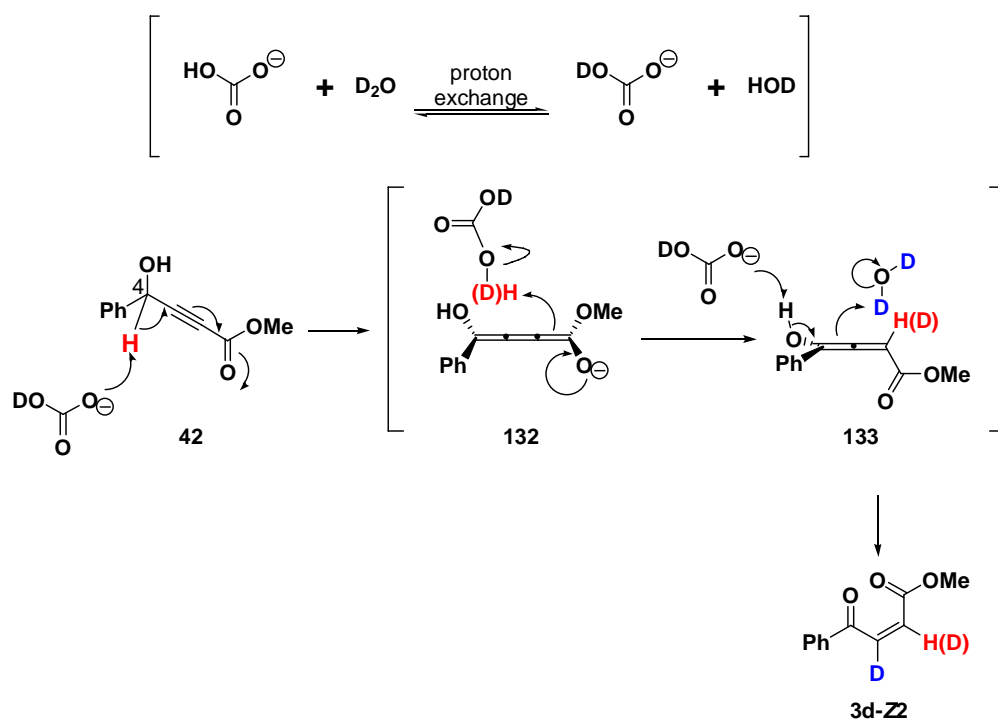


**Scheme 57.** NaHCO<sub>3</sub>-catalyzed redox isomerization: D<sub>2</sub>O incorporation experiment.

To determine the most plausible mechanism the deuterium-enriched alkynoate **4d-42** was subjected to the optimized NaHCO<sub>3</sub>-catalyzed redox isomerization conditions (Scheme 58). Upon the isolation of the product, a 50 % incorporation of deuterium was found only on the 2-C position which was consistent with mechanism A. Also, the 50 % deuterium enrichment at 2-C was consistent with a proton exchange between the base and water.



**Scheme 58.** NaHCO<sub>3</sub>-catalyzed redox isomerization: deuterium isotope effect.



**Scheme 59.** Mechanism for NaHCO<sub>3</sub>-catalyzed redox isomerization.

Therefore, the most plausible mechanism is a modification of methine deprotonation mechanism. NaHCO<sub>3</sub> deprotonates at the 4-H, and the resulting cumulenolate **132** (Scheme 59) abstracts a proton from the more acidic carbonic acid rather than water (pK<sub>a</sub> in DMSO = 32) in the reaction system to give allenol **133**. This allenol tautomerizes with D<sub>2</sub>O adding on the less

hindered side<sup>42</sup> to give alkenoate **3d-Z43**. Finally, during this reaction, the NaHCO<sub>3</sub> could undergo a proton exchange with water or D<sub>2</sub>O to yield a less or more deuterium enriched compound at 2-C respectively.

### 2.3.2 Reaction Scope of NaHCO<sub>3</sub>-Catalyzed Redox Isomerization

**Table 18.** NaHCO<sub>3</sub> isomerization: aromatic and vinylogous substrates.

Entry	R	Time (h)	% Yield
1		18	<b>Z92</b> - 58
2		3.0	<b>Z94</b> - 50
3		54	<b>Z96</b> - 50% conversion
4		38	<b>Z98</b> - 22
5		5.8 <sup>a</sup> 8.0 <sup>b</sup>	<b>100</b> - 1 : 1.67 <i>E:Z</i> <sup>a</sup> <b>Z100</b> - 57 <sup>b</sup>
6		8.0	<b>Z102</b> - 53
7		22	<b>Z104</b> - 52

<sup>a</sup>standard conditions

<sup>b</sup>with 0.9 equivalents of LiBr

**Aromatic and Vinylogous Substrates:** Upon the optimization (0.5 mol% of NaHCO<sub>3</sub>, 0.1 mol% hydroquinone, in an 8:1 DMSO water mixture with initial alkynoate concentration of 0.2 M) of the NaHCO<sub>3</sub> catalyzed redox isomerization, the scope of the reaction was explored. Compared to the DABCO-catalyzed redox isomerization, the yields for NaHCO<sub>3</sub>-catalyzed redox isomerization were lower but this is the first time *Z*-alkenoate was prepared from the alkynoate. In agreement with the mechanism, the electron rich *p*-methoxyphenyl derivative **91** had a slower reaction time (Table 18, Entry 1) of 18 h than alkynoate **42** and gave 58 % yield. Likewise the electron withdrawing *p*-trifluoromethylphenyl derivative **93** (Entry 2) reacted in 3.0 h with a 50 % yield. Interestingly *o*-substituted aromatic derivatives were poorly amenable to the *Z*-selective redox isomerization conditions. The *o*-bromophenyl derivative **95** only showed a 50 % conversion (Entry 3) after 54 h presumably due to the bulkiness the bromine atom that interfered with the methine deprotonation. Even with a smaller substituent in the *o*-position (fluorine) **97** (Entry 4), the *Z*-selective redox isomerization still only yielded **Z98** in a 22 % yield after 38 h. Another interesting anomaly was the furanyl derivative **99** (Entry 5) in which the standard conditions, gave a 1:1.7 *E:Z* mixture of the alkenoate after 5.8 h. The addition of 90 mol% of LiBr to standard conditions yielded the desired *Z*-alkenoate in a 57 % yield after 8.0 h showing that the *Z*-selective redox isomerization was amenable to heteroaromatics. The styrenyl derivative **101** (Entry 6) yielded the corresponding *Z*-alkenoate in 53 % yield after 8.0 h. Finally, unlike the DABCO-catalyzed redox isomerization, the NaHCO<sub>3</sub>-catalyzed redox isomerization was able to convert the hexenyl derivative **103** (Entry 7) to the **Z104** in a 52 % yield showing that the NaHCO<sub>3</sub>-catalyzed redox isomerization was amenable to vinylogous substrates.

**Aliphatic Substrates:** Although the aromatic and vinylogous substrates gave reasonable yields, the aliphatic alkynoates did not proceed desirably. Treatment of the hexyl derivative **107** (Table 19, Entry 1) with the standard conditions resulted in the formation of a complex mixture. During the monitoring of the reaction using TLC, the desired *Z*-alkenoate appeared to form but with large quantities of by-products. At the end of the reaction, there was no sign of the *Z*-alkenoate. During the reaction, the *Z*-alkenoate was formed and underwent further reactions such as an aldol or Dieckmann condensation. This also seemed likely for the cyclohexyl derivative **108** (Entry 2), which also yielded a complex mixture after 44 h. These results were the reason stronger bases were not pursued for the *E*-selective redox isomerization. However, the epoxide

derivative **109** (Entry 3) appeared to be inert to the reaction conditions and only gave a thermal decomposition when heated to 80 °C for 26 h.

**Table 19.** NaHCO<sub>3</sub> isomerization: aliphatic substrates.

Entry	R	Temperature (°C)	Time (h)	% Yield
1	n-Hex <b>107</b>	23	75	complex mixture
2	 <b>108</b>	23	44	complex mixture
3	 <b>109</b>	23 to 80	26	decomposition

**Table 20.** NaHCO<sub>3</sub> isomerization: other electron withdrawing groups.

Entry	R	EWG	Time (h)	% Yield
1		 <b>90</b>	7.3	55
2		 <b>113</b>	23.5	no reaction

**Different Electron Withdrawing Groups:** Another way to test the scope of the NaHCO<sub>3</sub> catalyzed redox isomerization was to vary the electron withdrawing group at the 1-position. Using the ethyl ester **90** in the NaHCO<sub>3</sub>-catalyzed redox isomerization (Table 20, Entry 1), resulted in the formation of the desired alkenoate in 55 % yield after 7.3 h. This demonstrated that the redox isomerization was amenable to different ester functionalities. However,

phosphonate **113** was inert to the NaHCO<sub>3</sub>-catalyzed redox isomerization (Entry 2) resulting in the recovery of the starting alkyne phosphonate. This was not completely surprising because 4-H was not sufficiently acidic.

Treatment of the phosphonate **115** with the standard *Z*-selective redox isomerization conditions (Table 21, Entry 1) resulted in a 45 % yield of 2:1 mixture of *E*:*Z*-alkene phosphonates. In an attempt to increase *Z*-selectivity, different metal cations were used as based on the optimization reactions (see Table 14). However, using different metals such as Li (Entry 2), K (Entry 3) and Cs (Entry 4) only increased the *E*-selectivity (*E*:*Z* = approximately >1:99 for Li, 4:1 for K, 10:1 for Cs respectively). Although the *Z*-selectivity could not be increased, using cesium bicarbonate (CsHCO<sub>3</sub>) at 40 °C (Entry 5) resulted in an excellent *E*-selectivity which could be used as an alternate way to prepare **E116**.

**Table 21.** NaHCO<sub>3</sub> isomerization: phosphonate studies.

Entry	Metal	Temperature (°C)	Time (h)	% Yield	<i>E</i> : <i>Z</i>
1	Na	23	52	45	2 : 1
2	Li (0.90 equiv LiBr)	23	52	50% conversion	no detectable <i>Z</i>
3	K	23	50	n.d.	4:1
4	Cs	23	29	n.d.	10:1
5	Cs	40	23.5	38	no detectable <i>Z</i>

Treatment of the alkyne amide derivative **111** with the standard redox isomerization condition resulted in the isolation of the starting material. Since the amide is not as electron withdrawing as the ester, a stronger base, Na<sub>2</sub>CO<sub>3</sub>, was added to the reaction mixture (Table 22, Entry 1). However, this again resulted in isolation of the starting material after 24 h. Repeating the experiment with only Na<sub>2</sub>CO<sub>3</sub> (Entry 2) showed that Na<sub>2</sub>CO<sub>3</sub> was mostly insoluble even after

28 h, leading to no apparent reaction. Since the amide was less likely to undergo a hydrolysis, NaOH was used (Entry 3) but it did not lead to **112**. Finally, using NaOAc (Entry 4) caused the reaction to proceed extremely slowly with at least half the starting material remaining after 74 h. This final result may appear odd for the combination of NaOAc and DABCO was used to prepare the *E*-alkene amide. However, one explanation for the *E*-alkene amide formation was that the NaOAc and DABCO acted in a synergistic manner, in which NaOAc might not deprotonate 4-H as originally perceived. Instead, NaOAc might keep the DABCO doubly-deprotonated which increased DABCO's basicity leading to 4-H's deprotonation.

**Table 22.** NaHCO<sub>3</sub> isomerization: amide studies.

Entry	Base	Mol%	Time (h)	Result
1	NaHCO <sub>3</sub> /Na <sub>2</sub> CO <sub>3</sub>	50 / 50	23.5	no reaction
2	Na <sub>2</sub> CO <sub>3</sub>	75	28	base is mostly insoluble
3	NaOH	20	4.3	complex mixture
4	NaOAc	saturated solution	72	25 % conversion?

## 2.4 SYNTHETIC APPLICATIONS OF $\gamma$ -OXO- $\alpha,\beta$ -ALKENOATES

Not only *E* or *Z*-alkenoates are biologically active molecules, but also they can be useful synthetic intermediates. We envisioned that syn- $\beta$ -hydroxy esters, which can be found explicitly in natural products such as yohimbine<sup>44,45</sup> or found as a masked benzoyl functionality as in cocaine,<sup>46</sup> could be prepared from either the *E* or *Z*-alkenoates. For example, **136** could undergo a cycloaddition with **137**(Scheme 60) to give cyclic moiety **138**. This cyclic moiety reacts with

an oxidant to undergo a Baeyer-Villiger oxidation where the aliphatic cyclic moiety would migrate instead of the phenyl ring<sup>47-49</sup> to give **139**.

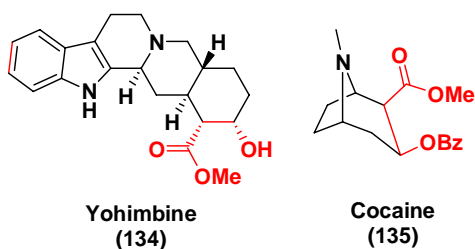
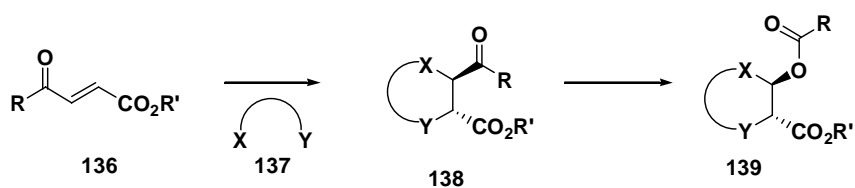
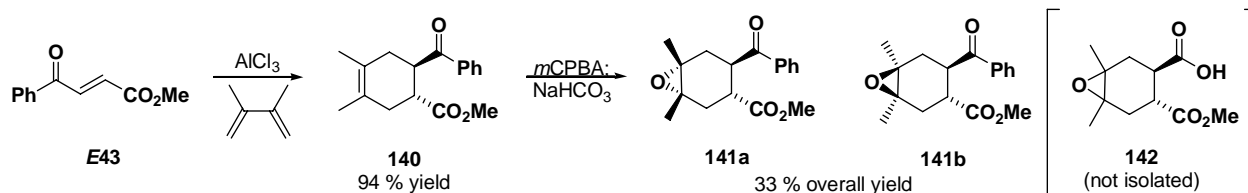


**Figure 12.** Natural products containing syn- $\beta$ -hydroxy esters.



**Scheme 60.** Preparation of syn- $\beta$ -hydroxy ester precursor.

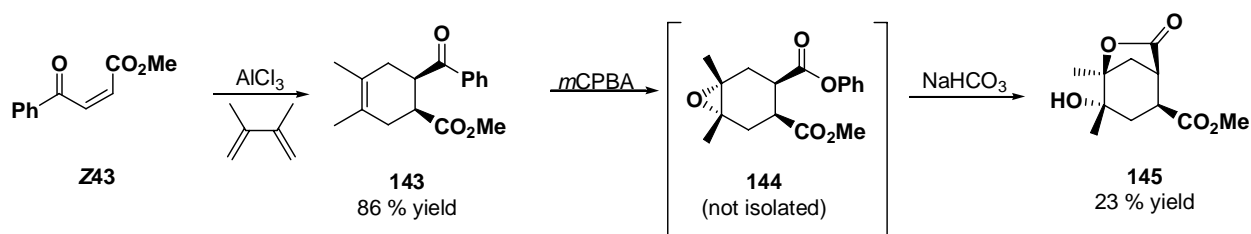
The Diels-Alder reaction of **E43** and 2,3-dimethyl-1,3-butadiene (Scheme 61) gave the desired product **140** as one diastereomer in 94 % yield. Since the ketone and ester functionality are distant from the olefin, the subsequent Baeyer-Villiger oxidation and epoxidation gave a 1:1 mixture of diastereomers **141a** and **141b** with an overall yield of 33 % as the epoxidized product only. The lower yield was from the phenyl migration product in the Baeyer-Villiger oxidation, in which the phenyl ester was converted to the acid **142** by hydrolysis conditions. This reaction favored the phenyl migration and other conditions will be sought to facilitate the cyclohexyl migration.



**Scheme 61.** Formation of cyclohexyl esters from the *E*-alkenoates.

The Diels-Alder reaction of **Z43** and 2,3-dimethyl-1,3-butadiene (Scheme 62) gave the desired product **143** as one diastereomer in 86 % yield. This time the ketone and ester

functionalities were syn to each other, which should invoke a diastereoselective epoxidation when treated with *m*CPBA. Although treatment of **143** gave one epoxidized product, the Baeyer-Villiger gave the phenyl migration product **144** instead of the desired cyclohexyl migration product. Upon hydrolysis with NaHCO<sub>3</sub>, the carboxylate opened the epoxide ring to yield the  $\gamma$ -lactone **145** as a single diastereomer in 23 % yield. The loss of yield was due to the incomplete lactonization where the free carboxylate anion that was lost during aqueous workup. Although the desired cyclohexanol could not be formed, the  $\gamma$ -lactone was a skeletally diverse structure that could be used in future work.

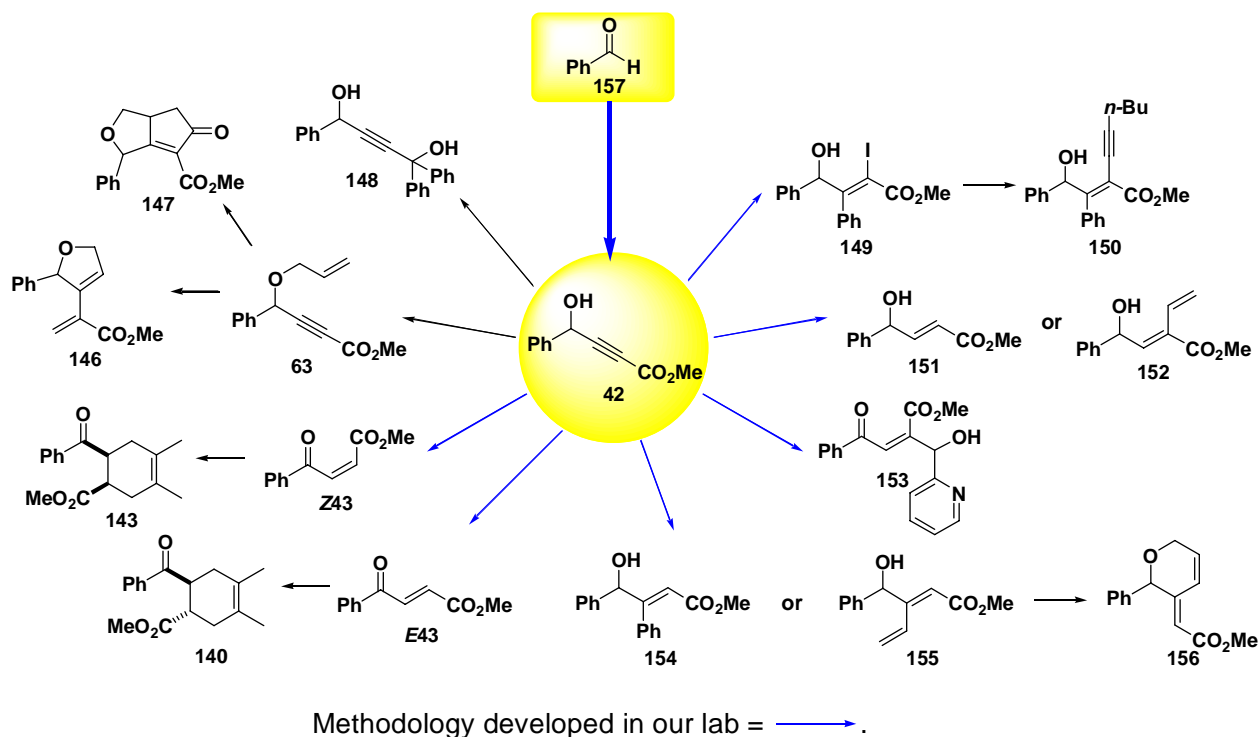


**Scheme 62.** Formation of  $\gamma$ -lactone from *Z*-alkenoates.

## 2.5 BIOLOGICAL STUDIES OF LIBRARY COMPOUNDS IN ZEBRAFISH EMBRYOS

A second objective of my research was to build a library<sup>50</sup> containing molecules that have a carbon skeletons that were easily diversified with minimal transformations. Although an easily-diversifiable substrate may sound common, only a few of these molecules have been demonstrated.<sup>51-53</sup> In our lab, we previously developed chemistry to convert  $\gamma$ -hydroxy- $\alpha,\beta$ -alkynoates to skeletally diverse structures in one or two steps (Scheme 63). The majority of the library members contain an unsaturated ester system which should invoke some reactivity in a biological system.<sup>20</sup> Also, their skeletal differences should affect different phenotypes in cells or organisms. After their preparation, these molecules, with the exception of **63**, **142**, and **145**,

were then tested in zebrafish embryos by Professor Nathan Bahary at the University of Pittsburgh.



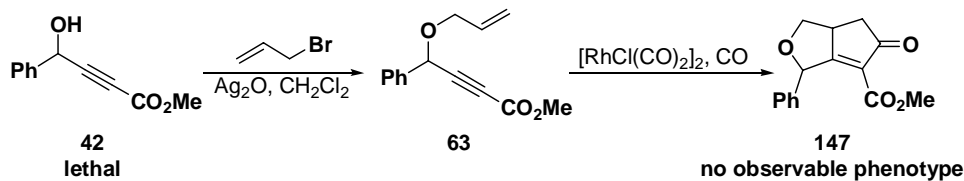
Alkynylation: Shahi, S. P.; Koide, K. *Angew. Chem. Int. Ed.*, **2004**, 43,2525-2527.  
Red-Al Reduction: Meta, C. T.; Koide, K. *Org Lett.* **2004**, 6, 1785-1787.

**Scheme 63.** DOS library derived from  $\gamma$ -hydroxy- $\alpha,\beta$ -alkynoates.

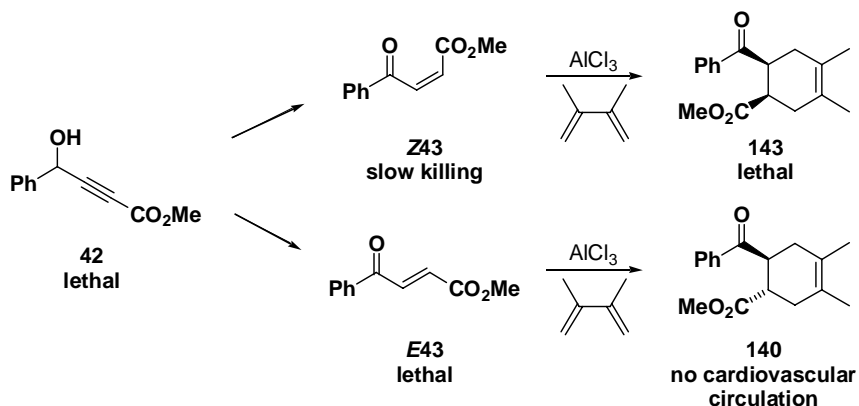
There were several reasons why zebrafish were chosen instead of the more common animal model, mice. Since zebrafish are smaller than mice, the resources to maintain them (food, living space) are less than mice's. Likewise the eggs are less than 1mm in diameter so they can easily fit in the single well of a 384-well plate and the female zebrafish can also lay up to 300 eggs at time.<sup>54</sup> Despite the fact that they are not mammals, zebrafish contain a genomic complexity similarly to humans.<sup>55</sup> Finally, the eggs and embryos are transparent, allowing for the studying of the embryo's development using light microscopy.<sup>56</sup>

Therefore, Professor Nathan Bahary introduced the molecules to 96-well plates containing 10 zebrafish eggs in embryo rearing media to give a final concentration of 10 or 50  $\mu\text{M}$ .<sup>57</sup> The embryos' developments were monitored each day for 3 days. If any interesting phenotypes were observed, that experiment was then repeated using 30 embryos in 1mL of

media. After these initial experiments, several types of phenotypes were present. Some of the molecules were lethal to zebrafish, while some had no observable phenotype. Others lead to no brain development or caused heart failure. The  $\gamma$ -hydroxy- $\alpha,\beta$ -alkynoate **42** was lethal; killing the zebrafish embryos after one day. However, the lethality of the substrate was eliminated in two steps. Treatment of alkynoate **42** with allylbromide and silver oxide in  $\text{CH}_2\text{Cl}_2$  yielded enyne **63**<sup>57</sup> which was then converted to the bicyclic molecule **147** in 24 % yield (unoptimized conditions) using  $[\text{RhCl}(\text{CO})_2]_2$  under a carbon monoxide atmosphere (Scheme 64). Despite the electron withdrawing ketone, ester and ether oxygen moieties, the tetra-substituted olefin **147** was too hindered, so this molecule did not cause an observable phenotype. This skeletal change from two steps completely negated its toxicity in the zebrafish.



**Scheme 64.** Biological effects of Pauson-Khand product **147**.

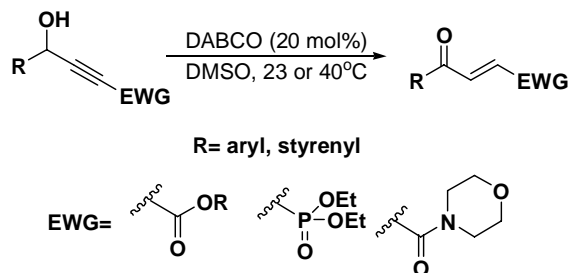


**Scheme 65.** Biological activity of Diels-Alder products.

Another interesting set of phenotypes dealt with the *E* and *Z*- $\gamma$ -oxo- $\alpha,\beta$ -alkenoates. Analogous to the Dal Pozzo paper, **E43** was the more reactive substrate killing the zebrafish embryos after one day while **Z43** killed the zebrafish after three days (Scheme 65). These results prompted the development of *E* and *Z*-selective redox isomerization conditions. Another interesting result was observed when **E43** and **Z43** were converted to their Diels-Alder products.

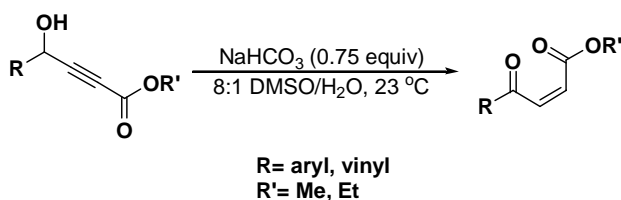
Compound **143**, prepared from the less reactive **Z43**, was deadly to the zebrafish. On the other hand, compound **130**, prepared from the more reactive **E43**, caused no cardiovascular circulation in the zebrafish embryos after three days. The zebrafish treated with compound **140** eventually died after their yolk sac was consumed, but these results showed a reversal of lethality after one skeletal transformation. Although these mentioned compounds are not being studied, other library members are currently being studied for their phenotypes.

### 3.0 CONCLUSION



**Scheme 66.** Summary of *E*-selective redox isomerization.

We have developed a mild *E*-selective redox isomerization using DABCO in DMSO (Scheme 66).<sup>58</sup> From the reaction optimization and mechanistic studies, the mechanism was eluded to precede via mechanism A (See Scheme 36). We also determined the scope of this *E*-selective redox isomerization in which the reaction proceeded well with aryl and styrenyl alkynoates.<sup>59</sup> Although aliphatic alkynoates do not yield the *E*-alkenoates, we have developed the first *E*-selective redox isomerization using an aryl alkyne phosphonate and aryl alkyne amide.



**Scheme 67.** Summary of *Z*-selective redox isomerization.

Also we have developed the first *Z*-selective redox isomerization using  $\text{NaHCO}_3$  (Scheme 67).<sup>60</sup> From the reaction optimization and mechanistic studies, the mechanism was eluded to precede via mechanism A (See Scheme 59). We also determined the scope of this *Z*-selective redox isomerization showing that the reaction preceded well using aryl and vinyl alkynoates.

## 4.0 EXPERIMENTAL

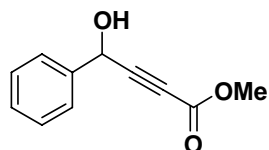
**General Techniques** All reactions were carried out with dry, freshly distilled solvents under anhydrous conditions, unless otherwise noted. Tetrahydrofuran (THF) was distilled from sodium-benzophenone, and methylene chloride ( $\text{CH}_2\text{Cl}_2$ ) was distilled from calcium hydride. Dimethylsulfoxide (DMSO) was distilled from calcium hydride under reduced pressure and kept dry over 3 angstrom sieves. Yields refer to chromatographically and spectroscopically ( $^1\text{H}$  NMR) homogenous materials, unless otherwise stated.

All reactions were monitored by thin-layer chromatography (TLC) carried out on 0.25-mm E. Merck silica gel plates (60F-254) using UV-light (254 nm) with anisaldehyde in ethanol and heat as developing agents. TSI silica gel (230–400 mesh) was used for flash column chromatography. Merck silica gel (60 PF<sub>254</sub>) was used to make preparative TLC (prep-TLC) plates for further purification of select compounds in which the prep-TLC plates were prepared as specified by the silica gel manufacturer. NMR spectra were recorded on AM300 or AM500 (Bruker) instruments and calibrated using the solvent or tetramethylsilane as an internal reference. The following abbreviations are used to indicate the multiplicities; app, apparent; s, singlet; d, doublet; t, triplet; q, quartet; sex, sextet; m, multiplet; br, broad. High-resolution mass spectra were obtained by using EBE geometry.

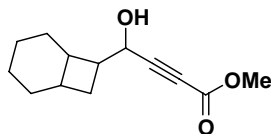
Alkynes were synthesized by one of the two following methods.

**Method A** - Using the procedure from Shahi, S. P., Koide, K. *Angew. Chem., Int. Ed.* **2004**, *43*, 2525–2527.

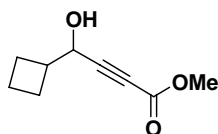
**Method B** - Using the procedure from Krause, N., *Liebigs Ann. Chem.* **1990**, 603–604.



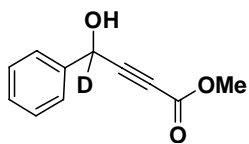
**Preparation of 42:** See: Shahi, S. P.; Koide, K. *Angew. Chem., Int. Ed.* **2004**, *43*, 2525–2527.



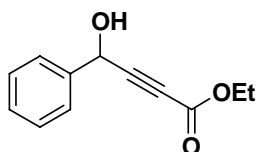
**Preparation of 76:** Method A.



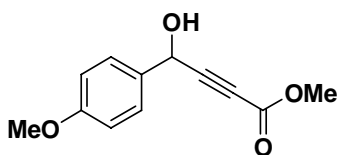
**Preparation of 77:** Method A.



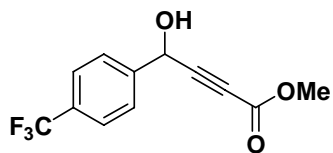
**Preparation of 4d-42:** Method A. Silica gel chromatography (5 → 20 % EtOAc in hexanes) afforded **4d-42** (70.3 mg, 70 %) as a pale yellow oil;  $R_f$  = 0.33 (30 % EtOAc in hexanes).



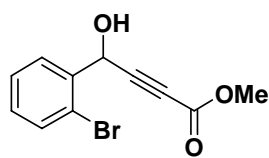
**Preparation of 90:** Method A. Spectral data were in agreement with the literature: Herrmann, J. L., Berger, M. H., Schlessinger, R. H., *J. Am. Chem. Soc.* **1979**, *101*, 1544–1549.



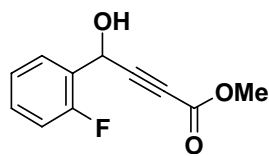
**Preparation of 91:** See: Shahi, S. P.; Koide, K. *Angew. Chem., Int. Ed.* **2004**, *43*, 2525–2527.



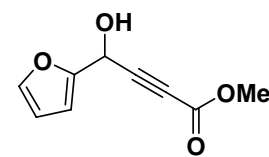
**Preparation of 93:** Method A. Silica gel chromatography (5 → 20 % EtOAc in hexanes) afforded **93** (303.0 mg, 61 %) as a yellow oil;  $R_f$  = 0.33 (30 % EtOAc in hexanes); IR (film) 3420 (br, O-H), 3011, 2959, 2242 (C≡C), 1717 (C=O), 1438, 1329, 1260, 1167, 1128, 1017, 857  $\text{cm}^{-1}$ ;  $^1\text{H}$  NMR (300 MHz, 293K,  $\text{CDCl}_3$ )  $\delta$  7.65 (br s, 4H), 5.61 (br s, 1H), 3.80 (s 3H);  $^{13}\text{C}$  NMR (125 MHz, 293 K,  $\text{CDCl}_3$ )  $\delta$  153.8, 142.4, 130.7 (q,  $J$  = 32.3 Hz), 126.8, 125.6 (q,  $J$  = 3.8 Hz), 123.8 (q,  $J$  = 270.4 Hz), 86.2, 77.5, 63.1, 52.9; HRMS (EI $^+$ ) calc'd for  $\text{C}_{12}\text{H}_9\text{F}_3\text{O}_3$  ( $\text{M}^+$ ) 258.0503; found 258.0500.



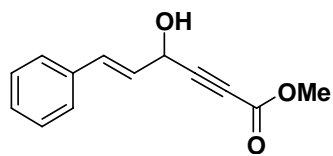
**Preparation of 95:** Method B. Silica gel chromatography (5 → 20 % EtOAc in hexanes) afforded **95** (459.0 mg, 46 %) as a yellow oil;  $R_f = 0.40$  (30 % EtOAc in hexanes); IR (film) 3411 (br, O-H), 2954, 2923, 2238 (C≡C), 1716 (C=O), 1436, 1255, 1019, 942, 751  $\text{cm}^{-1}$ ;  $^1\text{H}$  NMR (500 MHz, 293 K,  $\text{CDCl}_3$ ),  $\delta$  7.72 (dd, 1H,  $J = 7.8, 1.5$  Hz), 7.57 (d, 1H,  $J = 8.0$  Hz), 7.38 (t, 1H,  $J = 7.6$  Hz), 7.22 (td, 1H,  $J = 7.8, 1.6$  Hz), 5.87 (s, 1H), 3.79 (s, 3H);  $^{13}\text{C}$  NMR (125 MHz, 293 K,  $\text{CDCl}_3$ )  $\delta$  153.8, 137.7, 132.9, 130.2, 128.4, 127.9, 122.4, 86.0, 76.9, 63.4, 52.9; HRMS ( $\text{EI}^+$ ) calc'd for  $\text{C}_{11}\text{H}_9\text{BrO}_3$  ( $\text{M}^+$ ); 267.9735; found 267.9742.



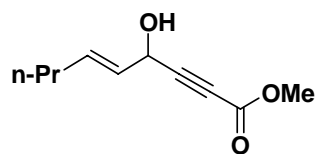
**Preparation of 97:** Method B. Silica gel chromatography (7.5 → 30 % EtOAc in hexanes) afforded **97** (632.3 mg, 63 %) as a pale yellow oil;  $R_f = 0.36$  (30 % EtOAc in hexanes); IR (film) 3419 (br, O-H), 3070, 3048, 2956, 2241 (C≡C), 1716 (C=O), 1616, 1491, 1457, 1256, 1175, 1009, 758  $\text{cm}^{-1}$ ;  $^1\text{H}$  NMR (300 MHz, 293 K,  $\text{CDCl}_3$ )  $\delta$  7.62 (td, 1H,  $J = 7.5, 1.8$  Hz), 7.39–7.31 (m, 1H), 7.19 (td, 1H,  $J = 7.5, 1.1$  Hz), 7.08 (ddd, 1H,  $J = 10.2, 8.2, 1.2$  Hz), 5.82 (br s, 1H), 3.79 (s, 3H);  $^{13}\text{C}$  NMR (75 MHz, 293 K,  $\text{CDCl}_3$ )  $\delta$  159.4 (d,  $J = 247.2$  Hz), 153.7, 130.3 (d,  $J = 8.2$  Hz), 128.0 (d,  $J = 3.1$  Hz), 125.7 (d,  $J = 13.3$  Hz), 124.2 (d,  $J = 3.5$  Hz), 115.3 (d,  $J = 20.9$  Hz), 85.9, 76.4, 57.7 (d,  $J = 5.1$  Hz), 52.7; HRMS ( $\text{EI}^+$ ) calc'd for  $\text{C}_{11}\text{H}_9\text{FO}_3$  ( $\text{M}^+$ ) 208.0535; found 208.0534.



**Preparation of 99:** Method A. Silica gel chromatography (5 → 20 % EtOAc in hexanes) afforded **99** (236.0 mg, 67 %) as a yellow oil;  $R_f = 0.30$  (30 % EtOAc in hexanes); IR (film) 3408 (br, O-H), 2957, 2244 (C≡C), 1719 (C=O), 1500, 1438, 1263, 1144, 1073, 1023, 952, 918, 884, 750  $\text{cm}^{-1}$ ;  $^1\text{H}$  NMR (300 MHz, 293 K,  $\text{CDCl}_3$ )  $\delta$  7.44 (dd, 1H,  $J = 1.8, 0.6$  Hz), 6.50 (dd, 1H,  $J = 3.3, 0.6$  Hz), 6.38 (dd, 1H,  $J = 3.3, 1.8$  Hz), 5.57 (br d, 1H,  $J = 6.8$  Hz), 3.80 (s, 3H), 2.62 (br d, 1H,  $J = 6.8$  Hz);  $^{13}\text{C}$  NMR (75 MHz, 293 K,  $\text{CDCl}_3$ )  $\delta$  153.6, 150.7, 143.4, 110.5, 108.5, 84.2, 76.4, 57.7, 52.9; HRMS ( $\text{EI}^+$ ) calc'd for  $\text{C}_9\text{H}_8\text{O}_4$  ( $\text{M}^+$ ) 180.0423; found 180.0419.

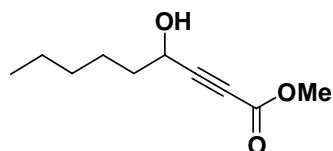


**Preparation of 101:** See: Shahi, S. P.; Koide, K. *Angew. Chem., Int. Ed.* **2004**, *43*, 2525–2527.

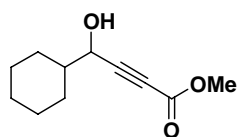


**Preparation of 103:** Method B. Silica gel chromatography (5 → 20 %

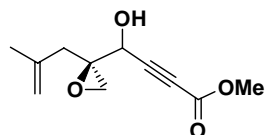
EtOAc in hexanes) afforded **103** (646.0 mg, 65 %) as a pale yellow oil;  $R_f = 0.42$  (30 % EtOAc in hexanes); IR (film) 3407 (br, O-H), 3033, 2959, 2932, 2238 (C≡C), 1716 (C=O), 1436, 1256, 1066, 968, 752  $\text{cm}^{-1}$ ;  $^1\text{H}$  NMR (300 MHz,  $\text{CDCl}_3$ )  $\delta$  5.91 (dtd, 1H,  $J = 15.3, 7.1, 1.1$  Hz), 5.59 (dtd, 1H,  $J = 15.3, 6.2, 1.3$  Hz), 4.92 (br d,  $J = 6.2$  Hz), 3.79 (s, 1H), 2.05 (app br q, 2H,  $J = 7.1$  Hz), 1.43 (app sex, 2H,  $J = 7.3$ ), 0.91 (t, 3H,  $J = 7.3$  Hz);  $^{13}\text{C}$  NMR (75 MHz, 293 K,  $\text{CDCl}_3$ )  $\delta$  153.9, 134.8, 126.8, 87.0, 76.3, 62.0, 52.6, 33.8, 21.6, 13.3; HRMS ( $\text{EI}^+$ ) calc'd for  $\text{C}_{10}\text{H}_{14}\text{O}_3$  ( $\text{M}^+$ ) 182.0943; found 182.0948.



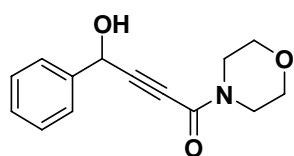
**Preparation of 107:** See: Shahi, S. P.; Koide, K. *Angew. Chem., Int. Ed.* **2004**, *43*, 2525–2527.



**Preparation of 108:** See: Shahi, S. P.; Koide, K. *Angew. Chem., Int. Ed.* **2004**, *43*, 2525–2527.

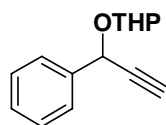


**Preparation of 109:** See: Shahi, S. P.; Koide, K. *Angew. Chem., Int. Ed.* **2004**, *43*, 2525–2527.

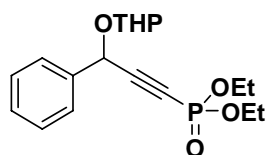


**Preparation of 111:** Method B. Silica gel chromatography (20 → 80 %

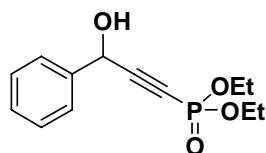
EtOAc in hexanes) afforded **111** (58.0 mg, 26 %) as a yellow oil;  $R_f = 0.15$  (80 % EtOAc in hexanes); IR (film) 3347 (br, O-H), 3032, 2965, 2858, 2237 (C≡C), 1613 (C=O), 1434, 1276, 1248, 1114, 996, 700  $\text{cm}^{-1}$ ;  $^1\text{H}$  NMR (300 MHz, 293 K,  $\text{CDCl}_3$ )  $\delta$  7.53–7.49 (m, 2H), 7.43–7.34 (m, 3H), 5.57 (s, 1H), 3.74–3.62 (m, 8H);  $^{13}\text{C}$  NMR (125 MHz, 293 K,  $\text{CDCl}_3$ )  $\delta$  152.8, 139.2, 128.7, 128.6, 126.5, 92.6, 66.7, 66.3, 64.0, 47.2, 41.9; HRMS ( $\text{EI}^+$ ) calc'd for  $\text{C}_{14}\text{H}_{15}\text{NO}_3$  ( $\text{M}^+$ ) 245.1052; found 245.1046.



**Preparation of 118:** *p*TsOH (143.9 mg, 0.7567 mmol), was added in one portion to a solution of **117** (920  $\mu$ L, 7.57 mmol) and dihydropyran (755  $\mu$ L, 8.25 mmol) in CH<sub>2</sub>Cl<sub>2</sub> (30 mL) at 23 °C. The resulting mixture was then stirred for 1 h and then diluted with Et<sub>2</sub>O (45 mL). The mixture was then washed with saturated NaHCO<sub>3</sub> solution (1  $\times$  15 mL) and brine (1  $\times$  30 mL). The aqueous layer was then extracted with Et<sub>2</sub>O (2  $\times$  15 mL). The organic layers were combined, dried over Na<sub>2</sub>SO<sub>4</sub>, filtered, and concentrated under reduced pressure. The resulting residue was then purified by silica gel chromatography (2.5  $\rightarrow$  10 % EtOAc in hexanes) to afford the THP ether **118** as a mixture of diastereomers (1.551 g, 95 %), which was used in the subsequent step without further purification.



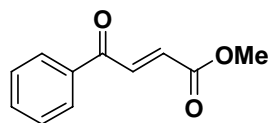
**Preparation of 119:** *n*-Butyllithium (1.6 M in hexanes) was added drop wise to a solution of **118** (432.6 mg, 2.000 mmol) in THF (2 mL) at -78 °C. Diethylchlorophosphate (320  $\mu$ L, 2.20 mmol) in THF (2.2 mL) was then added drop wise to solution at -78 °C and the resulting mixture was allowed to stir at the same temperature for 1.5 h. The reaction flask was then placed in an ice water bath and quenched with water (2.4 mL) at 0 °C. The solvent was removed under pressure and the resulting residue was extracted with Et<sub>2</sub>O (4  $\times$  6 mL). The organic layers were then washed with brine (1  $\times$  6 mL), dried over Na<sub>2</sub>SO<sub>4</sub>, filtered, and concentrated under reduced pressure. The resulting residue was then subjected to silica gel chromatography (10  $\rightarrow$  50 % EtOAc in hexanes) to remove unreacted starting materials and to afford the THP ether phosphonate **119** as a mixture of diastereomers (298.6 mg, 42 %), which was used in the subsequent step without further purification.



**Preparation of 115:** PPTS (16.9 mg, 0.0673 mmol) was added in one portion to a solution of **119** (236.6 mg, 0.6731 mmol) in EtOH (4.5 mL). The reaction mixture was heated to 55 °C. After an additional 7.3 h at the same temperature, the solvent was removed under reduced pressure. The resulting residue was then purified by silica gel chromatography (15  $\rightarrow$  60 % EtOAc in hexanes) to afford **115** (162.9 mg 90 %) as a pale yellow oil;  $R_f$  = 0.25 (80 % EtOAc in hexanes); IR (film) 3319 (br, O-H), 3032, 2986, 2909, 2203 (C $\equiv$ C), 1455, 1252 (P=O), 1051, 781, 701 cm<sup>-1</sup>; <sup>1</sup>H NMR (300 MHz, 293 K, CDCl<sub>3</sub>)  $\delta$  7.53–7.49 (m, 2H), 7.42–7.34 (m, 3H), 5.52 (d, 1H,  $J$  = 3.5 Hz), 4.20–4.09 (m, 4H), 1.73 (br s, 1H), 1.35 (td, 6H,  $J$  = 7.1, 3.2 Hz); <sup>13</sup>C NMR (75 MHz, 293 K, CDCl<sub>3</sub>)  $\delta$  138.9,

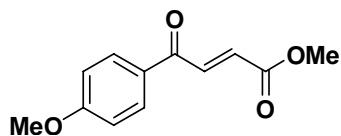
128.4, 128.2, 126.4, 101.3 (d,  $J = 49.2$  Hz), 74.3 (d,  $J = 295.4$  Hz), 63.6 (br s), 63.3 (d,  $J = 5.6$  Hz), 15.8 (d,  $J = 7.1$  Hz); HRMS (EI<sup>+</sup>) calc'd for C<sub>13</sub>H<sub>17</sub>PO<sub>4</sub> (M<sup>+</sup>) 268.0864; found 268.0874.

**General procedure for the formation of *E*-olefins (Method C):** To a solution of **A** (0.2500 mmol) in DMSO (1.25 mL) at 23 °C, DABCO (5.6 mg, 0.050 mmol) was added in one portion, and the resulting solution was stirred at the same temperature for the indicated time. The reaction was then diluted with water (25 mL), and then acidified to pH 3 with pH 3 phosphate buffer. The resulting aqueous mixture was extracted with Et<sub>2</sub>O (25 mL × 3 or 4). The combined organic layers were then washed with water (25 mL) then brine (25 mL), dried over Na<sub>2</sub>SO<sub>4</sub>, filtered, and concentrated under reduced pressure. The resulting residue was purified by silica gel chromatography (EtOAc in hexanes) to afford the corresponding trans olefin **B**.

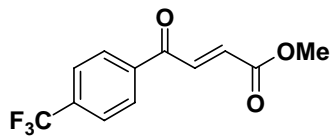


**Preparation of *E*43:** Method C. Silica gel chromatography (5 → 20 % EtOAc in hexanes) afforded **E43** (734 mg, 73 %) as a pale yellow oil. Spectral data were in agreement with the literature: Bonete, P., Najera, C.,

*J. Org. Chem.* **1994**, *59*, 3202–3209.

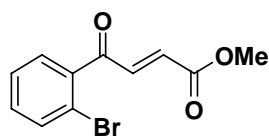


**Preparation of *E*92:** Method C. Silica gel chromatography (5 → 20 % EtOAc in hexanes) afforded **E92** (42.4 mg, 77 %) as a yellow solid;  $R_f = 0.33$  (30 % EtOAc in hexanes); mp = 65.5–66.0 °C; IR (film) 3014, 2956, 2924, 2848, 1737(C=O), 1727 (C=O), 1668, 1596, 1439, 1306, 1264, 1165, 1028, 975, 833, 766 cm<sup>-1</sup>; <sup>1</sup>H NMR (300 MHz, 293 K, CDCl<sub>3</sub>) δ 8.02 (dt, 2H,  $J = 8.9, 2.1$  Hz), 7.94 (d, 1H,  $J = 15.5$  Hz), 6.99 (dt, 2H,  $J = 8.9, 2.1$  Hz) 6.88 (d, 1H,  $J = 15.5$  Hz), 3.90 (s, 3H), 3.85 (s, 3H); <sup>13</sup>C NMR (125 MHz, 293 K, CDCl<sub>3</sub>) δ 187.5, 166.2, 164.2, 136.7, 131.2, 131.2, 129.6, 114.1, 55.5, 52.2; HRMS (EI<sup>+</sup>) calc'd for C<sub>12</sub>H<sub>12</sub>O<sub>4</sub> (M<sup>+</sup>) 220.0736; found 220.0741.



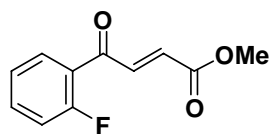
**Preparation of *E*94:** Method C. Silica gel chromatography (5 → 20 % EtOAc in hexanes) afforded **E94** (40.0 mg, 62 %) as a pale yellow solid;  $R_f = 0.41$  (20 % EtOAc in hexanes); mp = 73.5–74.0 °C; IR (film) 3079, 2927, 1731 (C=O), 1669 (C=O), 1628, 1410, 1319, 1306, 1164, 1126, 970, 773, 722 cm<sup>-1</sup>; <sup>1</sup>H NMR (300 MHz, 293K, CDCl<sub>3</sub>) δ 8.11 (br d, 2H,  $J = 8.8$  Hz), 7.90 (d, 1H,  $J = 15.6$  Hz),

7.79 (br d, 1H,  $J = 8.8$  Hz), 6.93 (d, 1H,  $J = 15.6$  Hz), 3.87 (s, 3H);  $^{13}\text{C}$  NMR (125 MHz, 293 K,  $\text{CDCl}_3$ )  $\delta$  188.6, 165.6, 139.1, 135.7, 135.0 (q,  $J = 32.5$  Hz), 133.0, 129.0, 125.9, 123.4 (q,  $J = 273.8$  Hz), 52.4; HRMS ( $\text{ES}^+$ ) calc'd for  $\text{C}_{12}\text{H}_9\text{F}_3\text{O}_3$  ( $\text{M}^+$ ) 258.0504; found 258.0538.



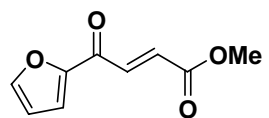
**Preparation of E96:** Method C. Silica gel chromatography (5  $\rightarrow$  20 % EtOAc in hexanes) afforded **E96** (24.0 mg, 36 %) as a yellow oil;  $R_f = 0.46$  (30 % EtOAc in hexanes); IR (film) 2952, 2923, 2851, 1728 (C=O),

1675 (C=O), 1434, 1309, 1275, 1256, 1169, 1025, 751  $\text{cm}^{-1}$ ;  $^1\text{H}$  NMR (300 MHz, 293 K,  $\text{CDCl}_3$ )  $\delta$  7.65 (d, 1H,  $J = 7.1$  Hz), 7.50 (d, 1H,  $J = 15.8$  Hz), 7.45–7.35 (m, 3H), 6.64 (d, 1H,  $J = 15.8$  Hz), 3.83 (s, 3H);  $^{13}\text{C}$  NMR (125 MHz, 293 K,  $\text{CDCl}_3$ )  $\delta$  193.1, 165.7, 139.4, 139.1, 133.6, 132.7, 132.4, 129.5, 127.5, 119.6, 52.3; HRMS ( $\text{EI}^+$ ) calc'd for  $\text{C}_{11}\text{H}_9\text{BrO}_3$  ( $\text{M}^+$ ) 267.9735; found 267.9745.



**Preparation of E98:** Method C. Alumina chromatography (15 % EtOAc in hexanes) afforded **E98** (31.3 mg, 60 %) as a orange oil;  $R_f = 0.45$  (30 % EtOAc in hexanes); IR (film) 2954, 2923, 2851, 1728 (C=O), 1673 (C=O),

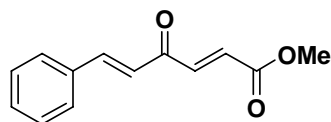
1610, 1454, 1311, 1279, 977, 757  $\text{cm}^{-1}$ ;  $^1\text{H}$  NMR (300 MHz, 293 K,  $\text{CDCl}_3$ )  $\delta$  7.84 (dd, 1H,  $J = 7.4, 1.6$  Hz), 7.77 (dd, 1H,  $J = 15.6, 3.4$  Hz), 7.62–7.55 (m, 1H), 7.28 (td, 1H,  $J = 7.7, 1.1$  Hz), 7.18 (ddd, 1H,  $J = 10.8, 8.3, 0.8$  Hz), 6.83 (dd, 1H,  $J = 15.6, 1.3$  Hz), 3.84 (s, 3H);  $^{13}\text{C}$  NMR (125 MHz, 293 K,  $\text{CDCl}_3$ )  $\delta$  188.0 (d,  $J = 2.6$  Hz), 165.9, 161.5 (d,  $J = 253.8$  Hz), 139.3 (d,  $J = 6.9$  Hz), 135.2 (d,  $J = 9.0$  Hz), 131.7, 131.0 (d,  $J = 2.1$  Hz), 125.4 (d,  $J = 12.2$  Hz), 124.7 (d,  $J = 3.3$  Hz), 116.7 (d,  $J = 22.8$  Hz), 52.3; HRMS ( $\text{EI}^+$ ) calc'd for  $\text{C}_{11}\text{H}_9\text{FO}_3$  ( $\text{M}^+$ ) 208.0535; found 208.0542.



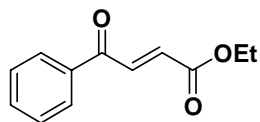
**Preparation of E100:** Method C. Silica gel chromatography (5  $\rightarrow$  20 % EtOAc in hexanes) afforded **E100** (36.0 mg, 78 %) as a pale yellow solid;

$R_f = 0.31$  (30 % EtOAc in hexanes); mp = 87.5–88.5  $^\circ\text{C}$ ; IR (film) 3154, 3133, 3096, 3005, 2959, 2853, 1720 (C=O), 1665 (C=O), 1622, 1463, 1337, 982, 767  $\text{cm}^{-1}$ ;  $^1\text{H}$  NMR (300 MHz, 293 K,  $\text{CDCl}_3$ )  $\delta$  7.77 (d, 1H,  $J = 15.6$  Hz), 7.70 (dd, 1H,  $J = 1.7, 0.7$  Hz), 7.39 (dd 1H  $J = 3.6, 0.7$  Hz), 6.98 (d, 1H,  $J = 15.6$  Hz), 6.62 (dd, 1H,  $J = 3.6, 1.7$  Hz), 3.84 (s, 3H);  $^{13}\text{C}$  NMR (75 MHz, 293

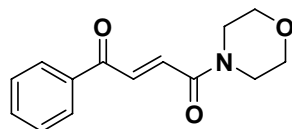
K, CDCl<sub>3</sub>)  $\delta$  176.4, 165.9, 152.7, 147.9, 135.6, 131.6, 119.6, 112.9, 52.3; HRMS (ES<sup>+</sup>) calc'd for C<sub>9</sub>H<sub>8</sub>O<sub>4</sub>Na 203.0320 (M + Na)<sup>+</sup>; found 203.0318.



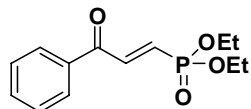
**Preparation of E102:** Method C. Silica gel chromatography (5 → 20 % EtOAc in hexanes) afforded **E102** (65.5 mg, quantitative yield) as a yellow solid; Spectral data were in agreement with the literature: Baraldi, P. G., Bazzanini, R., Bigoni, A., Manfredini, S., Simoni, D., *Synthesis* **1993**, 1206–1208.



**Preparation of E104:** Method C. Silica gel chromatography (5 → 20 % EtOAc in hexanes) afforded **E104** (37.0 mg, 72 %) as a yellow oil; Spectral data were in agreement with the literature: Ronsheim, M. D., Zercher, C. K., *J. Org. Chem.* **2003**, 68, 4535–4538.



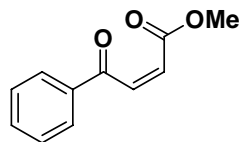
**Preparation of E112:** Method C was used to generate **E112** with the modification of an addition of NaOAc (1.6 mg, 0.020 mmol, 20 mol%) in one portion after the DABCO addition. Silica gel chromatography (20 → 80 % EtOAc in hexanes) yielded **E112** (18.5 mg, 76 %) as a white solid;  $R_f$  = 0.19 (80 % EtOAc in hexanes); mp = 126.5–127.5 °C; IR (film) 2958, 2922, 2853, 1671 (C=O), 1636 (C=O), 1434, 1289, 1114, 1043, 891, 722 cm<sup>-1</sup>; <sup>1</sup>H NMR (300 MHz, 293 K, CDCl<sub>3</sub>)  $\delta$  8.04 (d, 2H,  $J$  = 7.2 Hz), 7.97 (d, 1H,  $J$  = 15.0 Hz), 7.65–7.60 (m, 1H), 7.54–7.49 (m, 2H), 7.47 (d, 1H,  $J$  = 15.0 Hz), 3.75–3.68 (m, 8H); <sup>13</sup>C NMR (125 MHz, 293 K, CDCl<sub>3</sub>)  $\delta$  189.5, 164.0, 136.8, 134.6, 133.8, 131.7, 128.8, 128.8, 66.7, 46.4, 42.6; HRMS (EI<sup>+</sup>) calc'd for C<sub>14</sub>H<sub>15</sub>NO<sub>3</sub> (M<sup>+</sup>) 245.1052; found 245.1042.



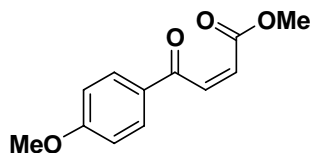
**Preparation of E116:** Method C was used to afford **E116** with the modification of heating the reaction to 40 °C (oil bath) after DABCO addition. Silica gel chromatography (15 → 60 % EtOAc in hexanes) yielded **E116** (25.4 mg, 95 %) as a yellow oil containing a 10:1 E/Z mixture. Stereochemically pure **E116** was afforded under different conditions (50 mol % of CsHCO<sub>3</sub> in DMSO, 23 °C) in lower yield (31.0 mg, 50 %) which was used for characterization;  $R_f$  = 0.15 (80 % EtOAc in hexanes); IR (film) 3064, 2984, 2929, 1671, 1448, 1260 (P=O), 1051, 1024, 975, 692 cm<sup>-1</sup>; <sup>1</sup>H NMR (300 MHz, 293 K,

CDCl<sub>3</sub>)  $\delta$  8.04–8.00 (m, 2H), 7.84 (dd, 1H,  $J$  = 21.2, 16.9, Hz), 7.64 (tt, 1H,  $J$  = 7.5, 1.3 Hz), 7.55–7.50 (m, 2H), 6.94 (dd, 1H,  $J$  = 19.4, 16.9 Hz), 4.18 (m, 4H), 1.38 (t, 3H,  $J$  = 7.1 Hz); <sup>13</sup>C NMR (125 MHz, 293 K, CDCl<sub>3</sub>)  $\delta$  188.5 (d,  $J$  = 22.5 Hz), 140.3, 136.3, 133.9, 131.4, 129.9, 128.9, 62.5, 16.3; HRMS (EI<sup>+</sup>) calc'd for C<sub>13</sub>H<sub>17</sub>PO<sub>4</sub> (M<sup>+</sup>) 268.0864; found 268.0863.

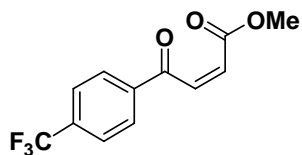
**General procedure for the preparation of Z-olefins (Method D):** To a solution of **alkynoate** (0.2500 mmol) in 1:8 H<sub>2</sub>O/DMSO (1.25 mL total) at 23 °C, a 0.01M solution of hydroquinone in DMSO was added (25  $\mu$ L, 0.002500 mmol). Subsequently, NaHCO<sub>3</sub> (15.8 mg, 0.05000 mmol) was then added in one portion and the resulting solution was stirred at the same temperature for the indicated time. The reaction was then diluted with water (25 mL), and then acidified to pH 3 with pH 3 phosphate buffer. The resulting aqueous mixture was extracted with Et<sub>2</sub>O (25 mL  $\times$  3 or 4). The combined organic layers were then washed with water (25 mL) then brine (25 mL), dried over Na<sub>2</sub>SO<sub>4</sub>, filtered, and concentrated under reduced pressure. The resulting residue was purified by silica gel chromatography (EtOAc in hexanes) to afford the corresponding cis olefin.



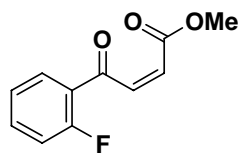
**Preparation of Z42:** Method D. Silica gel chromatography (5  $\rightarrow$  20 % EtOAc in hexanes) afforded **Z42** (39.0 mg, 76 %) as a yellow oil; Spectral data were in agreement with the reference: Etrick, M. R., Miller, M., Heeds, L. S., *J. Am. Chem. Soc.* **1992**, *114*, 4079–4088.



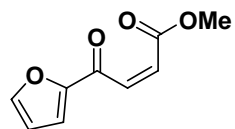
**Preparation of Z92:** Method D. Silica gel chromatography (5  $\rightarrow$  20 % EtOAc in hexanes) afforded **Z92** (29.9 mg, 58 %) as a yellow oil;  $R_f$  0.31 (30 % EtOAc in hexanes); IR (film) 2924, 1723 (C=O), 1661 (C=O), 1596, 1573, 1251, 1217, 1160 cm<sup>-1</sup>; <sup>1</sup>H NMR (300 MHz, 293K, CDCl<sub>3</sub>)  $\delta$  7.91 (dt, 2H,  $J$  = 9.0, 2.1 Hz), 6.96 (dt, 2H,  $J$  = 8.9, 2.1 Hz) 6.90 (d, 1H,  $J$  = 12.1 Hz), 6.26 (d, 1H,  $J$  = 12.1 Hz), 3.87 (s, 3H), 3.62 (s, 3H); <sup>13</sup>C NMR (125 MHz, 293 K, CDCl<sub>3</sub>)  $\delta$  192.6, 165.4, 164.0, 141.3, 131.0, 128.9, 125.3, 114.0, 55.5, 51.8; HRMS (EI<sup>+</sup>) calc'd for C<sub>12</sub>H<sub>12</sub>O<sub>4</sub> (M<sup>+</sup>) 220.0736; found 220.0726  $m/z$ .



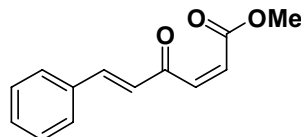
**Preparation of Z94:** Method D. Silica gel chromatography (5 → 20 % EtOAc in hexanes) afforded **Z94** (32.4 mg, 50 %) as an orange oil;  $R_f$  0.38 (30 % EtOAc in hexanes); IR (film) 2956, 1727 (C=O), 1683 (C=O), 1412, 1326, 1224, 1169, 1129, 1067, 820  $\text{cm}^{-1}$ ;  $^1\text{H}$  NMR (300 MHz, 293K,  $\text{CDCl}_3$ )  $\delta$  8.05 (br d, 2H,  $J = 8.8$  Hz), 7.76 (br d, 2H,  $J = 8.8$  Hz), 6.90 (d, 1H,  $J = 12.0$  Hz), 6.36 (d, 1H,  $J = 12.0$  Hz), 3.62 (s 3H);  $^{13}\text{C}$  NMR (125 MHz, 293 K,  $\text{CDCl}_3$ )  $\delta$  193.2, 165.1, 140.7, 138.3, 134.7 (q,  $J = 32.5$  Hz), 128.8, 126.3, 125.7, 123.4 (q,  $J = 271.2$  Hz), 52.0; HRMS ( $\text{EI}^+$ ) calc'd for  $\text{C}_{12}\text{H}_9\text{F}_3\text{O}_3$  ( $\text{M}^+$ ) 258.0504; found 258.0504  $m/z$ .



**Preparation of Z98:** Method D. Silica gel chromatography (5 → 20 % EtOAc in hexanes) afforded **Z98** (11.1 mg, 22 %) as a yellow oil;  $R_f$  0.39 (30 % EtOAc in hexanes); IR (film) 2923, 2850, 1722 (C=O), 1670 (C=O), 1608, 1453, 1384, 1215, 1170, 11153, 761  $\text{cm}^{-1}$ ;  $^1\text{H}$  NMR (300 MHz, 293 K,  $\text{CDCl}_3$ )  $\delta$  7.95 (td, 1H,  $J = 7.5, 1.8$  Hz), 7.60 – 7.52 (m, 1H), 7.28 (td, 1H,  $J = 7.9, 0.7$  Hz), 7.13 (dd, 1H,  $J = 10.9, 8.3$  Hz), 6.96 (dd, 1H,  $J = 12.0, 4.7$  Hz), 6.18 (dd, 1H,  $J = 12.0, 0.8$  Hz), 3.66 (s, 3H);  $^{13}\text{C}$  NMR (125 MHz, 293 K,  $\text{CDCl}_3$ )  $\delta$  190.7, 165.6, 162.0 (d,  $J = 255$  Hz), 142.2, 135.2 (d,  $J = 8.9$  Hz), 130.7, 124.6, 116.6 (d,  $J = 22.3$  Hz), 51.9; HRMS ( $\text{EI}^+$ ) calc'd for  $\text{C}_{11}\text{H}_9\text{O}_3\text{F}$  ( $\text{M}^+$ ) 208.0536; found 208.0535  $m/z$ .

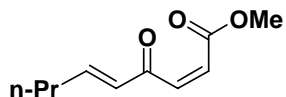


**Preparation of Z100:** Method D but with the addition of LiBr (20.0 mg, 90 mol%) before the addition of  $\text{NaHCO}_3$ . Silica gel chromatography (5 → 20 % EtOAc in hexanes) afforded **Z100** (26.0 mg, 57 %) as a pale yellow oil;  $R_f$  0.28 (30 % EtOAc in hexanes); IR (film) 3131, 2953, 2923, 2852, 1726 (C=O), 1661 (C=O), 1464, 1220, 1177, 1159, 1042, 1007  $\text{cm}^{-1}$ ;  $^1\text{H}$  NMR (300 MHz, 293K,  $\text{CDCl}_3$ )  $\delta$  7.64 (dd, 1H,  $J = 1.6, 0.6$  Hz), 7.23 (dd, 1H,  $J = 3.6, 0.6$  Hz), 6.86 (d, 1H,  $J = 12.0$  Hz), 6.58 (dd, 1H,  $J = 3.6, 1.7$  Hz), 6.33 (d, 1H,  $J = 12.0$  Hz), 3.71 (s 3H);  $^{13}\text{C}$  NMR (75 MHz, 293 K,  $\text{CDCl}_3$ )  $\delta$  179.8, 165.9, 152.0, 147.3, 135.6, 128.6, 118.8, 112.6, 52.1; HRMS ( $\text{ES}^+$ ) calc'd for  $\text{C}_9\text{H}_8\text{O}_4$  203.0320 ( $\text{M} + \text{Na}$ ); found 203.0313  $m/z$ .

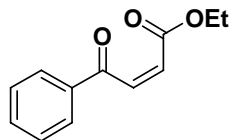


**Preparation of Z102:** Silica gel chromatography (5 → 20 % EtOAc in hexanes) afforded **Z102** (28.7 mg, 53 %) as a yellow oil;  $R_f$  0.34 (30 %

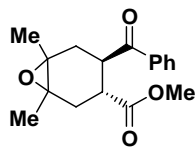
EtOAc in hexanes); IR (film) 2951, 2924, 2851, 1725 (C=O), 1653 (C=O), 1625, 1602, 1388, 1215, 1198, 1160, 1101, 977, 690  $\text{cm}^{-1}$ ;  $^1\text{H}$  NMR (300 MHz, 293K,  $\text{CDCl}_3$ )  $\delta$  7.55 (m, 3H), 7.45 (d, 1H,  $J = 16.5$  Hz), 7.41 (m, 2H), 6.85 (d, 1H,  $J = 16.3$  Hz), 6.73 (d, 1H,  $J = 12.1$  Hz), 6.24 (d, 1H,  $J = 12.1$  Hz), 3.73 (s, 3H);  $^{13}\text{C}$  NMR (75 MHz, 293 K,  $\text{CDCl}_3$ )  $\delta$  193.5, 165.5, 145.6, 140.5, 134.1, 130.9, 128.9, 128.4, 126.2, 125.9, 52.0; HRMS ( $\text{ES}^+$ ) calc'd for  $\text{C}_{13}\text{H}_{12}\text{O}_3$  239.0684 (M + Na); found 239.0668  $m/z$ .



**Preparation of Z104:** Method D. Alumina chromatography (20 % EtOAc in hexanes) afforded **Z104** (23.8 mg, 52 %) as a yellow oil;  $R_f$  0.42 (30 % EtOAc in hexanes); IR (film) 2959, 2931, 2874, 1731 (C=O), 1665 (C=O), 1636, 1437, 1214, 1167, 979  $\text{cm}^{-1}$ ;  $^1\text{H}$  NMR (300 MHz, 293 K,  $\text{CDCl}_3$ )  $\delta$  6.80 (dt, 1H,  $J = 16.0$ , 6.9 Hz), 6.62 (d, 1H,  $J = 12.1$  Hz), 6.22 (dt, 1H,  $J = 16.0$ , 1.5 Hz), 6.15 (d, 1H,  $J = 12.1$  Hz), 3.72 (s, 3H), 2.25 (qd, 2H,  $J = 7.4$ , 1.5 Hz), 1.51 (sextet, 2H,  $J = 7.4$  Hz), 0.94 (t, 3H,  $J = 7.4$  Hz);  $^{13}\text{C}$  NMR (125 MHz, 293 K,  $\text{CDCl}_3$ )  $\delta$  193.7, 165.4, 151.0, 140.6, 130.5, 125.5, 51.9, 34.6, 21.2, 13.6; HRMS ( $\text{EI}^+$ ) calc'd for  $\text{C}_{10}\text{H}_{14}\text{O}_3$  182.0943 ( $\text{M}^+$ ); found 182.0944  $m/z$ .

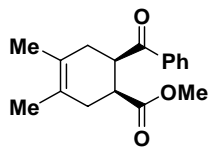


**Preparation of Z25:** Method D. Silica gel chromatography (5  $\rightarrow$  20 % EtOAc in hexanes) afforded **Z25** (28.2 mg, 55 %) as a yellow oil; Spectral data were in agreement with the reference: Lin, C. C., Wu, H. J., *J. Org. Chem.* **1996**, *61*, 3820–3828.

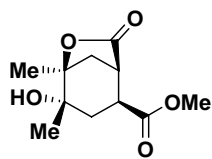


**Preparation of 141a and 141b:** *m*CPBA (70 % purity, 147.9 mg, 0.6000 mmol) was added to a solution of **143** (51.9 mg, 0.1907 mmol) in  $\text{CH}_2\text{Cl}_2$  (1.0 mL) at  $-50$   $^\circ\text{C}$ . The solution was allowed to warm to  $23$   $^\circ\text{C}$  over 21.0 h and then was quenched with 2-methyl-2-butene (85  $\mu\text{L}$ , 0.8000 mmol). 1,4 dioxane (2 mL) and concentrated  $\text{NaHCO}_3$  (2 mL) were then added to the solution and the resulting mixture was stirred overnight. 1,4-dioxane was then removed under reduced pressure and the aqueous layer was extracted with EtOAc (4.0 mL  $\times$  1). The organic layer were washed with water (2 mL  $\times$  2), brine (2 mL  $\times$  2), dried over  $\text{Na}_2\text{SO}_4$ , filtered, and concentrated under reduced pressure. The resulting residue was purified by medium-pressure silica gel chromatography (0  $\rightarrow$  30 % EtOAc in hexanes) to afford the corresponding **141a** and **141b** as pale yellow oils; **141a**  $R_f$  0.35 (30 % EtOAc in hexanes); IR

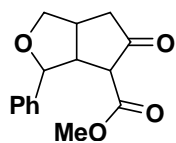
(film) 2924, 2852, 1735 (C=O), 1682 (C=O), 1448, 1196, 1173, 708  $\text{cm}^{-1}$ ;  $^1\text{H}$  NMR (300 MHz, 293K,  $\text{CDCl}_3$ )  $\delta$  7.99–7.96 (m, 2H), 7.58 (tt, 1H,  $J = 7.4, 1.3$  Hz), 7.50–7.45 (m, 2H), 3.89 (ddd, 1H,  $J = 11.6, 9.9, 4.5$  Hz), 3.58 (s, 3H), 2.92 (ddd, 1H,  $J = 11.6, 10.7, 6.3$  Hz), 2.30–2.21 (m, 2H), 2.10 (dd, 1H,  $J = 15.2, 11.6$  Hz), 1.71 (dd, 1H,  $J = 14.7, 11.6$  Hz) 1.38 (s, 3H), 1.33 (s, 3H);  $^{13}\text{C}$  NMR (75 MHz, 293 K,  $\text{CDCl}_3$ )  $\delta$  202.9, 174.5, 135.9, 133.2, 128.7, 128.5, 77.2, 62.5, 61.1, 51.8, 41.2, 40.5, 34.9, 32, 9, 20.8, 19.1; HRMS ( $\text{ES}^+$ ) calc'd for  $\text{C}_{17}\text{H}_{20}\text{O}_5\text{Na}$  ( $\text{M}^+ \text{Na}$ ) 327.1208; found 327.1212  $m/z$ . **141b**  $R_f$  029 (30 % EtOAc in hexanes); IR (film) 2954, 2923, 2851, 1734 (C=O), 1681 (C=O), 1448, 1435, 1195, 1173, 714  $\text{cm}^{-1}$ ;  $^1\text{H}$  NMR (300 MHz, 293K,  $\text{CDCl}_3$ )  $\delta$  7.95–7.92 (m, 2H), 7.57 (tt, 1H,  $J = 7.3, 1.3$  Hz), 7.50–7.45 (m, 2H), 3.70–3.60 (m, 1H), 3.59 (s, 3H), 3.10 (ddd, 1H,  $J = 12.5, 11.6, 4.4$  Hz), 2.44 (dd, 1H,  $J = 14.5, 4.4$  Hz), 2.12 (dd, 1H,  $J = 15.3, 6.8$  Hz), 1.94–1.82 (m, 2H) 1.38 (s, 3H), 1.33 (s, 3H);  $^{13}\text{C}$  NMR (75 MHz, 293 K,  $\text{CDCl}_3$ )  $\delta$  202.0, 175.7, 136.2, 133.1, 128.7, 128.3, 62.3, 60.8, 51.8, 43.1, 39.0, 34.7, 33.9, 21.0, 19.0; HRMS ( $\text{ES}^+$ ) calc'd for  $\text{C}_{17}\text{H}_{20}\text{O}_4\text{Na}$  ( $\text{M}^+ \text{Na}$ ) 311.1259; found 311.1251  $m/z$ .



**Preparation of 143:** 2,3-dimethyl-1,3-butadiene (2.1 mL, 18.40 mmol) was added to a solution of **Z43** (350.1 mg, 1.840 mmol) in  $\text{CH}_2\text{Cl}_2$  (18.5 mL) at 23  $^\circ\text{C}$  under a nitrogen atmosphere. The solution was cooled to  $-78$   $^\circ\text{C}$  followed by the addition  $\text{AlCl}_3$  (49.1 mg, 0.3680 mmol). The solution was allowed to warm to  $-74$   $^\circ\text{C}$  over 2.0 h then was quenched with 3 M HCl (2 mL). The layers were separated and the aqueous layer was extracted with  $\text{CH}_2\text{Cl}_2$  (25 mL  $\times$  2). The combined organic layers were then washed with water (25 mL  $\times$  1) and then stirred with 1M  $\text{Na}^+, \text{K}^+$  tartrate (1 mL) for 30 min at 23  $^\circ\text{C}$ . The layers were then separated and the organic layer was washed with water (25 mL  $\times$  1), brine (25 mL  $\times$  1), dried over  $\text{Na}_2\text{SO}_4$ , filtered, and concentrated under reduced pressure. The resulting oil was purified by silica gel (6 mL) chromatography (5  $\rightarrow$  20 % EtOAc in hexanes) to afford **143** (431 mg, 86 % yield) as a yellow oil;  $R_f$  0.34 (15 % EtOAc in hexanes); IR (film) 3059, 2917, 2856 1735 (C=O), 1683 (C=O), 1596, 1579, 1445, 1379, 1356, 1288, 1221, 1118, 1021, 969, 762, 698  $\text{cm}^{-1}$ ;  $^1\text{H}$  NMR (300 MHz, 293K,  $\text{CDCl}_3$ )  $\delta$  7.85 (m, 2H), 7.55 (tt, 1H,  $J = 7.3, 1.4$  Hz), 7.45 (m, 2H), 3.90 (dt, 1H,  $J = 3.9, 6.5$  Hz), 3.62 (s, 3H), 3.00 (dt, 1H,  $J = 3.9, 6.6$  Hz), 2.67–2.60 (m, 1H), 2.41–2.38 (m, 3H), 1.66 (br s, 3H), 1.58 (br s, 3H);  $^{13}\text{C}$  NMR (75 MHz, 293 K,  $\text{CDCl}_3$ )  $\delta$  201.7, 174.1, 136.9, 132.5, 128.5, 128.2, 124.3, 123.0, 51.6, 42.6, 40.6, 32.5, 32.2, 18.9, 18.9; HRMS ( $\text{ES}^+$ ) calc'd for  $\text{C}_{17}\text{H}_{20}\text{O}_3\text{Na}$  ( $\text{M}^+ \text{Na}$ ) 295.1310; found 295.1316  $m/z$ .



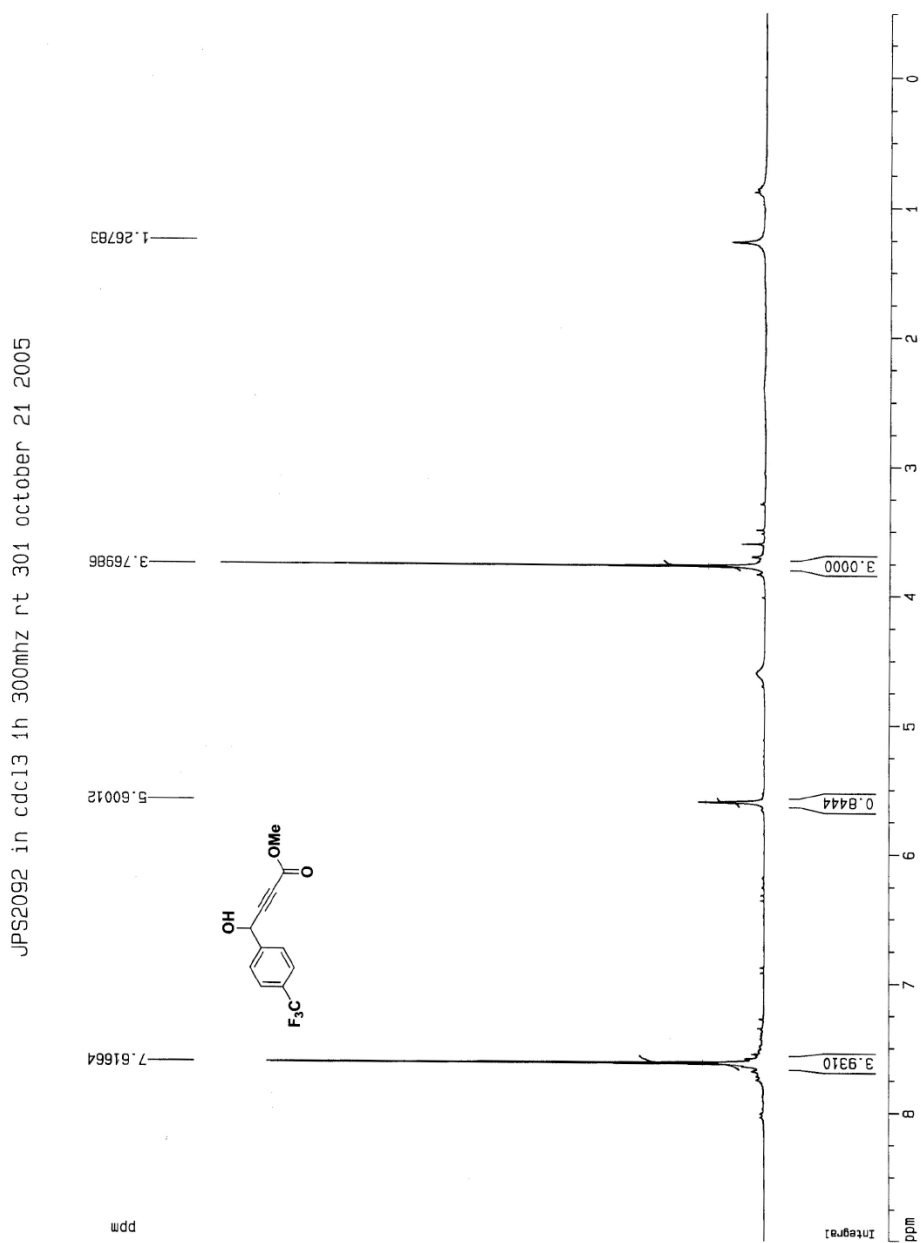
**Preparation of 145:** *m*CPBA (70 % purity, 310 mg, 1.250 mmol) dissolved in CH<sub>2</sub>Cl<sub>2</sub> (3.0 mL) was added in 1.0 equiv increments, to a solution of **143** (64.9 mg, 0.2500 mmol) in CH<sub>2</sub>Cl<sub>2</sub> (0.5 mL) at 0 °C. until the epoxide intermediate was consumed. The solution was allowed to warm to 16 °C over 51.0 h and then was quenched with 2-methyl-2-butene (140 μL, 1.300 mmol). 1,4 dioxane (3 mL) and concentrated NaHCO<sub>3</sub> (3 mL) were then added to the solution and the resulting mixture was stirred overnight. 1,4-dioxane was then removed under reduced pressure and the aqueous layer was extracted with Et<sub>2</sub>O (4 mL × 3) and EtOAc (4.0 mL × 1). The combined organic layers were washed with water (4 mL × 1), brine (4 mL × 1), dried over Na<sub>2</sub>SO<sub>4</sub>, filtered, and concentrated under reduced pressure. The resulting residue was purified by medium-pressure silica gel chromatography (0 → 80 % EtOAc in hexanes) to afford the corresponding **145** as a pale yellow oil; *R<sub>f</sub>* 0.33 (60 % EtOAc in hexanes); IR (film) 3500, 2953, 2853, 1782 (C=O), 1759 (C=O), 1736 (C=O), 1456, 1255, 1202, 1146, 1086, 927 cm<sup>-1</sup>; <sup>1</sup>H NMR (300 MHz, 293K, CDCl<sub>3</sub>) δ 3.73 (s 3H), 3.13–3.10 (m, 1H), 2.92 (dddd, 1H *J* = 11.6, 8.1, 6.3, 1.8 Hz), 2.55 (d, 1H, *J* = 12.1 Hz), 2.03–1.94 (m, 3H), 1.43, (s, 3H), 1.32 (s, 3H); <sup>13</sup>C NMR (75 MHz, 293 K, CDCl<sub>3</sub>) δ 175.9, 172.1, 87.2, 77.2, 52.2, 42.6, 40.0, 38.7, 37.1, 25.1, 18.9; HRMS (ES<sup>+</sup>) calc'd for C<sub>11</sub>H<sub>16</sub>O<sub>5</sub> (M<sup>+</sup> Na) 251.0895; found 251.0898 *m/z*.



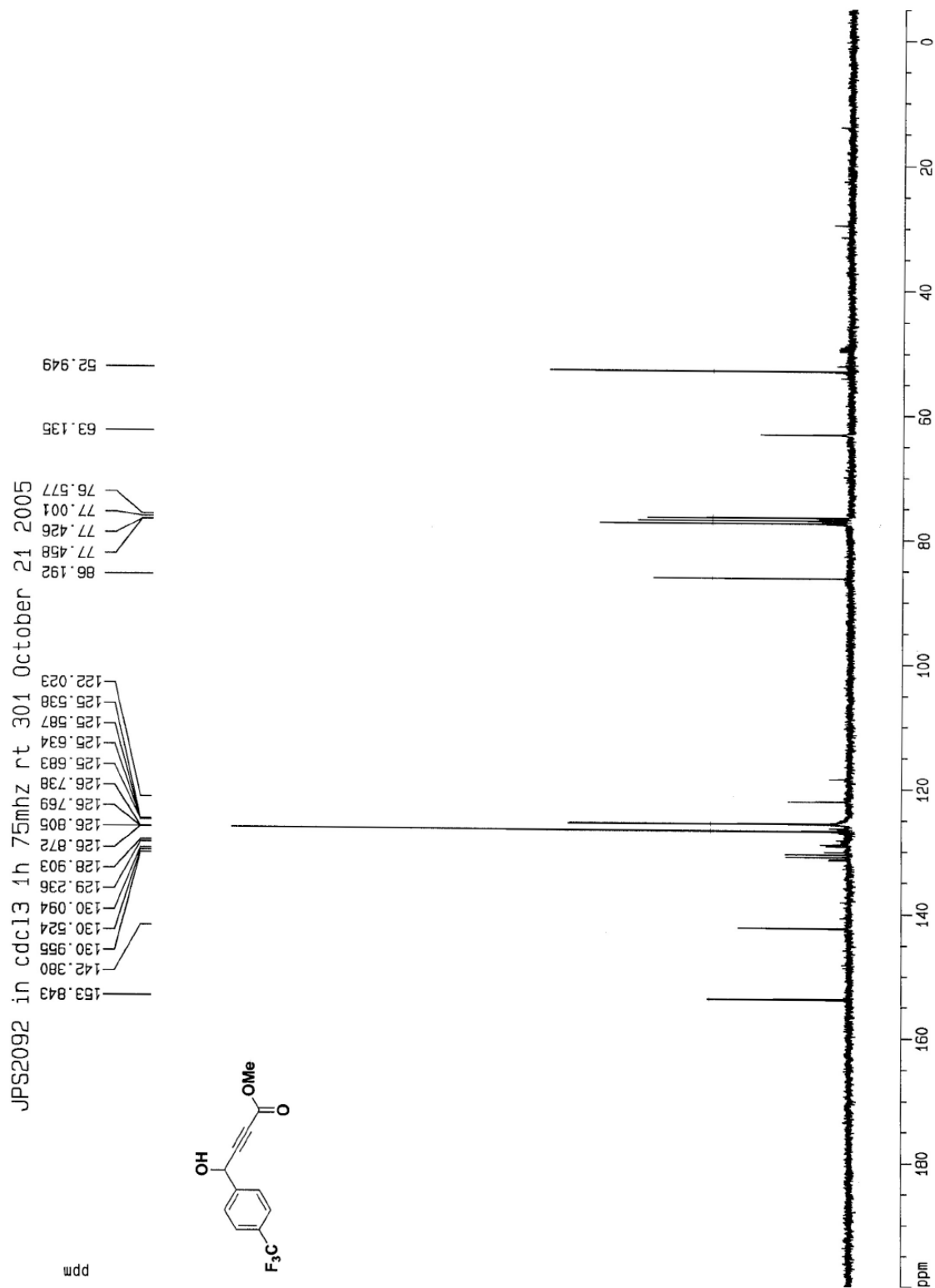
**Preparation of 147:** Enyne **63** (324.7 mg, 1.41 mmol) in degassed (CH<sub>2</sub>Cl)<sub>2</sub> (8.1 mL) was added to a solution of [RhCl(CO)<sub>2</sub>]<sub>2</sub> (6.2 mg 0.0141 mmol) in degassed (CH<sub>2</sub>Cl)<sub>2</sub> (6.0 mL) at 23°C under a CO atmosphere. The reaction mixture is then stirred at 80°C for 15 h, then cooled to 23°C, and concentrated under reduced pressure. The resulting oil was purified by silica gel (30 mL) chromatography (15 → 60 % EtOAc in hexanes) to afford **147** (106.0 mg, 24 % yield) as a yellow solid. Further purification was performed via preparative HPLC (C<sub>18</sub>-reverse phase, *t<sub>R</sub>* = 17.8 min 5 → 95 % CH<sub>3</sub>CN in water) for biological testing; *R<sub>f</sub>* 0.29 (60 % EtOAc in hexanes); IR (film) 2923, 2853, 1716 (C=O), 1650 (C=O), 1453, 1322, 1224, 1018, 698 cm<sup>-1</sup>; <sup>1</sup>H NMR (300 MHz, 293K, CD<sub>3</sub>CN) δ 7.47-7.33 (m, 5H), 5.89 (br s, 1H), 4.48 (br t, 1H, *J* = 0.9, 8.1, 8.1 Hz), 3.68 (s, 3H), 3.68-3.60 (m, 1H), 3.43 (dd, 1H, *J* = 7.9, 11.1 Hz), 2.69 (dd, 1H, *J* = 6.6, 17.7 Hz), 2.34 (ddd, 1H, *J* = 0.7, 3.8, 17.7 Hz); <sup>13</sup>C NMR (75 MHz, 293 K, CD<sub>3</sub>CN) δ 203.3, 194.2, 162.6, 139.6, 129.5, 129.4, 129.3, 128.4, 79.6, 71.3, 52.0, 44.4, 41.0; HRMS (ES<sup>+</sup>) calc'd for C<sub>17</sub>H<sub>20</sub>O<sub>3</sub> (M<sup>+</sup> Na) 281.0790; found 281.0779 *m/z*.

## 5.0 $^1\text{H}$ AND $^{13}\text{C}$ NMR SPECTRA

$^1\text{H}$  NMR spectrum of **93**:  $\text{CDCl}_3$ , 293 K, 300 MHz

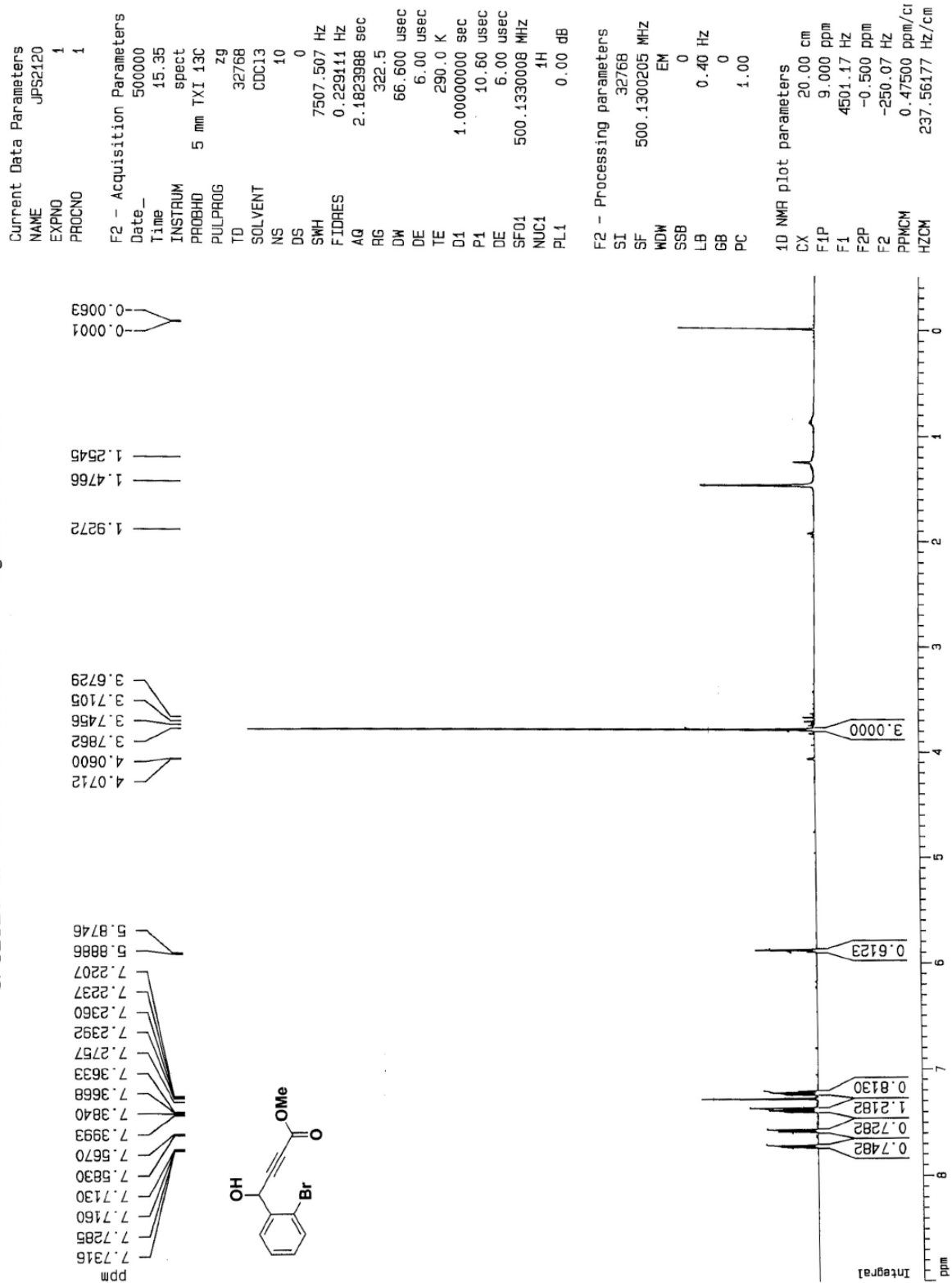


$^{13}\text{C}$  NMR of **93**:  $\text{CDCl}_3$ , 293 K, 75 MHz



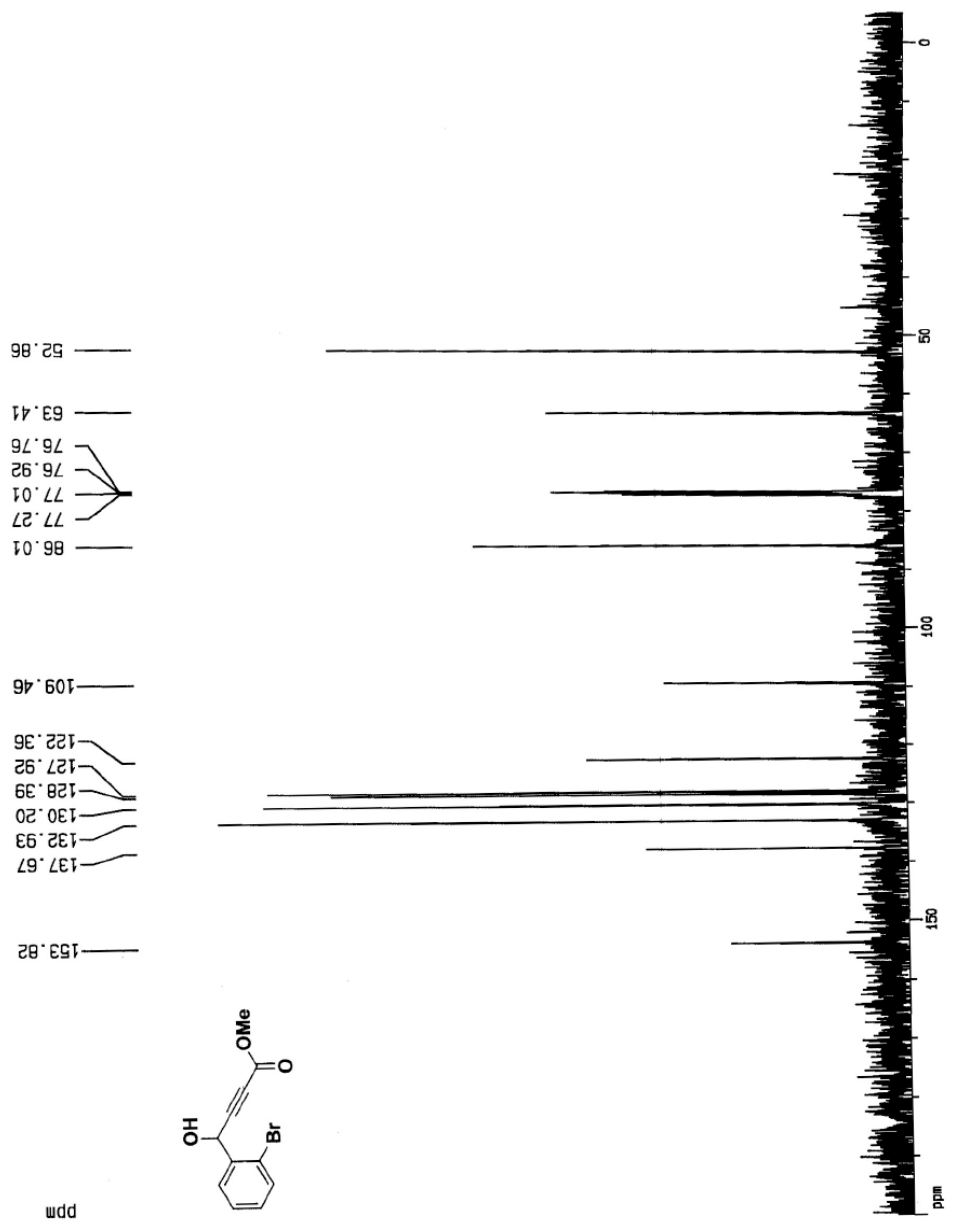
<sup>1</sup>H NMR spectrum of **95**: CDCl<sub>3</sub>, 293 K, 500 MHz

JPS2120 in cdcl3 1h 500mhz rt August 23 2005



<sup>13</sup>C NMR spectrum of **95**: CDCl<sub>3</sub>, 293 K, 125 MHz

JPS2120 in cdc13 13c 125mhz rt 500 December 12 2005



Current Data Parameters  
 NAME JPS2120  
 EXPNO 2  
 PROCNO 1

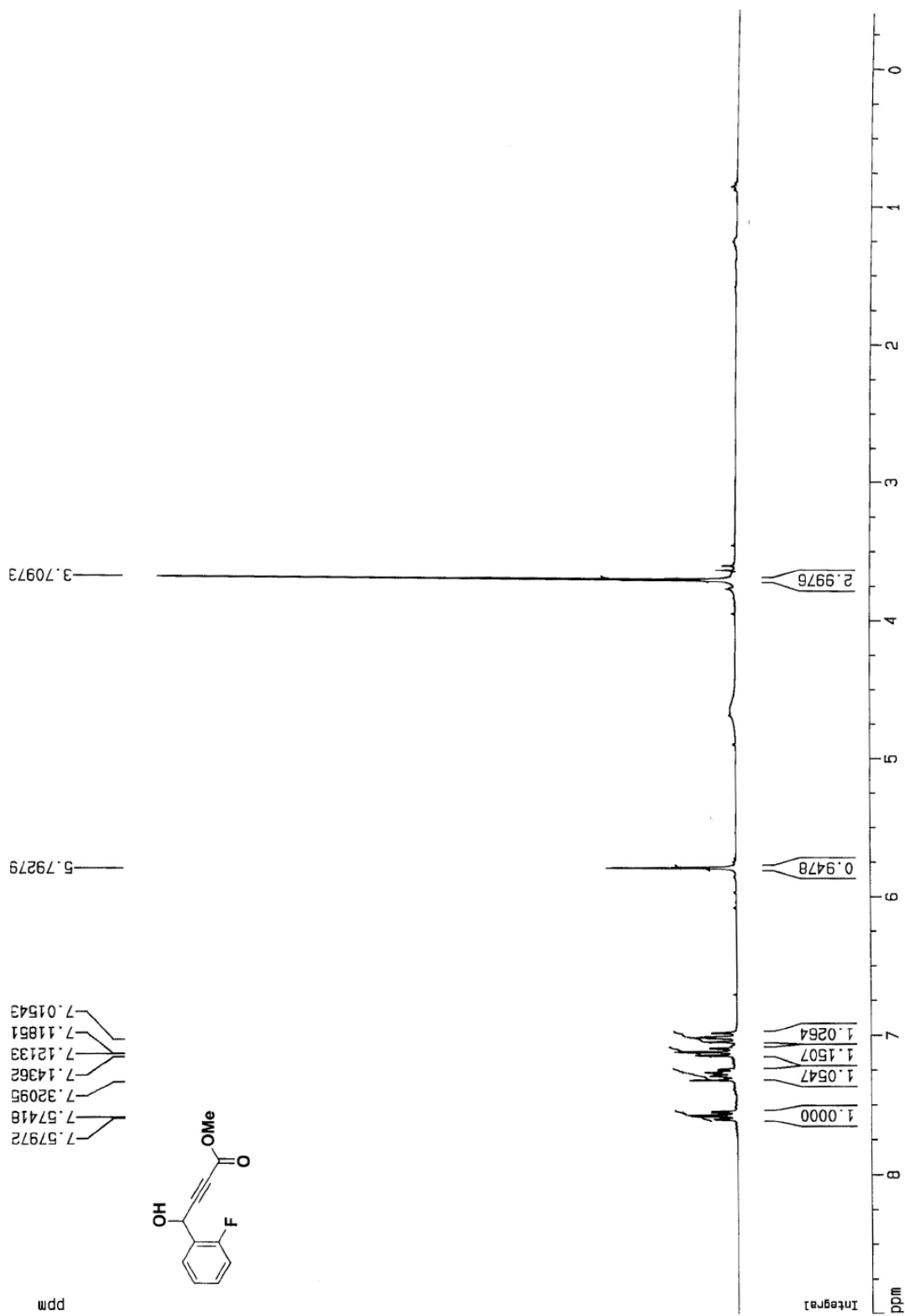
F2 - Acquisition Parameters  
 Date\_ 500000  
 Time 15.34  
 INSTRUM spect  
 PROBHD 5 mm TXI 13C  
 PULPROG c13winoe  
 TD 32768  
 SOLVENT CDCl3  
 NS 44  
 DS 0  
 SWH 32679.738 Hz  
 FIDRES 0.997305 Hz  
 AQ 0.5014004 sec  
 RG 8192  
 DW 15.300 usec  
 DE 6.00 usec  
 TE 290.0 K  
 D3 0.00100000 sec  
 PL12 6.00 dB  
 D1 6.00000000 sec  
 CPDPRG2 waltz16  
 PCPD2 100.00 usec  
 SF02 500.1330008 MHz  
 NUC2 1H  
 PL2 120.00 dB  
 P1 21.60 usec  
 DE 6.00 usec  
 SF01 125.7745724 MHz  
 NUC1 13C  
 PL1 0.00 dB

F2 - Processing parameters  
 SI 8192  
 SF 125.7578080 MHz  
 WDW EM  
 SSB 0  
 LB 4.00 Hz  
 GB 0  
 PC 1.00

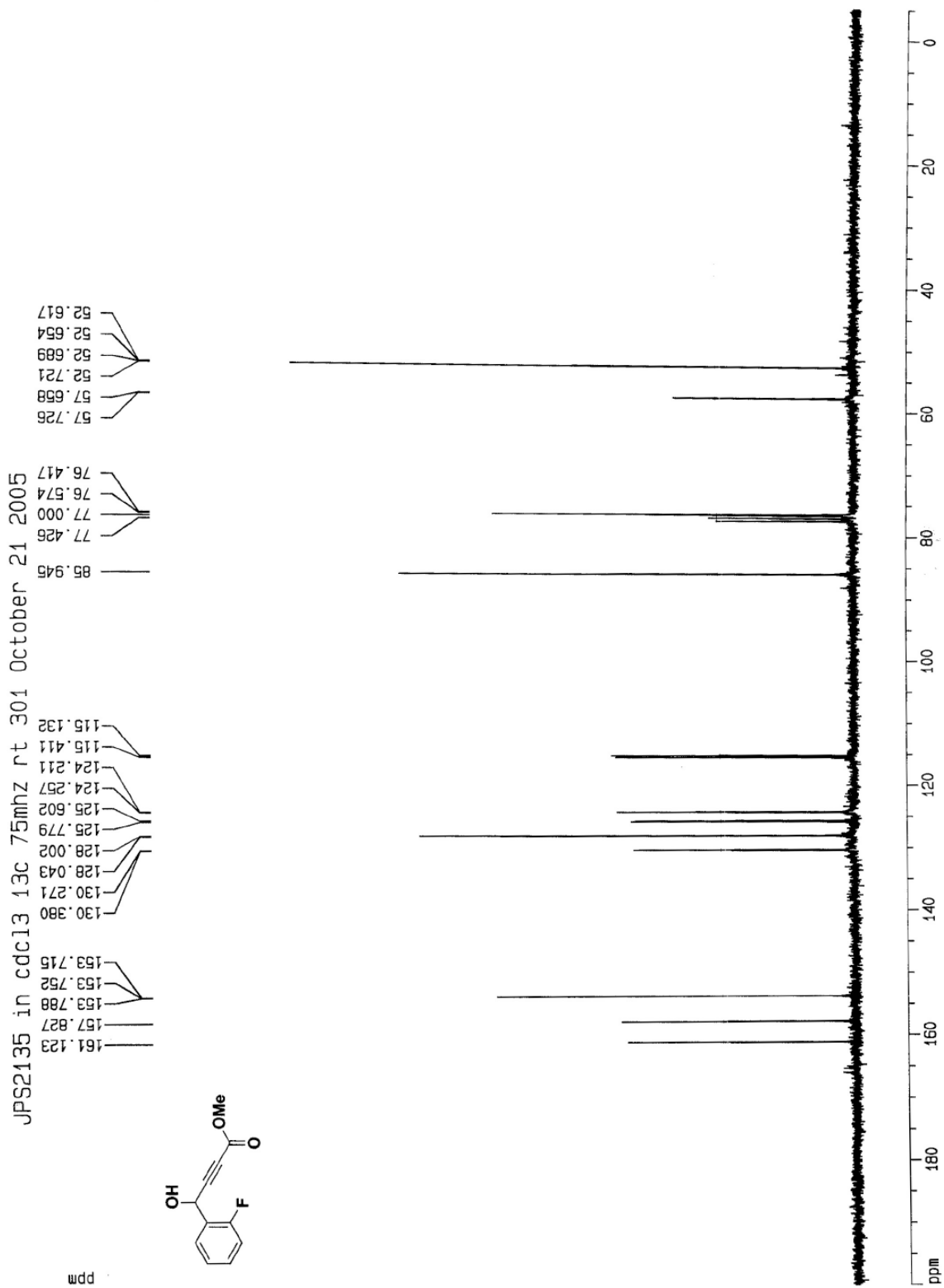
1D NMR plot parameters  
 CX 20.00 cm  
 F1P 200.000 ppm  
 F1 25151.56 Hz  
 F2P -5.000 ppm  
 F2 -628.79 Hz  
 PPMCM 10.25000 ppm/cm  
 HZCM 1289.01758 Hz/cm

<sup>1</sup>H NMR spectrum of **97**: CDCl<sub>3</sub>, 293 K, 300 MHz

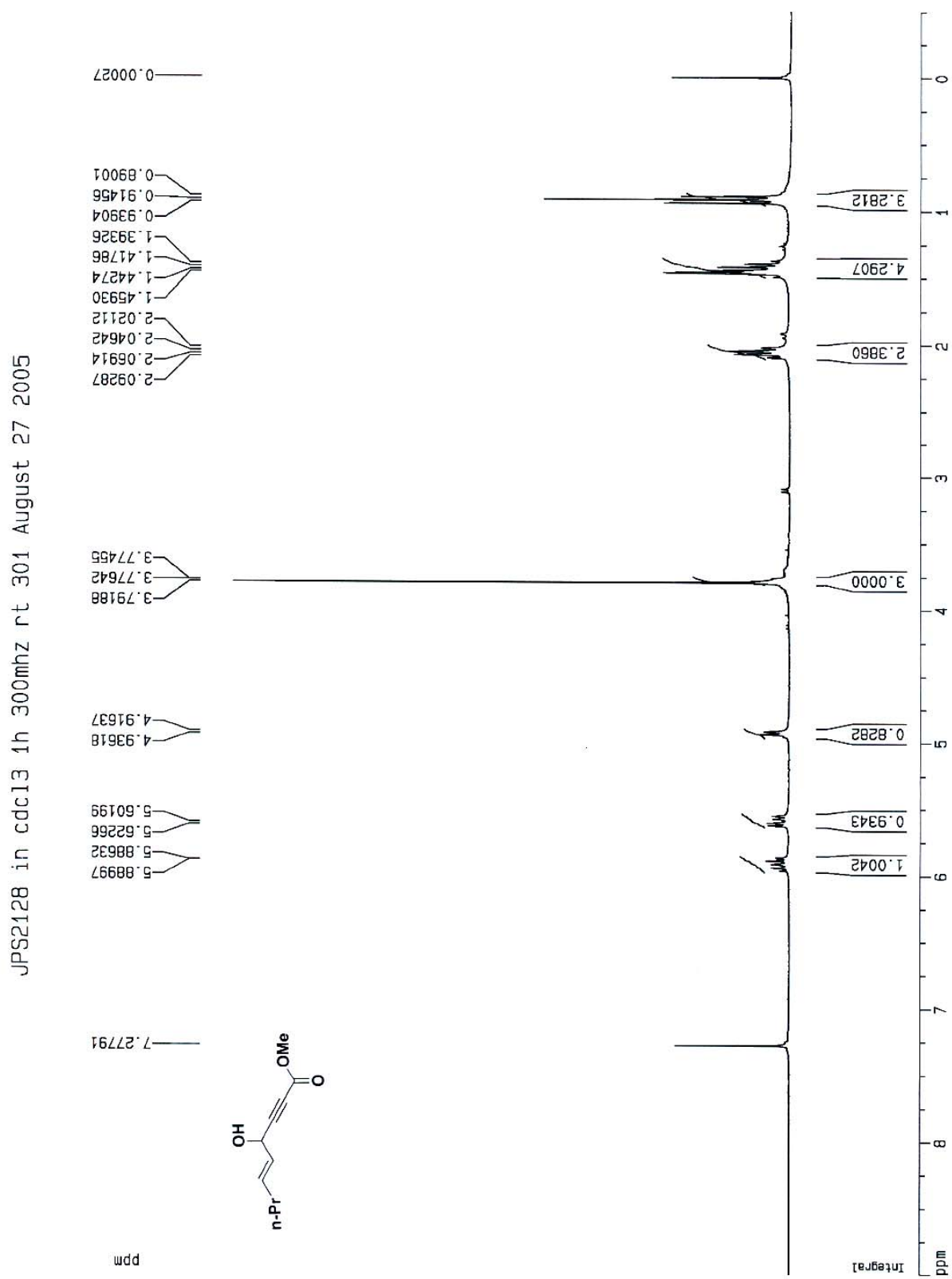
JPS2135 in cdcl3 1h 300mhz rt 301 October 21 2005



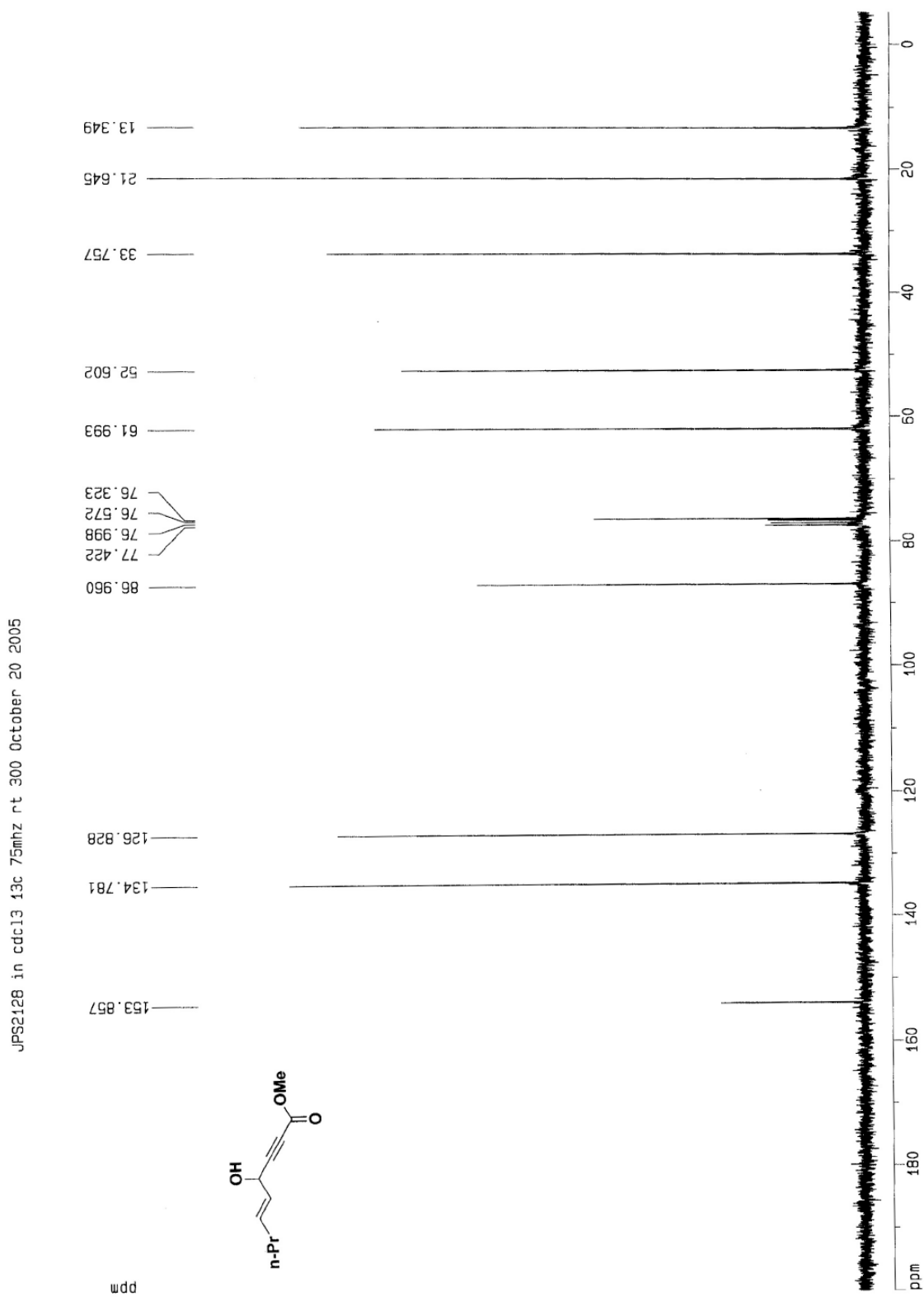
$^{13}\text{C}$  NMR spectrum of **97**:  $\text{CDCl}_3$ , 293 K, 75 MHz



<sup>1</sup>H NMR spectrum of **103**: CDCl<sub>3</sub>, 293 K, 300 MHz

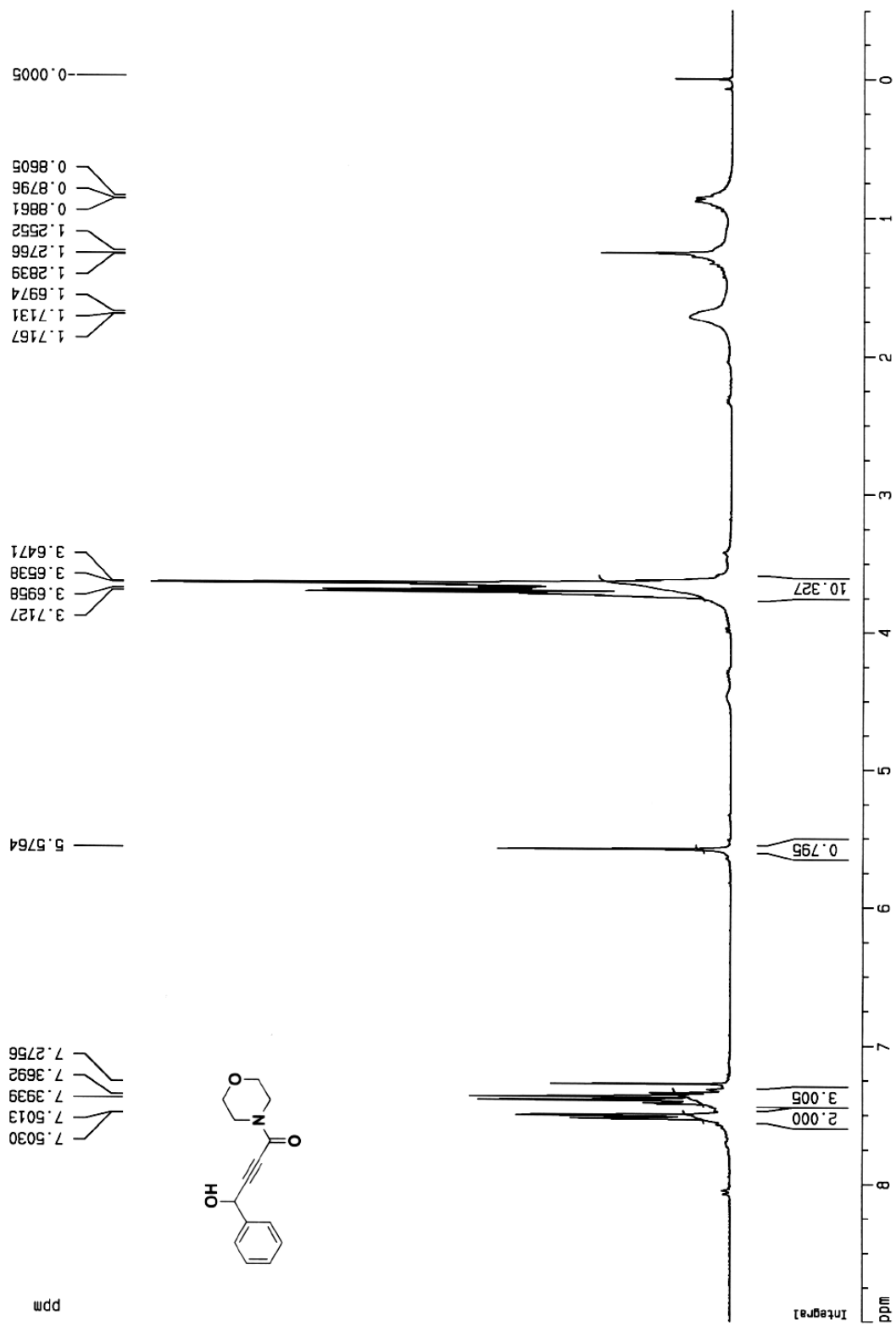


$^{13}\text{C}$  NMR spectrum of **103**:  $\text{CDCl}_3$ , 293 K, 75 MHz

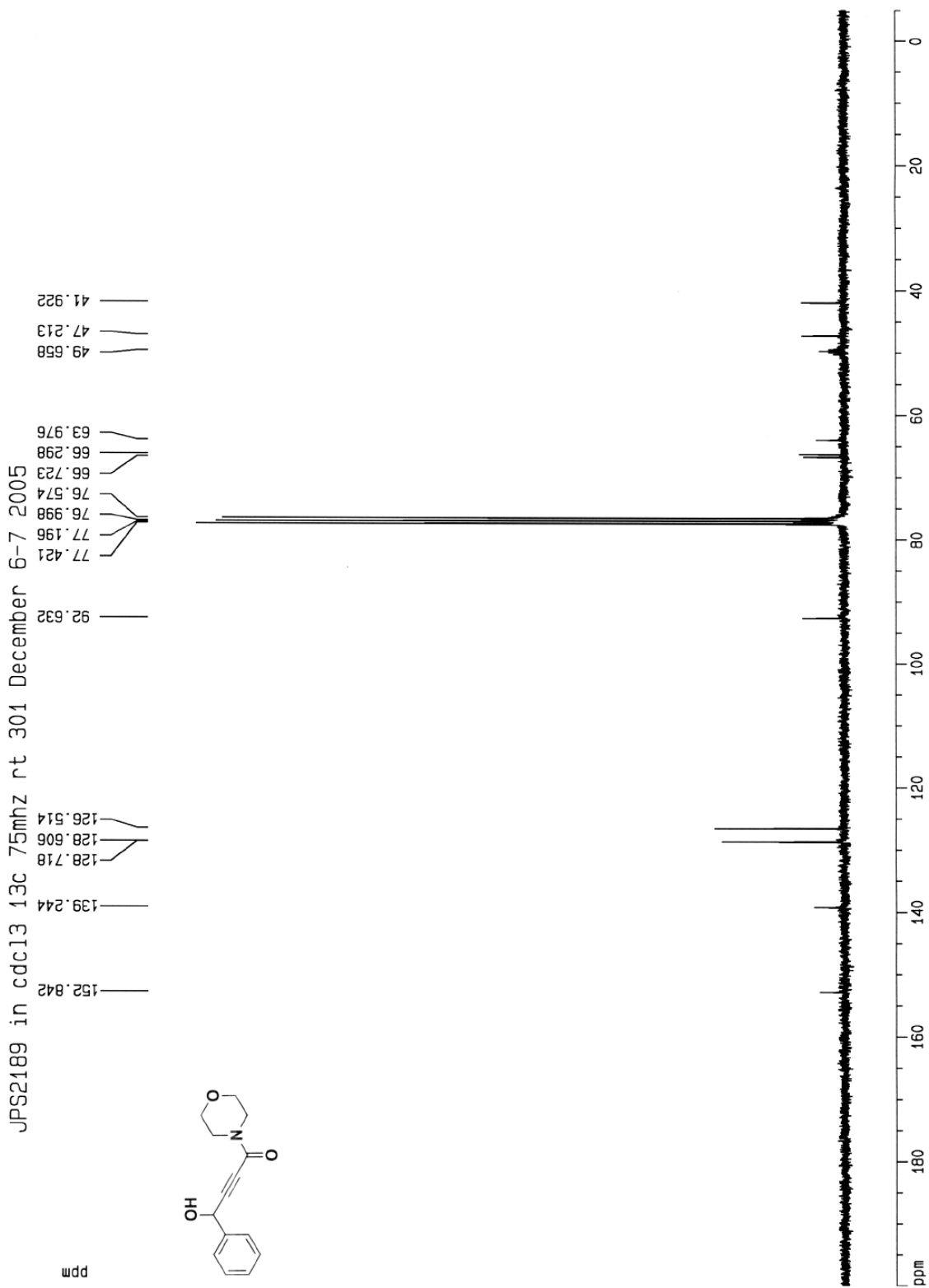


<sup>1</sup>H NMR spectrum of **111**: CDCl<sub>3</sub>, 293 K, 300 MHz

JPS2189 in cdc13 1h 300mhz rt 301 December 6 2005

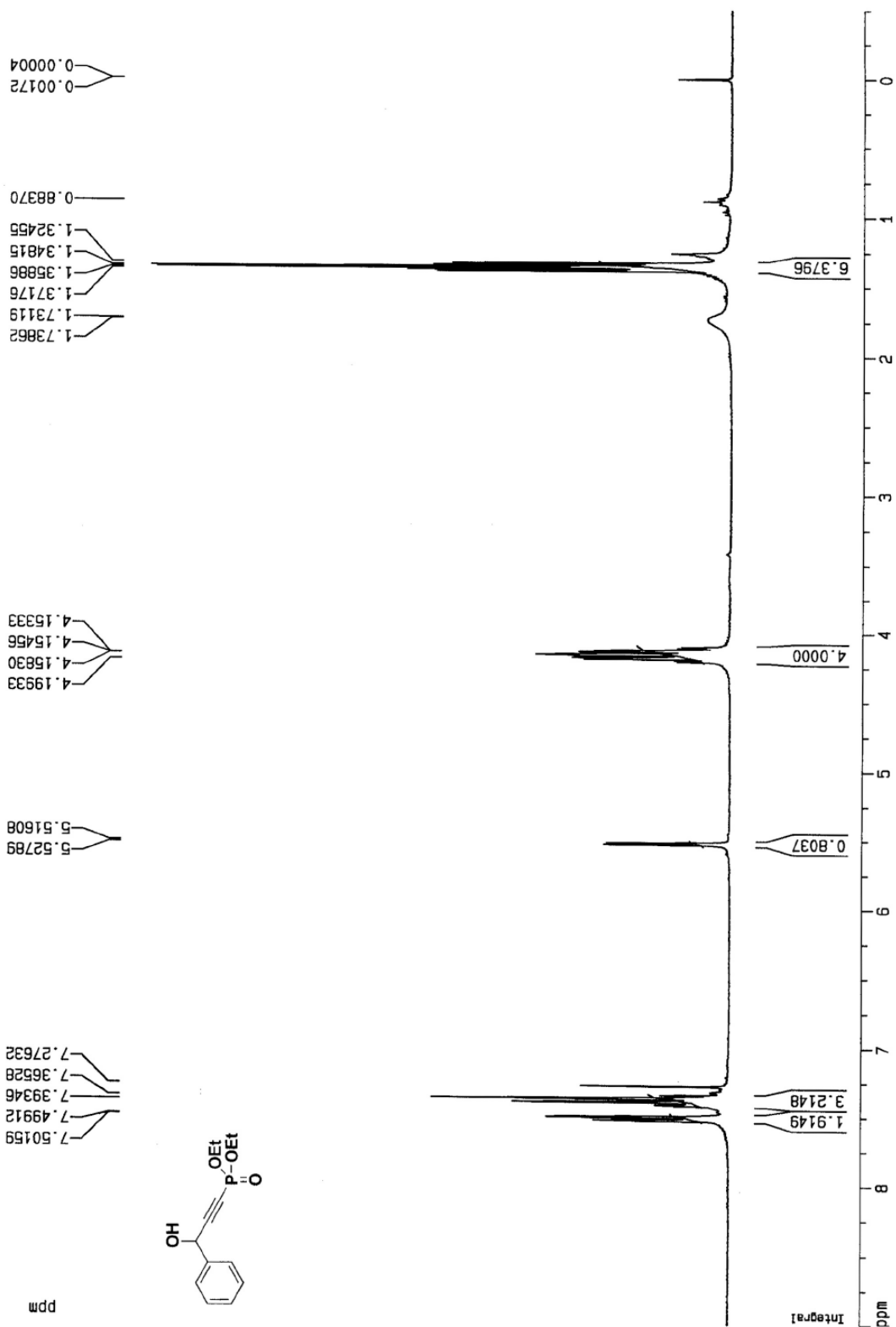


$^{13}\text{C}$  NMR spectrum of **111**:  $\text{CDCl}_3$ , 293 K, 75 MHz

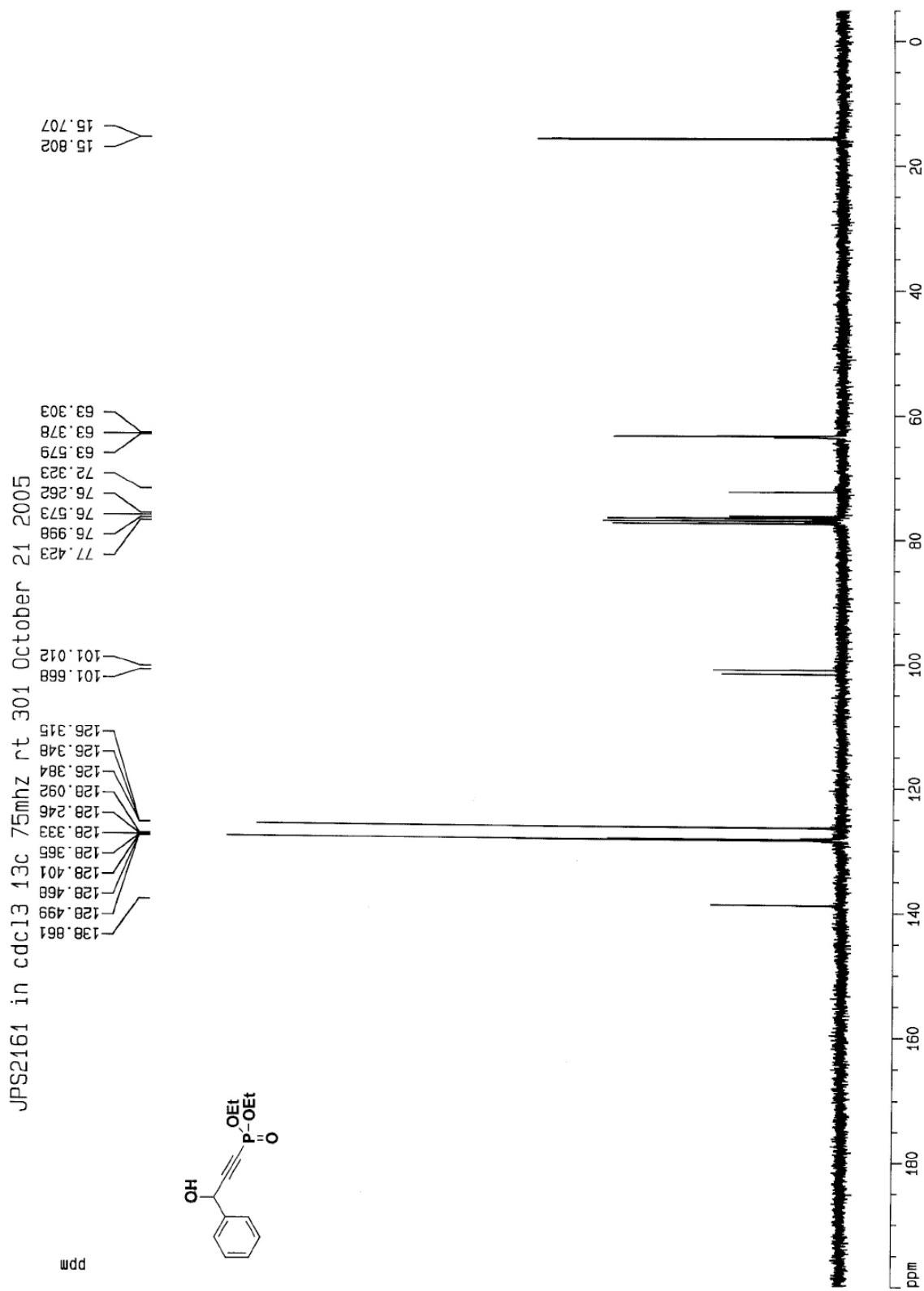


<sup>1</sup>H NMR spectrum of **115**: CDCl<sub>3</sub>, 293 K, 300 MHz

JPS2161 in cdc13 1h 300mhz rt 301 December 6 2005



$^{13}\text{C}$  NMR spectrum of **115**:  $\text{CDCl}_3$ , 293 K, 125 MHz



HMBC of **E43**: CDCl<sub>3</sub>, 293 K, 500 MHz.

Current Data Parameters  
 NAME JPS2142T  
 EXPNO 4  
 PROCNO 1

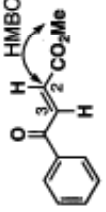
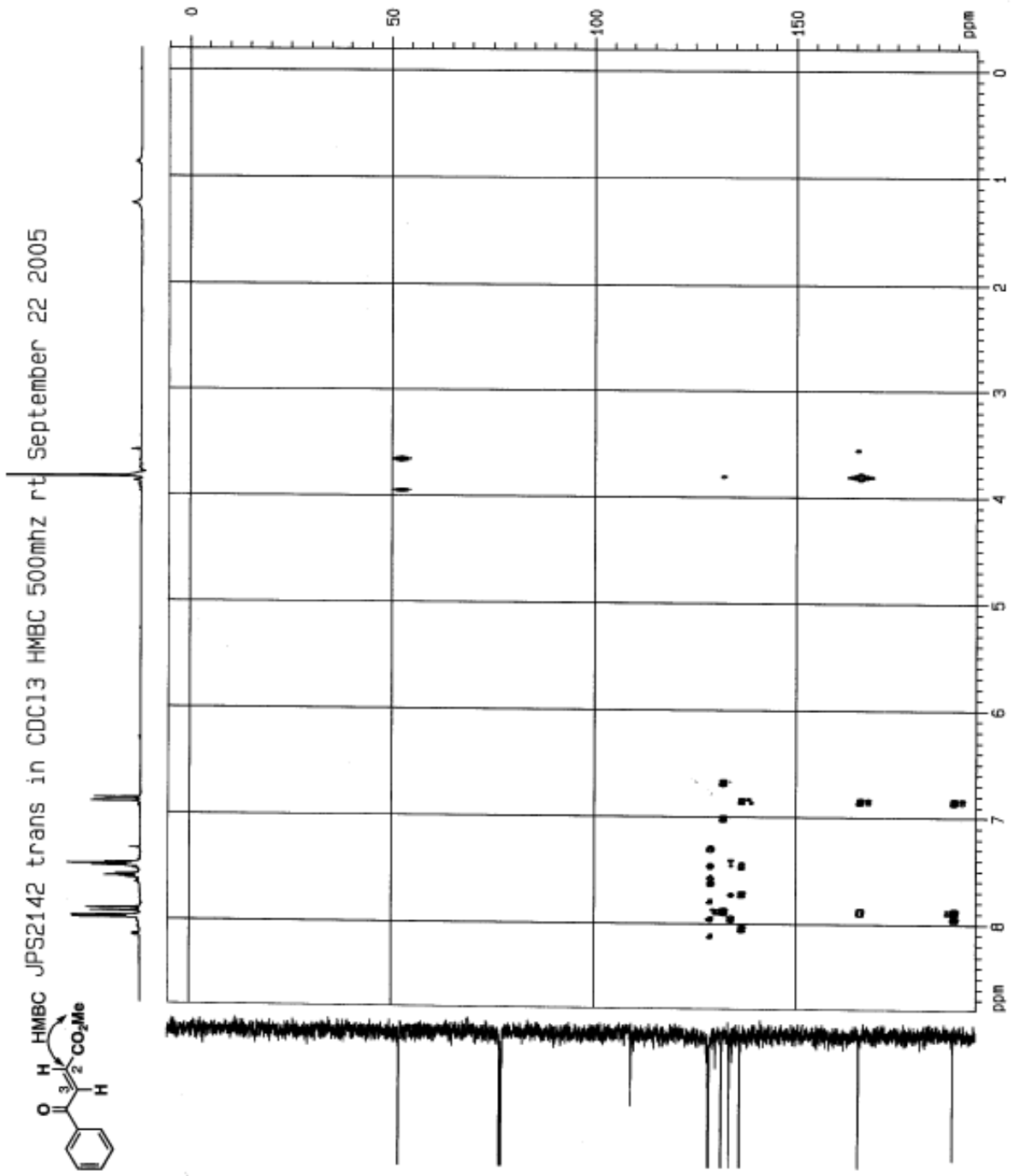
F2 - Acquisition Parameters  
 Date\_ 500000  
 Time 15.18  
 INSTRUM spect  
 PULPROG zgpg30  
 PALPROG Inv4puls  
 TO 4095  
 SOLVENT CDCl3  
 NS 16  
 DS 16  
 SWH 4456.403 Hz  
 FIDRES 1.267755 Hz  
 AQ 0.482528 sec  
 RG 32708  
 DM 111.200 uSAC  
 DE 6.00 uSAC  
 TE 310.3 K  
 F1 19.09 uSAC  
 PC 21.2 uSAC  
 GC 0.000000 sec  
 GZ 0.000000 sec  
 SI 1.000000 sec  
 SF 6.1000000 MHz  
 SW 15.00 uSAC  
 SF02 125.7629000 MHz  
 NU22 128  
 PL2 -8.00 dB  
 P16 1000.00 uSAC  
 D16 0.0000000 sec  
 DE 6.00 uSAC  
 SF04 500.1321000 MHz  
 MUX1 1H  
 PL1 0.00 dB  
 IN3 0.00001000 sec

F1 - Acquisition parameters  
 MD 2  
 TO 266  
 SF01 525.7807 MHz  
 FIDRES 08.268256 Hz  
 SN 200.004 ppm

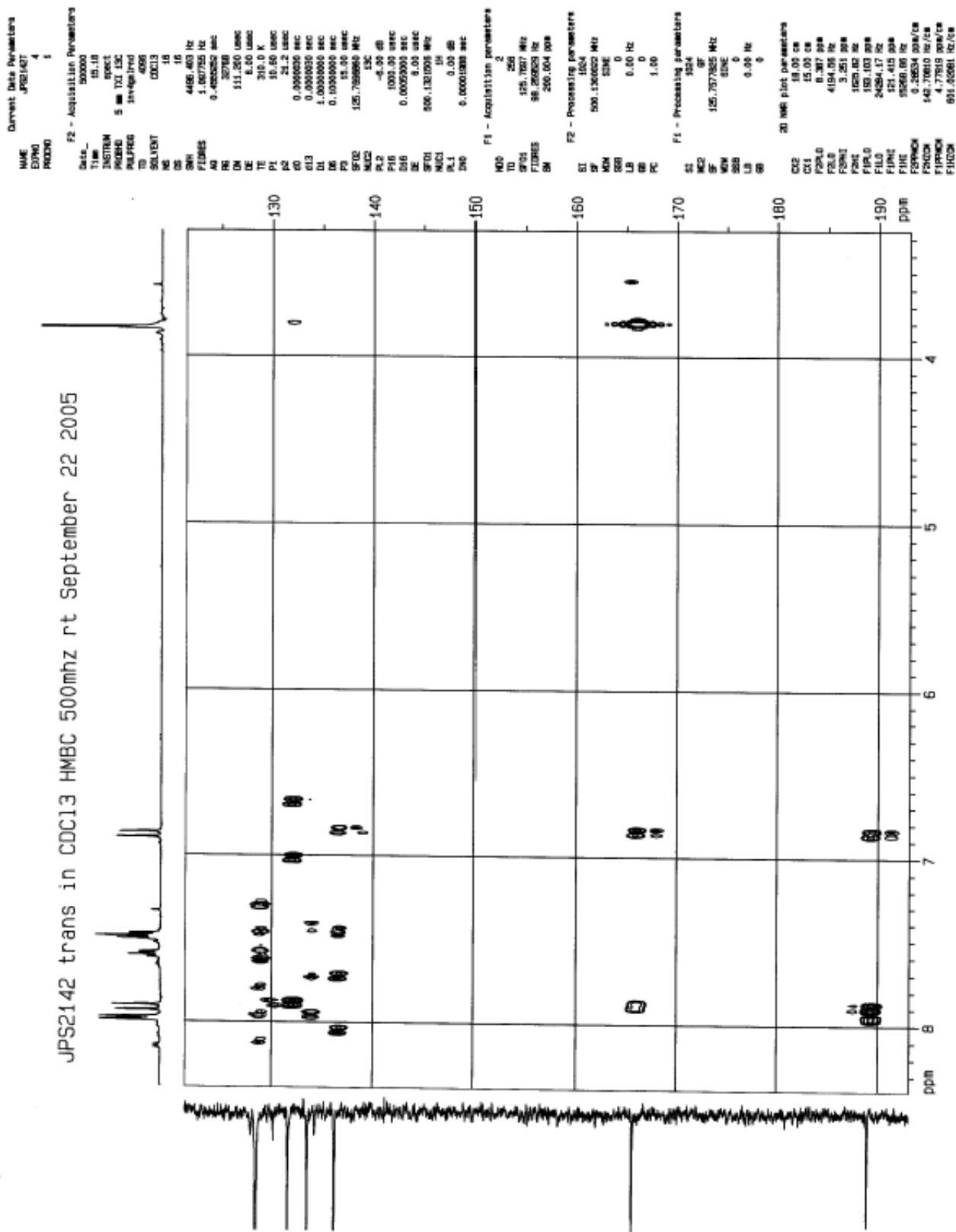
F2 - Processing parameters  
 SI 1624  
 SF 500.1300000 MHz  
 WDM 0  
 SINE 0  
 LB 0.00 Hz  
 GB 0  
 PC 1.00

F1 - Processing parameters  
 SI 1624  
 SF 125.7627000 MHz  
 WDM 0  
 SINE 0  
 LB 0.00 Hz  
 GB 0

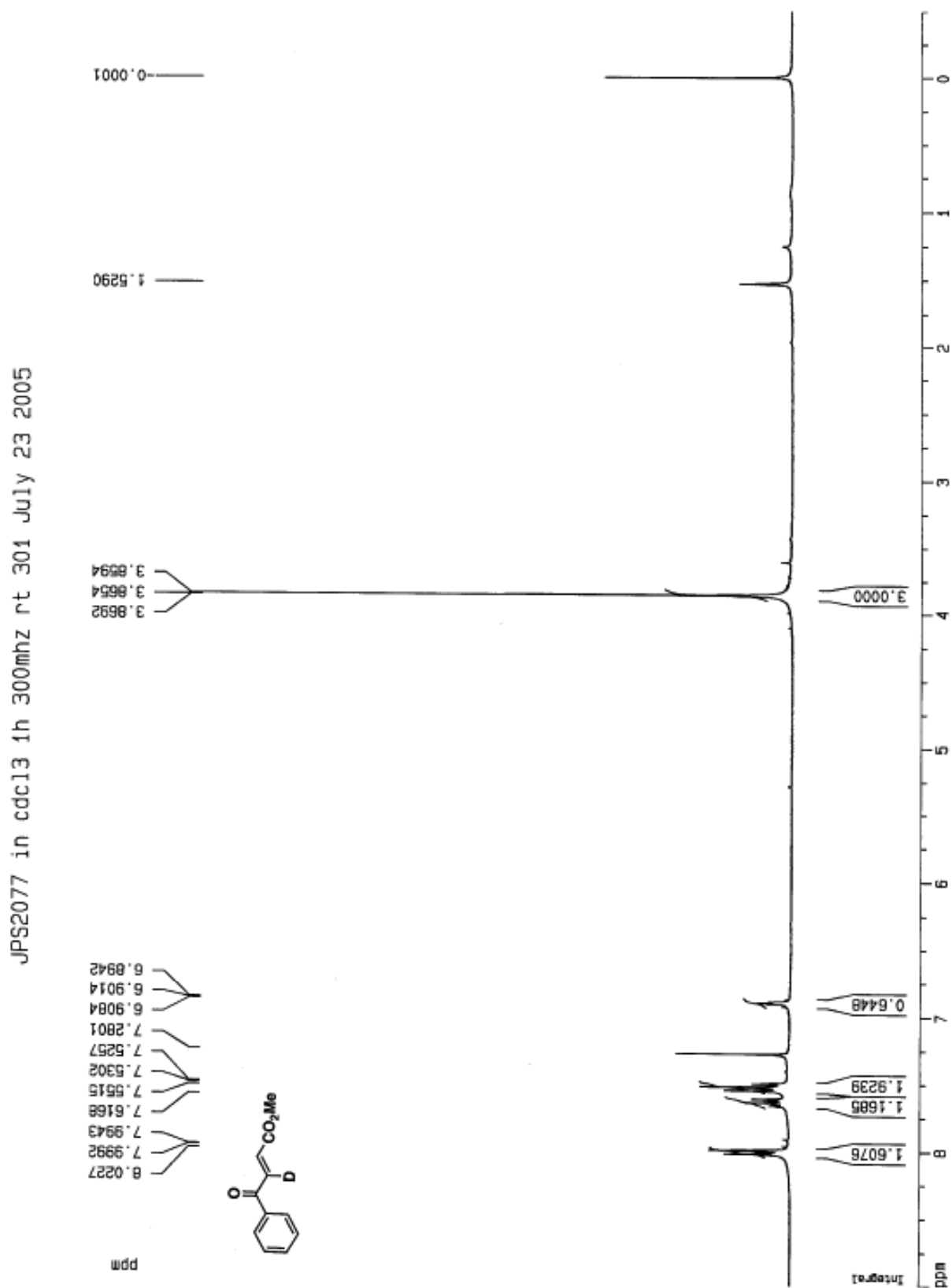
2D NMR plot parameters  
 CQ2 10.00 cm  
 CX1 15.00 cm  
 F2PQ0 0.791 ppm  
 F3LQ0 4350.05 Hz  
 F2PQ1 -0.200 ppm  
 F3PQ1 -59.80 Hz  
 F1PQ0 194.655 ppm  
 F1LQ0 24480.00 Hz  
 F1PQ1 -6.200 ppm  
 F1LQ1 -673.70 Hz  
 F2PQ0M 0.43847 ppm/cm  
 F2PQ1M 245.80016 Hz/cm  
 F1PQ0M 13.20486 ppm/cm  
 F1LQ0M 1075.38522 Hz/cm



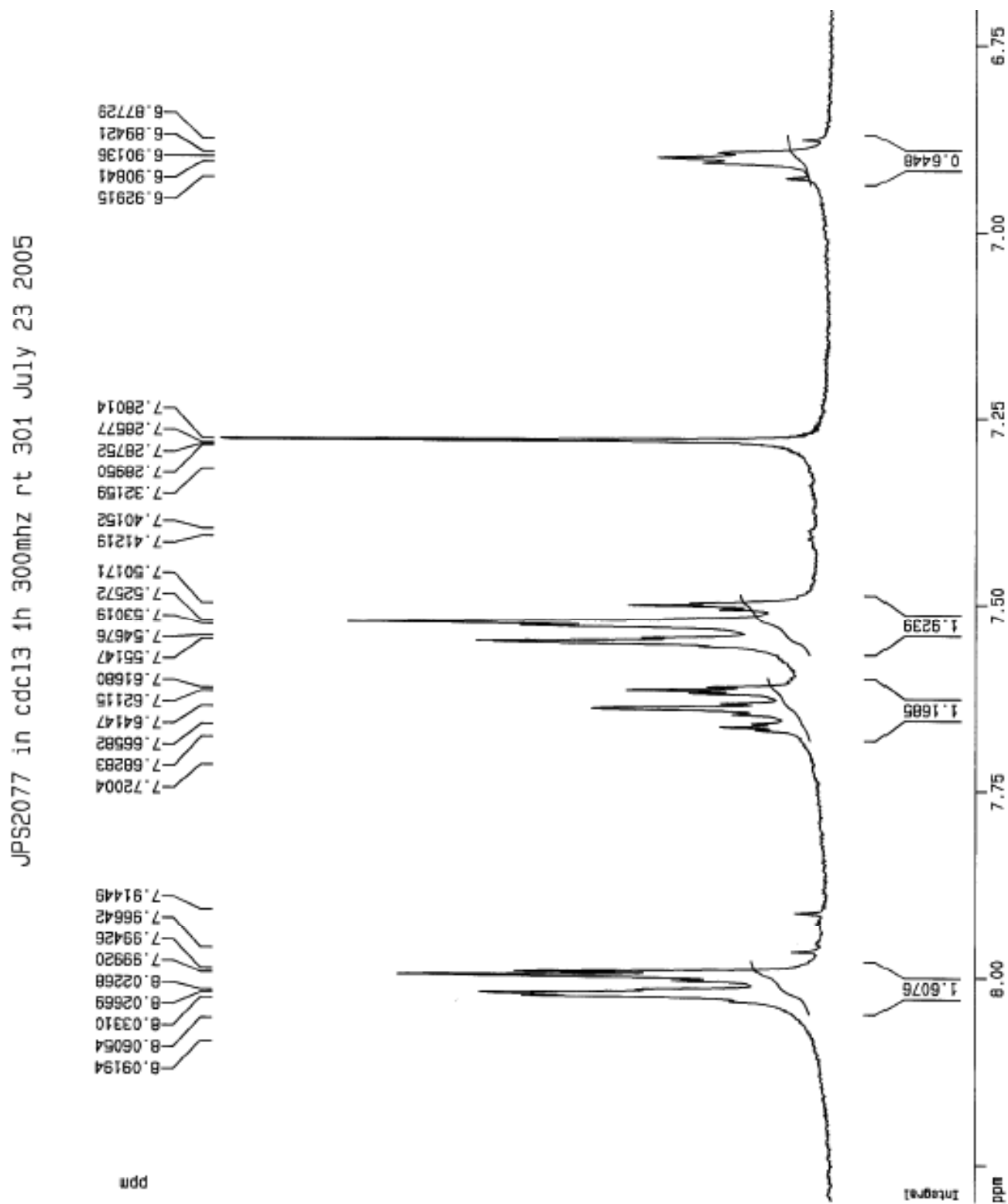
HMBC of **E43**: CDCl<sub>3</sub>, 293 K, 500 MHz.



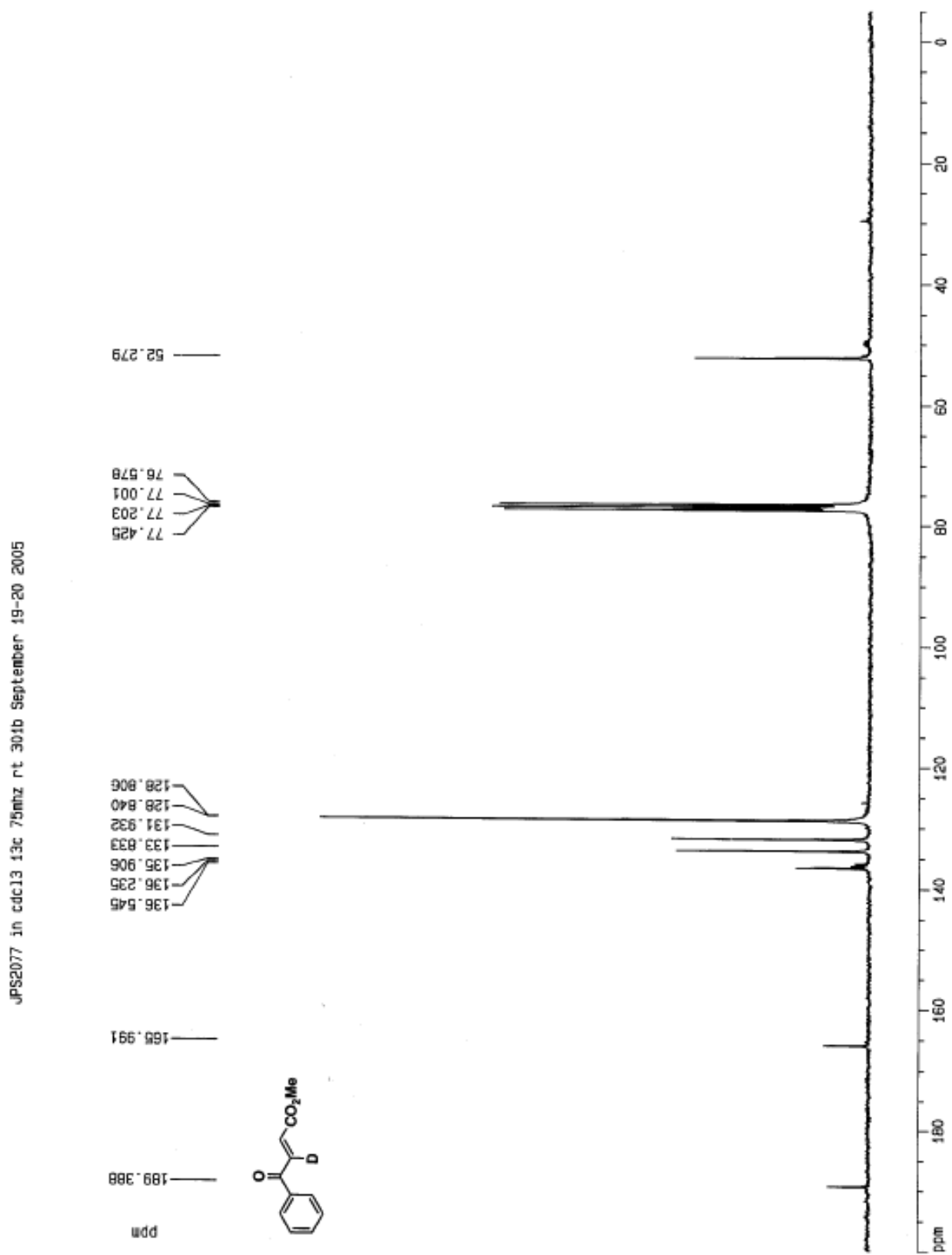
$^1\text{H}$  NMR of **3d-E43**:  $\text{CDCl}_3$ , 293 K, 300 MHz.



$^1\text{H}$  NMR of **3d-E43**:  $\text{CDCl}_3$ , 293 K, 300 MHz.

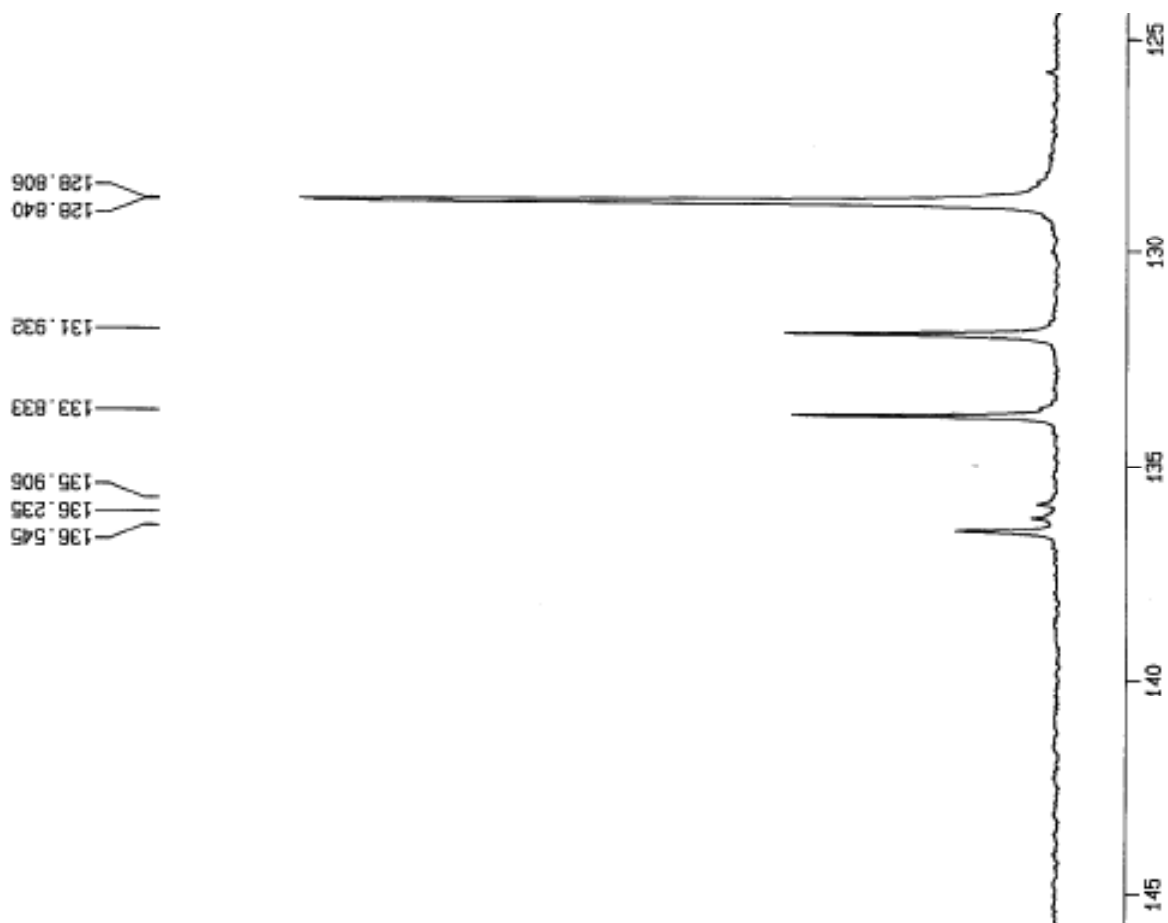


$^{13}\text{C}$  NMR spectrum of **3d-E43**:  $\text{CDCl}_3$ , 293 K, 125 MHz



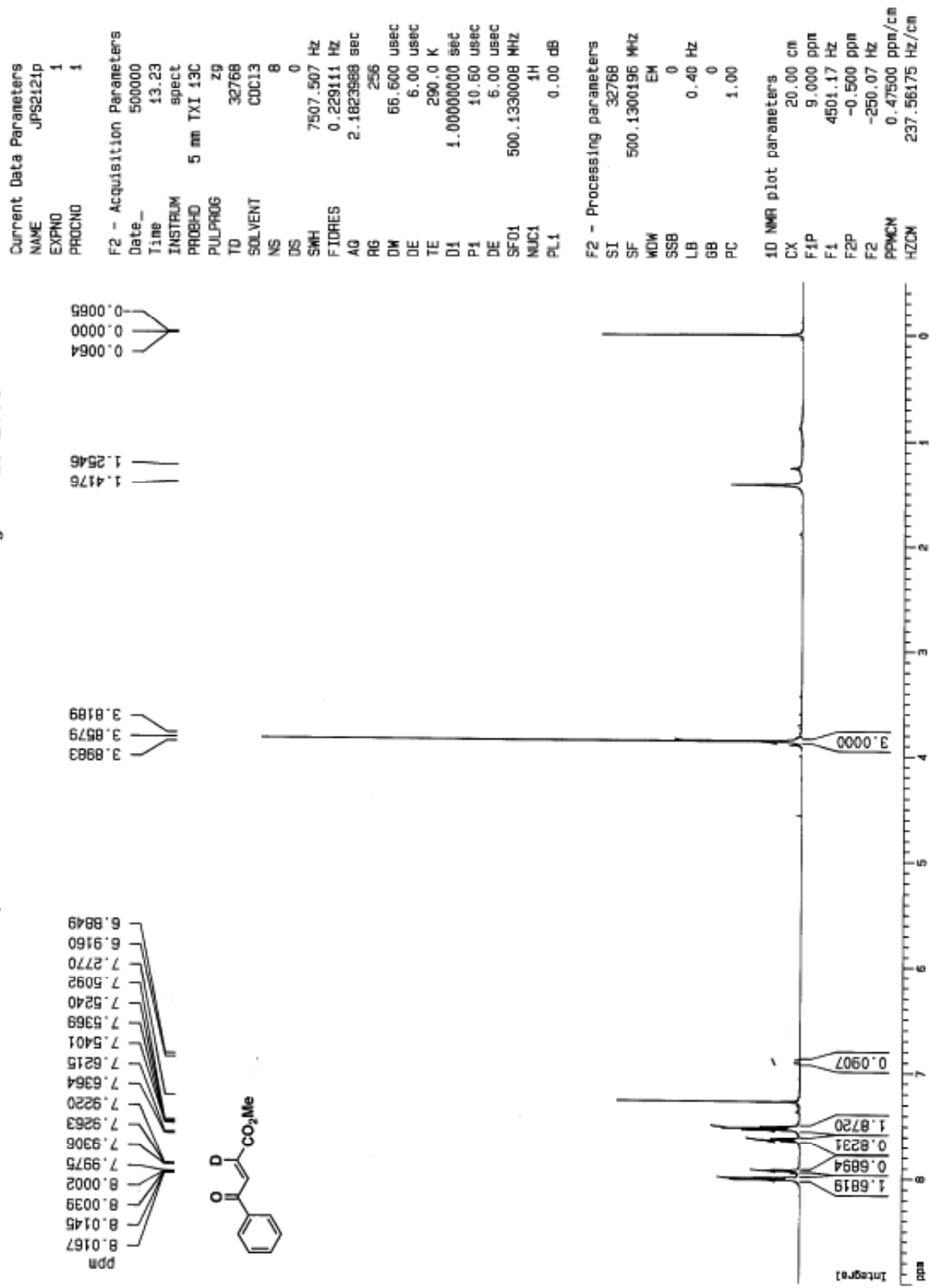
$^{13}\text{C}$  NMR spectrum of **3d-E43**:  $\text{CDCl}_3$ , 293 K, 125 MHz

JPS2077 in cdc13 13c 75mhz rt 301b September 19-20 2005

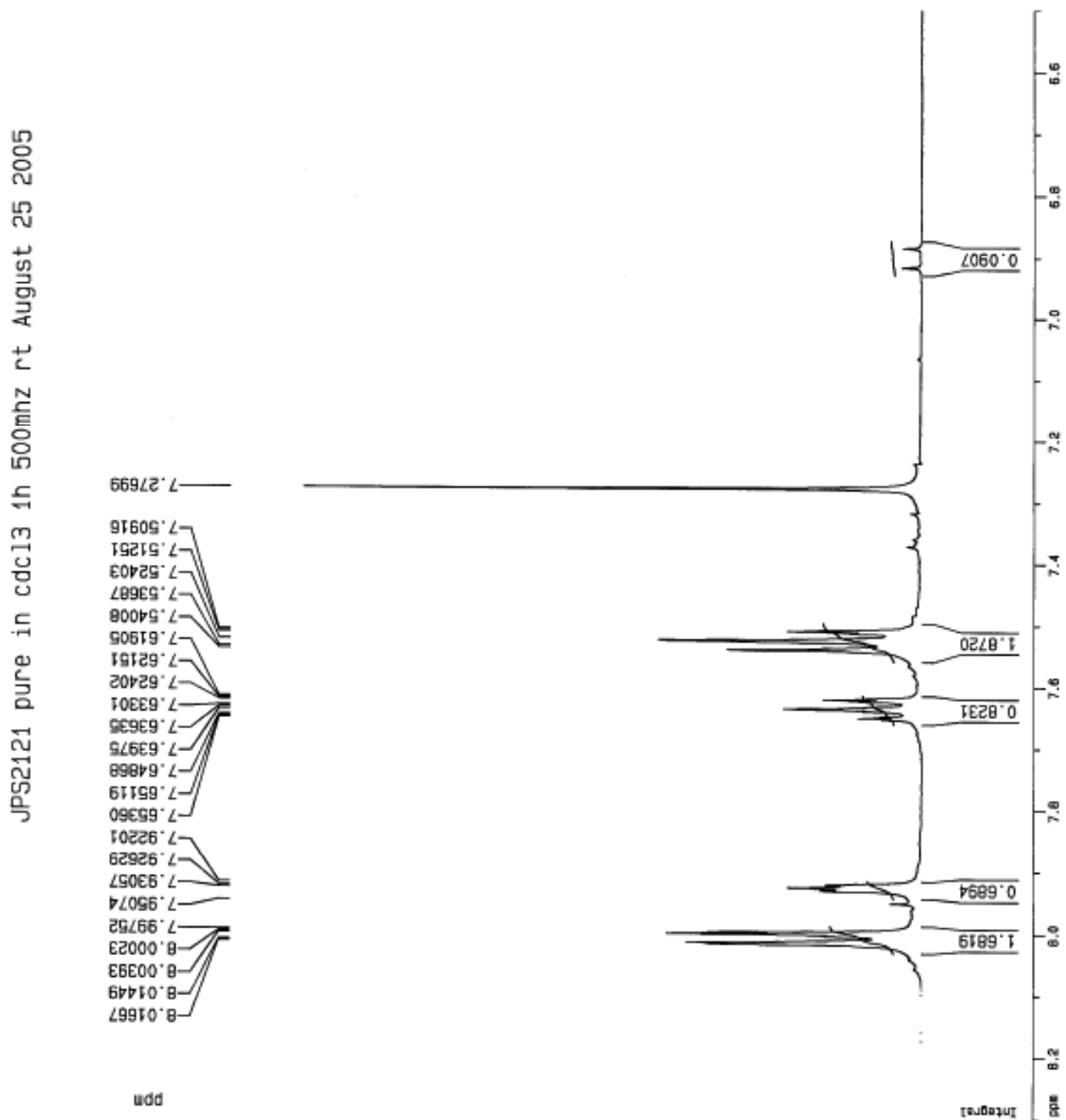


<sup>1</sup>H NMR of **2d-E43**: CDCl<sub>3</sub>, 293 K, 500 MHz

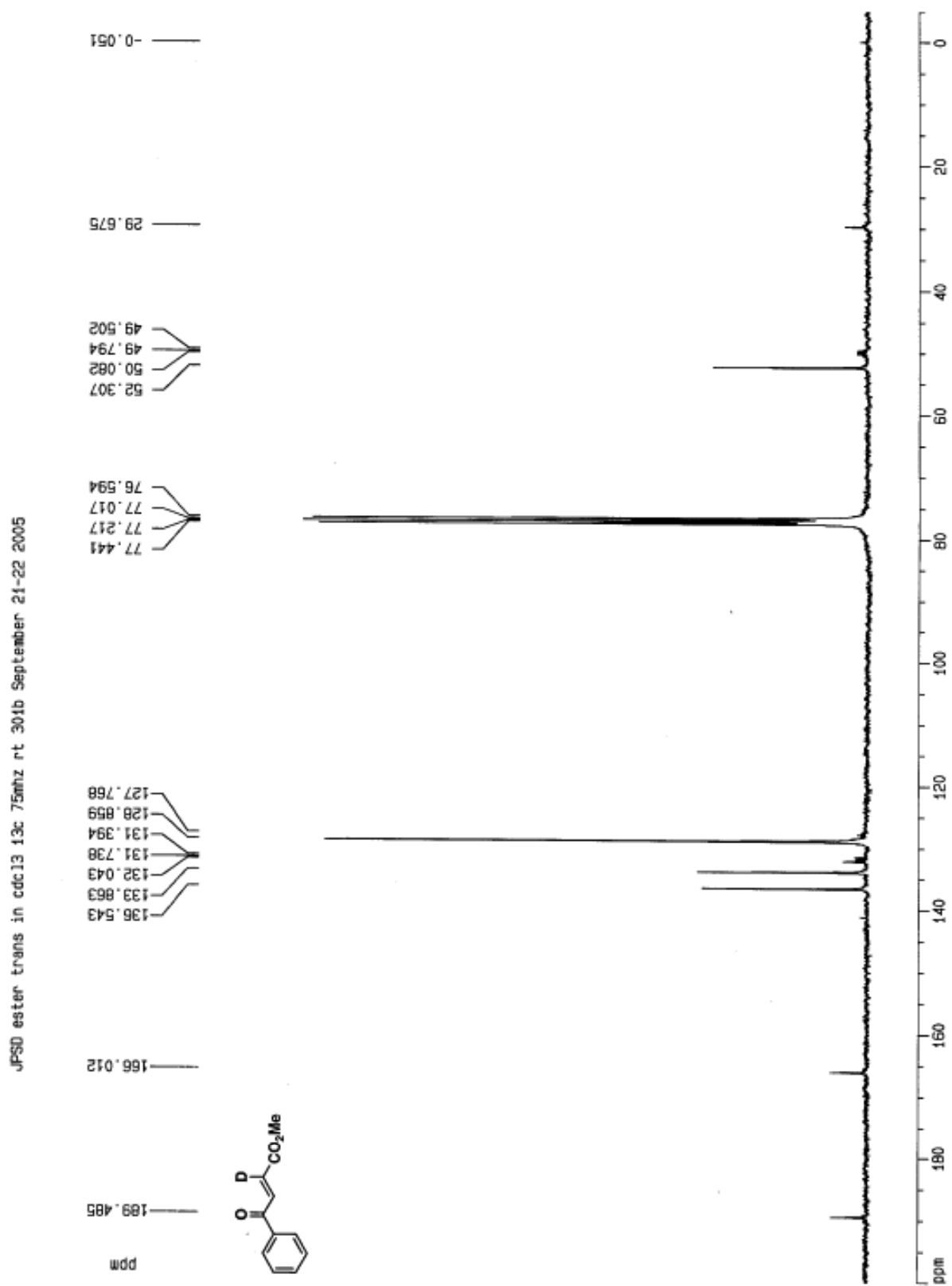
JPS2121 pure in cdcl3 1h 500mhz rt August 25 2005



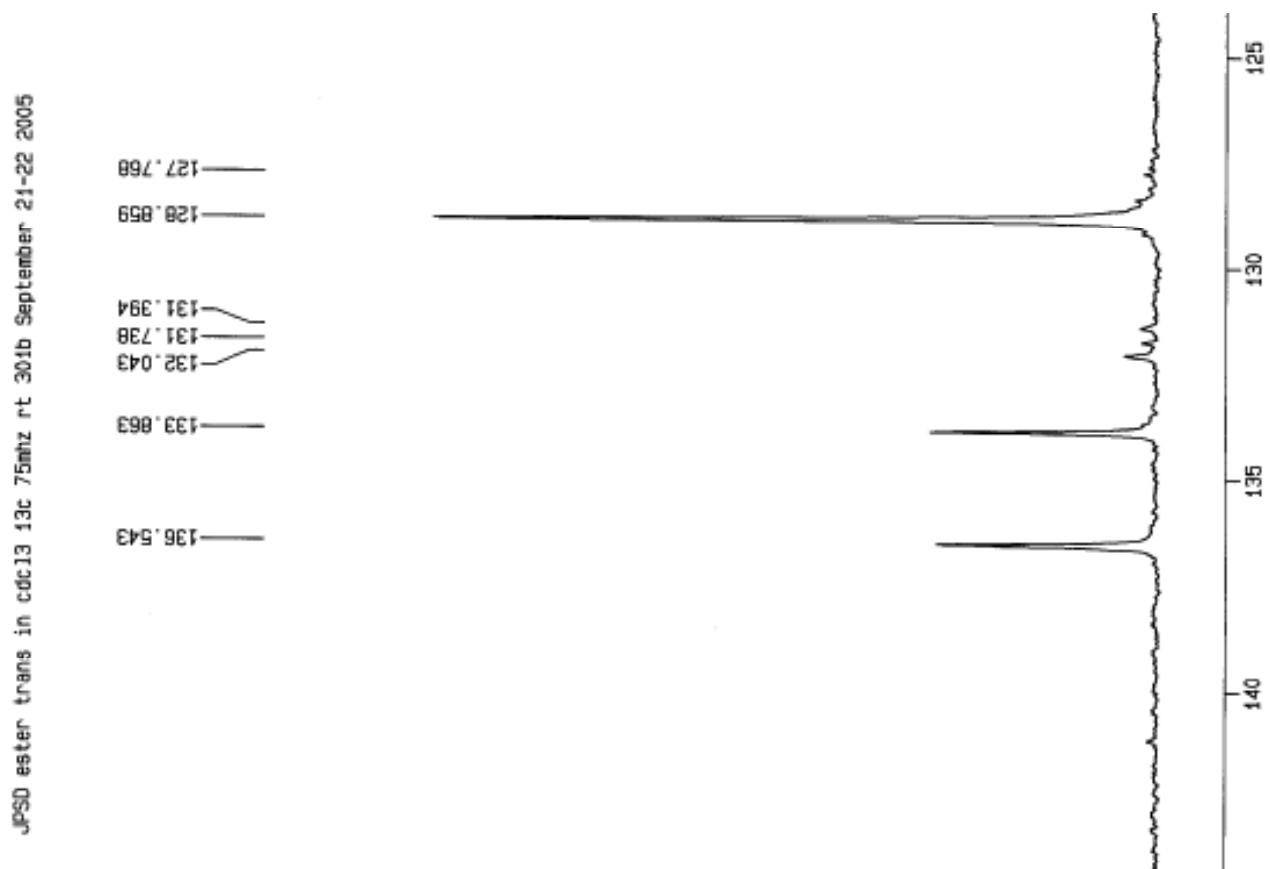
$^1\text{H}$  NMR of **2d-E43**:  $\text{CDCl}_3$ , 293 K, 500 MHz



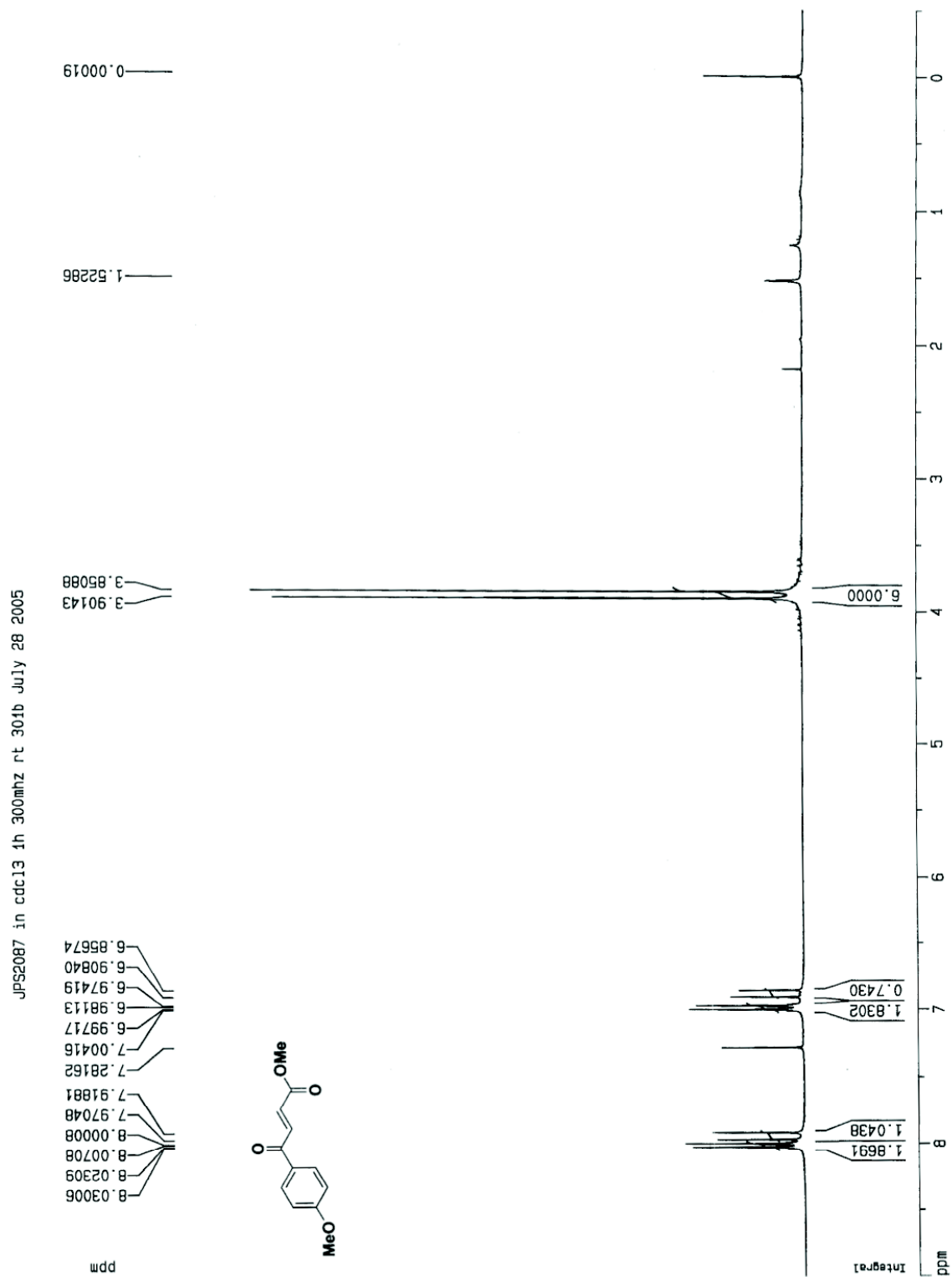
$^{13}\text{C}$  NMR of **2d-E43**:  $\text{CDCl}_3$ , 293 K, 125 MHz



$^{13}\text{C}$  NMR of **2d-E43**:  $\text{CDCl}_3$ , 293 K, 125 MHz



$^1\text{H}$  NMR spectrum of **E92**:  $\text{CDCl}_3$ , 293 K, 300 MHz



<sup>13</sup>C NMR spectrum of **E92**: CDCl<sub>3</sub>, 293 K, 125 MHz

JPS2087 in cdc13 13c 125mhz rt 500 August 5 2005

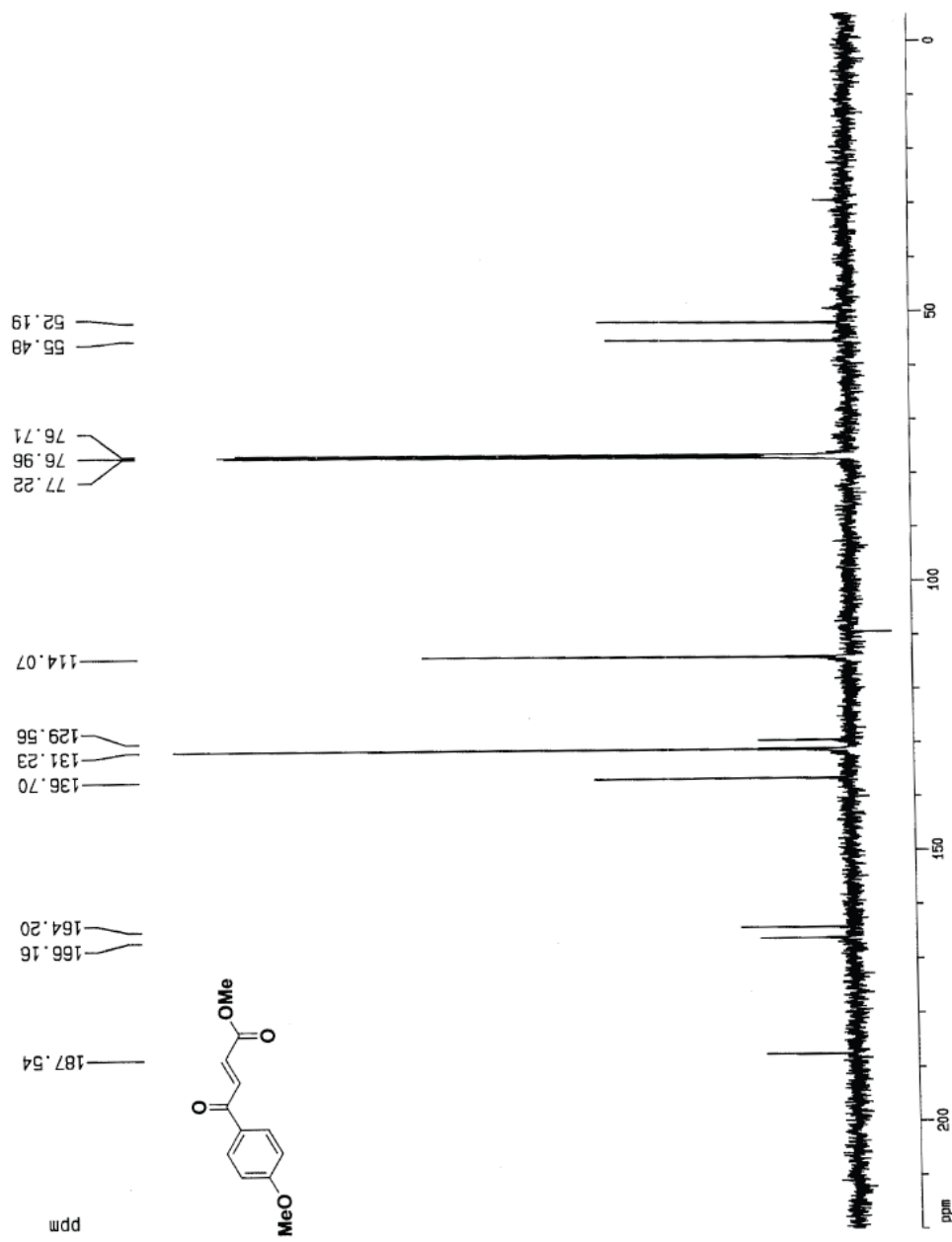
```

Current Data Parameters
NAME      JPS2087
EXPNO    2
PROCNO   1

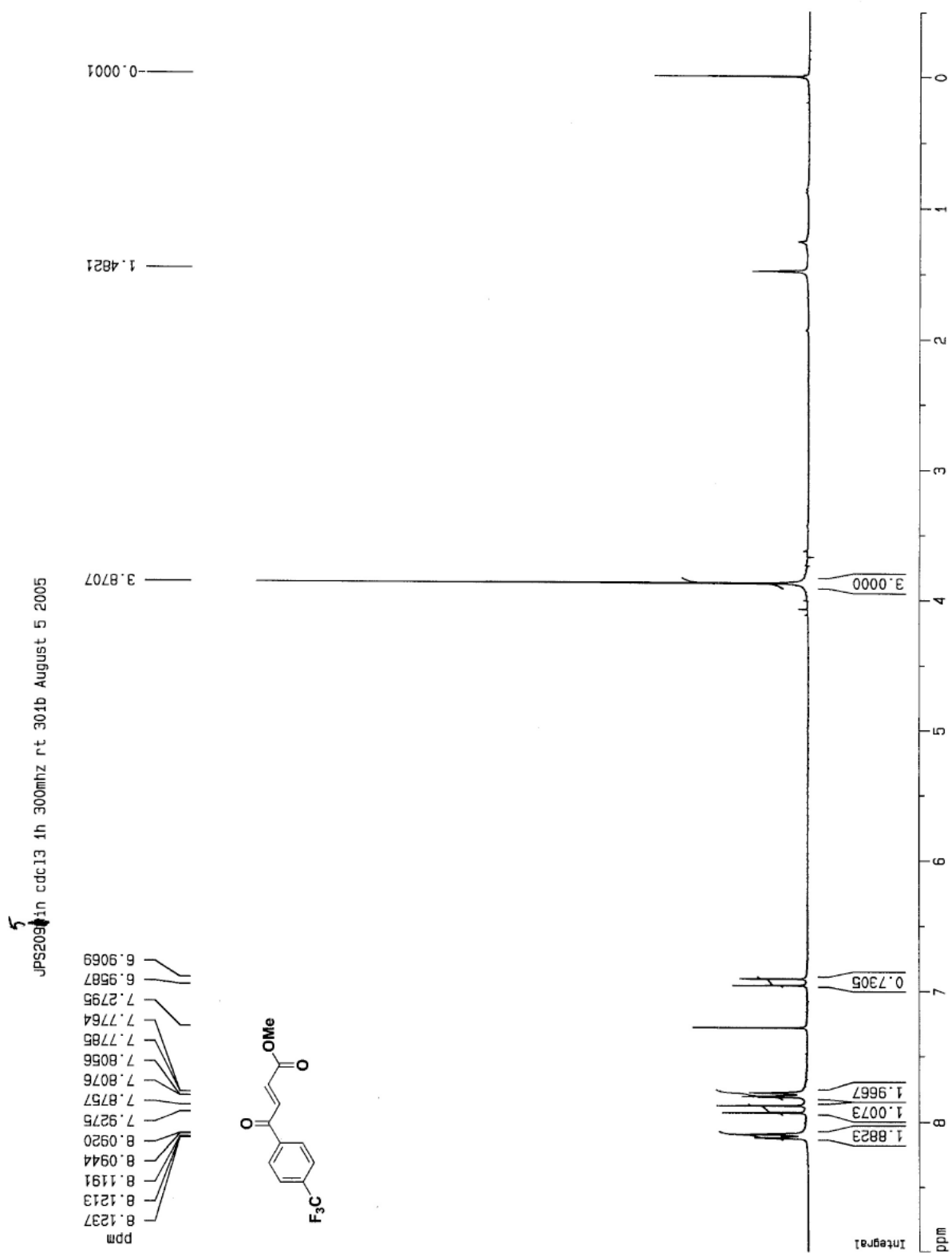
F2 - Acquisition Parameters
Date_    500000
Time     21.04
INSTRUM  spect
PROBHD   5 mm TXI 13C
PULPROG  zgpg
TD        32768
SOLVENT  CDCl3
NS        220
DS        0
SWH       32679.798 Hz
FIDRES    0.997305 Hz
AQ         0.5014004 sec
RG         7298.2
DM         15.300 usec
DE         6.00 usec
TE         290.0 K
d11        0.0300000 sec
d12        0.0000200 sec
PL13       20.00 dB
D1         6.00000000 sec
CPDPRG2   waltz16
PCPD2     65.00 usec
SF02      500.1330008 MHz
NUC2       1H
PL2        120.00 dB
PL12       18.00 dB
P1         9.00 usec
DE         6.00 usec
SF01      125.7715724 MHz
NUC1       13C
PL1        -6.00 dB

F2 - Processing parameters
SI         8192
SF         125.7578047 MHz
WDW        EM
SSB        0
LB         4.00 Hz
GB         0
PC         1.00

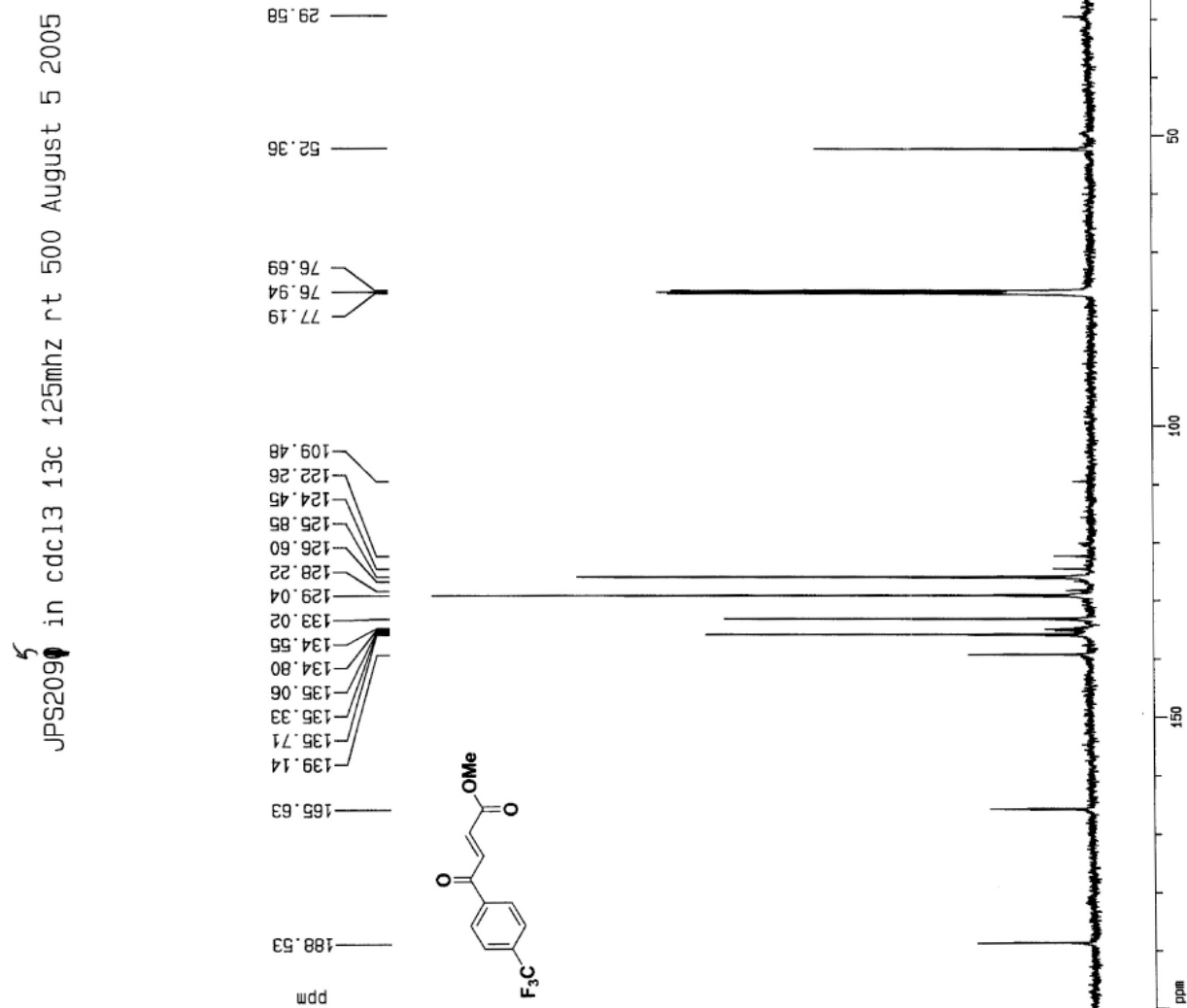
1D NMR plot parameters
CX         20.00 cm
F1P        220.000 ppm
F1         27566.71 Hz
F2P        -5.000 ppm
F2         -628.79 Hz
PPMCM      11.25000 ppm/cm
HZCM       1414.77527 Hz/cm
    
```



$^1\text{H}$  NMR spectrum of **E94**:  $\text{CDCl}_3$ , 293 K, 300 MHz



<sup>13</sup>C NMR spectrum of **E94**: CDCl<sub>3</sub>, 293 K, 75 MHz



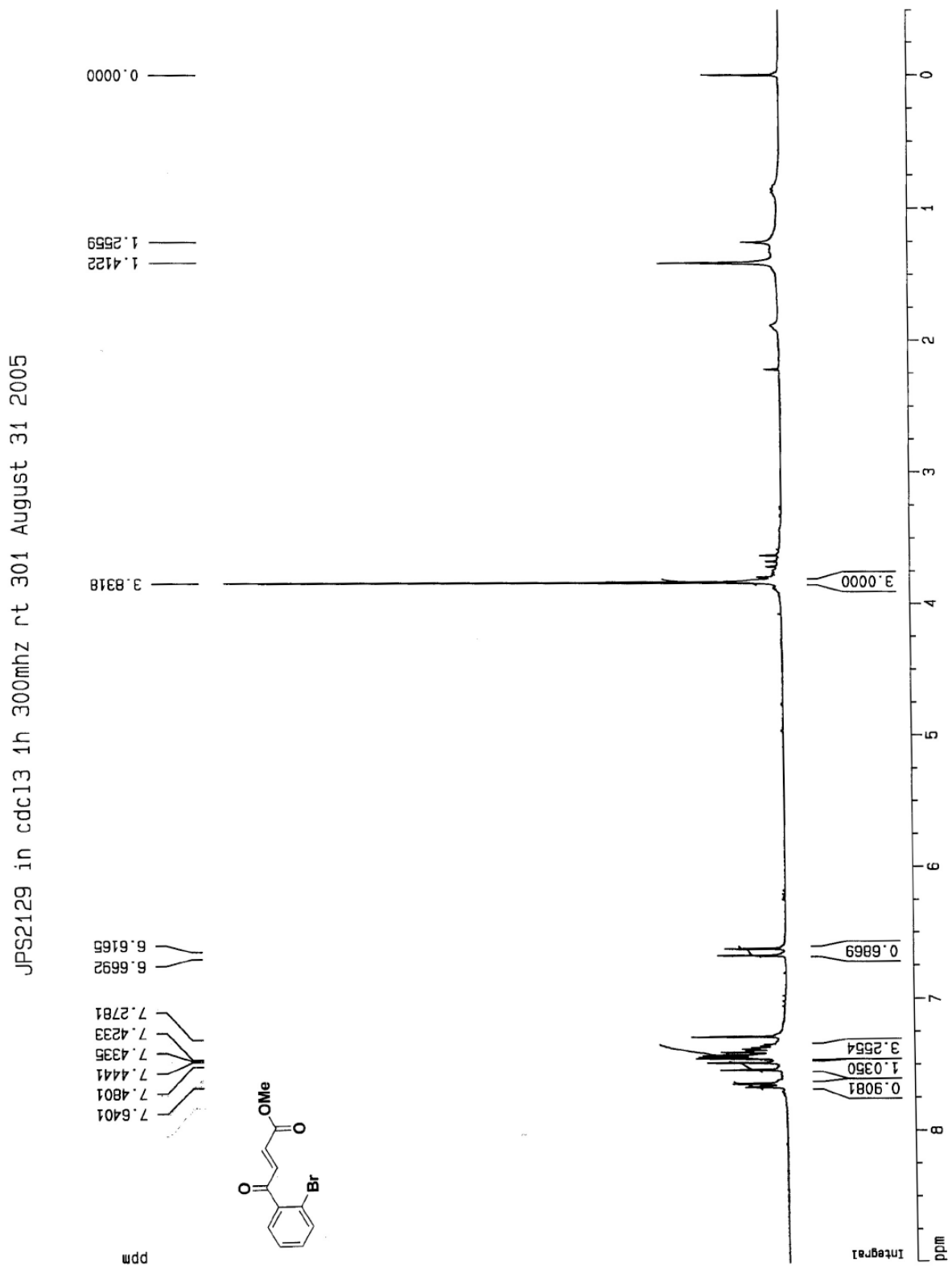
Current Data Parameters  
 NAME JPS2095  
 EXPNO 4  
 PROCNO 1

F2 - Acquisition Parameters  
 Date\_ 500000  
 Time 14.46  
 INSTRUM spect  
 PROBHD 5 mm TXI 13C  
 PULPROG zgpg  
 TD 32768  
 SOLVENT CDCl3  
 NS 1350  
 DS 0  
 SWH 32679.738 Hz  
 FIDRES 0.997306 Hz  
 AQ 0.5014004 sec  
 RG 7298.2  
 DM 15.300 usec  
 DE 6.00 usec  
 TE 290.0 K  
 d11 0.030000 sec  
 d12 0.0000200 sec  
 PL13 20.00 dB  
 D1 6.00000000 sec  
 CPDPRG2 waltz16  
 PCPD2 65.00 usec  
 SF02 500.1330008 MHz  
 NUC2 1H  
 PL2 120.00 dB  
 PL12 18.00 dB  
 P1 9.00 usec  
 DE 6.00 usec  
 SF01 125.7715724 MHz  
 NUC1 13C  
 PL1 -6.00 dB

F2 - Processing parameters  
 SI 8192  
 SF 125.7578047 MHz  
 KDW EM  
 SSB 0  
 LB 4.00 Hz  
 GB 0  
 PC 1.00

1D NMR plot parameters  
 CX 20.00 cm  
 F1P 200.000 ppm  
 F1 25151.56 Hz  
 F2P -5.000 ppm  
 F2 -628.79 Hz  
 PPMCM 10.25000 ppm/cm  
 HZCM 1289.01758 Hz/cm

$^1\text{H}$  NMR spectrum of **E96**:  $\text{CDCl}_3$ , 293 K, 300 MHz



<sup>13</sup>C NMR spectrum of **E96**: CDCl<sub>3</sub>, 293 K, 125 MHz

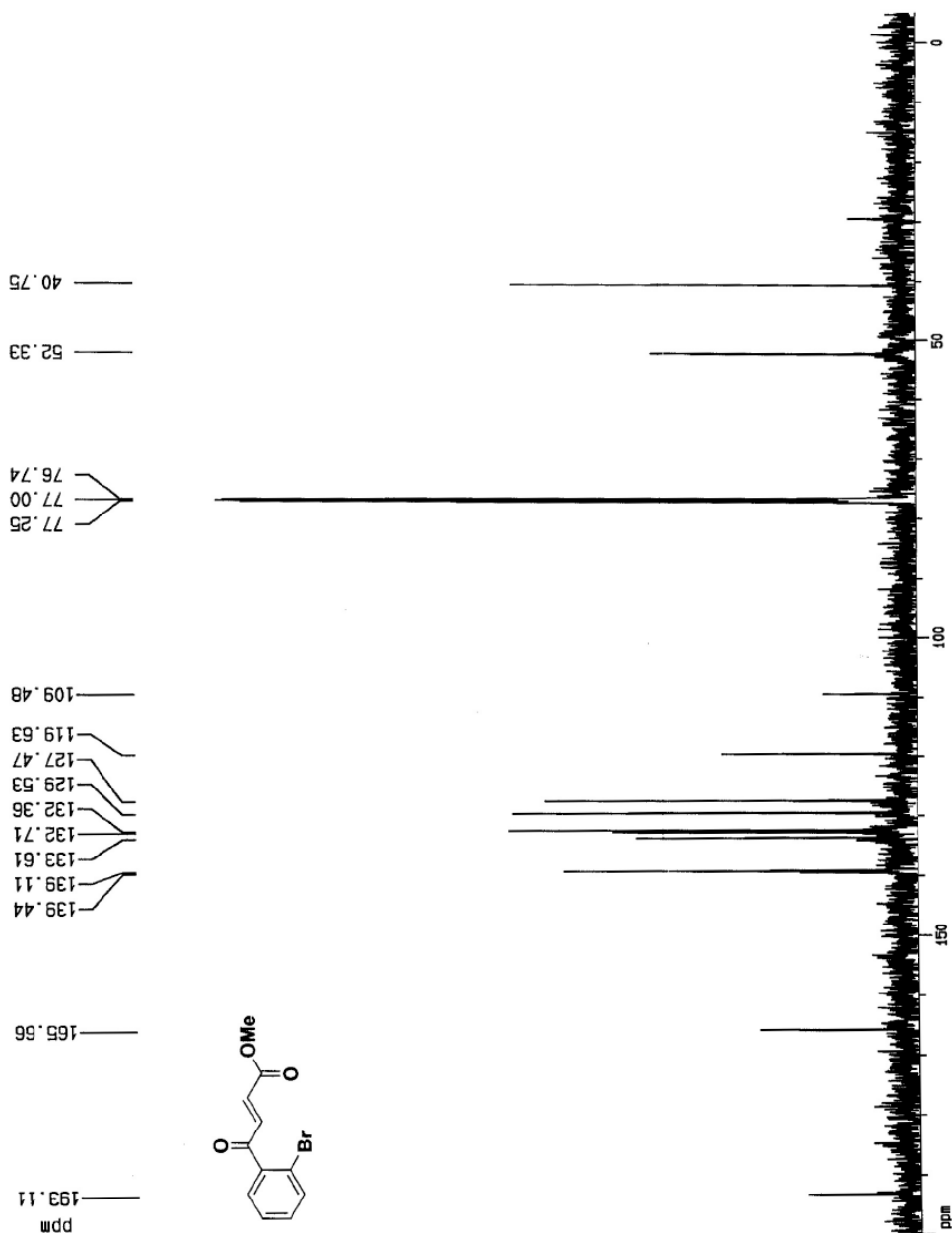
Current Data Parameters  
 NAME JPS2123  
 EXPNO 2  
 PROCNO 1

F2 - Acquisition Parameters  
 Date\_ 500000  
 Time 16.36  
 INSTRUM spect  
 PROBHD 5 mm TXI 13C  
 PULPROG c13nonde  
 TD 32768  
 SOLVENT CDCl3  
 NS 284  
 DS 0  
 SWH 32679.738 Hz  
 FIDRES 0.997306 Hz  
 AQ 0.5014004 sec  
 RG 4096  
 DM 15.300 usec  
 DE 6.00 usec  
 TE 290.0 K  
 D3 0.00100000 sec  
 PL12 6.00 dB  
 D1 6.00000000 sec  
 CPDPRG2 waltz16  
 PQRD2 100.00 usec  
 SF02 500.1330008 MHz  
 NUC2 1H  
 PL2 120.00 dB  
 P1 21.60 usec  
 DE 6.00 usec  
 SF01 125.7715724 MHz  
 NUC1 13C  
 PL1 0.00 dB

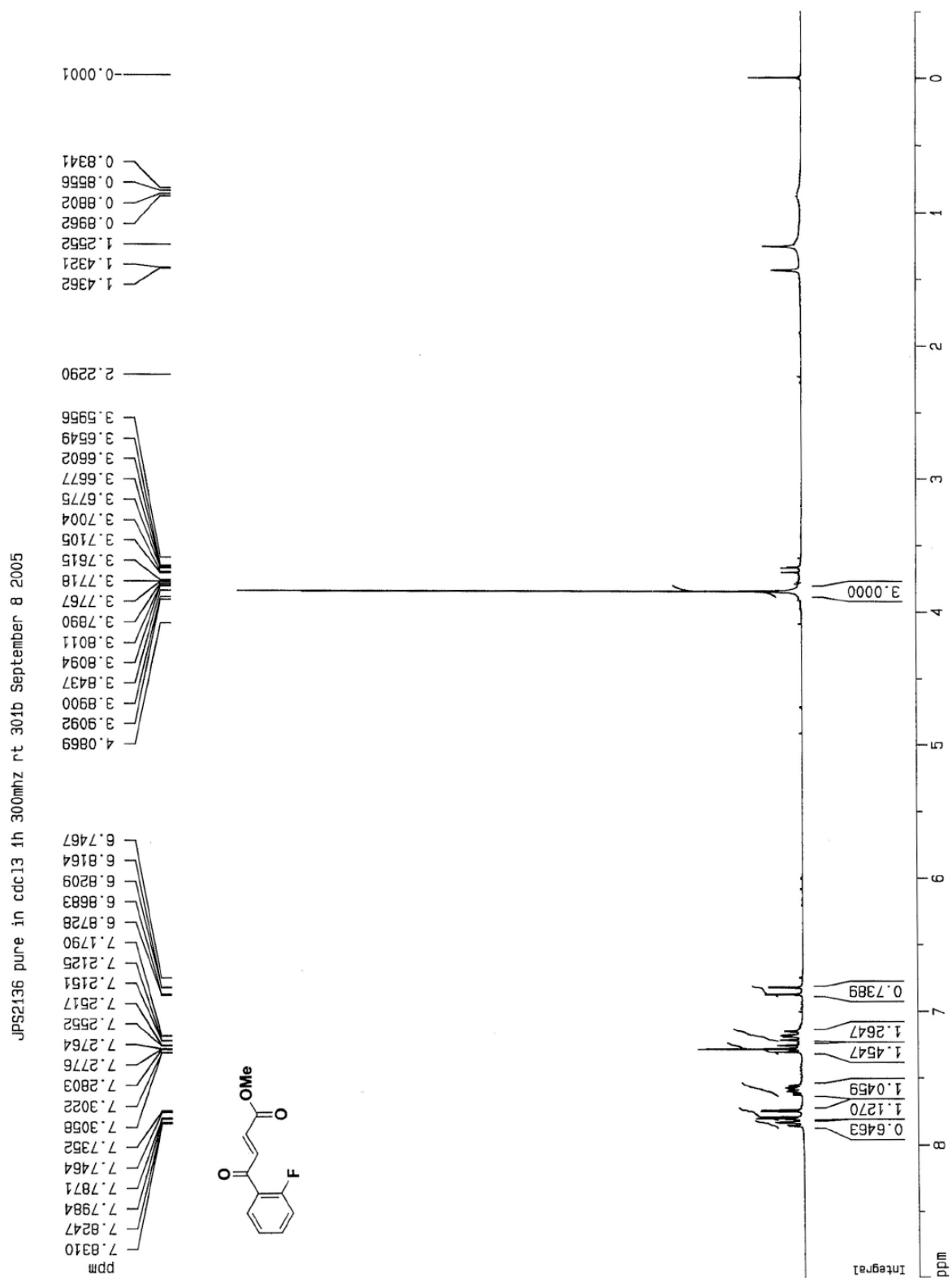
F2 - Processing parameters  
 SI 8192  
 SF 125.7578040 MHz  
 MDW EM  
 SSB 0  
 LB 4.00 Hz  
 GB 0  
 PC 1.00

1D NMR plot parameters  
 CX 20.00 cm  
 F1P 200.000 ppm  
 F1 25151.56 Hz  
 F2P -5.000 ppm  
 F2 -628.79 Hz  
 PPMCM 10.25000 ppm/cm  
 HZCM 1289.01758 Hz/cm

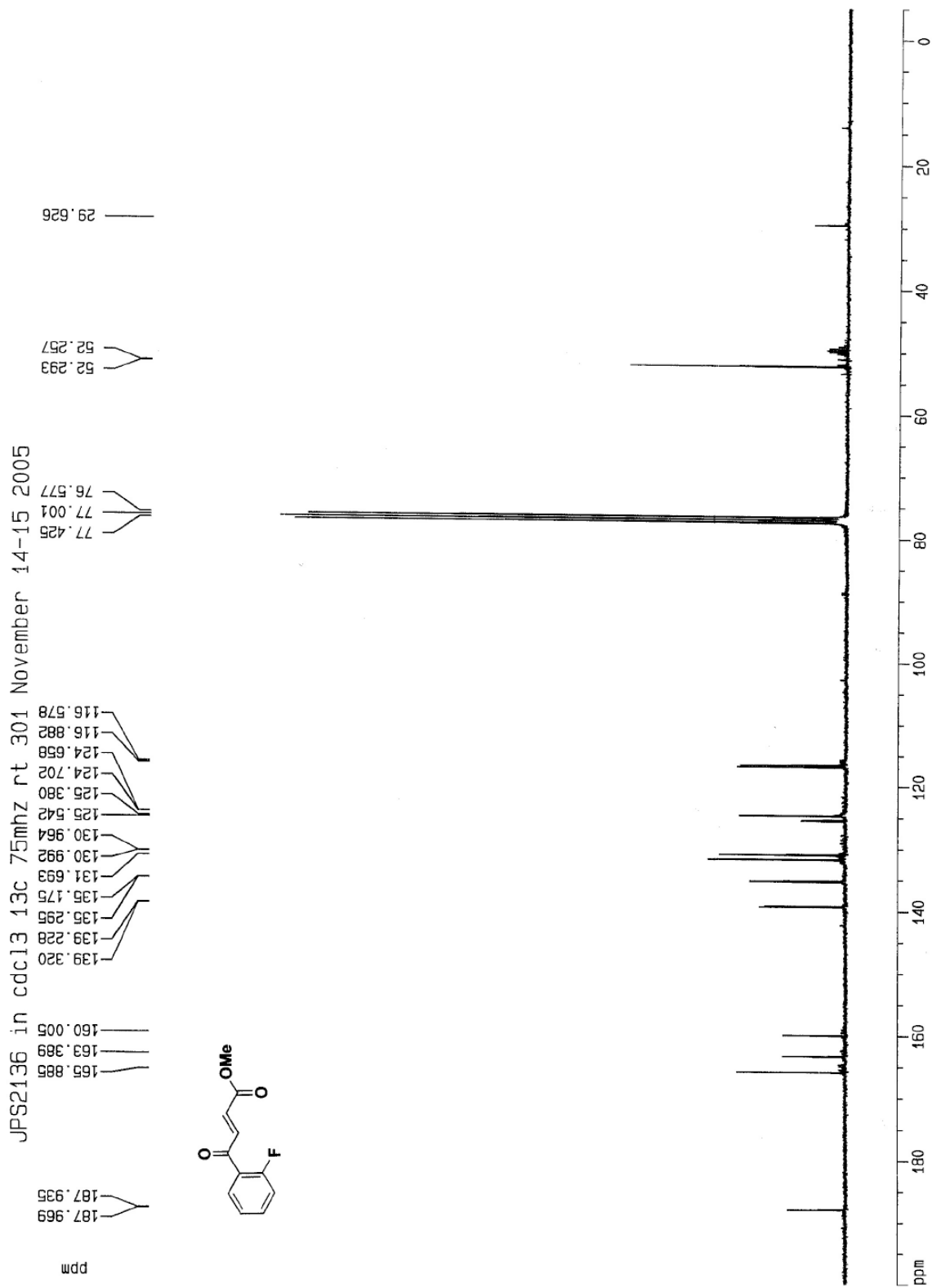
JPS2123 in cdc13 13c 125mhz rt 500 December 12 2005



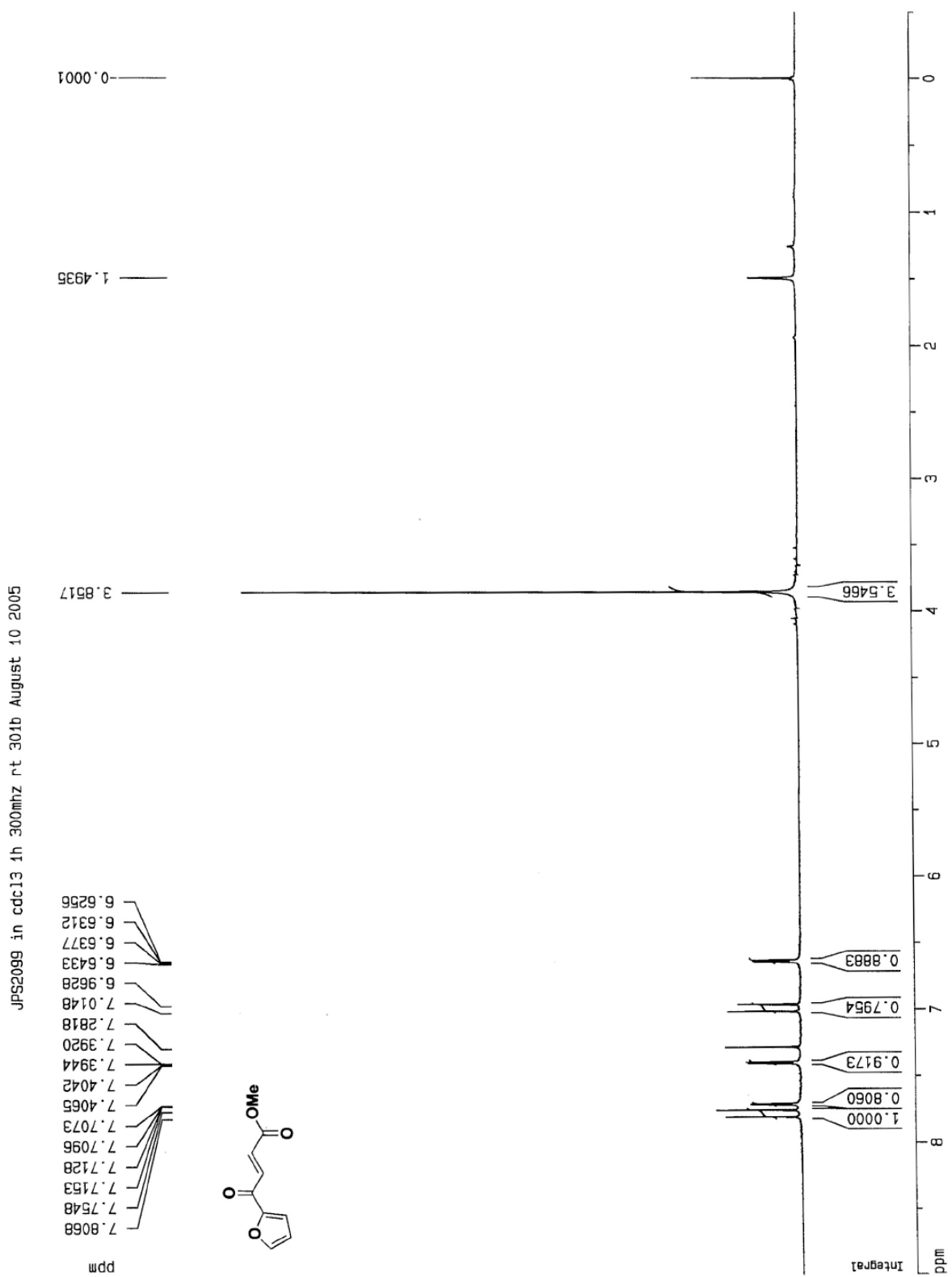
$^1\text{H}$  NMR spectrum of **E98**:  $\text{CDCl}_3$ , 293 K, 300 MHz



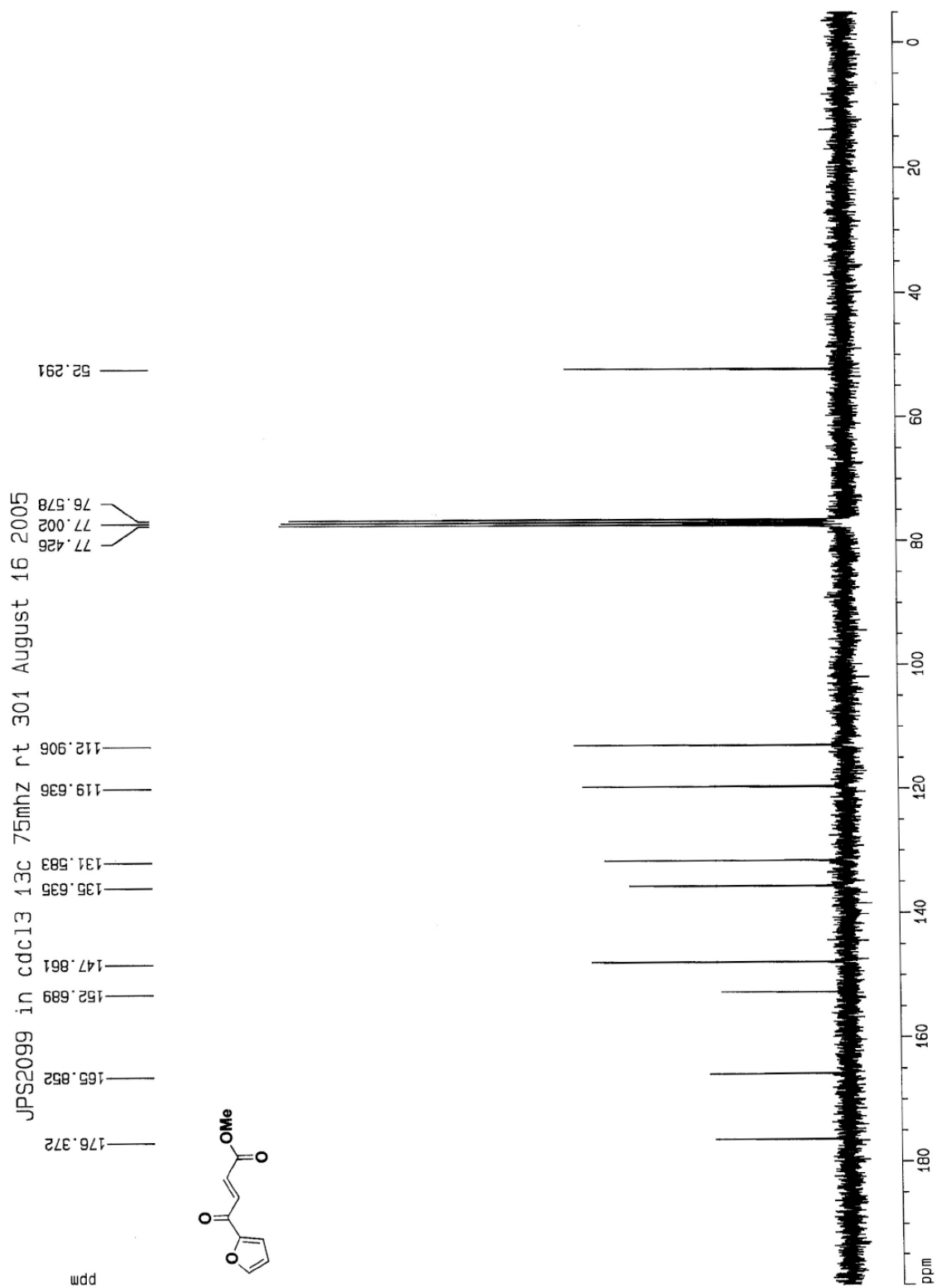
$^{13}\text{C}$  NMR spectrum of *E98*:  $\text{CDCl}_3$ , 293 K, 75 MHz



$^1\text{H}$  NMR spectrum of **E100**:  $\text{CDCl}_3$ , 293 K, 300 MHz

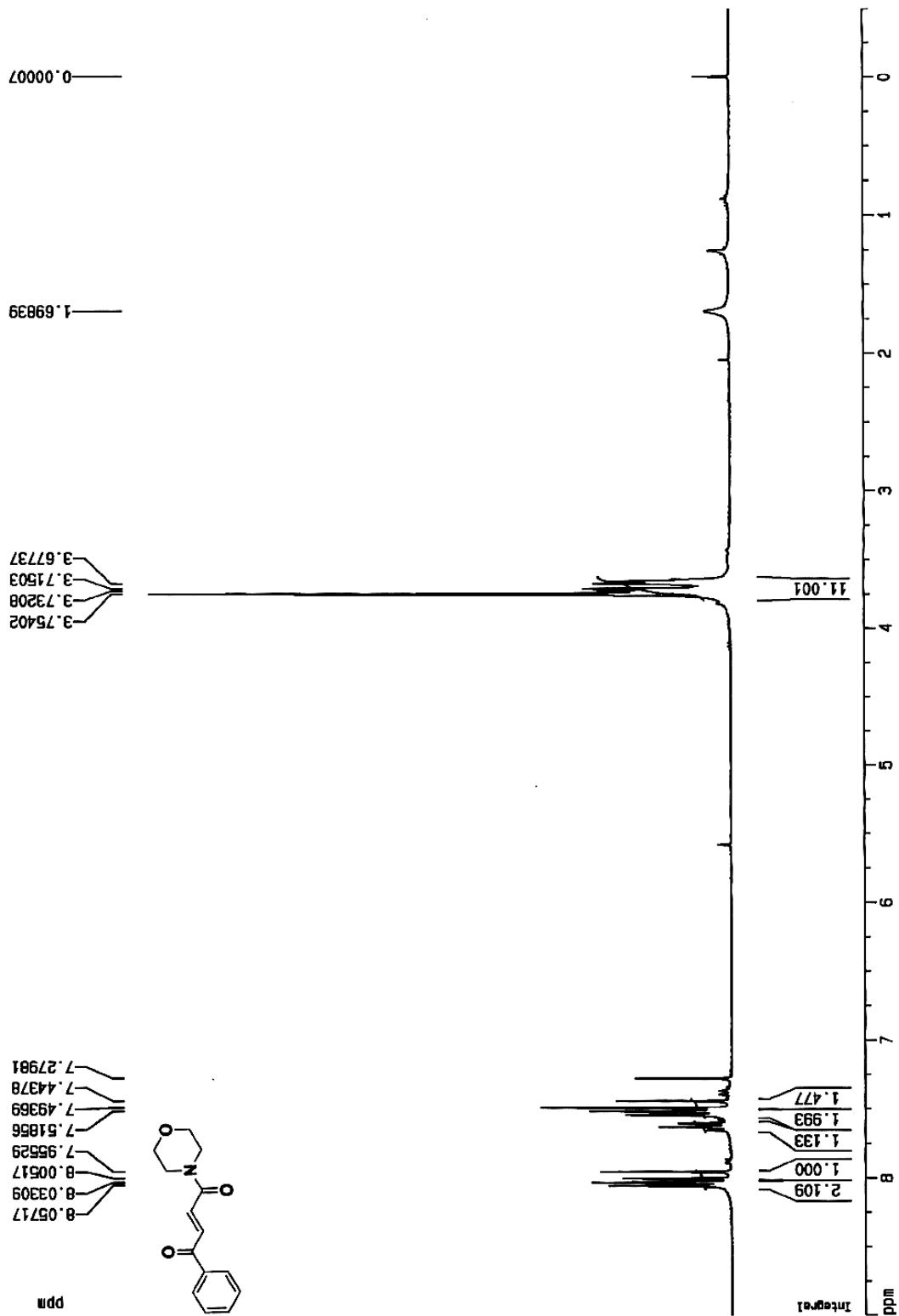


$^{13}\text{C}$  NMR spectrum of *E100*:  $\text{CDCl}_3$ , 293 K, 75 MHz



<sup>1</sup>H NMR spectrum of E112: CDCl<sub>3</sub>, 293 K, 300 MHz

JPS2193 in cdc13 1h 300mhz rt 301 December 3 2005



<sup>13</sup>C NMR spectrum of **E112**: CDCl<sub>3</sub>, 293 K, 125 MHz

JPS2193 after prep tlc 13c 125 mhz rt 500 December 12 2005

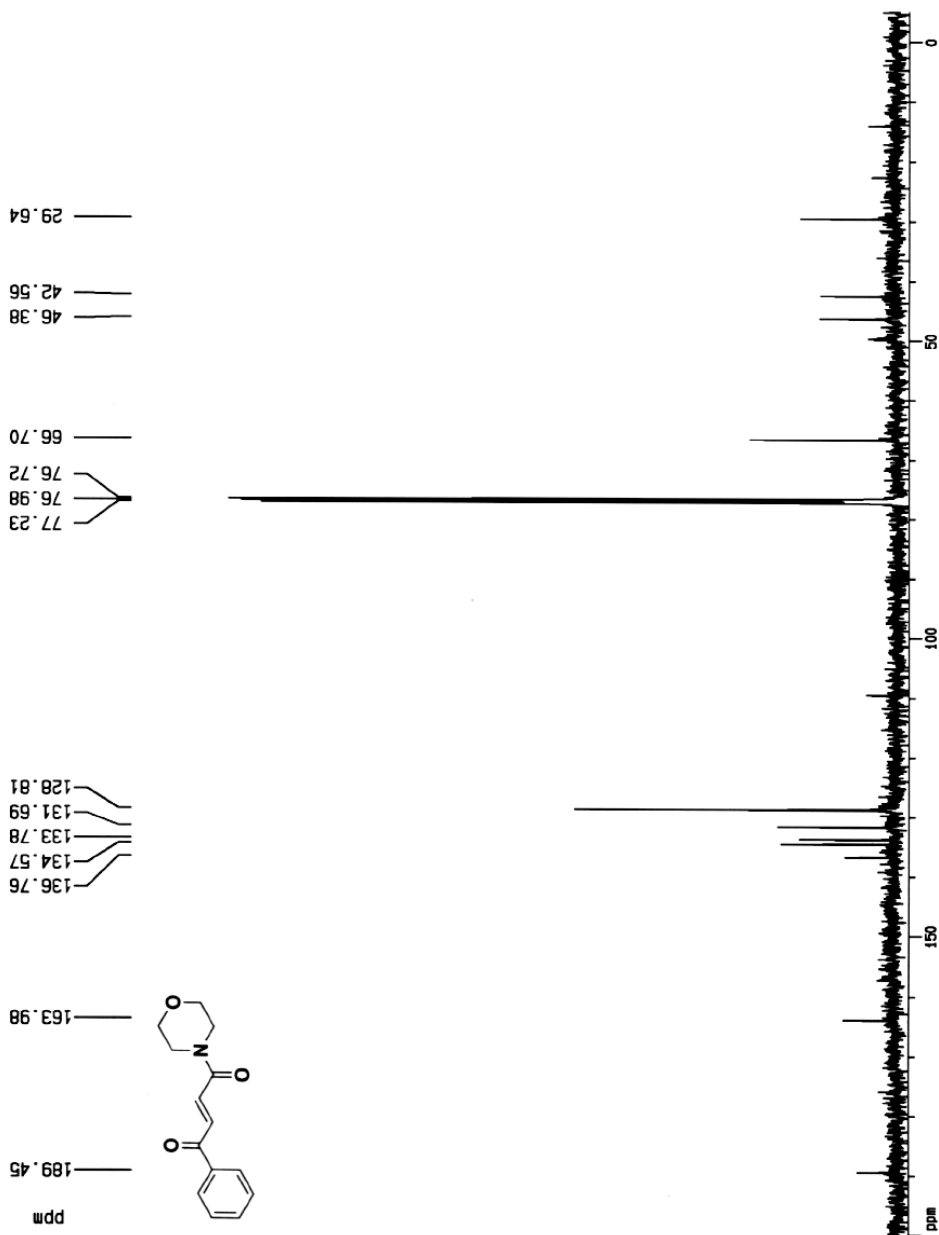
```

Current Data Parameters
NAME      JPS2193t1c
EXPNO     2
PROCNO    1

F2 - Acquisition Parameters
Date_     500000
Time      12.06
INSTRUM   spect
PROBHD    5 mm TXI 13C
PULPROG   c13winoe
TD         32768
SOLVENT   CDC13
NS         1147
DS         0
SWH        32679.738 Hz
FIDRES     0.997306 Hz
AQ         0.5014004 sec
RG         32768
DM         45.300 usec
DE         6.00 usec
TE         290.0 K
D3         0.00100000 sec
PL12      6.00 dB
D1         6.00000000 sec
CPDPRG2   waltz16
PCPD2     100.00 usec
SF02      500.1330008 MHz
NUC2      1H
PL2       120.00 dB
P1        21.60 usec
DE        6.00 usec
SF01      125.7715724 MHz
NUC1      13C
PL1       0.00 dB

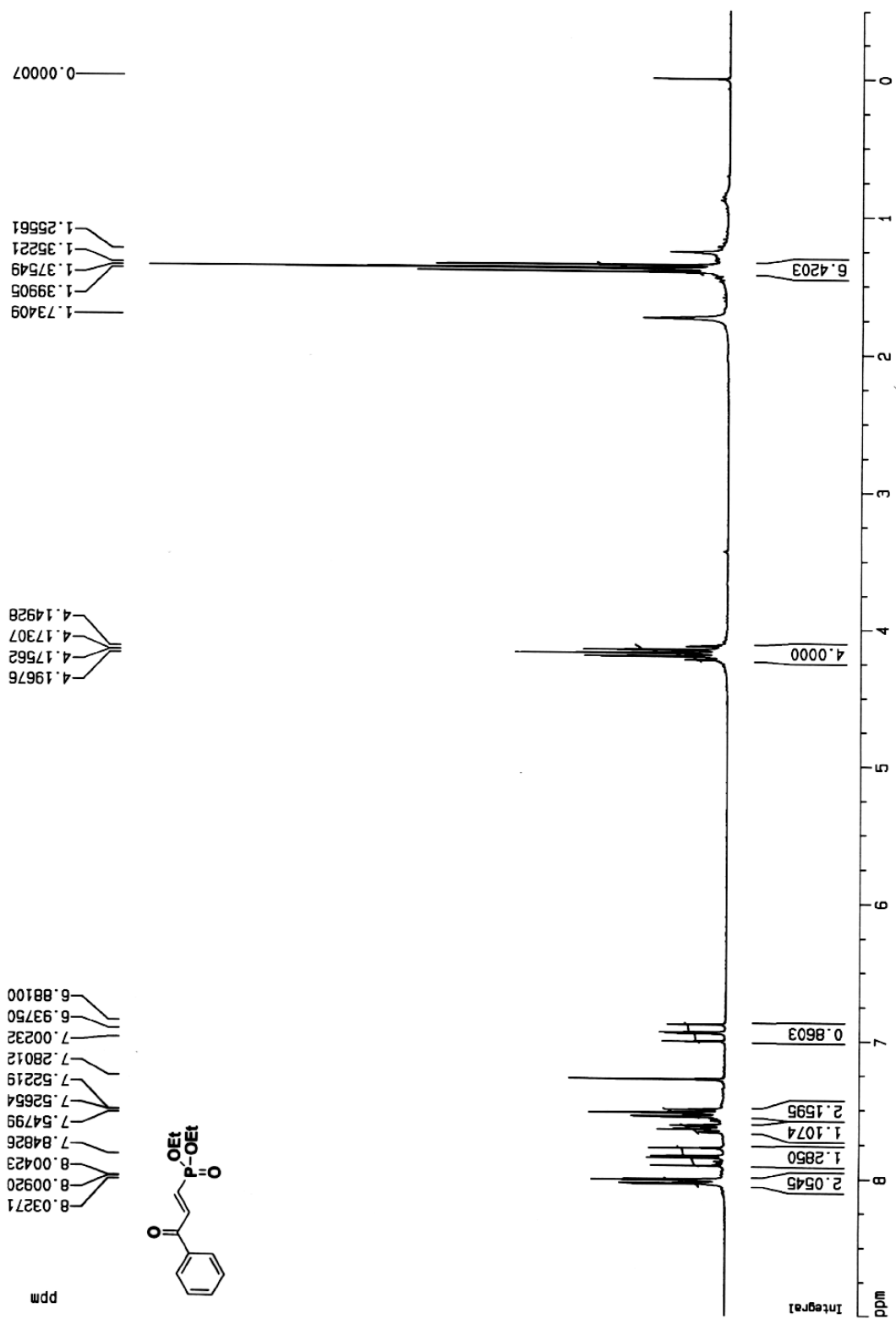
F2 - Processing parameters
SI         8192
SF         125.7578000 MHz
WDW        EM
SSB        0
LB         4.00 Hz
GB         0
PC         1.00

1D NMR plot parameters
CX         20.00 cm
F1P        200.000 ppm
F1         25151.56 Hz
F2P        -5.000 ppm
F2         -628.79 Hz
PPMCM      10.25000 ppm/cm
HZCM       1289.01758 Hz/cm
    
```



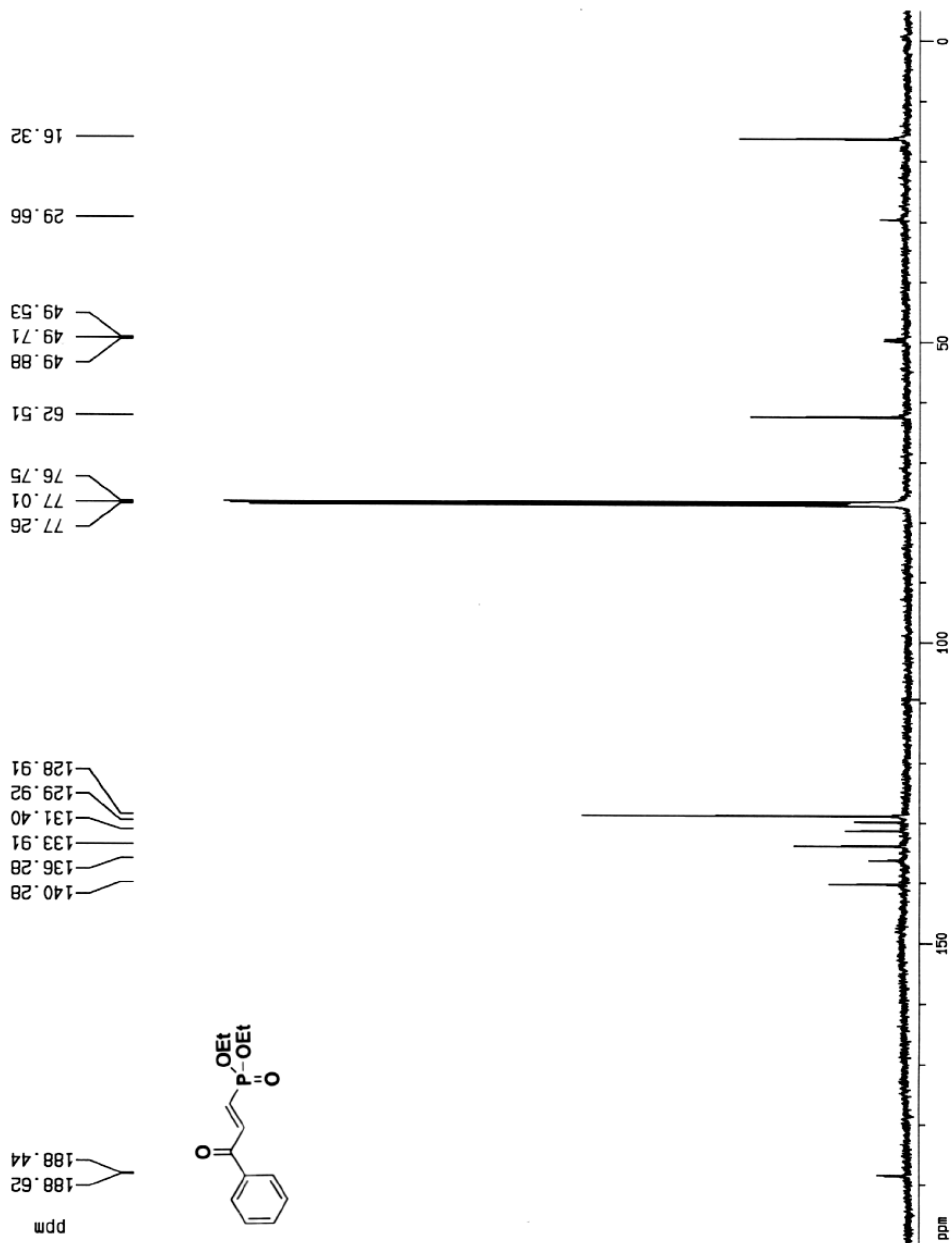
<sup>1</sup>H NMR spectrum of **E116**: CDCl<sub>3</sub>, 293 K, 300 MHz

JPS2168 in cdc13 1h 300mhz rt 301 October 26 2005



<sup>13</sup>C NMR spectrum of **E116**: CDCl<sub>3</sub>, 293 K, 125 MHz

JPS2168 in cdcl3 13c 125mhz rt November 30 - December 1 2005



```

Current Data Parameters
NAME      JPS2168
EXPNO    2
PROCNO   1

F2 - Acquisition Parameters
Date_    500000
Time     21.21
INSTRUM  spect
PROBHD   5 mm TXI 13C
PULPROG  c13winoe
TD        32768
SOLVENT  CDCl3
NS        6448
DS        0
SWH       32679.738 Hz
FIDRES    0.997306 Hz
AQ        0.5014004 sec
RG        32768
DM        15.300 usec
DE        6.00 usec
TE        290.0 K
D3        0.00100000 sec
PL12      6.00 dB
D1        6.00000000 sec
CPDPRG2  waltz16
PCPD2     100.00 usec
SF02      500.1330008 MHz
NUC2      1H
PL2       120.00 dB
P1        21.60 usec
DE        6.00 usec
SF01      125.7715724 MHz
NUC1      13C
PL1       0.00 dB

F2 - Processing parameters
SI         8192
SF         125.7577961 MHz
WDW        EM
SSB        0
LB         4.00 Hz
GB         0
PC         1.00

1D NMR plot parameters
CX         20.00 cm
F1P        200.000 ppm
F1         25151.56 Hz
F2P        -5.000 ppm
F2         -628.79 Hz
PPMCM      10.25000 ppm/cm
HZCM       1269.01758 Hz/cm
    
```

HMBC of Z43: CDCl<sub>3</sub>, 293 K, 500 MHz

Current Data Parameters  
 JPS1252  
 EXPNO 7  
 PROCNO 1

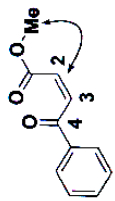
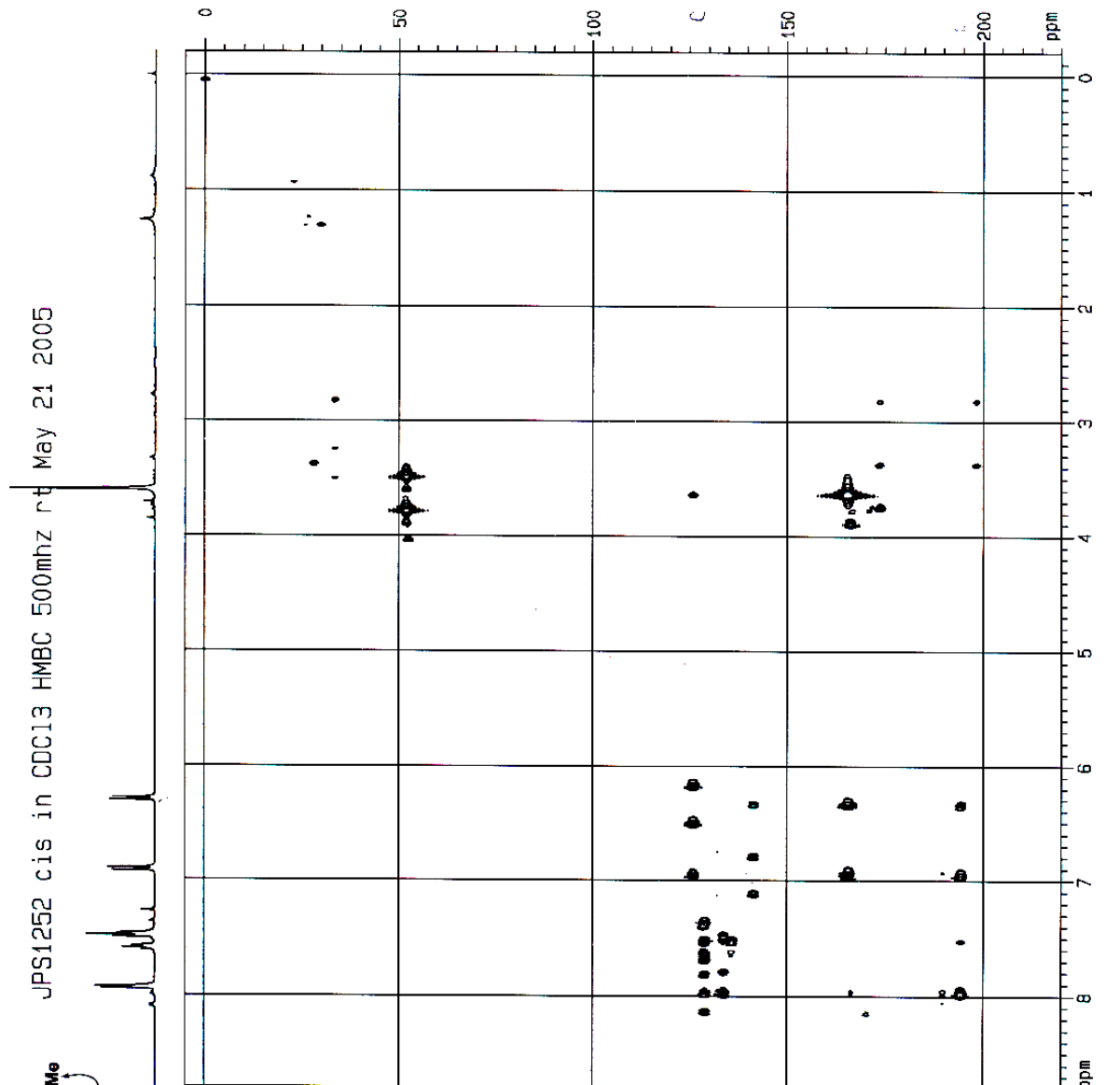
Date\_ 500000  
 Time 18.43  
 INSTRUM spect  
 PROBR0 13C  
 PULPROG zgpg30  
 ID 4058  
 SOLVENT cdcl3  
 NS 32  
 DS 4  
 SWH 4498.403 Hz  
 FIDRES 1.007765 Hz  
 AQ 0.485262 sec  
 RG 32768  
 IN 111.200 usec  
 DE 6.00 usec  
 TE 310.0 K  
 P1 11.50 usec  
 P2 23.0 usec  
 P3 0.000000 sec  
 d13 0.000000 sec  
 D1 1.0000000 sec  
 D6 0.1000000 sec  
 P3 14.00 usec  
 SFO2 125.770298 MHz  
 NUC2 13C  
 PL2 -6.00 dB  
 P18 1000.00 usec  
 D18 0.0000000 sec  
 DE 6.00 usec  
 SFO1 500.1321908 MHz  
 NUC1 1H  
 PL1 0.00 dB  
 TMO 0.0001325 sec

F1 - Acquisition parameters  
 NU0 235  
 TO 2  
 SFO1 125.770298 MHz  
 FIDRES 1.007765 Hz  
 SN 250.000 ppm

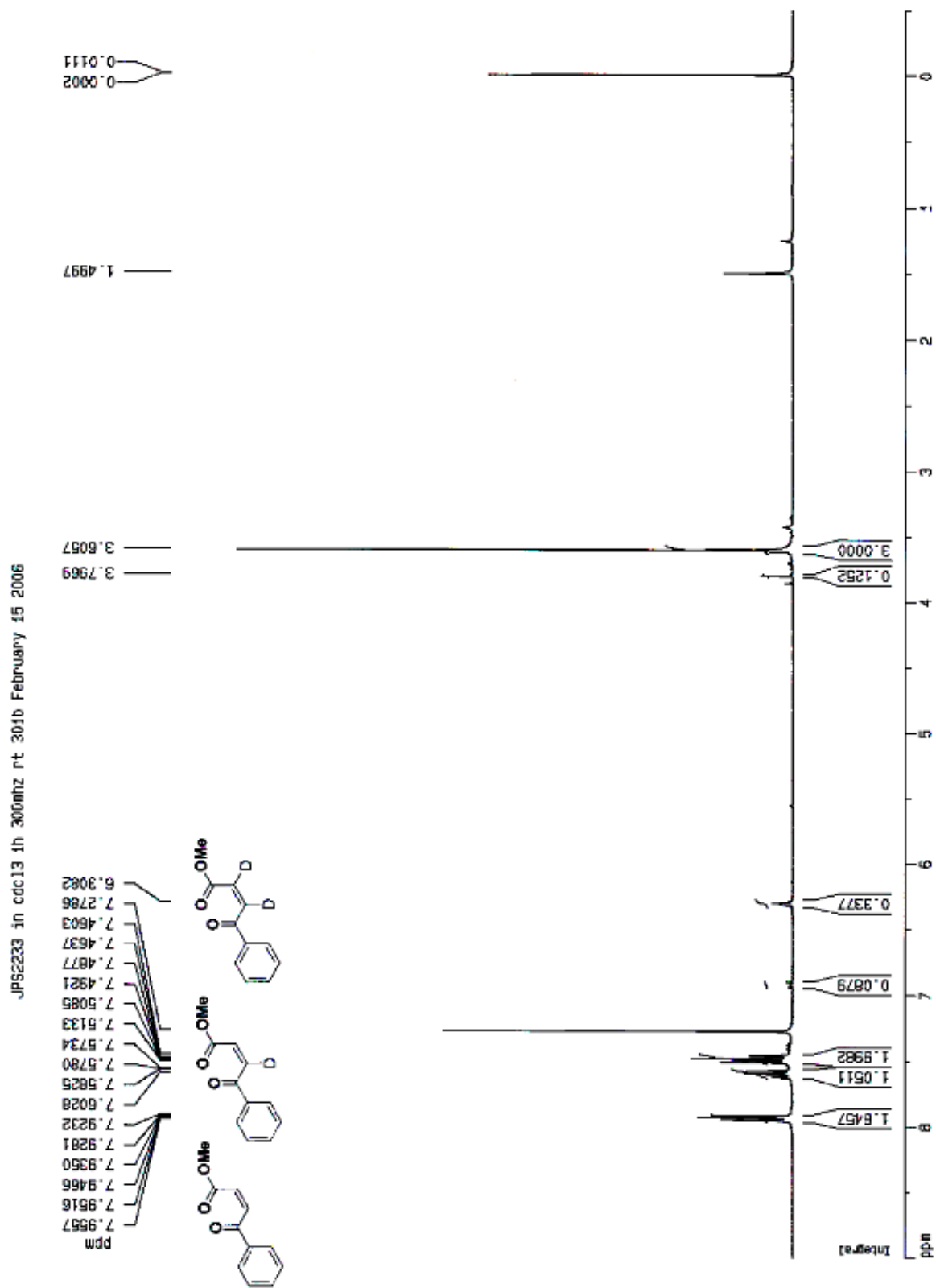
F2 - Processing parameters  
 SI 1024  
 SF 500.1300062 MHz  
 MSH 0  
 SSB 0  
 LB 0.00 Hz  
 GB 0  
 PC 1.00

F1 - Processing parameters  
 SI 1024  
 SF 125.7377629 MHz  
 MSH 0  
 SSB 0  
 LB 0.00 Hz  
 GB 0

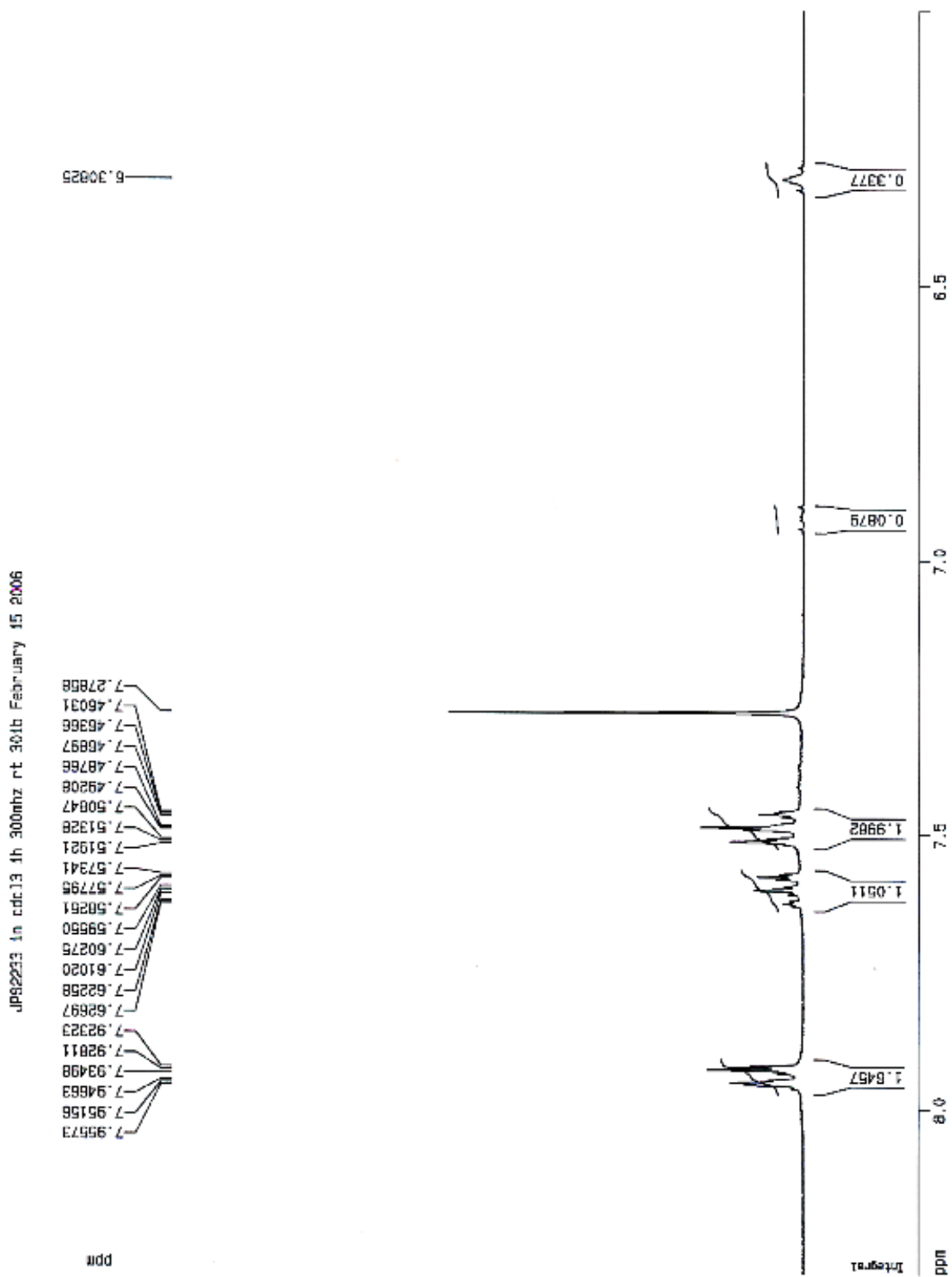
2D NMR plot parameters  
 CX2 18.00 cm  
 CY2 18.00 cm  
 F2P0 6.791 cm  
 F2P1 4986.55 Hz  
 F2P2 -0.200 ppm  
 F2P3 -59.85 Hz  
 F2P4 220.000 ppm  
 F2P5 27868.71 Hz  
 F2P6 -5.000 ppm  
 F2P7 -828.79 Hz  
 F2P8 0.49847 ppm/cm  
 F2P9 249.80016 Hz/cm  
 F2P10 15.00000 ppm/cm  
 F2P11 1696.36558 Hz/cm



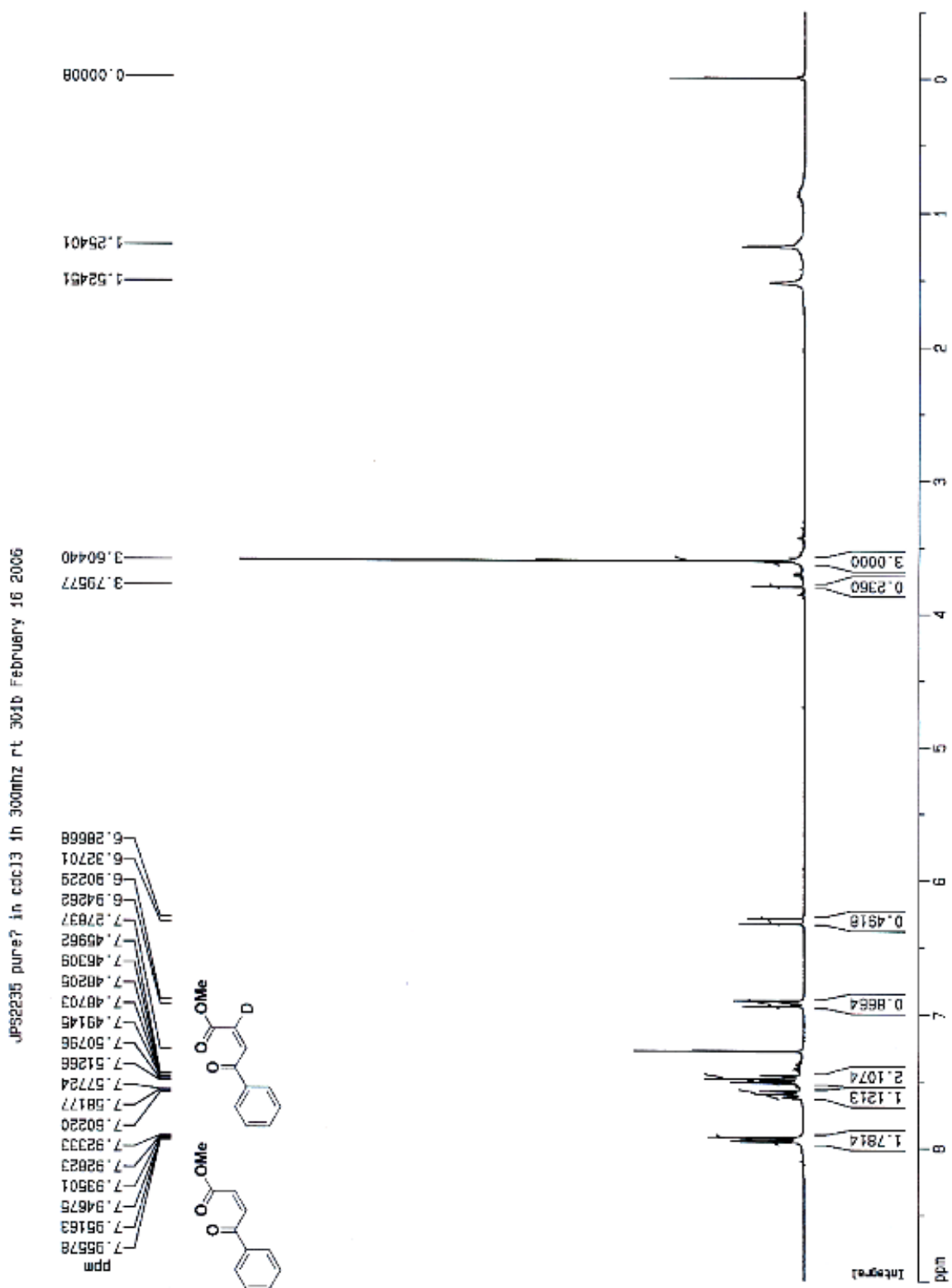
$^1\text{H}$  NMR spectrum of **3d-Z43**:  $\text{CDCl}_3$ , 293 K, 300 MHz



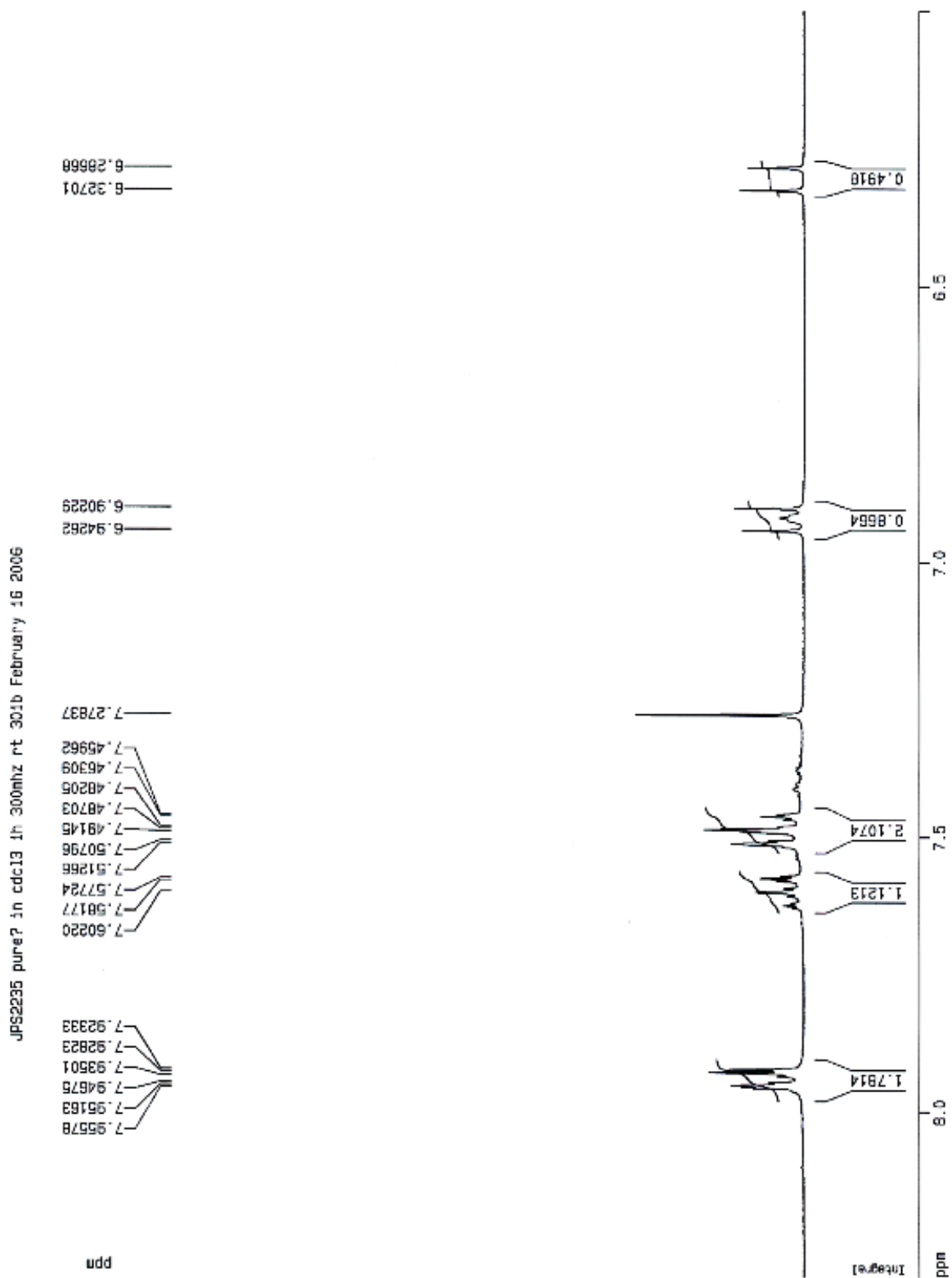
$^1\text{H}$  NMR spectrum of **3d-Z43**:  $\text{CDCl}_3$ , 293 K, 300 MHz



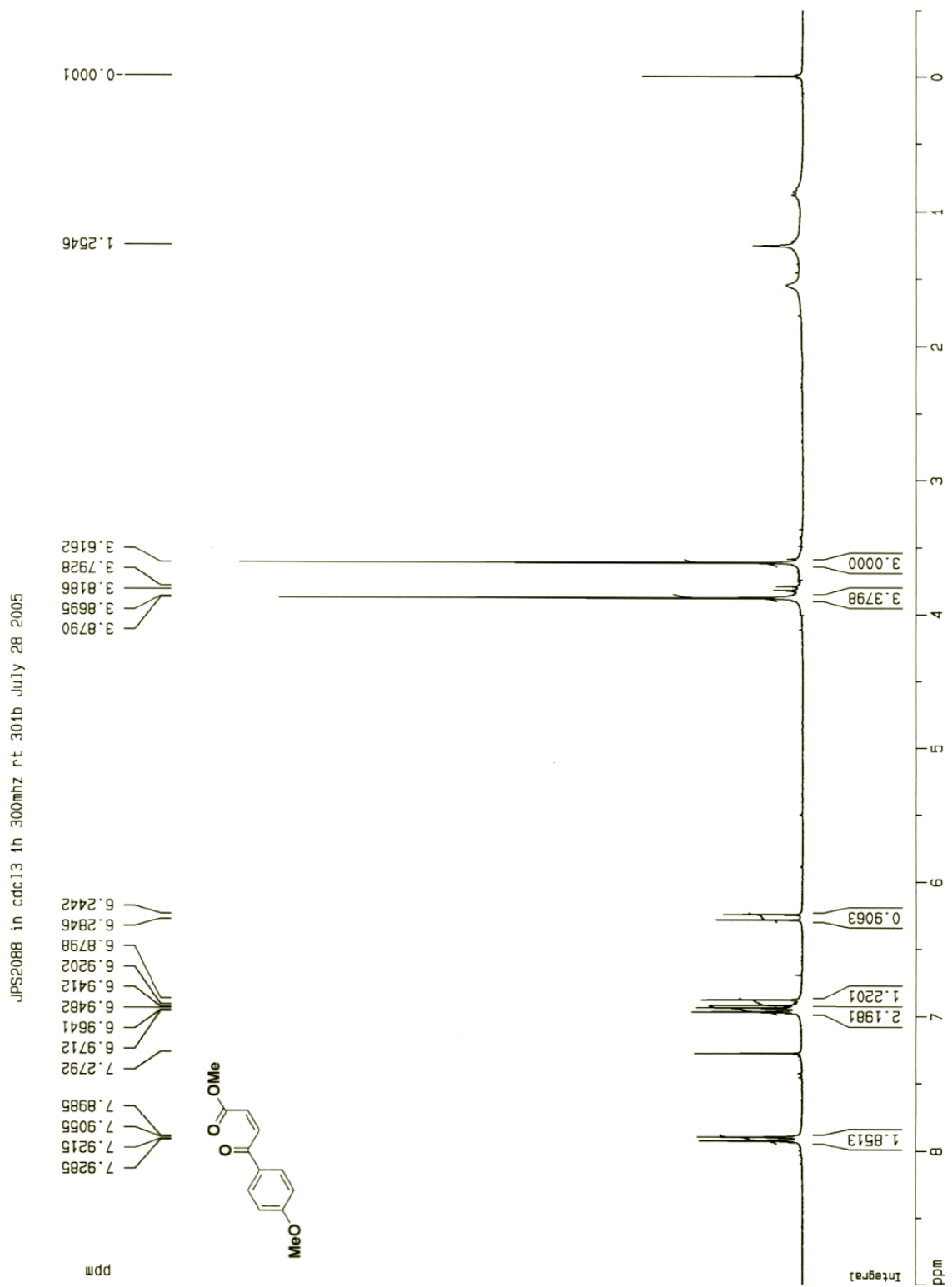
<sup>1</sup>H NMR spectrum of **2d-Z43**: CDCl<sub>3</sub>, 293 K, 300 MHz



$^1\text{H}$  NMR spectrum of **2d-Z43**:  $\text{CDCl}_3$ , 293 K, 300 MHz

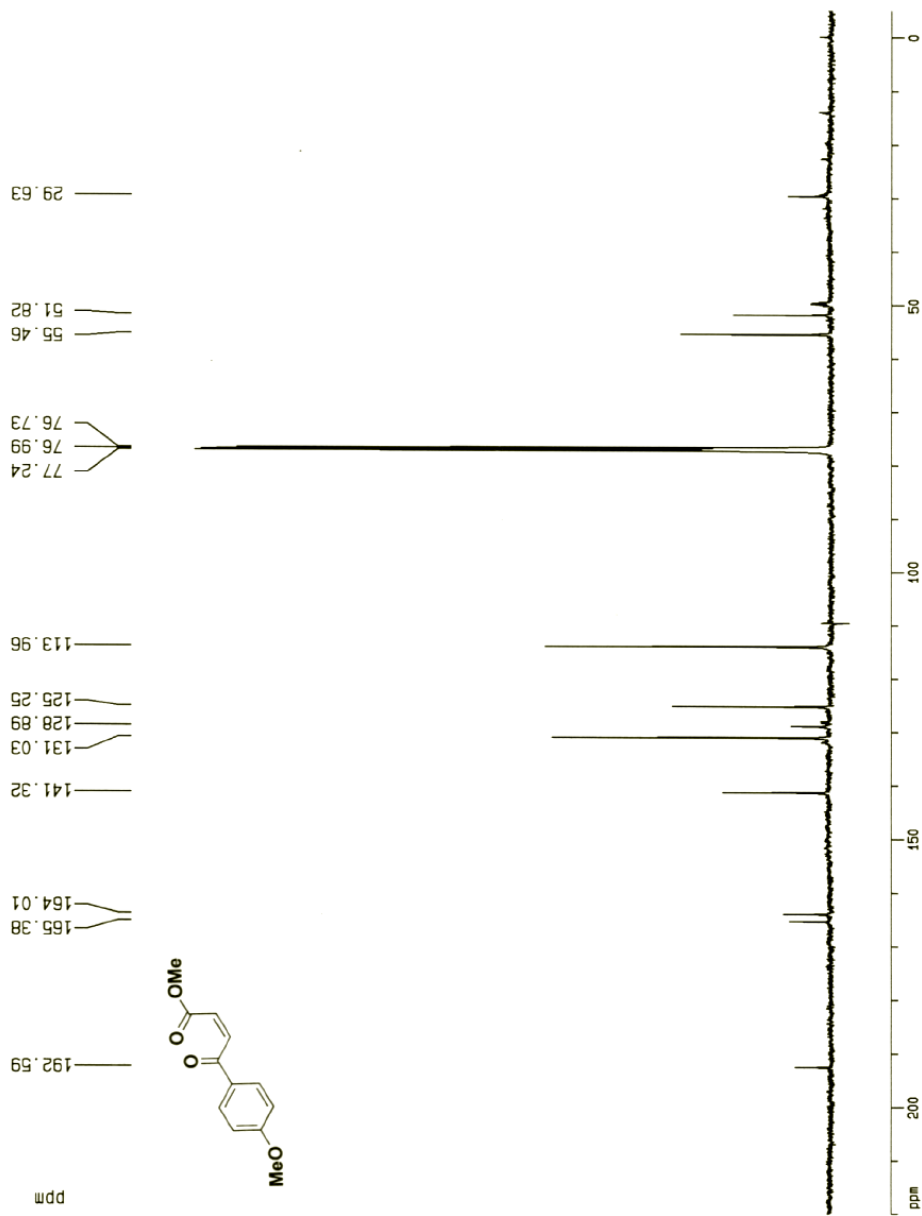


$^1\text{H}$  NMR spectrum of **Z92**:  $\text{CDCl}_3$ , 293 K, 300 MHz



<sup>13</sup>C NMR spectrum of **Z92**: CDCl<sub>3</sub>, 293 K, 125 MHz

JPS2088 in cdc13 13c 125mhz rt 500 August 5 2005



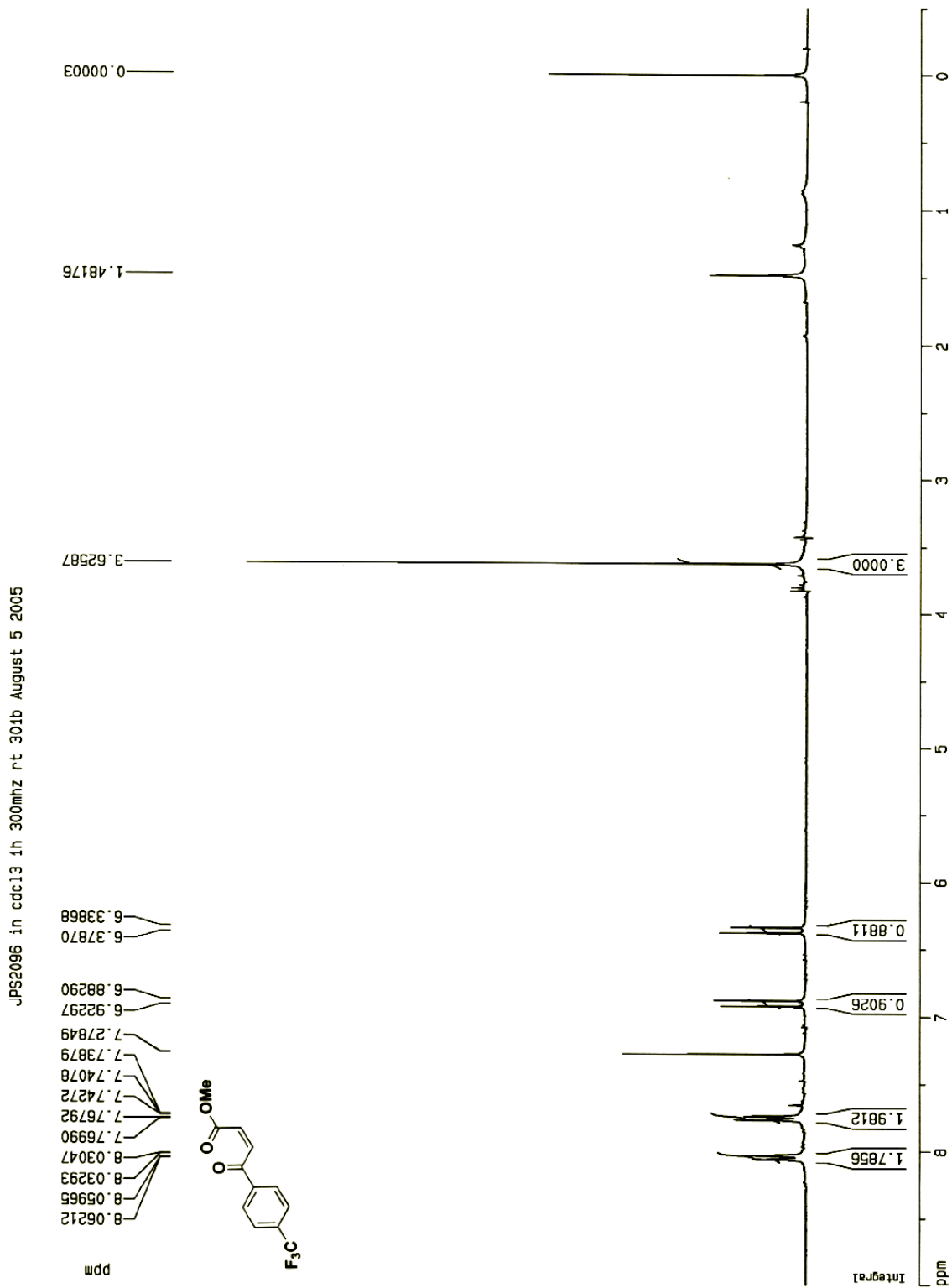
Current Data Parameters  
 NAME JPS2088  
 EXPNO 2  
 PROCNO 1

F2 - Acquisition Parameters  
 Date\_ 500000  
 Time 23.11  
 INSTRUM spect  
 PROBHD 5 mm TXI 13C  
 PULPROG zgpg  
 TD 32768  
 SOLVENT CDCl3  
 NS 6234  
 DS 0  
 SMH 32679.738 Hz  
 FIDRES 0.997306 Hz  
 AQ 0.5014004 sec  
 RG 8192  
 DW 15.300 usec  
 DE 6.00 usec  
 TE 290.0 K  
 d11 0.0300000 sec  
 d12 0.0000200 sec  
 PL13 20.00 dB  
 D1 6.0000000 sec  
 CPDPRG2 waltz16  
 PCPD2 65.00 usec  
 SF02 500.1330008 MHz  
 NUC2 1H  
 PL2 120.00 dB  
 PL12 18.00 dB  
 P1 9.00 usec  
 DE 6.00 usec  
 SF01 125.7715724 MHz  
 NUC1 13C  
 PL1 -6.00 dB

F2 - Processing parameters  
 S1 8192  
 SF 125.7578000 MHz  
 WDW EM  
 SSB 0  
 LB 4.00 Hz  
 GB 0  
 PC 1.00

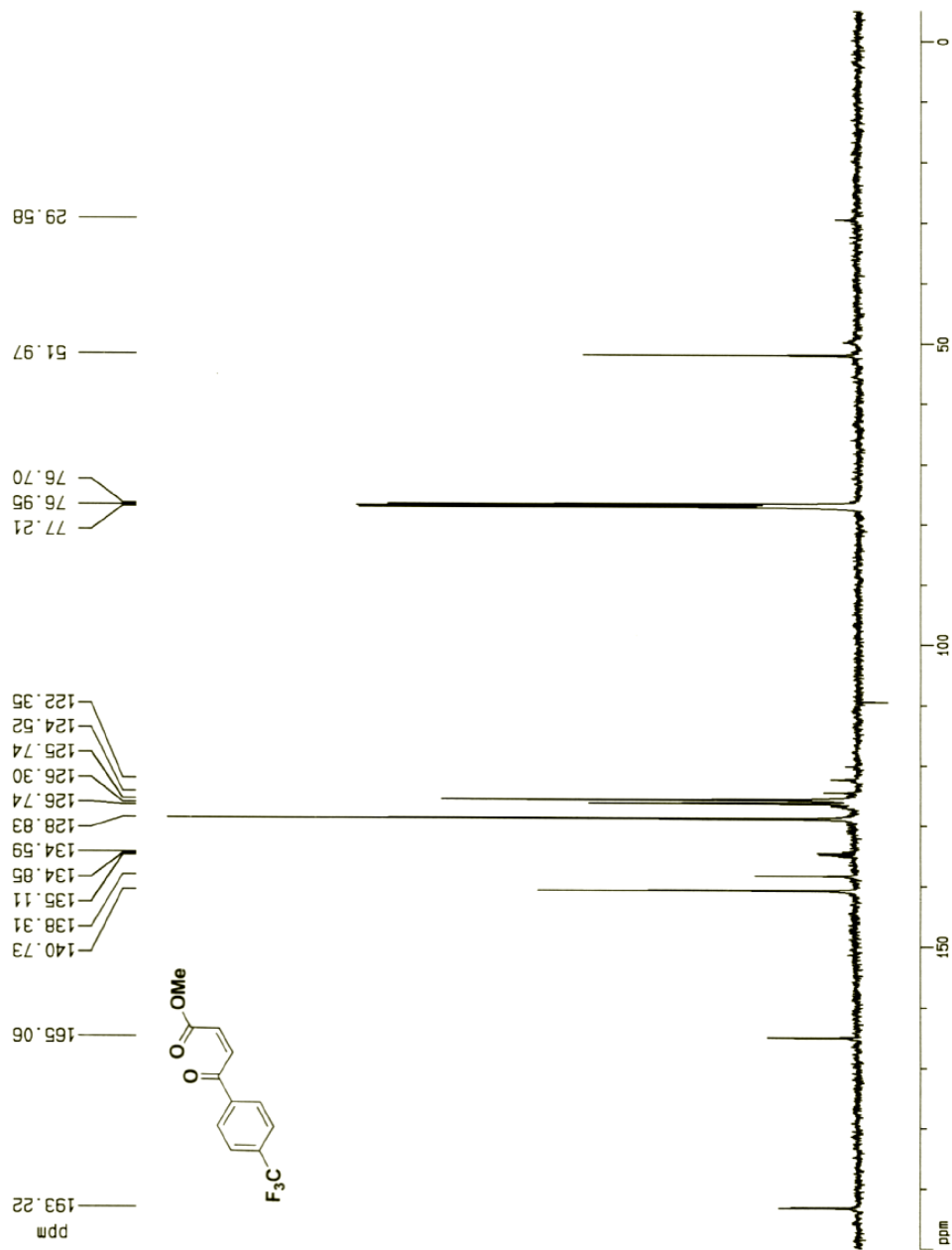
1D NMR plot parameters  
 CX 20.00 cm  
 F1P 220.000 ppm  
 F1 27666.71 Hz  
 F2P -5.000 ppm  
 F2 -628.79 Hz  
 PPMCM 11.25000 ppm/cm  
 HZCM 1414.77527 Hz/cm

<sup>1</sup>H NMR spectrum of **Z94**: CDCl<sub>3</sub>, 293 K, 300 MHz



<sup>13</sup>C NMR spectrum of **Z94**: CDCl<sub>3</sub>, 293 K, 125 MHz

JPS2096 in cdc13 13c 125mhz rt 500 August 5 2005



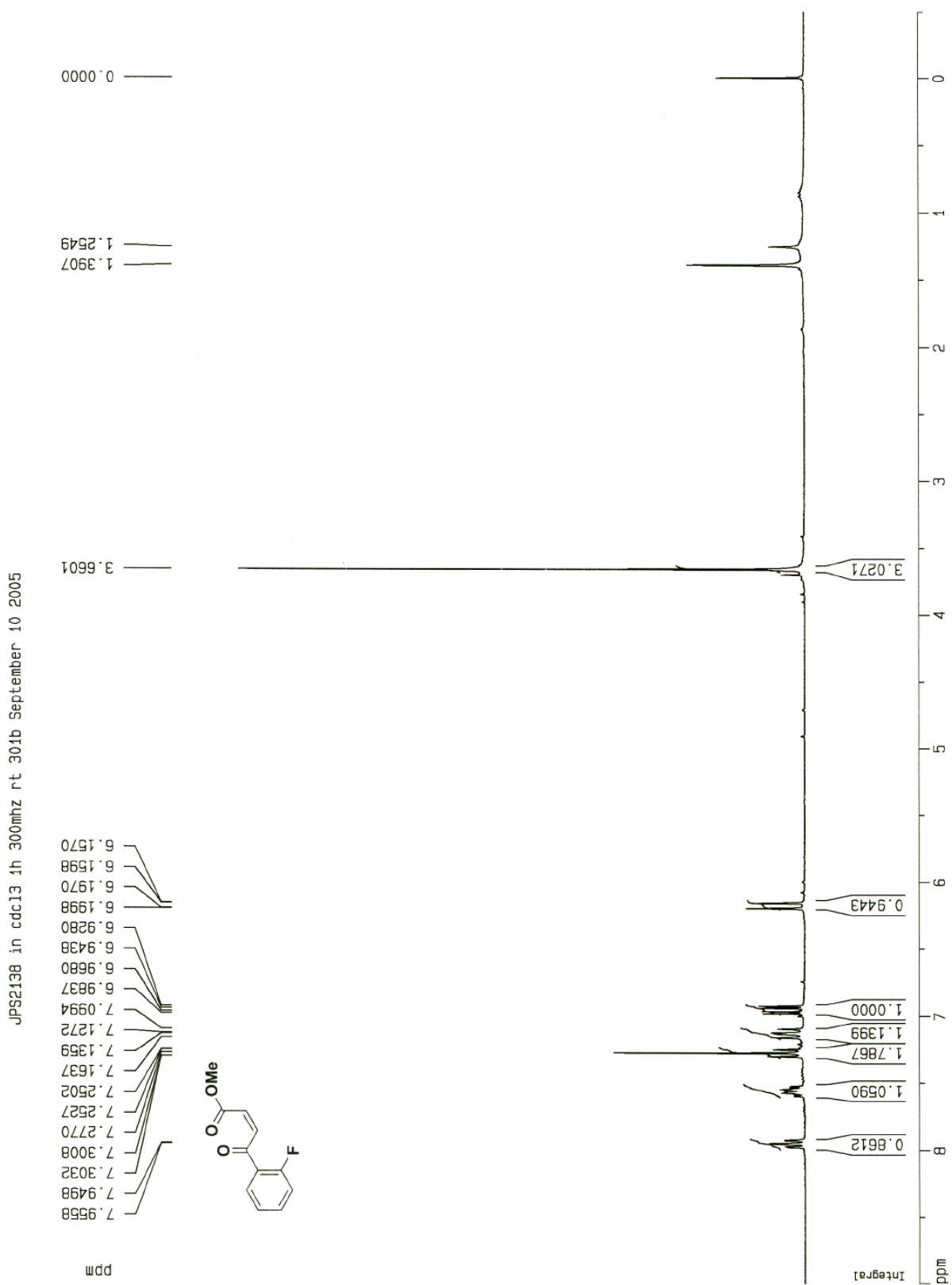
Current Data Parameters  
 NAME JPS2096  
 EXPNO 2  
 PROCNO 1

F2 - Acquisition Parameters  
 Date\_ 500000  
 Time 17.45  
 INSTRUM spect  
 PROBHD 5 mm TXI 13C  
 PULPROG zgpg  
 TO 32768  
 SOLVENT CDCl3  
 NS 1632  
 DS 0  
 SMH 32679.738 Hz  
 FIDRES 0.997306 Hz  
 AQ 0.5014004 sec  
 RG 7298.2  
 DM 15.300 usec  
 DE 6.00 usec  
 TE 290.0 K  
 d11 0.0300000 sec  
 d12 0.0002000 sec  
 PL13 20.00 dB  
 D1 6.00000000 sec  
 CPDPRG2 waltz16  
 PCPD2 65.00 usec  
 SF02 500.1330008 MHz  
 NUC2 1H  
 PL2 120.00 dB  
 PL12 18.00 dB  
 P1 9.00 usec  
 DE 6.00 usec  
 SF01 125.7715724 MHz  
 NUC1 13C  
 PL1 -6.00 dB

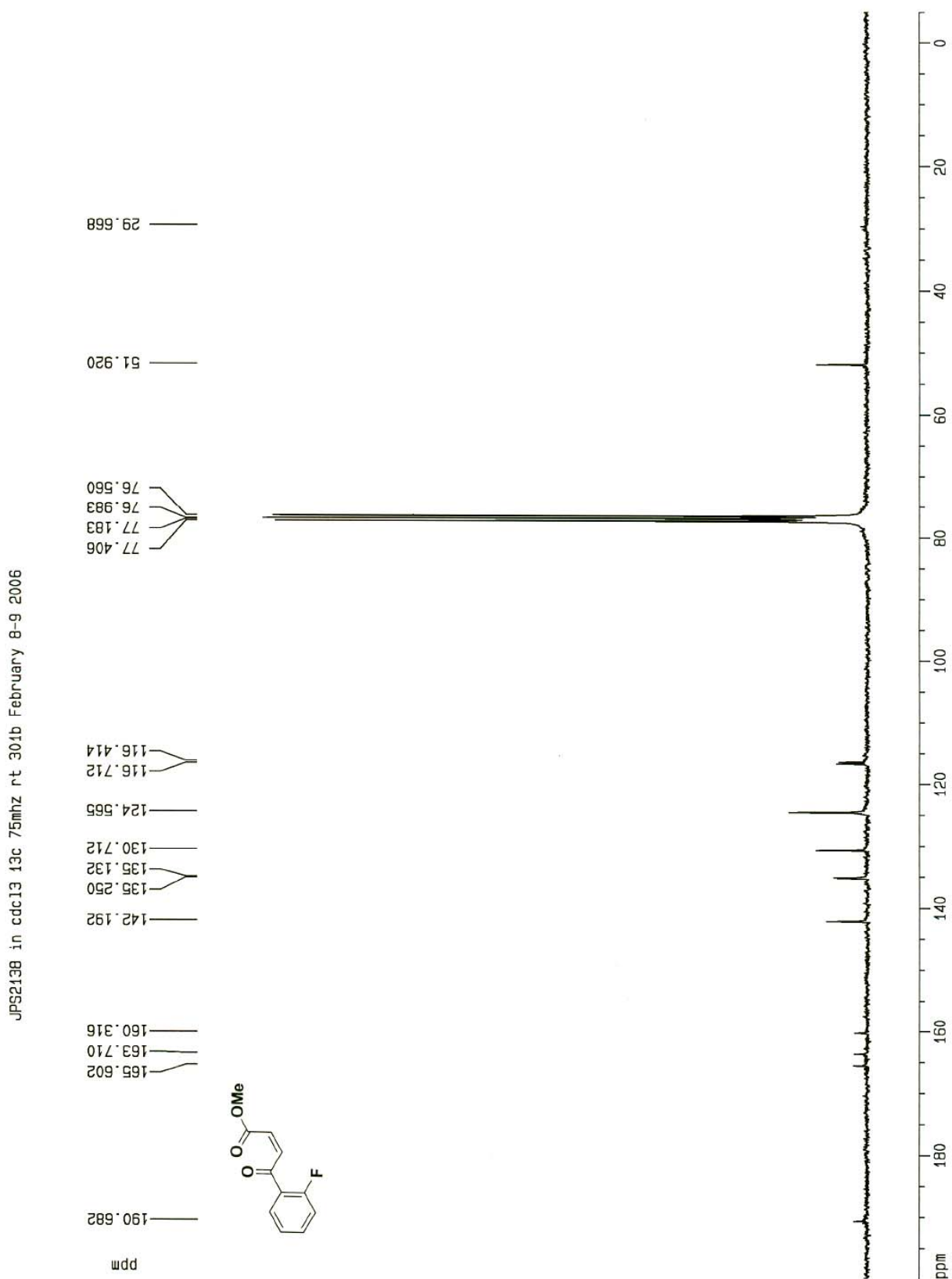
F2 - Processing parameters  
 SI 8192  
 SF 125.7578047 MHz  
 MDW EM  
 SSB 0  
 LB 4.00 Hz  
 GB 0  
 PC 1.00

1D NMR plot parameters  
 CX 20.00 cm  
 F1P 200.000 ppm  
 F1 25151.56 Hz  
 F2P -5.000 ppm  
 F2 -628.79 Hz  
 PPMCM 10.25000 ppm/cm  
 HZCM 1269.04758 Hz/cm

<sup>1</sup>H NMR spectrum of **Z98**: CDCl<sub>3</sub>, 293 K, 300 MHz

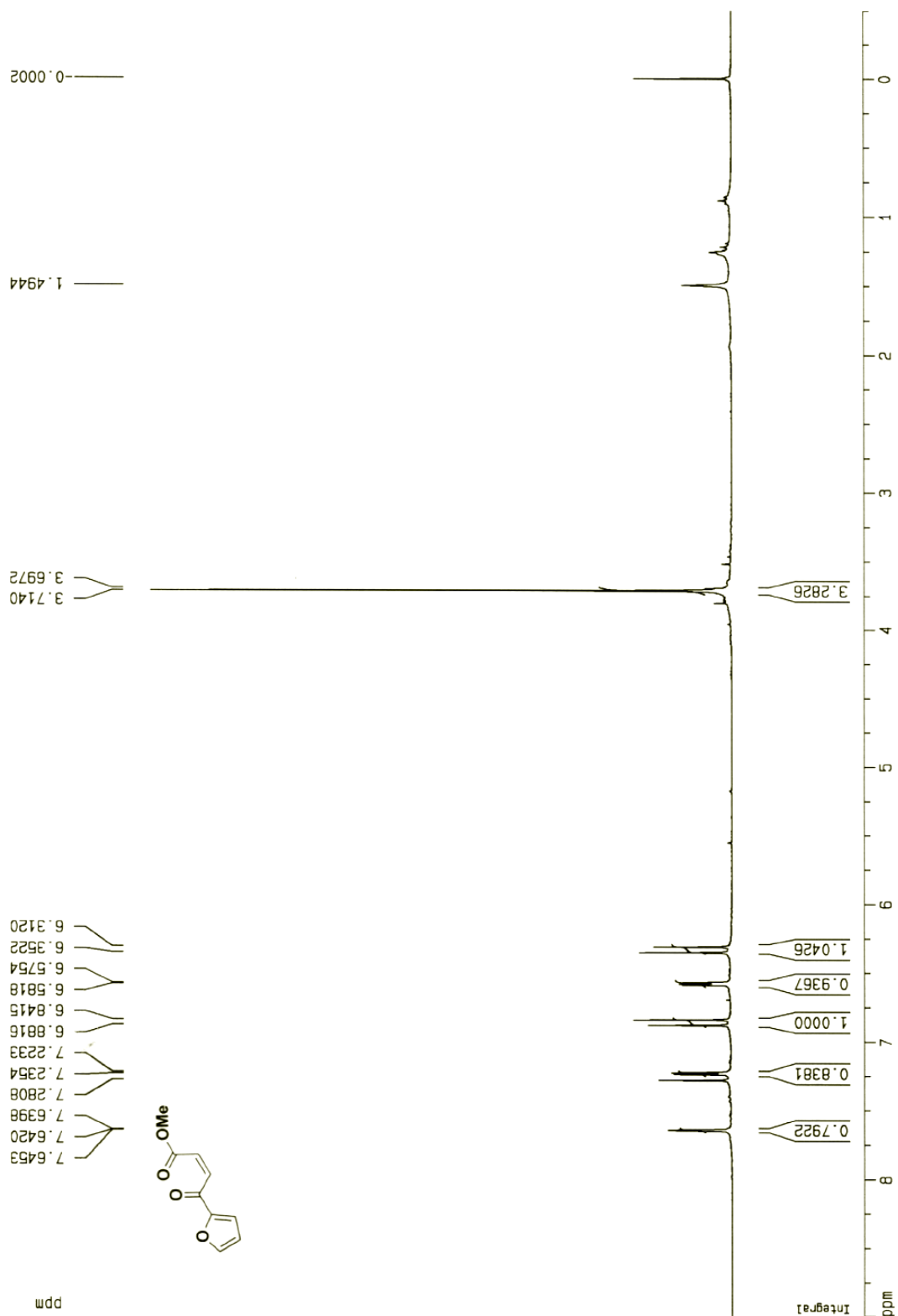


$^{13}\text{C}$  NMR spectrum of **Z98**:  $\text{CDCl}_3$ , 293 K, 75 MHz

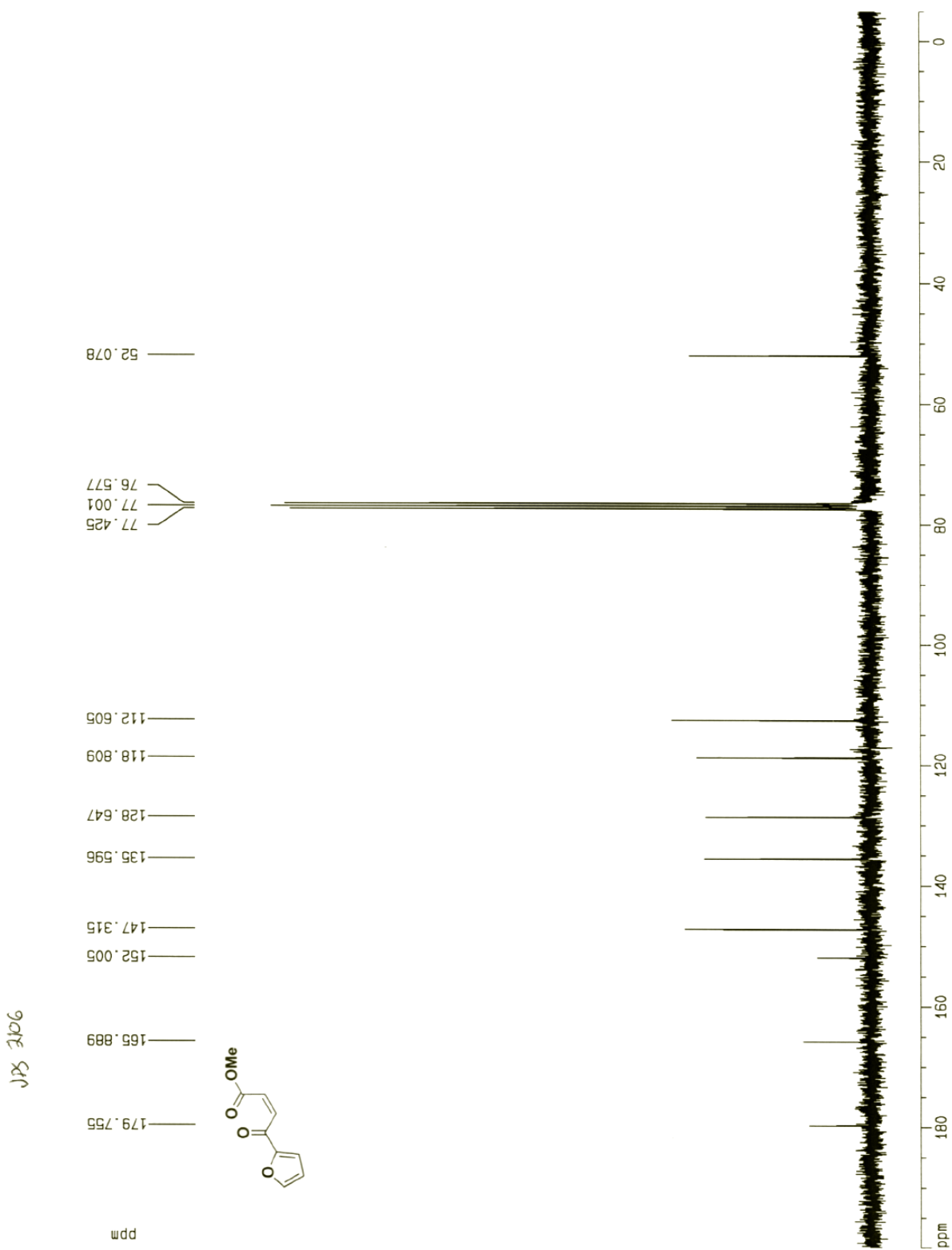


<sup>1</sup>H NMR spectrum of **Z100**: CDCl<sub>3</sub>, 293 K, 300 MHz

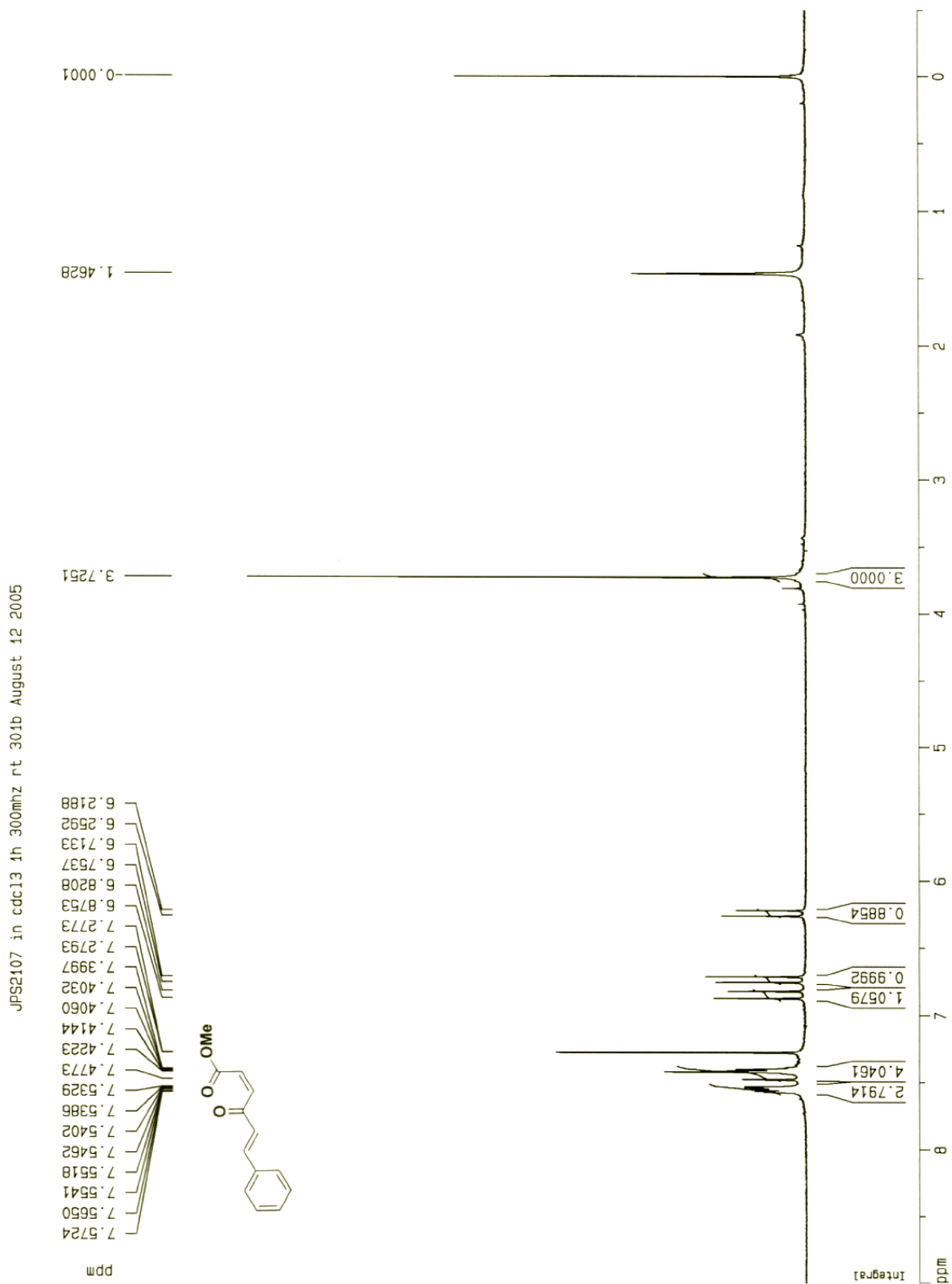
JPS2106 in cdcl3 1h 300mhz rt 301 August 11 2005



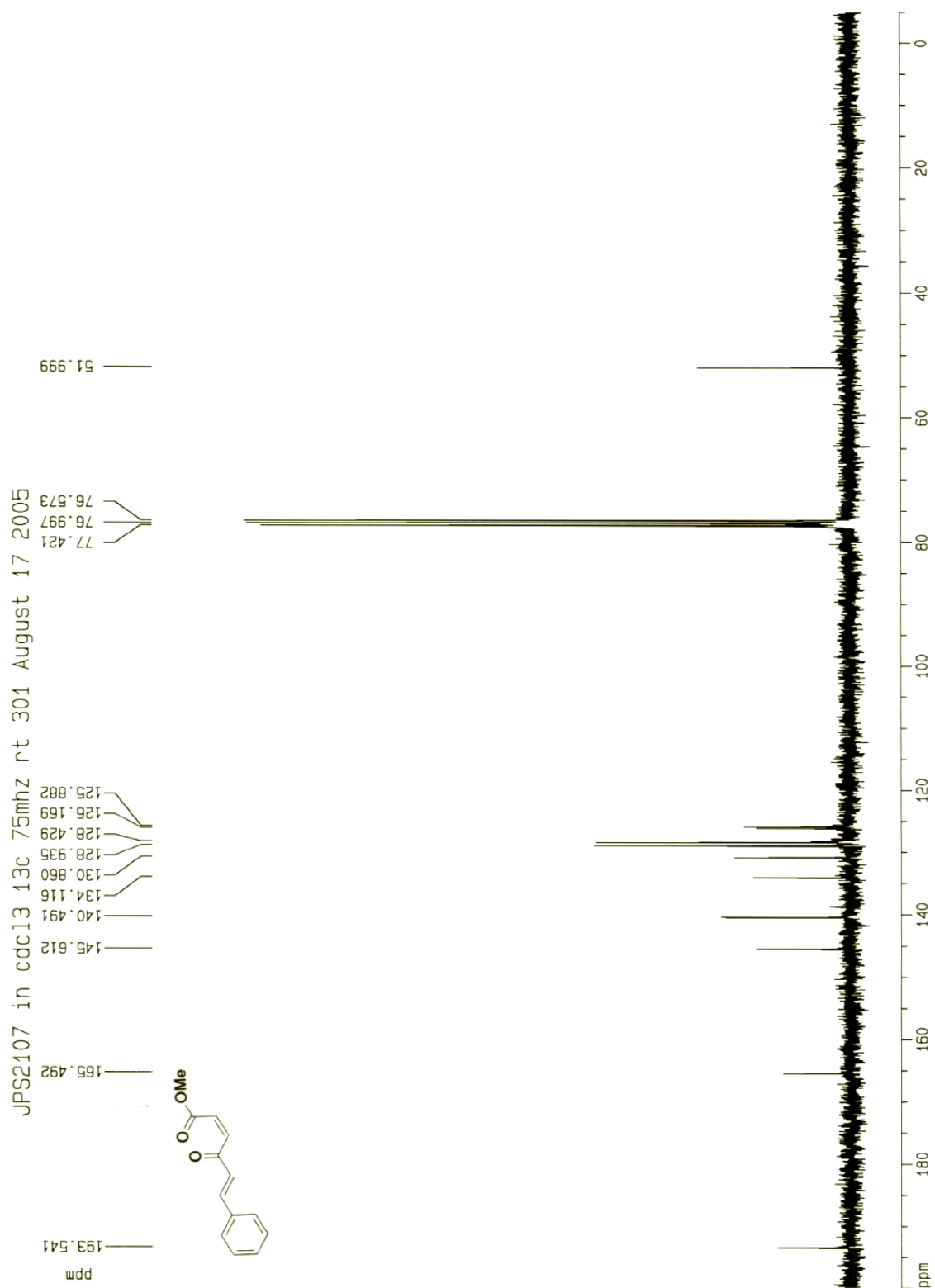
$^{13}\text{C}$  NMR spectrum of **Z100**:  $\text{CDCl}_3$ , 293 K, 75 MHz



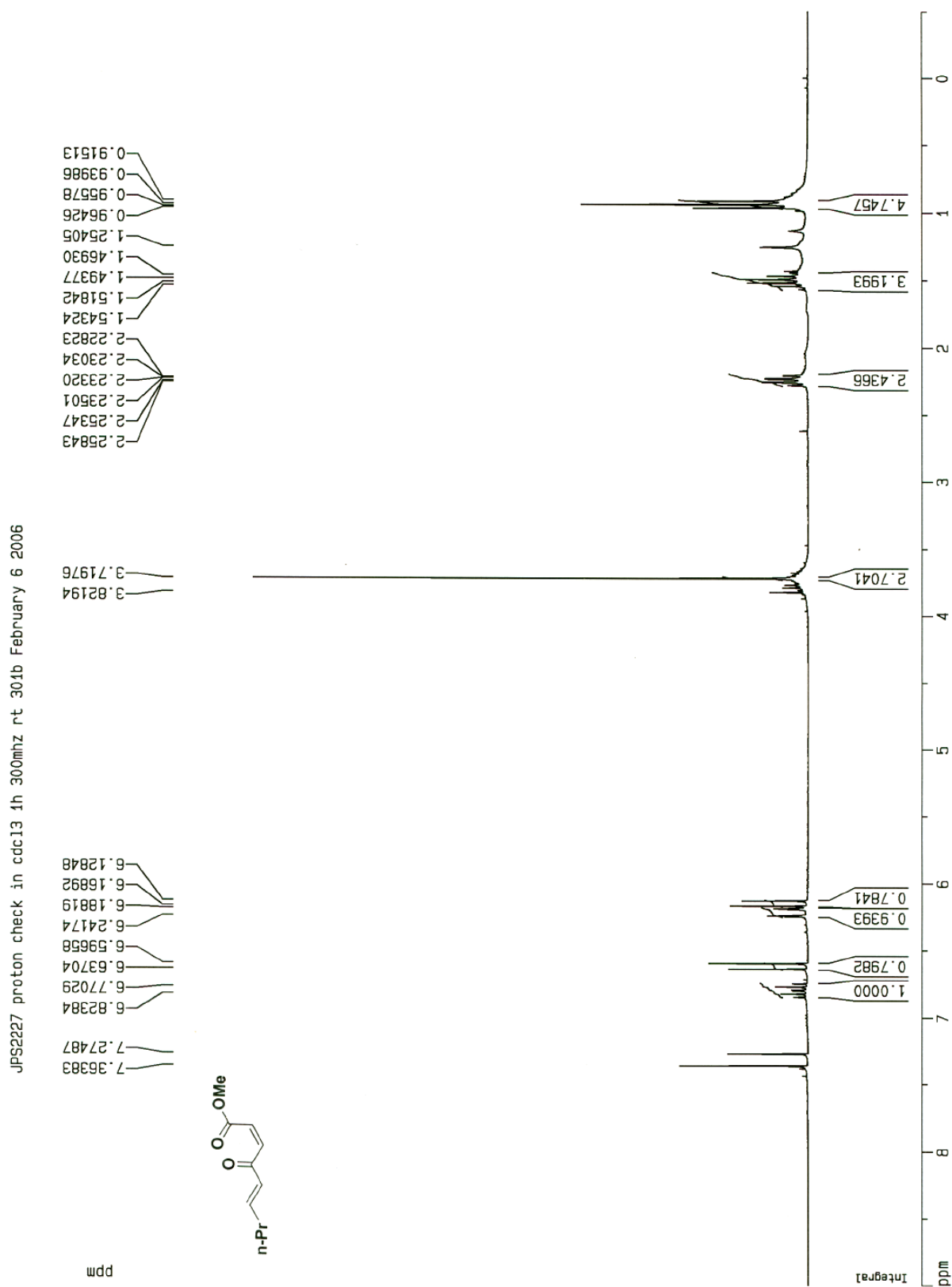
$^1\text{H}$  NMR spectrum of **Z102**:  $\text{CDCl}_3$ , 293 K, 300 MHz



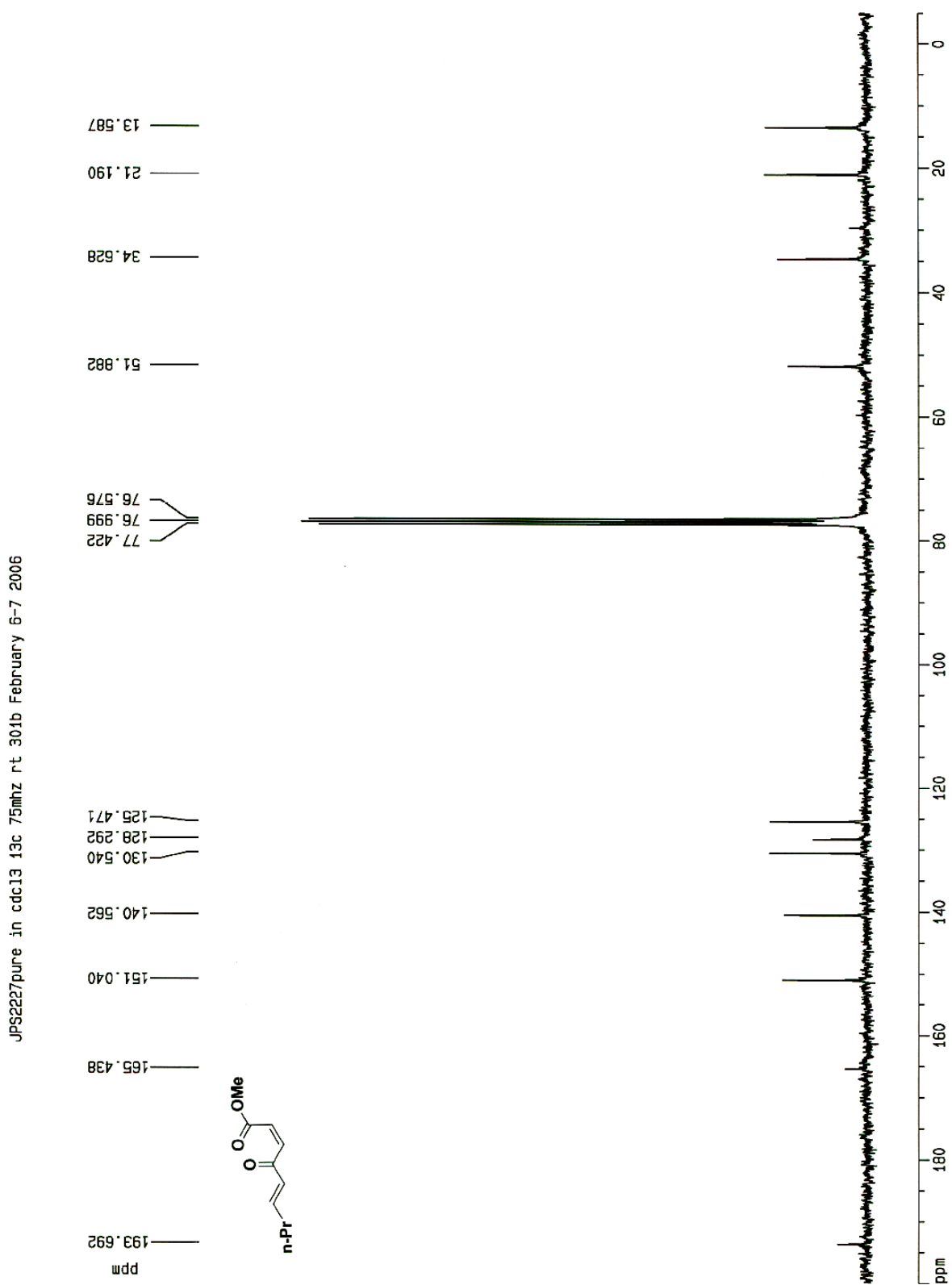
$^{13}\text{C}$  NMR spectrum of **Z102**:  $\text{CDCl}_3$ , 293 K, 75 MHz



$^1\text{H}$  NMR spectrum of **Z104**:  $\text{CDCl}_3$ , 293 K, 300 MHz

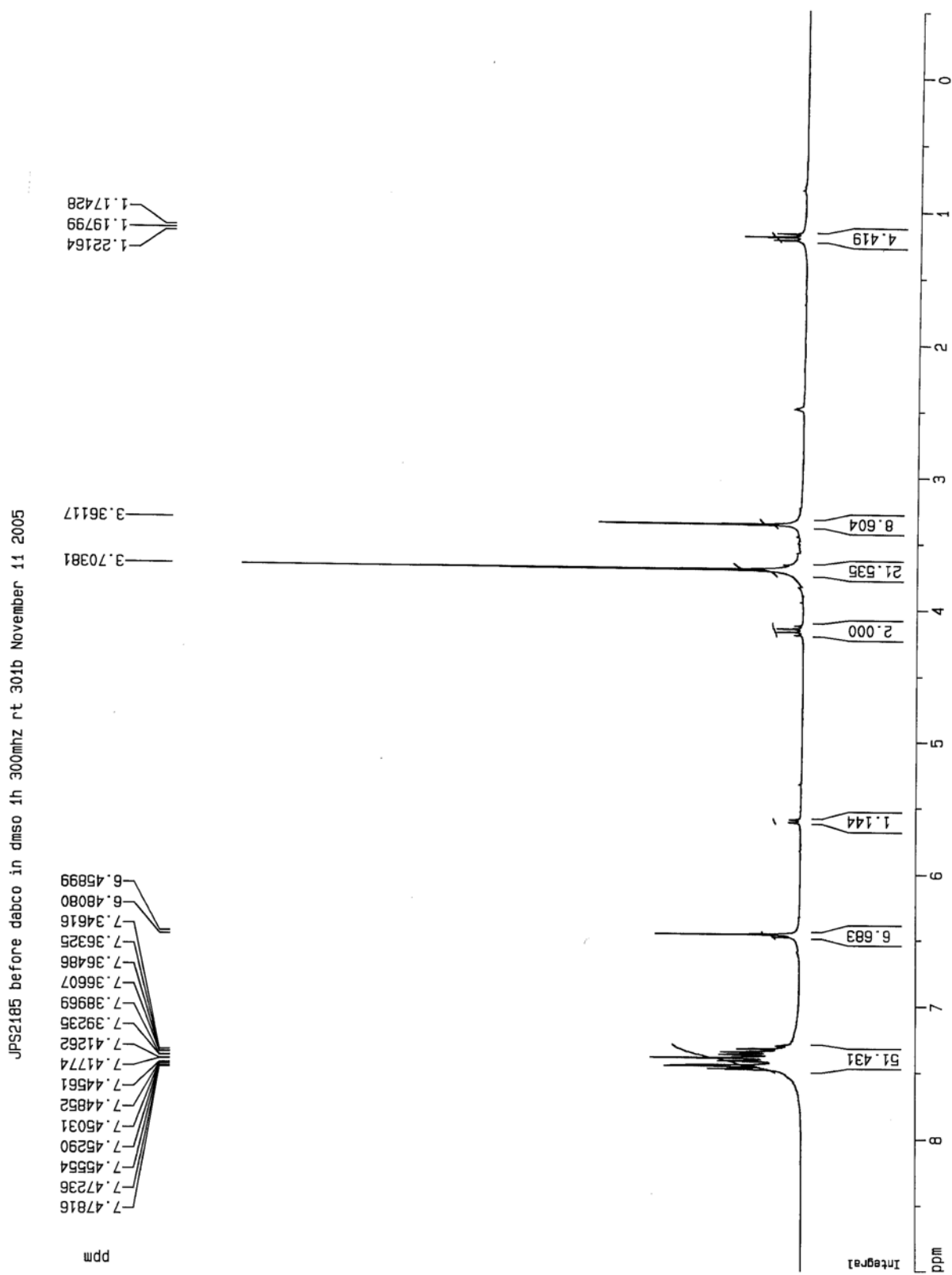


$^{13}\text{C}$  NMR spectrum of **Z104**:  $\text{CDCl}_3$ , 293 K, 75 MHz

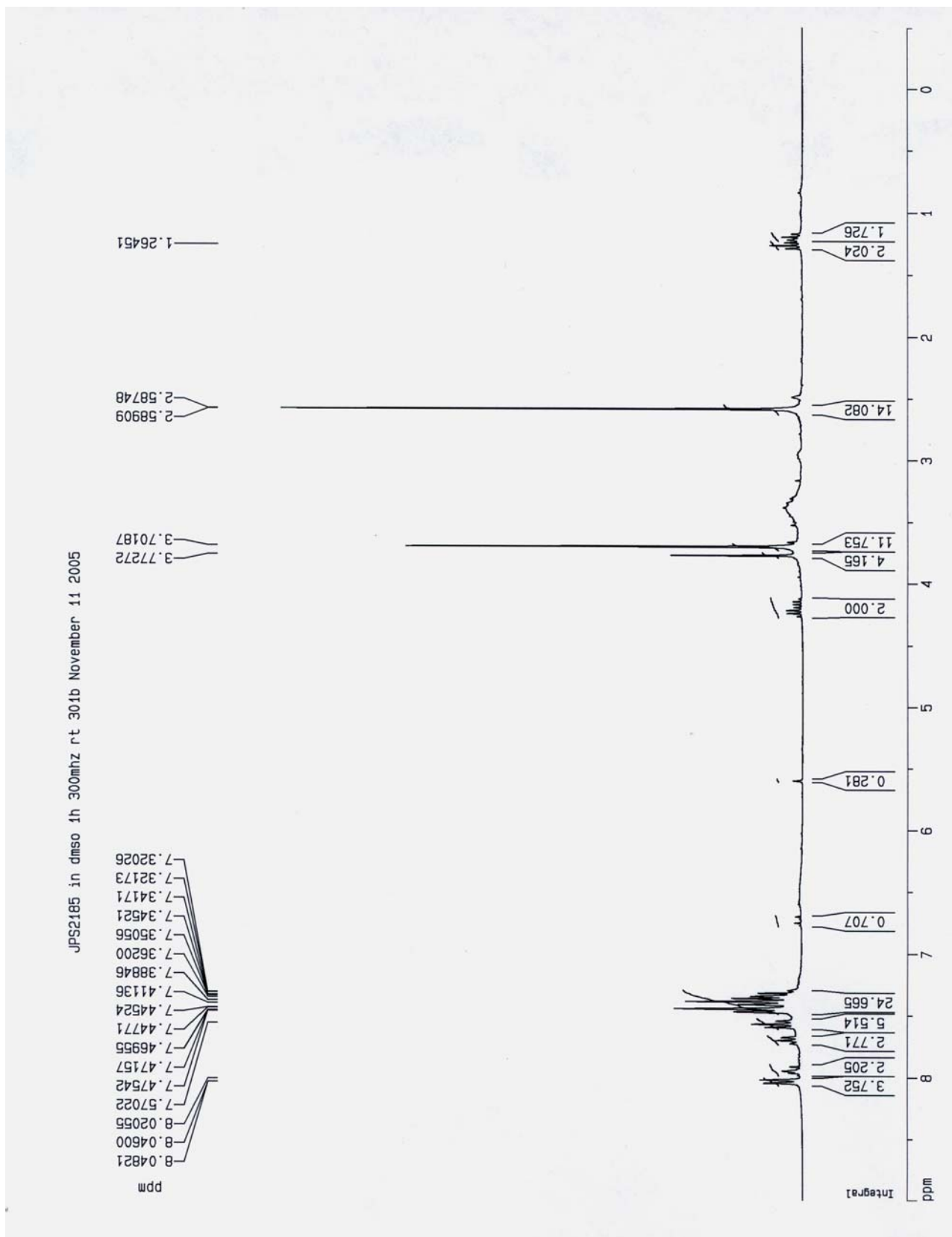




H-D crossover experiment before DABCO addition

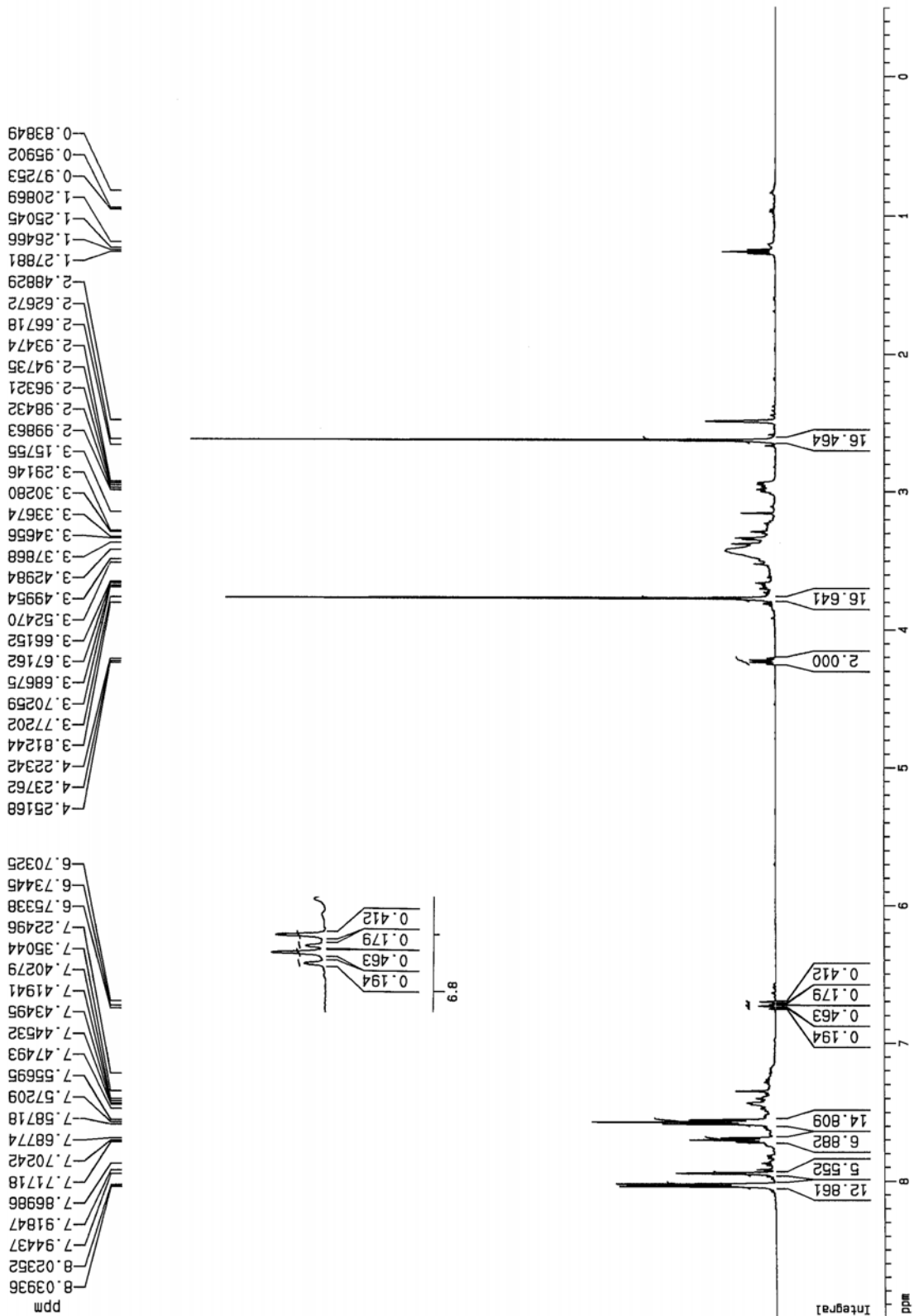


H-D crossover experiment sometime after the DABCO addition

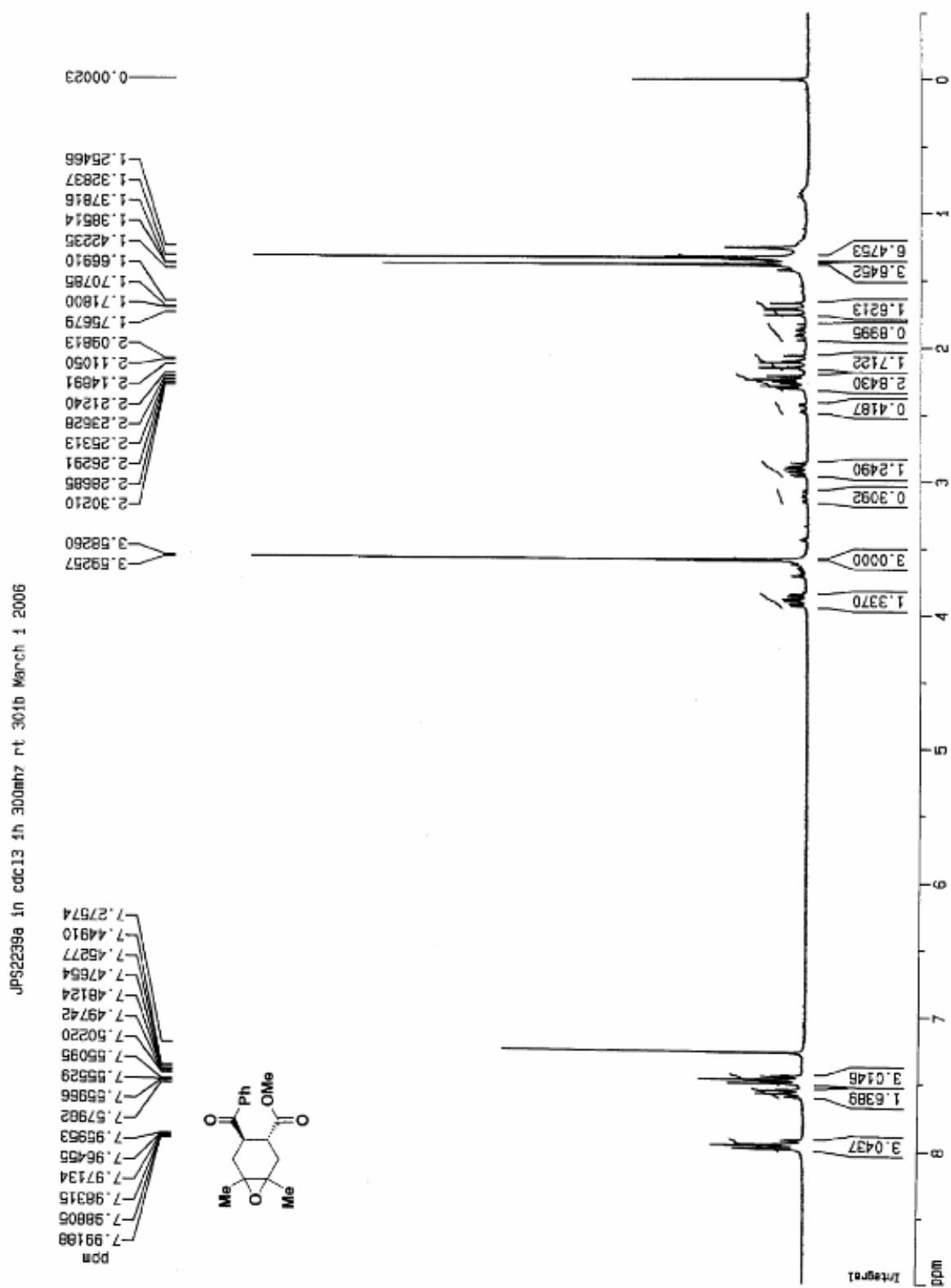


H-D crossover experiment after the redox isomerization

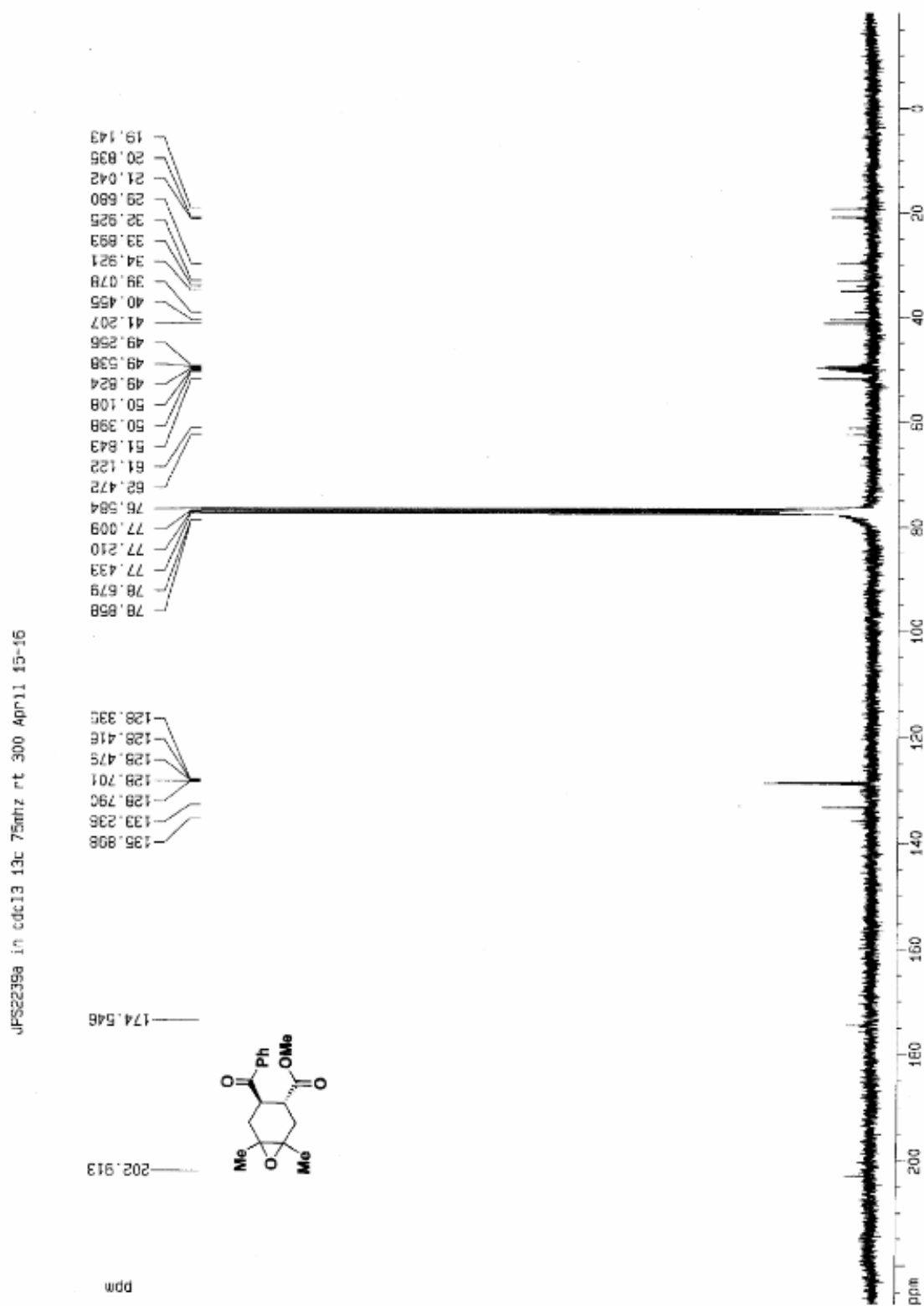
JPS2185 after particulate filtration 500mhz rt November 12 2005



$^1\text{H}$  NMR spectrum of **141a**:  $\text{CDCl}_3$ , 293 K, 300 MHz

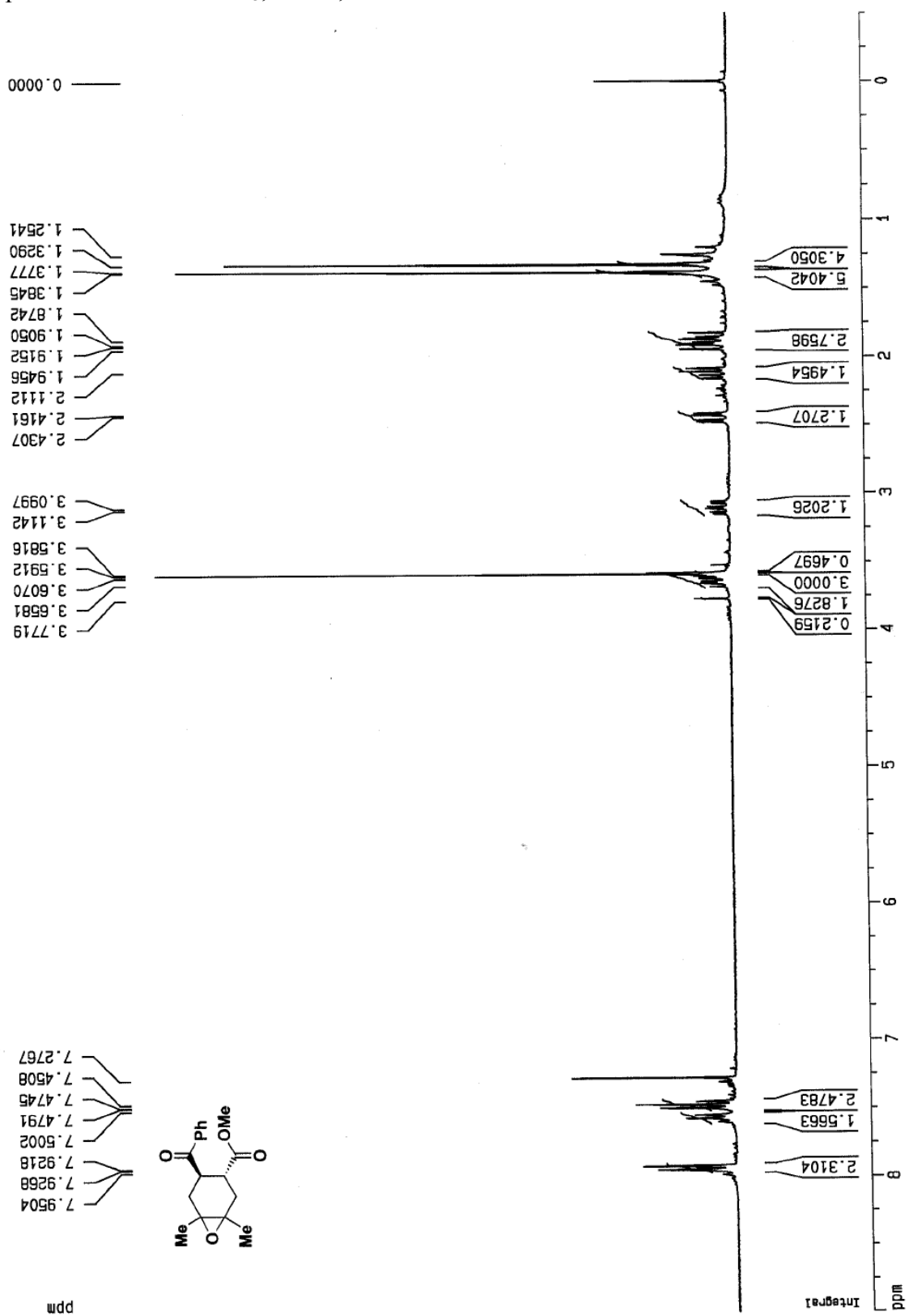


$^{13}\text{C}$  NMR spectrum of **141a**:  $\text{CDCl}_3$ , 293 K, 75 MHz



<sup>1</sup>H NMR spectrum of **141b**: CDCl<sub>3</sub>, 293 K, 300 MHz

JPS2239b in cdc13 1h 300mhz rt 301 March 1 2006



<sup>13</sup>C NMR spectrum of **141b**: CDCl<sub>3</sub>, 293 K, 125 MHz

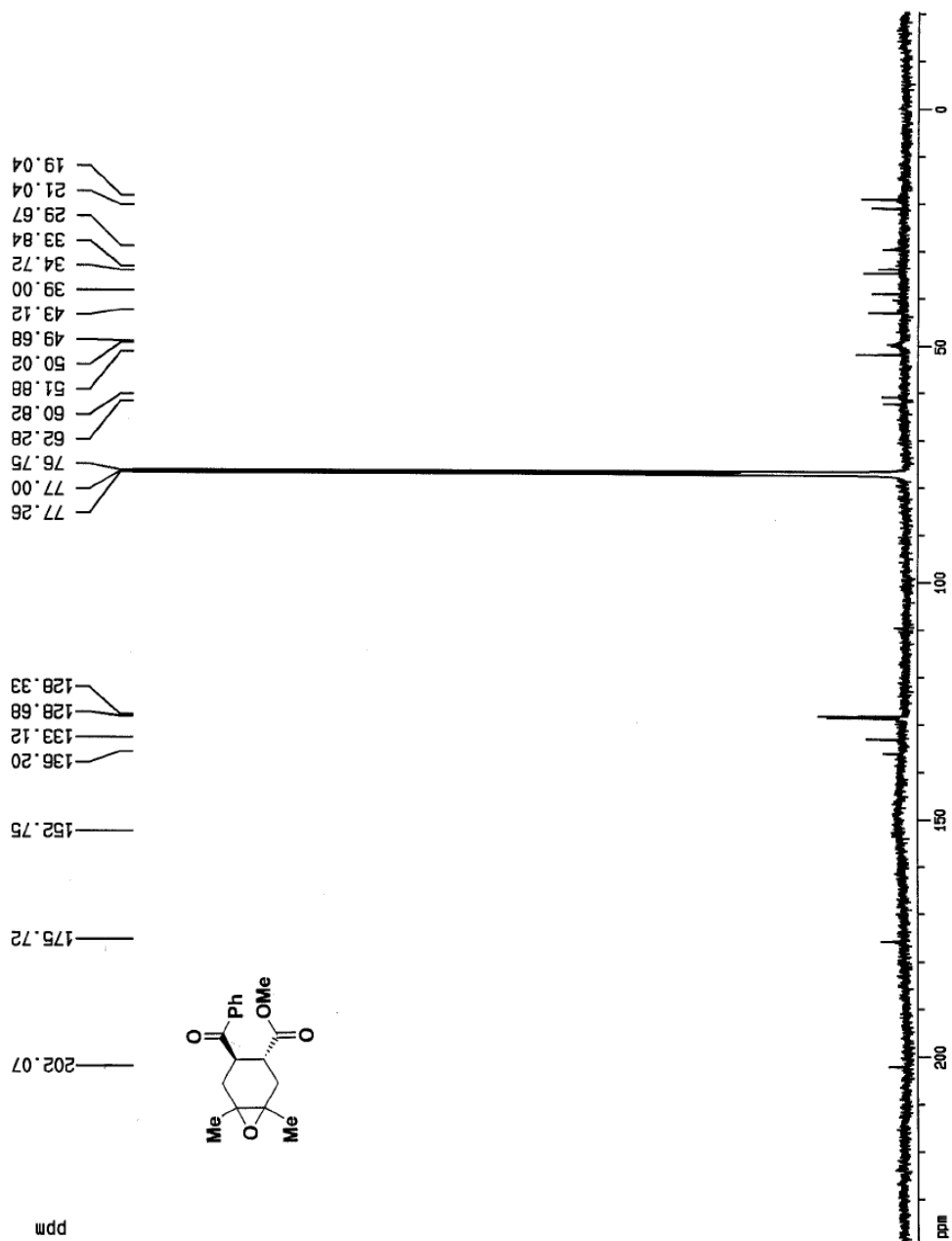
Current Data Parameters  
 NAME JPS2239b  
 EXPNO 2  
 PROCNO 1

F2 - Acquisition Parameters  
 Date\_ 500000  
 Time 11.31  
 INSTRUM spect  
 PROBHD 5 mm TXI 13C  
 PULPROG c13winoe  
 TD 32768  
 SOLVENT CDCl3  
 NS 11764  
 DS 0  
 SWH 32679.738 Hz  
 FIDRES 0.997306 Hz  
 AQ 0.5014004 sec  
 RG 8192  
 DM 15.300 usec  
 DE 6.00 usec  
 TE 290.0 K  
 D3 0.00100000 sec  
 PL12 6.00 dB  
 D1 6.00000000 sec  
 CPDPRG2 waltz16  
 PCPD2 100.00 usec  
 SF02 500.1330008 MHz  
 NUC2 1H  
 PL2 120.00 dB  
 P1 15.50 usec  
 DE 6.00 usec  
 SF01 125.7715724 MHz  
 NUC1 13C  
 PL1 0.00 dB

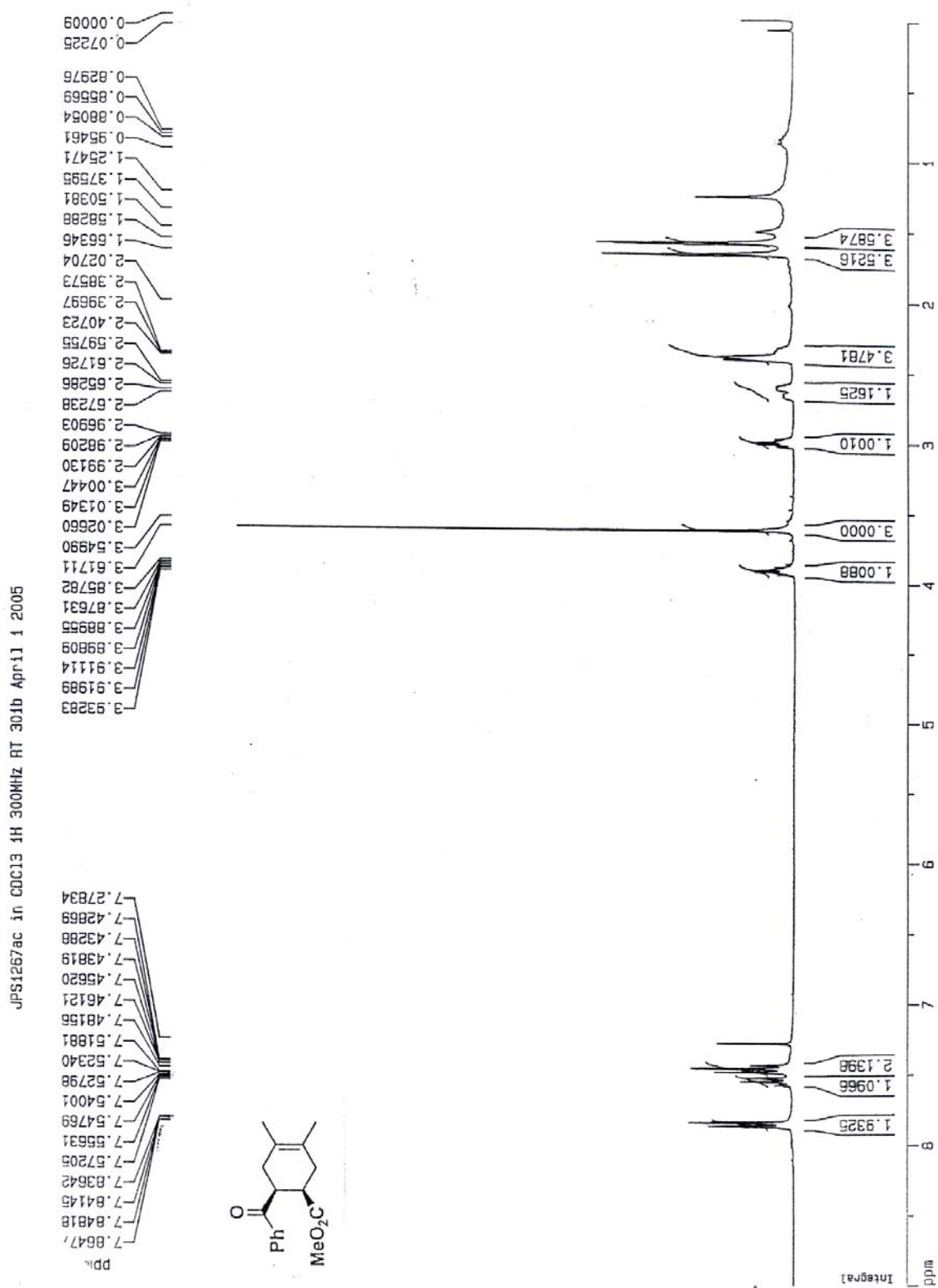
F2 - Processing parameters  
 SI 8192  
 SF 125.7577961 MHz  
 WDM EM  
 SSB 0  
 LB 4.00 Hz  
 GB 0  
 PC 1.00

1D NMR plot parameters  
 CX 20.00 cm  
 F1P 239.478 ppm  
 F1 30116.16 Hz  
 F2P -20.385 ppm  
 F2 -2563.57 Hz  
 PPMCM 12.95313 ppm/cm  
 HZCM 1633.98694 Hz/cm

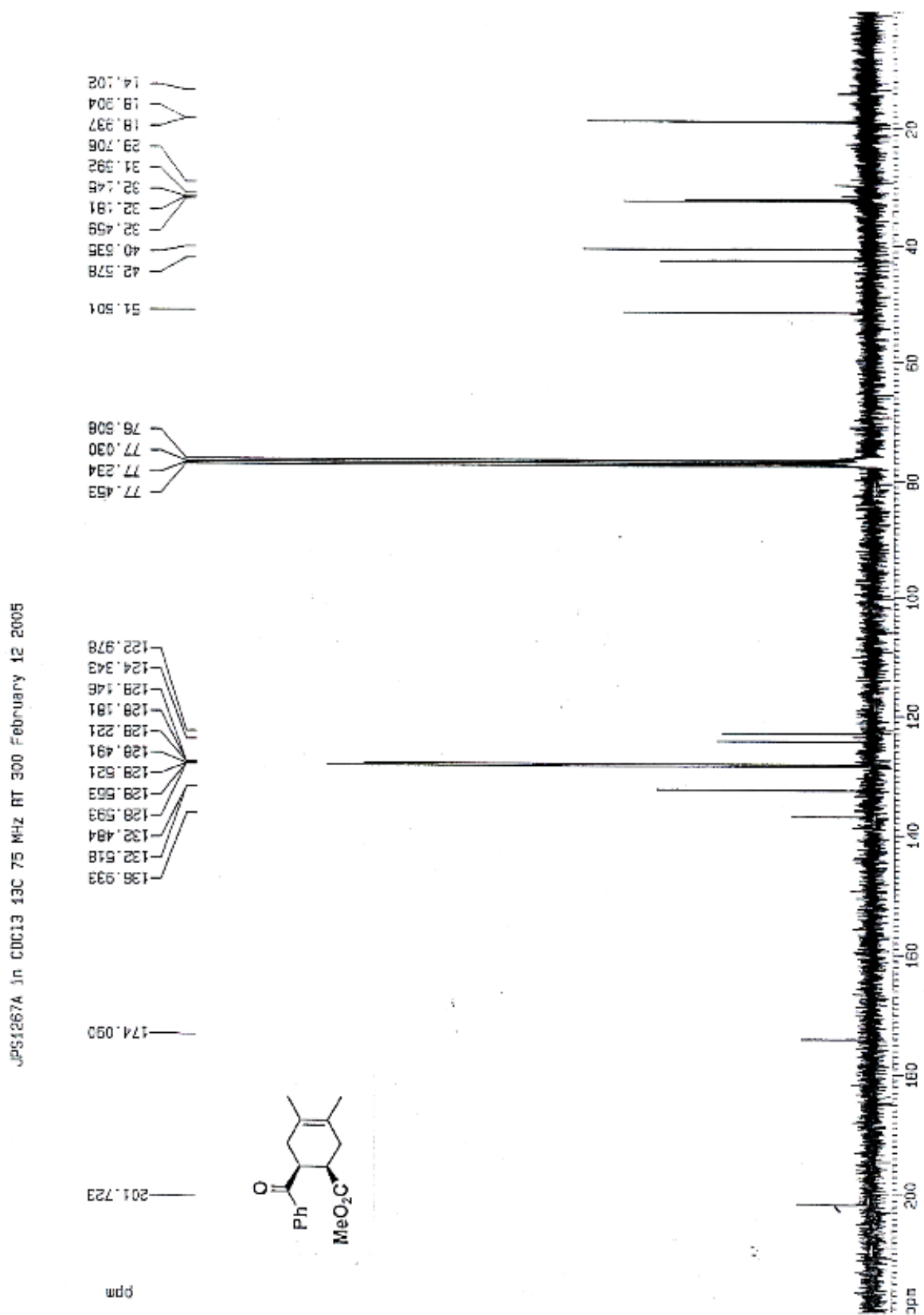
JPS2239b in cdc13 13c 125mhz rt April 24-26 2006



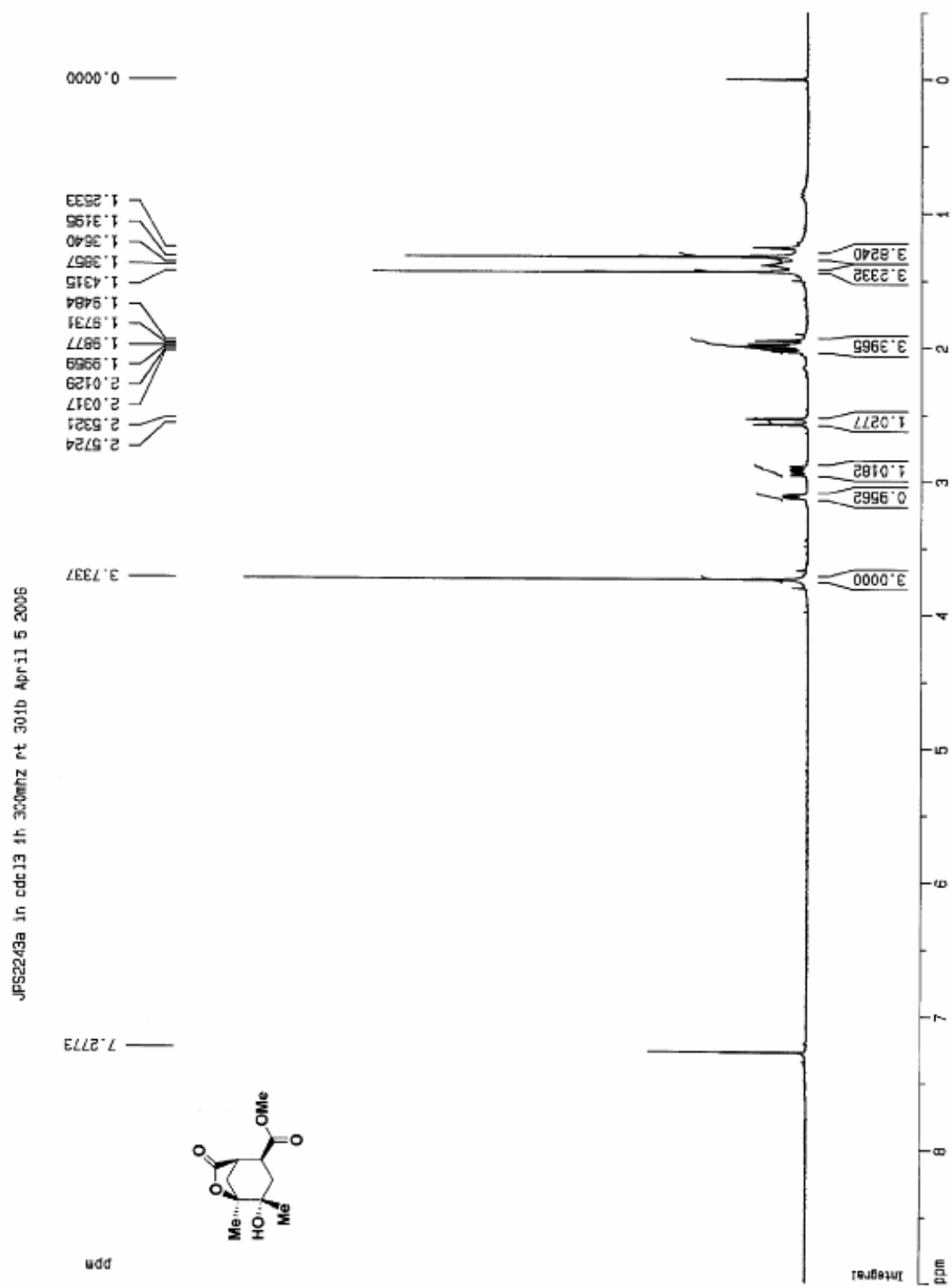
<sup>1</sup>H NMR spectrum of **143**: CDCl<sub>3</sub>, 293 K, 300 MHz



$^{13}\text{C}$  NMR spectrum of **143**:  $\text{CDCl}_3$ , 293 K, 75 MHz

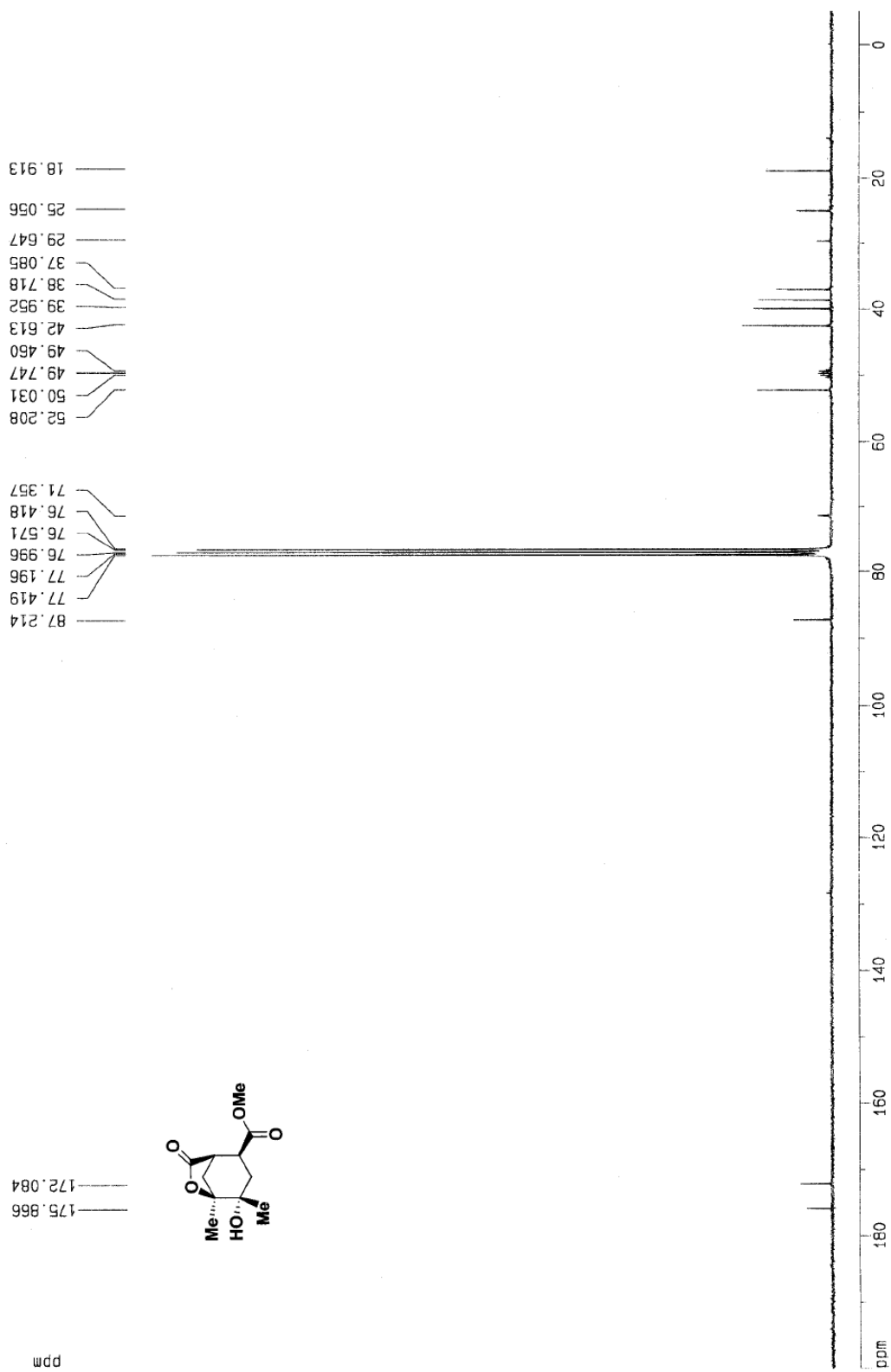


$^1\text{H}$  NMR spectrum of **145**:  $\text{CDCl}_3$ , 293 K, 300 MHz

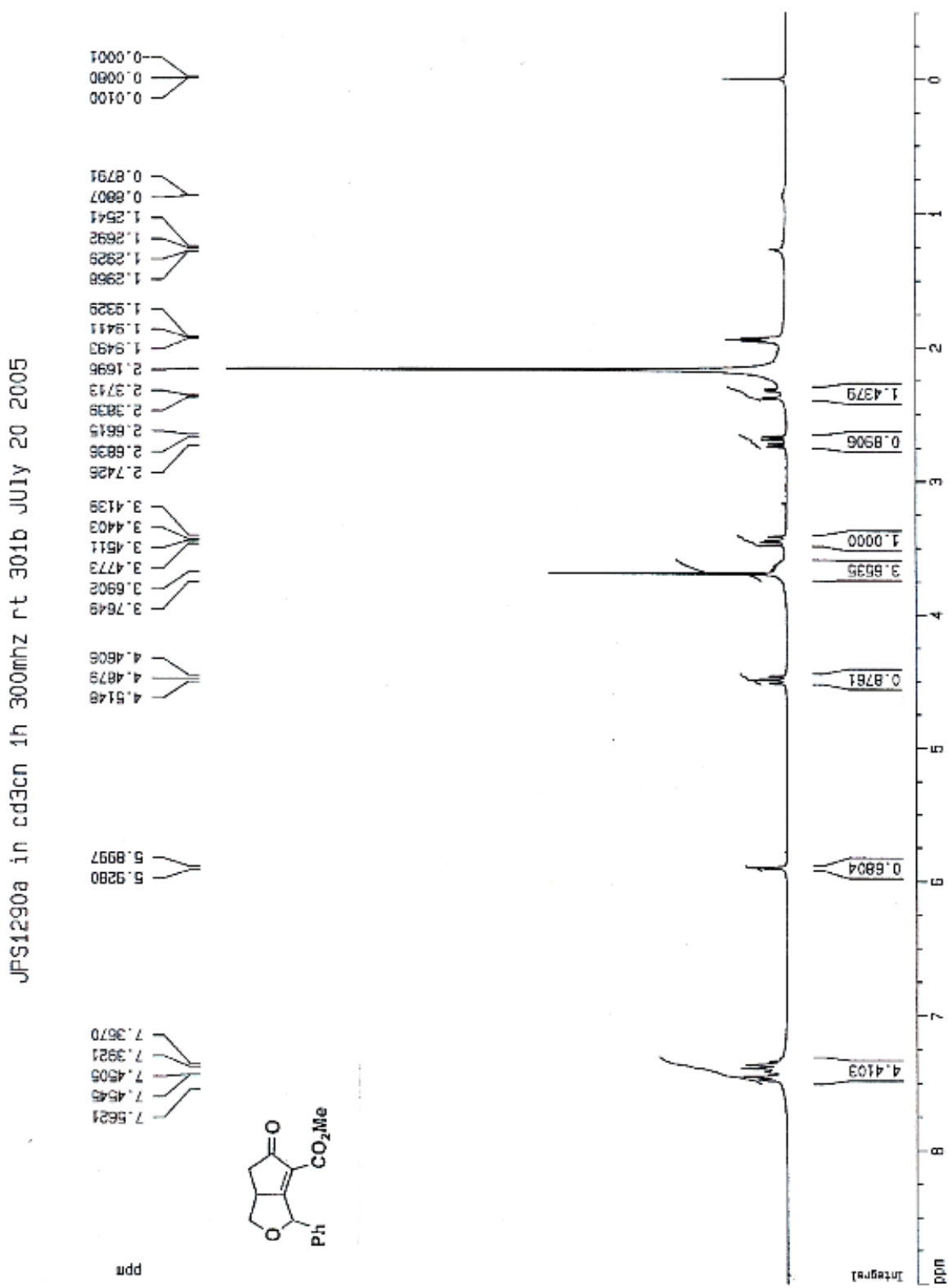


$^{13}\text{C}$  NMR spectrum of **145**:  $\text{CDCl}_3$ , 293 K, 75 MHz

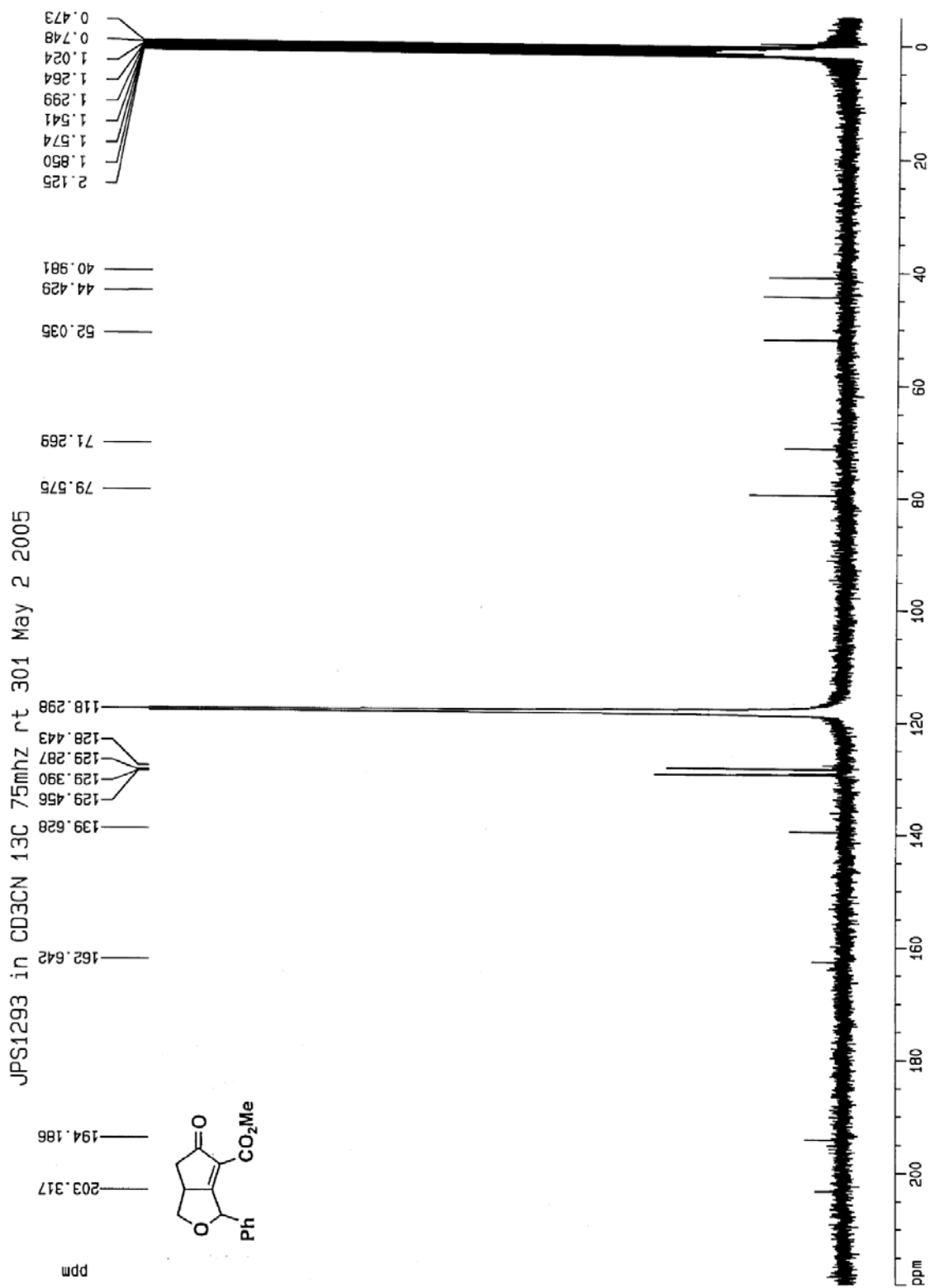
JPS2243a in cdcl3 13c 75mhz rt 300 April 10-11 2006



<sup>1</sup>H NMR spectrum of **147**: CDCl<sub>3</sub>, 293 K, 300 MHz



<sup>13</sup>C NMR spectrum of **147**: CDCl<sub>3</sub>, 293 K, 75 MHz



## 6.0 ENE-DIENE CROSS METATHESIS

### 6.1 INTRODUCTION

Olefin metathesis has become a useful transformation in synthetic organic chemistry. This was due to Robert Grubbs' ruthenium alkylidene catalyst, Grubbs I (Figure 12, **200**).<sup>61</sup> This catalyst was the basis for the next generation catalyst Grubbs II (**201**)<sup>62</sup> in which the phosphine ligand was replaced for a 1,3-dimesityl-4,5-dihydroimidazol-2-ylidene ligand increased catalyst stability and reactivity. Others then increased the reactivity by developing phosphine-free catalysts such as the Hoyveda-Grubbs catalyst (**202**)<sup>63</sup> and the nitro substituted Grela-Hoyveda-Grubbs catalyst (**203**).<sup>64</sup>

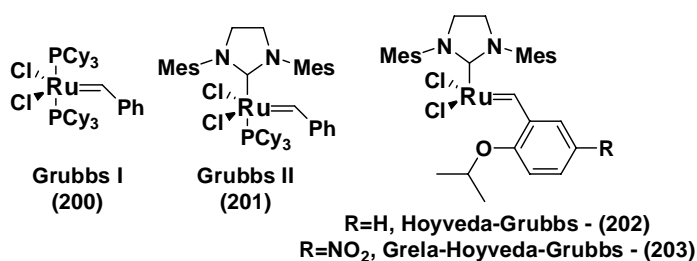
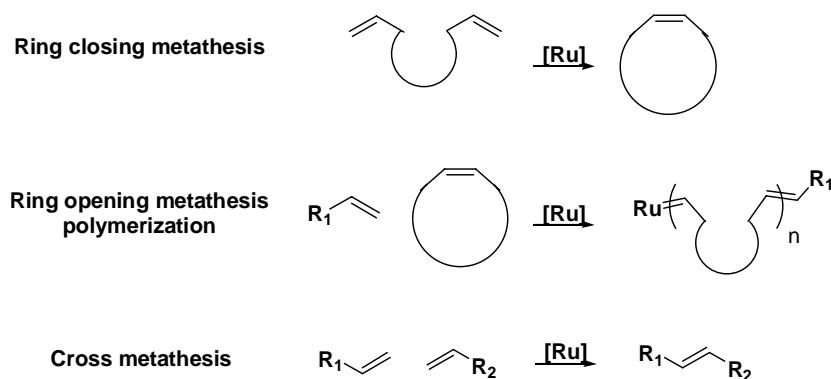


Figure 13. Ruthenium catalysts for olefin metatheses.

These catalysts have been used in ring closing metatheses (RCM), ring opening metathesis polymerizations (ROMP) and cross metatheses (CM) (Scheme 68). While RCM have been used in numerous syntheses of natural products,<sup>65</sup> CM have rarely been used, in particular a CM with an olefin and a 1,3-diene.<sup>66</sup> In fact, there were only two known examples of this type of reaction. The first example involved the coupling of electron-deficient olefins to 1,3-dienes<sup>67</sup> and the second example involved the coupling of 1,3-dienes that contained a sterically-hindered internal olefin.<sup>68</sup> Due to specificity of these two examples, the goal of this project was to determine the generality of the ene-diene cross metathesis (EDCM).



**Scheme 68.** Classes of olefin metathesis.

In order to attempt a particular cross metathesis, there are some general guidelines that have been established. Based on numerous results, Grubbs classifies olefins into four categories which are dependant on the structure and electronics of the olefin as well as the catalyst used.<sup>69</sup> Type I olefins are highly reactive and rapidly homodimerize, but these homodimers can react to yield the desired CM product (Table 23). Type II olefins are less reactive than Type I and they homodimerize slowly. Additionally, the homodimers of Type II olefins react slowly to give the CM product. Type III olefins are even less reactive and do not homodimerize at all. Finally Type IV olefins are inert to CM but do not deactivate the catalyst.

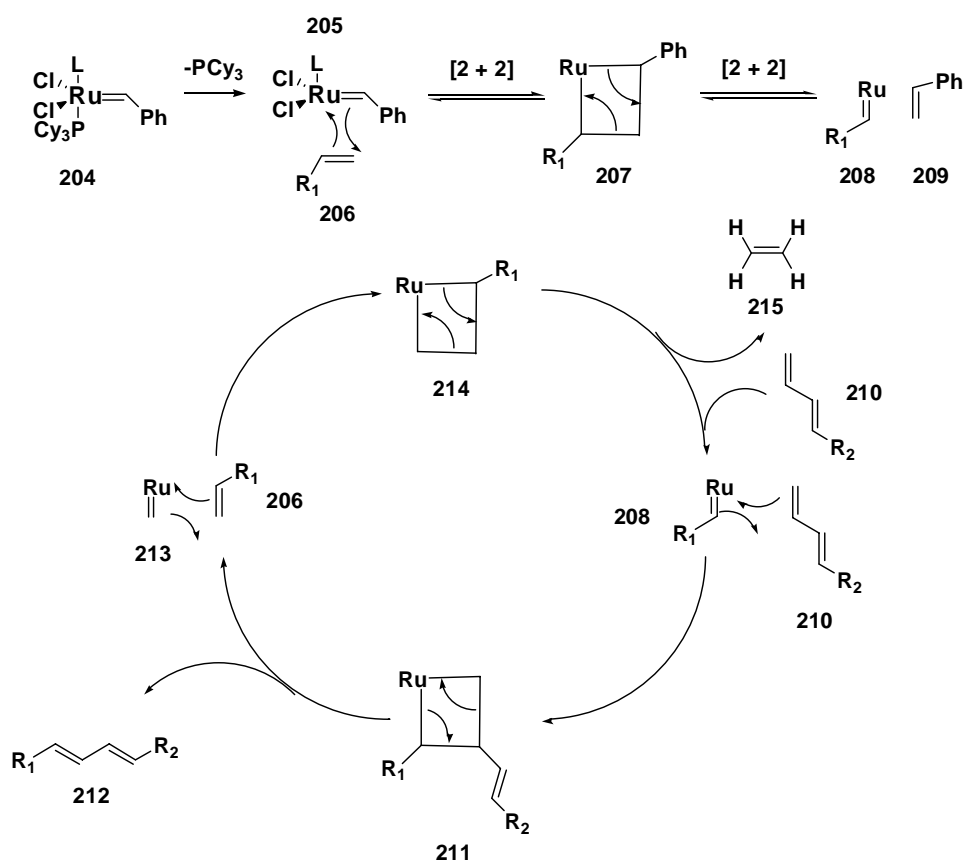
**Table 23.** Olefin classes in cross-metathesis.

Type I	Rapid homodimerization, homodimers consumable
Type II	Slow homodimerization, homodimers sparingly consumable
Type III	No homodimerization
Type IV	Olefins are inert to cross metathesis but do not deactivate the catalyst (spectator)

Based on the above classifications, if two olefins of the same type are coupled, this will lead to a non-selective metathesis in which many by-products are formed. However, if two olefins of differing types are coupled, a selective metathesis can be achieved. From this trend, we hypothesized that EDCM should be feasible and selective. Since most unconjugated terminal olefins are Type I,<sup>69</sup> we decided that the ene should be a terminal olefin so that its dimer can also react to give the desired CM product. Although 1,3-dienes are not classified as any of the olefin types, olefins that are in conjugation with a carbonyl or aromatic ring are categorized as

Type II or III. Therefore, we assumed that the terminal olefin of the 1,3-diene should be Type II due to its conjugation. Likewise, the internal olefin should be less reactive than the terminal one due to its conjugation and sterics.

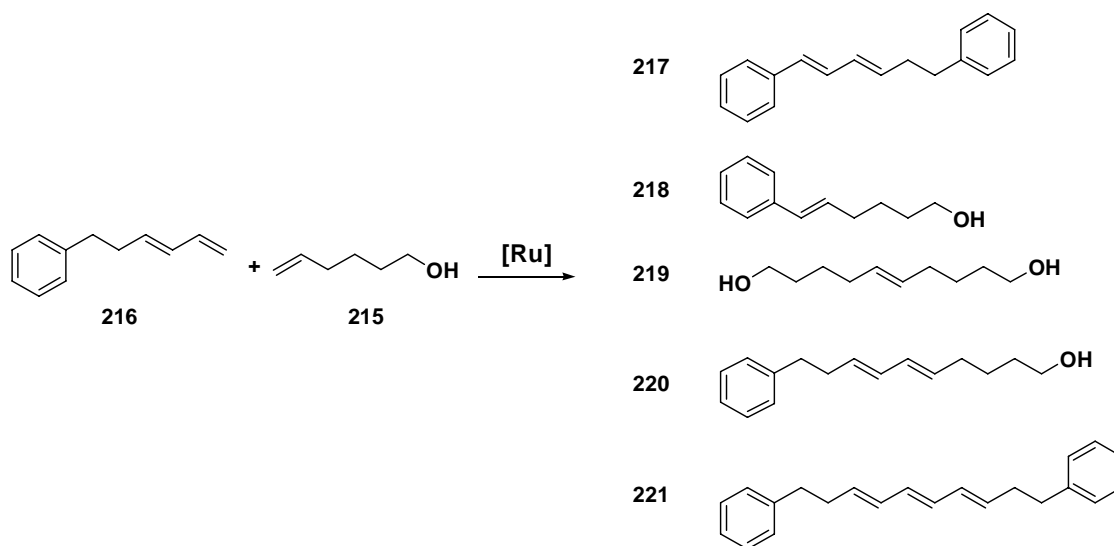
Thus, the ideal catalytic cycle should proceed as the following. The loss of the phosphine ligand from catalyst **204** leads to the activated form of the catalyst (**205**) which can react with the olefin of ene **206** to produce metallocycle **207** (Scheme 69). Metallocycle **207** then forms ruthenium alkylidene **208** and styrene **209**. Ruthenium alkylidene **208** can react with the terminal olefin of 1,3-diene **210** to give metallocycle **211**. Metallocycle **211** proceeds to eject the desired diene **212** and make a third ruthenium alkylidene **213**. This subsequently reacts with another ene **206** to form metallocycle **214** which in turn ejects ethylene gas **215** and makes **208** that continues in the cycle.



Scheme 69. Ideal catalytic cycle for EDCM.

If the catalytic cycle precedes in this pathway, the coupling of commercially available 5-hexene-1-ol **215** and diene **216**, which can be prepared in four steps from

dihydrocinnamaldehyde, should yield 4 possible by-products along with the desired CM product **220**. Since the diene or the ene could react with the styrene ligand, products **217** and **218** could be formed (Scheme 70). However, these should not be major products since because of the overall amount of catalyst present. Additionally, these products along with the dimer of the ene (**219**) should also be able to react to yield **220**. The only by-product that could be troublesome is the dimer of the diene **221**. Since the triene is more conjugated, it may not react as fast and conditions that lead to this product should be avoided.

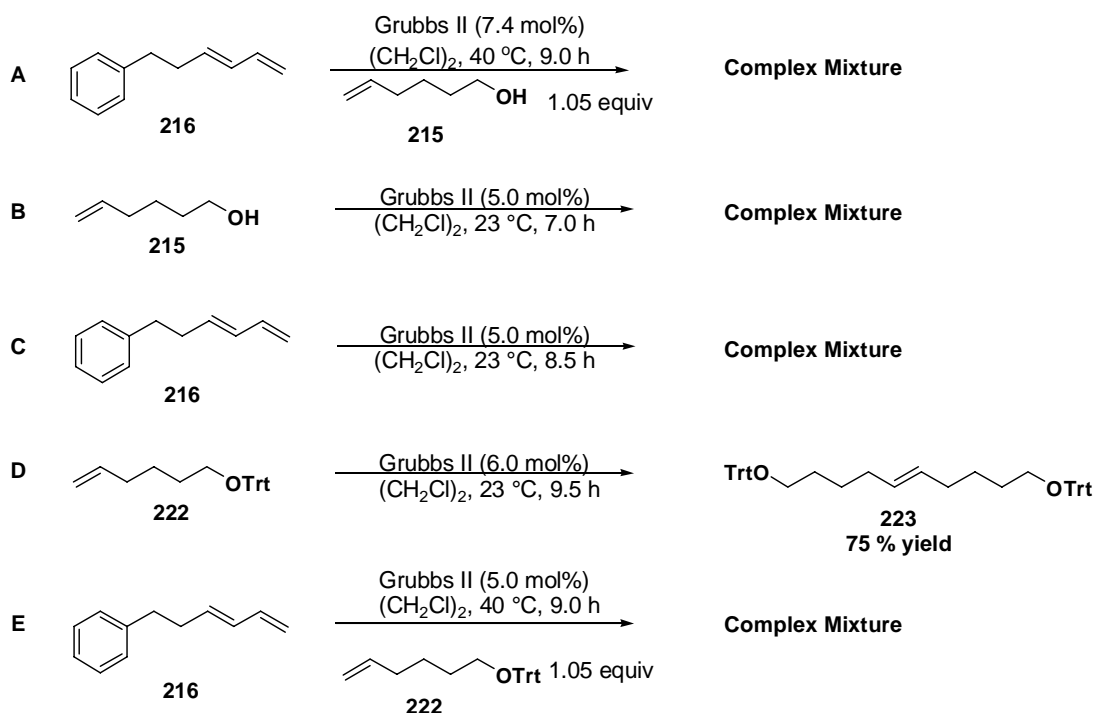


**Scheme 70.** Anticipated products from EDCM.

## 6.2 RESULTS AND DISCUSSION

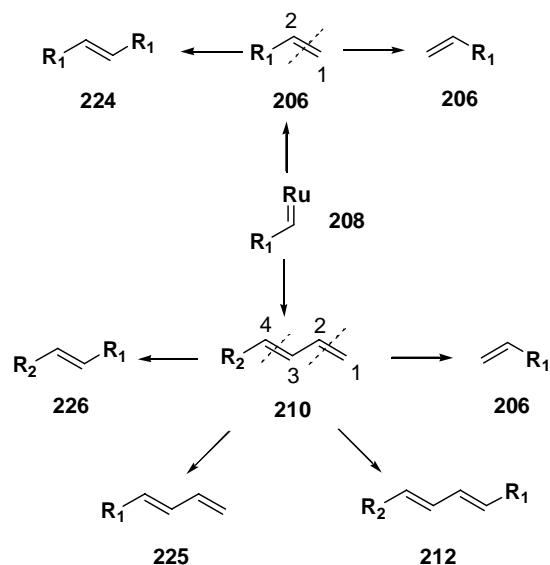
**Preliminary Couplings:** Although it was theorized that these couplings should precede, experimentally an approximate 1:1 mixture of ene and diene with 7.4 mol% of Grubbs II in 1,2-dichloroethane (Scheme 67, Reaction A) yielded a complex mixture. Likewise, the homocoupling control experiments (Reactions B and C) also yielded complex mixtures. The ene homocoupling yielded an aldehyde in which the structure could not be determined. Therefore to prevent this, 5-hexen-1-ol was protected as the triphenylmethyl (or trityl ether). These results appeared successful and the homocoupling control (Reaction D) of the trityl-protected ene **222**

proceeded to form the dimer **223** in 75 % yield by  $^1\text{H}$  NMR spectroscopy, but did not prevent the formation of a complex mixture in the EDCM reaction (Reaction E).



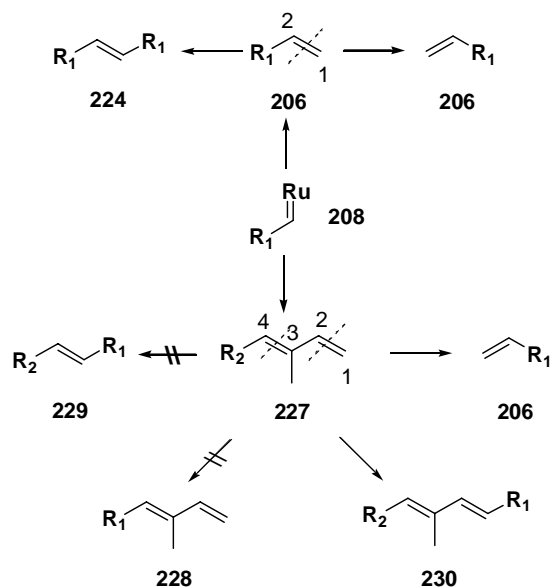
Scheme 71. Preliminary EDCM.

From these reactions, we deduced that both olefins of the diene must have reacted, which is demonstrated in Scheme 71. Once the more reactive ene coupled with the catalyst **208** it could react with either 2-C or 1-C of another ene **206** to regenerate the ene **206** or the ene-dimer **224** (Scheme 72). That pathway was effective because those two products were able to react again. However, **208** most likely reacted with 1-C, 2-C, 3-C or 4-C of the diene. If **208** reacted with 1-C or 2-C, it will generate the desired CM product **212** or the starting ene respectively. Experimentally, **208** most likely reacted with 4-C and 3-C of the diene to yield an unwanted diene **225** and an unwanted ene **226**. Both those products re-entered the catalytic cycle to lead to even more unwanted products.



**Scheme 72.** Reason for complex mixture in EDCM.

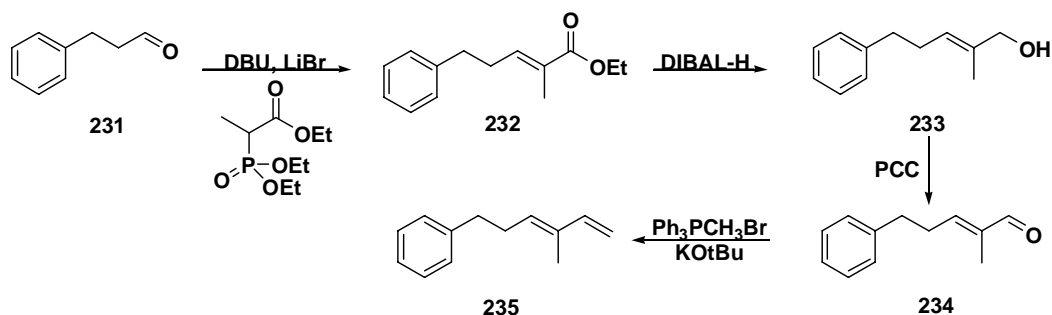
To minimize by-products, a new diene with a more hindered internal olefin **227** was prepared. The internal olefin was now trisubstituted (Scheme 73), less reactive, and should prevent pathways leading to the unwanted diene **228** and ene **229**. Thus, the remaining pathways should only lead to the desired CM-product **230** and the starting ene and ene-dimer.



**Scheme 73.** Diene **227** minimizing unwanted by-products.

The new diene **235** was prepared in four steps from dihydrocinnamaldehyde (Scheme 74). Even though the internal olefin should not react, the external olefin could react with another

external olefin of the diene to yield the diene-dimer, a triene (not shown). This extra conjugation should prevent this product from reacting, so conditions that yield the diene-dimer should be avoided.



**Scheme 74.** Preparation of diene **235**.

**Solvent Effects Studies:** Solvent effects were studied to determine the best yield. A 1:1 mixture of **235** and **222** was treated with 4.0 mol% of Grubbs II in a given solvent for 5 h at 23 °C. After 5 h, the reaction was halted and the crude reaction mixture was analyzed using  $^1\text{H}$  NMR spectroscopy. Acetonitrile (Table 24, Entry 1) appeared to decompose the catalyst and only starting materials were isolated. Likewise dimethoxyethane, dimethylformamide, and acetone (Entries 2, 3, and 4) gave low yields of **236** in 19 %, 10 %, and 20 % respectively. Ethanol (EtOH), toluene, and  $\text{CH}_2\text{Cl}_2$  (Entries 5, 6, and 7), gave yields of 25 %, 48 %, and 27 % of the CM product respectively but yielded diene-dimer in 19 %, 22 %, and 13 % yields. The two promising solvents were EtOAc and THF (Table 24, Entries 8 and 9) with **236** yields of 40 % and 24 % respectively. On a side note, these EDCM reactions caused a faster catalyst degradation than other types of metatheses for no appreciable conversion was observed between 4 and 5 h.

**Table 24.** Different solvents in EDCM.

Reaction scheme showing the reaction of diene **235** with dienophile **222** (1.01 equiv) to form product **236**. Reagents: Grubbs II (4.0 mol%), solvent, 23 °C, 5.0 h.

Entry	Solvent	Diene Result	Ene Result
1	CH <sub>3</sub> CN	100 % SM	100 % SM
2	dimethoxyethane	<b>19 % Product</b> 81 % SM 0 % Dimer	<b>16 % Product</b> 71 % SM 13 % Dimer
3	dimethylformamide	<b>10 % Product</b> 90 % SM 0 % Dimer	<b>10 % Product</b> 67 % SM 23 % Dimer
4	acetone	<b>20 % Product</b> 80 % SM 0 % Dimer	<b>22 % Product</b> 66 % SM 11 % Dimer
5	EtOH	<b>25 % Product</b> 56 % SM 19 % Dimer	<b>27 % Product</b> 52 % SM 21 % Dimer
6	toluene	<b>48 % Product</b> 30 % SM 22 % Dimer	<b>44 % Product</b> 30 % SM 26 % Dimer
7	CH <sub>2</sub> Cl <sub>2</sub>	<b>27 % Product</b> 60 % SM 13 % Dimer	<b>44 % Product</b> 30 % SM 26 % Dimer
8	EtOAc	<b>40 % Product</b> 46 % SM 14 % Dimer	<b>40 % Product</b> 36 % SM 24 % Dimer
9	THF	<b>24 % Product</b> 76 % SM 0 % Dimer	<b>24 % Product</b> 53 % SM 23 % Dimer

**Substrate Concentration Studies:** Once the solvents were chosen, substrate concentrations were studied. Since the reaction involved the coupling of two molecules, increasing the initial concentration of the substrates should increase the reaction rate. This faster reaction rate may also yield more product before the catalyst decomposed. Therefore, the reaction was repeated with the same conditions as the solvent studies using EtOAc, but the initial substrate concentration was increased to 0.5 M and 1.0 M (Table 25). Apparently, increasing the initial substrate concentration of 0.5 M and 1.0 M (Table 25, Entries 1 and 2) gave **236** yields of 34 % and 42 %. However, increasing the concentration caused an increase in the diene-dimer

formation with yields of 16 % for 0.5 M and 21% for 1.0 M. From these studies, we concluded that the best initial substrate concentration was 0.3 M (Entry 3).

**Table 25.** EDCM: substrate concentration studies.

Reaction scheme showing the conversion of diene **235** and dienophile **222** (1.01 equiv) to product **236** using Grubbs II (4.0 mol%), EtOAc, 23 °C, 5.0 h.

Entry	[Diene] <sub>initial</sub>	Diene Result	Ene Result
1	0.5	<b>34 % Product</b> 50 % SM 16 % Dimer	<b>38 % Product</b> 47 % SM 15 % Dimer
2	1.0	<b>42 % Product</b> 37 % SM 21 % Dimer	<b>51 % Product</b> 33 % SM 16 % Dimer
3	0.3	<b>40 % Product</b> 46 % SM 14 % Dimer	<b>40 % Product</b> 36 % SM 24 % Dimer

**Table 26.** EDCM: temperature studies.

Reaction scheme showing the conversion of diene **235** and dienophile **222** (1.01 equiv) to product **236** using Grubbs II (4.0 mol%) in THF, temperature, time.

Entry	Temperature (°C)	Time (h)	Diene Result	Ene Result
1	45	1.5	<b>5 % Product</b> 95 % SM 0 % Dimer	<b>4 % Product</b> 89 % SM 7 % Dimer
2	23	5.0	<b>24 % Product</b> 75 % SM 0 % Dimer	<b>24 % Product</b> 53 % SM 23 % Dimer
3	60	4.0	<b>27 % Product</b> 52 % SM 0 % Dimer 21 % Isomer	<b>36 % Product</b> 0 % SM 36 % Dimer 28 % Isomer
4	78 (EtOAc)	8.5	0 % SM Mostly by-products	0 % SM Mostly by-products

**Temperature Effects Studies:** Temperature effects were the next studied parameters. A 1:1 mixture of **235** and **222** was treated with 4.0 mol% of Grubbs II in THF and the reaction was heated to the given temperature for the specified time. Heating the reaction to 45 °C (Table 26, Entry 1) did not reduce the yield (5 % in 1.5 h ) when compared to 23 °C (24 %, Entry 2). However, heating the reaction to 65 (Entry 3) and 78 °C (Entry 4) caused the formation of other by-products instead of **236** (mostly by-products at 78 °C). On a side note the reaction at 65 °C appeared to yield the Z-isomer of **236** (Entry 3) in 21 % yield. Therefore increasing the temperature above 65 °C using Grubbs II was detrimental to the yield of **236**.

**Table 27.** EDCM: solvent studies using Grela-Hoyveda-Grubbs **203**.

Reaction scheme: **235** + **222** (1.01 equiv)  $\xrightarrow[\text{solvent, temperature, time}]{\text{203 (4.0 mol\%)}}$  **236**

Entry	Solvent	Temperature (°C)	Time (h)	Diene Result	Ene Result
1	THF	65	6.5	<b>8 % Product</b> 92 % SM 0 % Dimer	<b>7 % Product</b> 83 % SM 10 % Dimer
2	(ClCH <sub>2</sub> ) <sub>2</sub>	80	8.3	<b>10 % Product</b> 82 % SM 8 % Dimer	<b>12 % Product</b> 77 % SM 11 % Dimer
3	benzene	80	6.0	<b>20 % Product</b> 65 % SM 15 % Dimer	<b>22 % Product</b> 67 % SM 11 % Dimer
4	CH <sub>2</sub> Cl <sub>2</sub>	23	6.0	<b>21 % Product</b> 62 % SM 17 % Dimer	<b>23 % Product</b> 66 % SM 11 % Dimer
5	CH <sub>2</sub> Cl <sub>2</sub>	40	6.0	<b>41 % Product</b> 36 % SM 22 % Dimer	<b>48 % Product</b> 34 % SM 18 % Dimer

**Other Catalyst Studies:** Since the Grela-Hoyveda-Grubbs catalyst **203** was reported to be more active than Grubbs II, using it might prove fruitful. A 1:1 mixture of **235** and **222** was treated with 4.0 mol% of **203** in the given solvent and the reaction was heated to the given temperature for the specified time. THF, (Table 27, Entry 1) 1,2 dichloroethane (Entry 2), and benzene (Entry 3) heated to their reflux temperatures gave yields of 8 %, 10 %, and 20 % respectively. The low product and by-product yields were due to catalyst decomposition at the elevated temperatures. Finally, using CH<sub>2</sub>Cl<sub>2</sub> at 23 °C (Entry 4) and 40 °C (Entry 5) gave better

yields of 21 % and 41 % respectively. However, these yields were not as high as those with Grubbs II.

Since **203** was not useful, other ruthenium catalysts were pursued. A 1:1 mixture of **235** and **222** was treated with 4.0 mol% of the specified catalyst in the given solvent and the reaction was heated to the given temperature for 6 h. Not surprisingly, the less reactive Grubbs I in THF at 23 °C (Table 28, Entry 1) and 50 °C (Table 28, Entry 2) gave **236** yields of 11 % and 13 % respectively, even when the amount of catalyst was doubled. Likewise, the more active **202** in CH<sub>2</sub>Cl<sub>2</sub> at 23 °C (Entry 3) and 40 °C (Entry 4) gave **236** yields of 26 % and 44 % respectively. Grubbs reported that benzoquinone, may prevent the formation of ruthenium hydrides leading to olefin migration in the substrates.<sup>70</sup> Therefore, 8 mol% of benzoquinone was added to the reaction mixture before the catalyst addition and the reaction was heated to 50 °C in THF (Entry 5). This reaction yielded **236** in 41 % with 3 % formation of the diene-dimer. Therefore, using catalyst **202** or Grubbs II with or without benzoquinone resulted similarly.

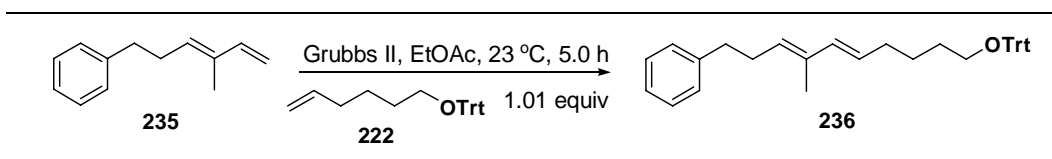
**Table 28.** EDCM: different catalyst studies.

Reaction scheme: **235** + **222** (1.01 equiv)  $\xrightarrow{\text{Ru catalyst, solvent, 6.0 h}}$  **236**

Entry	Catalyst	Catalyst Amount	Solvent	Temperature (°C)	Diene Result	Ene Result
1	Grubbs I	8.0 mol%	THF	23	<b>11 % Product</b> 89 % SM 0 % Dimer	<b>13 % Product</b> 63 % SM 24 % Dimer
2	Grubbs I	8.0 mol%	THF	50	<b>13 % Product</b> 87 % SM 0 % Dimer	<b>16 % Product</b> 53 % SM 31 % Dimer
3	Hoyveda Grubbs	4.0 mol%	CH <sub>2</sub> Cl <sub>2</sub>	23	<b>26 % Product</b> 59 % SM 15 % Dimer	<b>27 % Product</b> 60 % SM 13 % Dimer
4	Hoyveda Grubbs	4.0 mol%	CH <sub>2</sub> Cl <sub>2</sub>	40	<b>44 % Product</b>	<b>44 % Product</b>
5	Grubbs II benzoquinone	4.0 mol% 8.0 mol%	THF	50	<b>41 % Product</b> 56 % SM 3 % Dimer	<b>42 % Product</b> 40 % SM 18 % Dimer

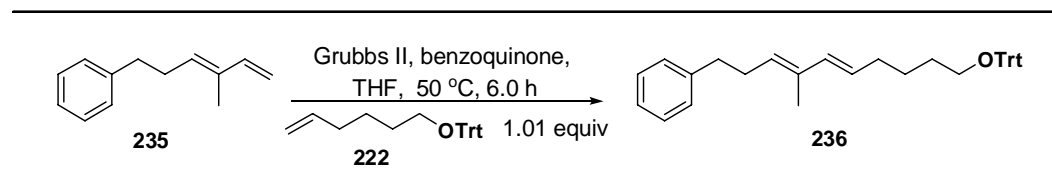
**Catalyst Amount Studies:** Although the three catalyst systems were found successful, the yield of these reactions could be improved. Since the catalyst was important, increasing the amount of catalyst might increase the yield. However, doubling the amount of Grubbs II in EtOAc at 23 °C (Table 29, Entry 1) gave a 40 % yield of **236**, identical to when 4.0 mol% of Grubbs II was used(Entry 2). When benzoquinone was added, doubling the amounts of Grubbs II and benzoquinone (Table 30, Entry 1) yielded **236** in 51 %, while the original catalysts' quantities (Entry 2) yielded **236** in 41 %. However, the amount of diene-dimer increased substantially. To conclude, doubling the amount of catalyst increased the yield.

**Table 29.** EDCM: catalyst amount studies using Grubbs II.



Entry	Catalyst Amount	Diene Result	Ene Result
1	8.0 mol%	<b>40 % Product</b> 41 % SM 19 % Dimer	<b>40 % Product</b> 41 % SM 19 % Dimer
2	4.0 mol%	<b>40 % Product</b> 46 % SM 14 % Dimer	<b>40 % Product</b> 36 % SM 24 % Dimer

**Table 30.** EDCM: catalyst amount studies using Grubbs II and benzoquinone.



Entry	Catalysts Amounts	Diene Result	Ene Result
1	8.0 mol%, 16.0 mol%	<b>51 % Product</b> 20 % SM 29 % Dimer	<b>80 % Product</b> 0 % SM 20 % Dimer
2	4.0 mol%, 8.0 mol%	<b>41 % Product</b> 56 % SM 3 % Dimer	<b>42 % Product</b> 40 % SM 18 % Dimer

**Ene-Diene Ratio Studies:** Although varying the catalyst amount proved useful, one final way was sought to improve the yield. If one of the substrates was not entirely stable to the reaction, increasing the amount of one substrate over the other might increase the yield of **236**. Therefore, treatment of **235** and **222** in varying ratios was treated with Grubbs II in CH<sub>2</sub>Cl<sub>2</sub> at 23 °C for 5 h. This time product was isolated to determine an isolated yield and not a <sup>1</sup>H NMR yield. As expected, tripling either the diene (Table 31, Entry 1) or the ene (Entry 2) gave **236** yields of 34 % and 29 % respectively which was higher than the first run of the 1:1 ratio of ene/diene (23 %, Entry 3). However, tripling the diene gave only a slightly better yield than tripling the ene. On a side note, the overall yield (40 % Entry 3) can be increased by isolating the product and re-subjecting the reaction mixture to the reaction conditions.

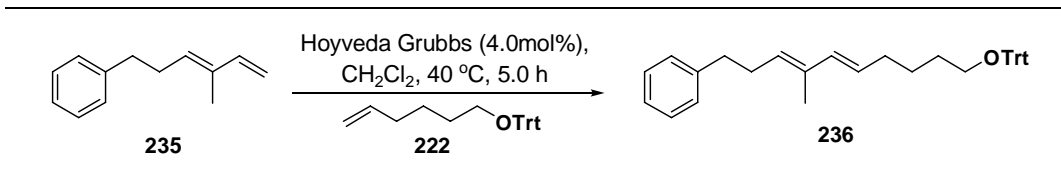
**Table 31.** EDCM: ene/diene ratio studies using Grubbs II.

Reaction scheme: Diene **235** (1-phenyl-1,3-butadiene) + Ene **222** (1-((tert-butyloxy)methyl)but-1-ene) → Product **236** (1-phenyl-1,3-bis(4-((tert-butyloxy)methyl)phenyl)but-1,3-diene).

Entry	Ene/Diene Ratio	% Yield
1	1 : 3	29
2	3 : 1	34
3	1 : 1	1 <sup>st</sup> 23 2 <sup>nd</sup> 17 Overall 40

Interestingly, the trend seemed to vary when the catalyst was switched to Hoyveda-Grubbs **202**. Tripling either the diene (Table 32, Entry 1) or ene (Entry 2) did increase the yield of **236** to 47 % and 52 % respectively when compared to the 1:1 ratio (44 %, Table 32, Entry 3). The more active **202** catalyst gave higher isolated yields (Table 32) than with Grubbs II (Table 31). The highest isolated yield of **236** was obtained with the tripled amount of ene (Entry 2) using **202**, and this was the best conditions thus far.

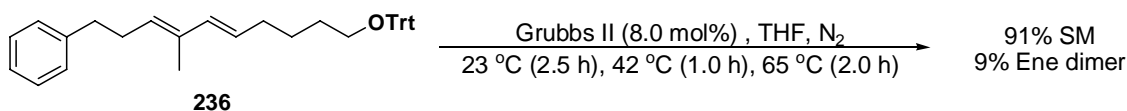
**Table 32.** EDCM: ene/diene ratio studies using catalyst **202**.



Reaction scheme showing the EDCM reaction of **235** and **222** to form **236**. Reagents: Hoyveda Grubbs (4.0 mol%), CH<sub>2</sub>Cl<sub>2</sub>, 40 °C, 5.0 h.

Entry	Ene/Diene Ratio	% Yield
1	1:3	47
2	3:1	52
3	1:1	44

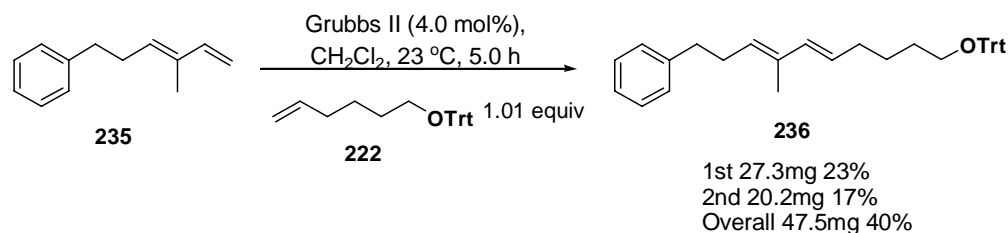
**Control Experiments:** During these experiments, some control experiments were pursued in order to gain insight into EDCM. One important issue with the metathesis reaction was the stability of the desired CM product **236**. Therefore, the product was treated with 8 mol% of Grubbs II in THF and the mixture was heated until a reaction was observed (Scheme 75). From the reaction, it appeared that the product was inert to the conditions at 23 and 42 °C. However once the reaction reached 65 °C, a small amount of ene-dimer was formed after 2.0 h. Since the <sup>1</sup>H NMR spectrum did not show any diene fragment, the fragment that contained the diene probably decomposed or was evaporated away. This showed that the product was stable at low temperature, so the metathesis must be performed at a lower temperature to prevent the product from reacting.



**Scheme 75.** EDCM: CM-product stability.

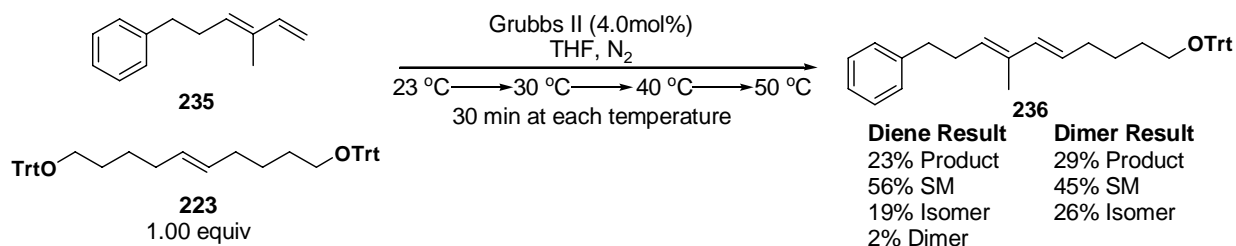
Another issue with the EDCM reaction was the low yield, which was from presence of remaining starting materials and dimers. Therefore, we hypothesized that the CM-product could be isolated and the remaining mixture could be further reacted to yield more CM-product. **235** and **222** in a 1:1 ratio were treated with 4.0 mol% of Grubbs II in CH<sub>2</sub>Cl<sub>2</sub> at 23 °C until no appreciable conversion occurred (between the 4 and 5 h mark) (Scheme 76). After 5 h, **236** (23 % yield) was isolated and the reaction mixture was treated with another 4.0 mol% of Grubbs II in

CH<sub>2</sub>Cl<sub>2</sub>. After another 5 h, **236** was isolated (17 % yield) to give an overall yield of 40 %. Although the yield was lower due to the lower temperature, this showed that the mixture can be used again to yield more **236**.



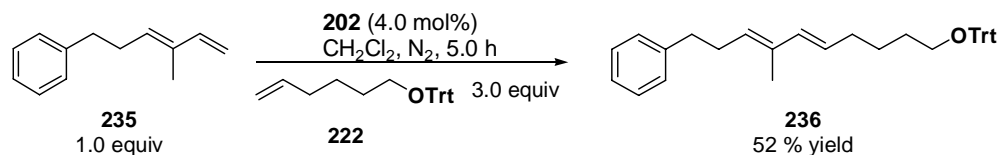
**Scheme 76.** EDCM: re-metathesis experiment.

One issue of metathesis is that the ruthenium catalyst will sometimes react at 2-C of a terminal olefin to produce a methyldiene on the ruthenium center leading to the decomposition of the catalyst.<sup>71-73</sup> To prevent this catalyst decomposition, the ene-dimer can be used in lieu of the ene. Diene **235** was reacted with **223** in the presence of 4 mol% of Grubbs II in THF (Scheme 77) (this reaction was done before the **202** was found to be the best catalyst) from 23 to 50 °C. The reaction proceeded slowly at the lower temperature so heating was used to expedite the reaction. Although the reaction yielded the Z-isomer of the desired CM-product, this reaction demonstrated that the ene-dimer can facilitate the CM-product formation.



**Scheme 77.** EDCM: Ene-dimer reaction.

### 6.3 CONCLUSION



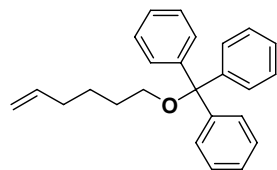
**Scheme 78.** Most promising conditions from EDCM.

From the experiments shown, good conditions to yield the CM-product were using an initial ene/diene ratio of 3:1 in presence of 4 mol% of catalyst **202** in refluxing dichloromethane (Scheme 78). Also, from the re-metathesis experiment, the yield can be increased by isolating the product and subjecting the remaining reaction mixture to the reaction conditions. Finally, since the ene and the diene did not contain any functionality, using any method to increase selectivity of the reaction, such as using coupling olefins that belong to different olefin types or increasing the sterics on the internal olefin of 1,3-diene, should help increase the yield of the CM-product substantially.

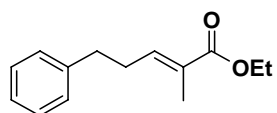
## 7.0 EXPERIMENTAL AND $^1\text{H}$ AND $^{13}\text{C}$ NMR SPECTRA

**General Techniques** All reactions were carried out with dry, freshly distilled solvents under anhydrous conditions, unless otherwise noted. Tetrahydrofuran (THF) was distilled from sodium-benzophenone, and methylene chloride ( $\text{CH}_2\text{Cl}_2$ ) was distilled from calcium hydride. Yields refer to chromatographically and spectroscopically ( $^1\text{H}$  NMR) homogenous materials, unless otherwise stated.

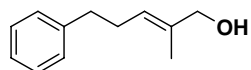
All reactions were monitored by thin-layer chromatography (TLC) carried out on 0.25-mm E. Merck silica gel plates (60F-254) using UV-light (254 nm) with anisaldehyde in ethanol and heat as developing agents. TSI silica gel (230–400 mesh) was used for flash column chromatography. Merck silica gel (60 PF<sub>254</sub>) was used to make preparative TLC (prep-TLC) plates for further purification of select compounds in which the prep-TLC plates were prepared as specified by the silica gel manufacturer. NMR spectra were recorded on AM300 or AM500 (Bruker) instruments and calibrated using the solvent or tetramethylsilane as an internal reference. The following abbreviations are used to indicate the multiplicities; app, apparent; s, singlet; d, doublet; t, triplet; q, quartet; sex, sextet; m, multiplet; br, broad. High-resolution mass spectra were obtained by using EBE geometry.



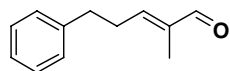
**Preparation of 222:** Using the procedure from Ren, T., Liu, D., *Biorg. Med. Chem. Lett.* **1999**, 9, 1247–1250. Silica gel chromatography (0 → 15 % EtOAc in hexanes) afforded **222** (2.724 g, 85 %) as a colorless oil; HRMS ( $\text{EI}^+$ ) calc'd for  $\text{C}_{25}\text{H}_{26}\text{O}$  ( $\text{M}^+$ ) 342.1984; found 342.1980  $m/z$ .



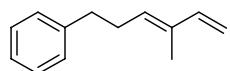
**Preparation of 232:** See: Browder, C. C., Marmsater, F. P., West, F. G., *Org. Lett.* **2001**, 3, 3033–3035.



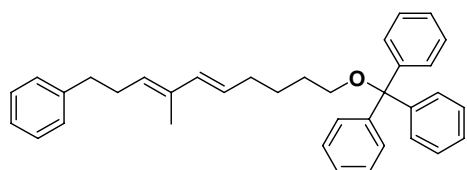
**Preparation of 233:** See: Browder, C. C., Marmsater, F. P., West, F. G., *Org. Lett.* **2001**, *3*, 3033–3035.



**Preparation of 234:** Alcohol **233** (2.331 g, 13.23 mmol) was added to a suspension of PCC (4.276 g, 1.5 mol%) and celite (8.5 g) in CH<sub>2</sub>Cl<sub>2</sub> (45 mL) at 23 °C. The resulting mixture was stirred for 15 min at the same temperature. The reaction was then diluted with Et<sub>2</sub>O (90 mL) and washed thru a plug of silica using Et<sub>2</sub>O (3 × 100 mL). The organic layer was then dried over Na<sub>2</sub>SO<sub>4</sub>, filtered, and concentrated under reduced pressure. Silica gel chromatography (0 → 10 % EtOAc in hexanes) afforded **234** (1.908 g, 83 % yield) as a colorless oil; Spectral data were in agreement with the literature: Browder, C. C., Marmsater, F. P., West, F. G., *Org. Lett.* **2001**, *3*, 3033–3035.

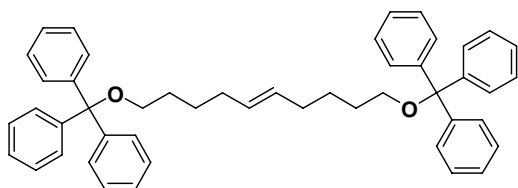


**Preparation of 235:** Aldehyde **S7** (1.856 g, 10.65 mmol) dissolved in THF (26 mL), was added in one portion via a cannula to a solution potassium t-butoxide (1.554 g, 13.85 mmol) and Ph<sub>3</sub>PCH<sub>3</sub>Br (5.329 g, 14.91 mmol) in THF (36 mL) at 0 °C. The resulting mixture was stirred for 2.8 h at the same temperature. The reaction was then quenched with H<sub>2</sub>O (77 mL) and hexanes (60 mL) and the mixture was allowed to warm to 23 °C for 14 h with stirring. The resulting mixture was extracted with Et<sub>2</sub>O (40 mL × 3). The combined organic layers were then washed with brine (40 mL), dried over Na<sub>2</sub>SO<sub>4</sub>, filtered, and concentrated under reduced pressure. The resulting residue was purified by silica gel chromatography (0 → 15 % EtOAc in hexanes) to afford **235** (1.304 g 71 % yield) as a colorless oil; *R<sub>f</sub>* 0.33 (1 % PhH in hexanes); IR (film) 3086, 3063, 3027, 2980, 2923, 1641, 1605, 1496, 1453, 990, 894, 748, 698 cm<sup>-1</sup>; <sup>1</sup>H NMR (300 MHz, 293K, CDCl<sub>3</sub>) δ 7.30–7.16 (m, 5H), 6.36 (dd, 1H, *J* = 17.4, 10.7 Hz), 5.53 (br t, 1H, *J* = 7.3 Hz), 5.08 (d, 1H, *J* = 17.4 Hz), 4.93 (d, 1H, *J* = 10.7 Hz), 2.70 (t, 2H, *J* = 7.3 Hz), 2.45 (app q, 2H, *J* = 7.7 Hz), 1.70 (s, 3H); <sup>13</sup>C NMR (125 MHz, 293 K, CDCl<sub>3</sub>) δ 141.7, 141.3, 134.5, 131.8, 128.3, 128.2, 125.7, 110.6, 35.6, 30.1, 11.5; HRMS (EI<sup>+</sup>) calc'd for C<sub>13</sub>H<sub>16</sub>(M<sup>+</sup>) 172.1252; found 172.1252 *m/z*.



**Preparation of 236:** Catalyst **202** (3.1 mg, 0.004931 mmol) was added to 3:1 mixture of **222** (126.6 mg, 0.3698 mmol) and **235** (21.2 mg, 1.232 mmol) dissolved in

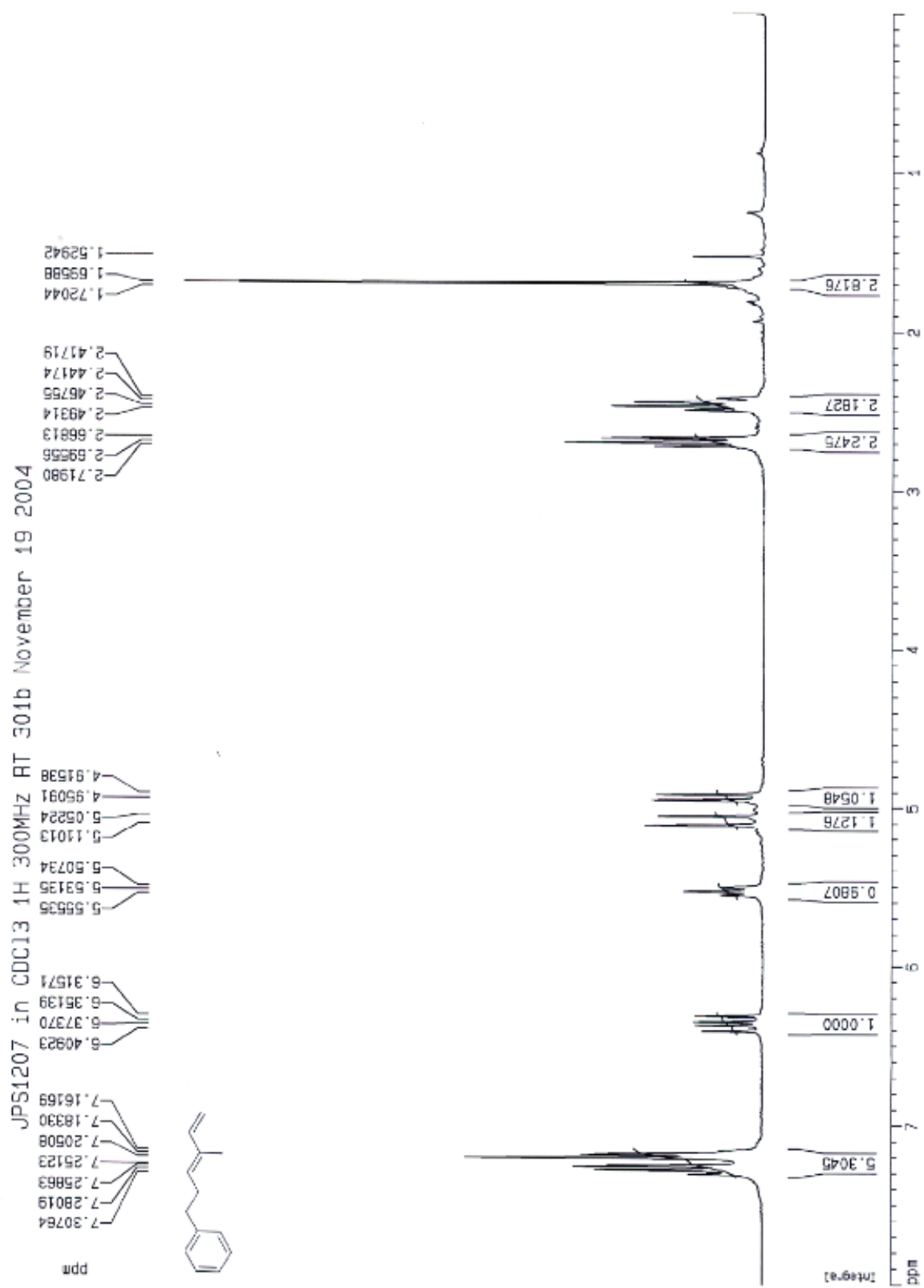
CH<sub>2</sub>Cl<sub>2</sub> (0.5 mL). The resulting mixture was heated to reflux for 5.0 h. The solvent was then removed under reduced pressure. The resulting residue was purified by silica gel chromatography (0 → 30 % PhH in hexanes) to afford **236** (37.0 mg, 52 % yield) as a colorless oil. *R<sub>f</sub>* 0.42 (5 % EtOAc in hexanes); IR (film) 3085, 3059, 3024, 2930, 2923, 1598, 1491, 1449, 1073 (C-O), 964, 899, 761, 745, 705, 633 cm<sup>-1</sup>; <sup>1</sup>H NMR (300 MHz, 293K, CDCl<sub>3</sub>) δ 7.44 (d, 6H, *J* = 7.3 Hz), 7.31–7.18 (m, 14H), 6.01 (d, 1H, *J* = 15.5 Hz), 5.53 (dt, 1H, *J* = 15.5, 6.9 Hz), 5.40 (br t, 1H, *J* = 7.1 Hz), 3.05 (t, 2H, *J* = 6.4 Hz), 2.68 (t, 2H, *J* = 7.1 Hz), 2.43 (app q, 2H, *J* = 7.7 Hz), 2.05 (app q, 2H, *J* = 7.1 Hz), 1.68 (s, 3H), 1.66–1.59 (m, 2H), 1.52–1.45 (m, 2H); <sup>13</sup>C NMR (125 MHz, 293 K, CDCl<sub>3</sub>) δ 144.5, 142.0, 134.7, 134.1, 129.2, 128.7, 128.4, 128.2, 127.9, 127.6, 126.7, 125.7, 86.3, 63.4, 35.8, 32.6, 30.1, 29.5, 26.3, 12.4; HRMS (EI<sup>+</sup>) calc'd for C<sub>36</sub>H<sub>38</sub>O (M<sup>+</sup>) 486.2923; found 486.2 *m/z*.



**Preparation of 223:** Product **223** was isolated as a by-product from the preparation of **236**. Silica gel chromatography (0 → 30 % PhH in hexanes) afforded **223** as a colorless oil. *R<sub>f</sub>* 0.38 (5 % EtOAc in hexanes);

IR (film) 3085, 3058, 2927, 2857, 1490, 1448, 1072 (C-O), 762, 745, 705, 633 cm<sup>-1</sup>; <sup>1</sup>H NMR (300 MHz, 293K, CDCl<sub>3</sub>) δ 7.45–7.42 (m, 12H), 7.30–7.18 (m, 18H), 5.34–5.32 (m, 2H), 3.06 (t, 4H, *J* = 6.5 Hz) 1.96–1.91 (m, 4H), 1.66–1.57 (m, 4H) 1.46–1.38 (m, 4H); <sup>13</sup>C NMR (125 MHz, 293 K, CDCl<sub>3</sub>) δ 144.5, 130.3, 128.7, 127.9, 127.6, 126.8, 86.2, 63.5, 32.3, 29.5, 26.2; HRMS (EI<sup>+</sup>) calc'd for C<sub>48</sub>H<sub>48</sub>O<sub>2</sub>Na (M<sup>+</sup>) 679.3552; found 679.3680 *m/z*.

$^1\text{H}$  NMR spectrum of **235**:  $\text{CDCl}_3$ , 293 K, 300 MHz



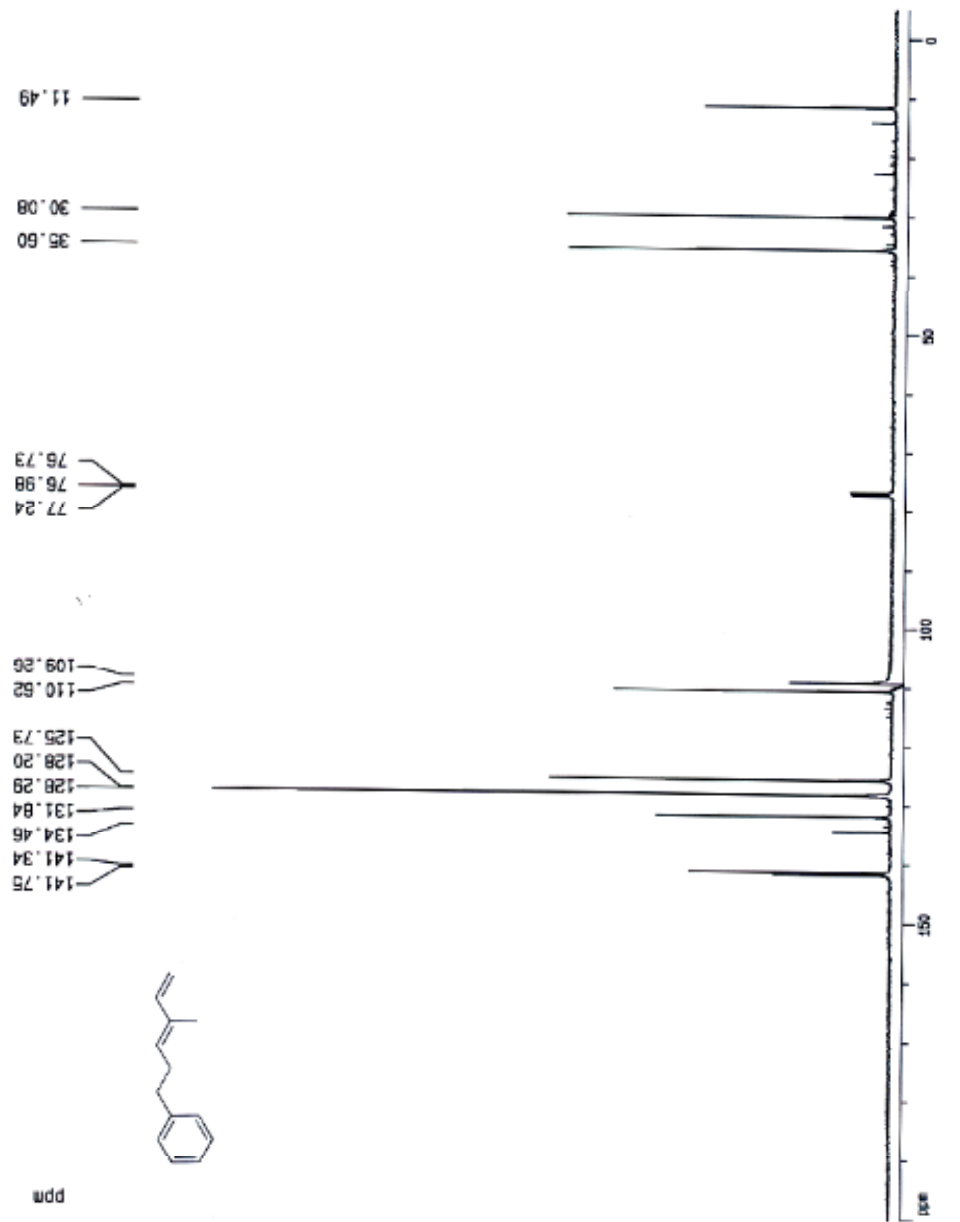
<sup>13</sup>C NMR spectrum of **235**: CDCl<sub>3</sub>, 293 K, 75 MHz

Current Data Parameters  
NAME JPS1207  
EXPNO 1  
PROCNO 1

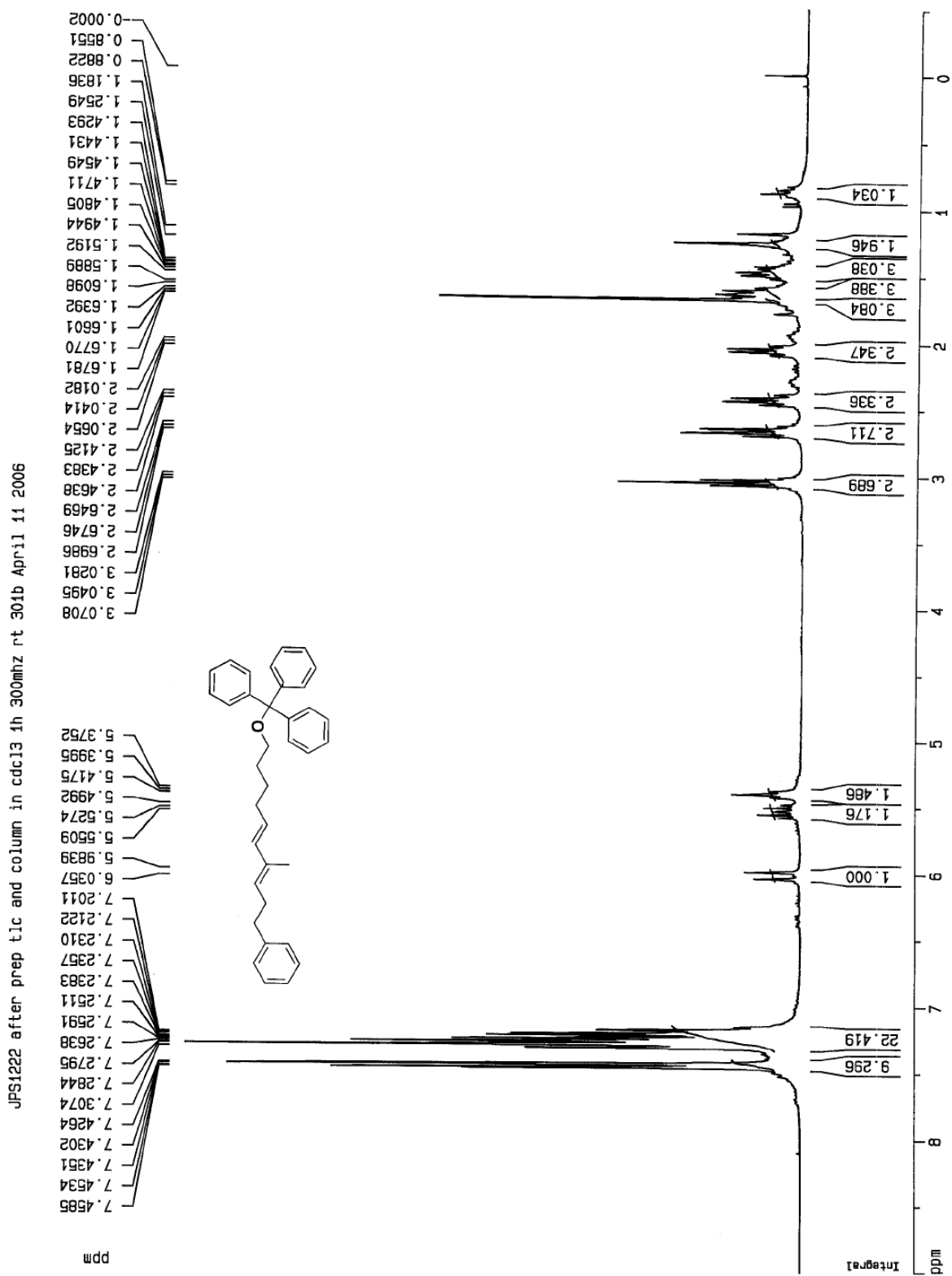
F2 - Acquisition Parameters  
Date\_ 500000  
Time 13.59  
INSTRUM spect  
PROBHD 5 mm TXI 13C  
PULPROG zgpg30  
SOLVENT CDCl3  
NS 979  
DS 0  
SWH 32679.738 Hz  
FIDRES 0.987306 Hz  
AQ 0.5014004 sec  
RG 8192  
CW 15.300 usec  
DE 6.00 usec  
TE 290.0 K  
D3 0.00100000 sec  
PL12 6.00 dB  
D1 5.00000000 sec  
PCPRG2 waltz16  
PCPD2 100.00 usec  
SFO2 500.1330006 MHz  
NUC2 1H  
PL2 120.00 dB  
P4 21.50 usec  
DE 6.00 usec  
SFO1 125.7715724 MHz  
NUC1 13C  
PL1 0.00 dB

F2 - Processing parameters  
SI 8152  
SF 125.7578260 MHz  
WDW EM  
SSB 0  
LB 4.00 Hz  
GB 0  
PC 1.00  
1D NMR plot parameters  
CX 20.00 cm  
FJP 200.000 ppm  
F1 25151.57 Hz  
F2 -5.000 ppm  
F2 -628.79 Hz  
PRMCM 10.25000 ppm/cm  
HZCM 1269.01782 Hz/cm

JPS1207 in cdcl3 1h 500mhz rt April 10 2006



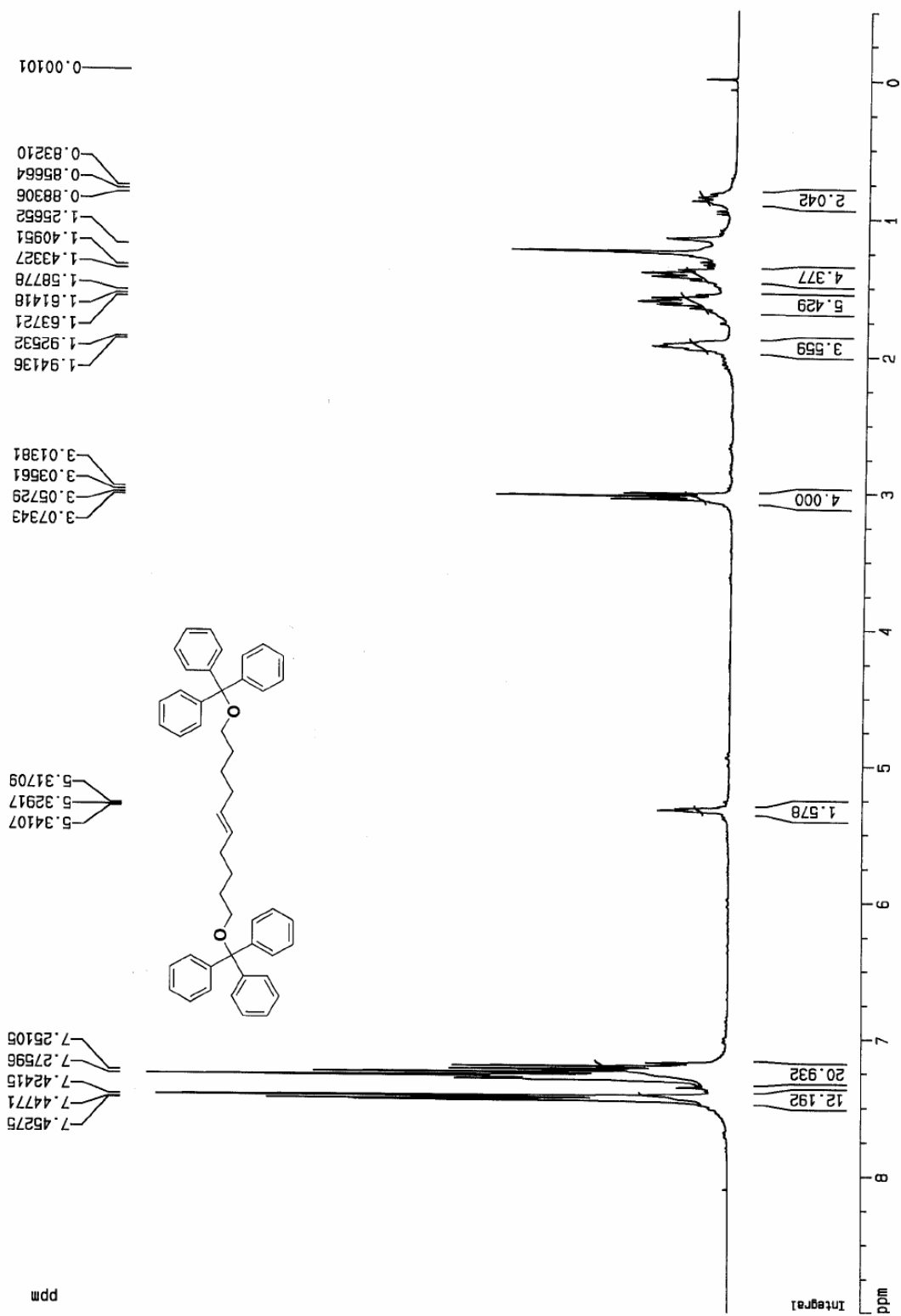
<sup>1</sup>H NMR spectrum of **236**: CDCl<sub>3</sub>, 293 K, 300 MHz



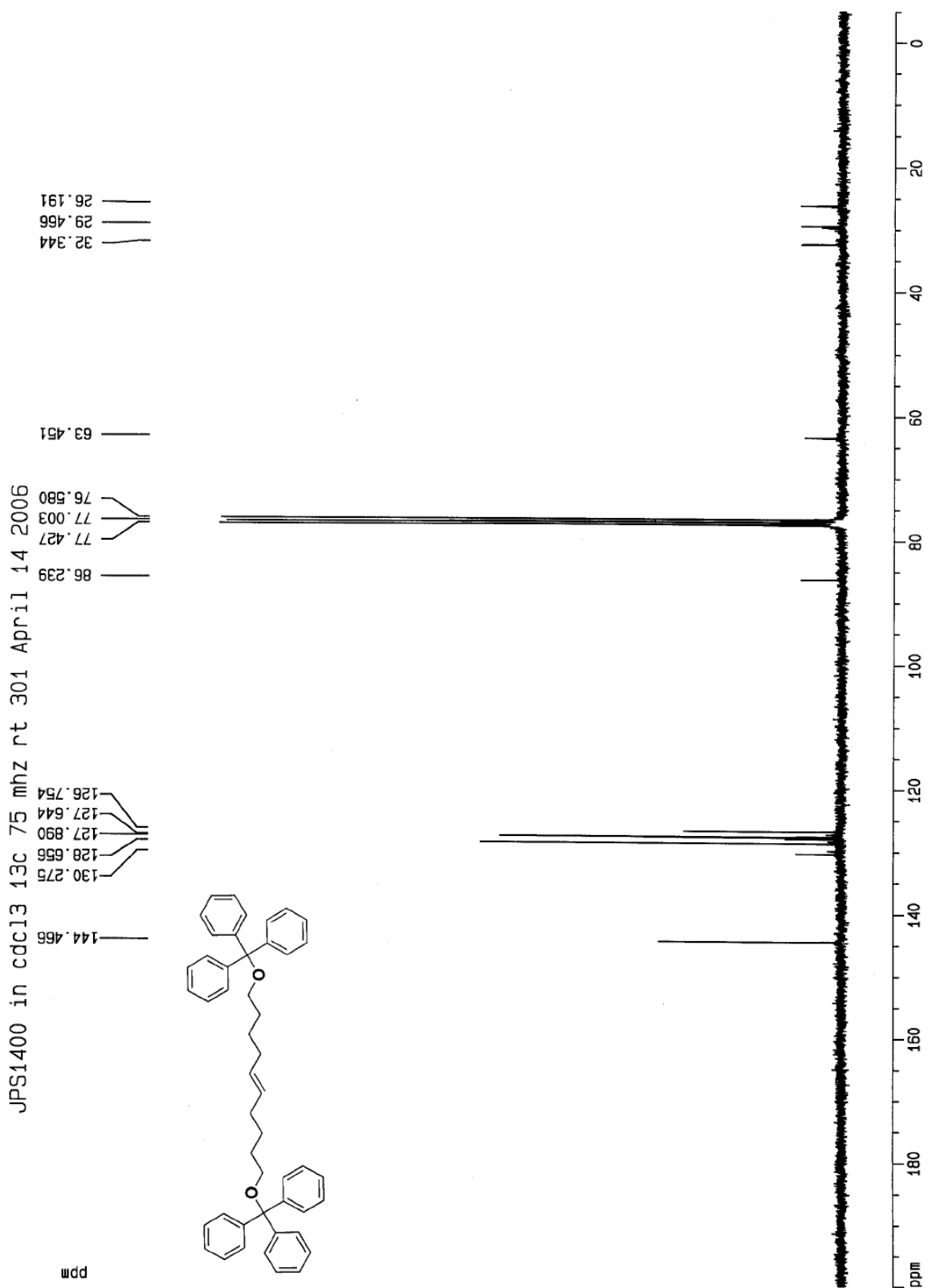


<sup>1</sup>H NMR spectrum of **223**: CDCl<sub>3</sub>, 293 K, 300 MHz

JPS1400 proton check in cdc13 1h 300mhz rt 301b April 14 2006



$^{13}\text{C}$  NMR spectrum of **223**:  $\text{CDCl}_3$ , 293 K, 75 MHz



## BIBLIOGRAPHY

- (1) Clardy, J., Walsh, C. *Nature* **2004**, *432*, 829–837.
- (2) Ishibashi, K. *J. Antibiot.* **1962**, *15*, 166.
- (3) Nozoe, S., Hirai, K., Tsuda, K. *Tetrahedron Lett.* **1965**, *51*, 4675–4677.
- (4) Fuska, J., Nemeč, P., Kuhr, I. *J. Antibiot. Ser. A* **1972**, *25*, 208.
- (5) Boeckman, R. K., Fayos, J., Clardy, J. *J. Am. Chem. Soc.* **1974**, *96*, 5954–5956.
- (6) Sekiguchi, J., Kuroda, H., Yamada, Y., Okada, H. *Tetrahedron Lett.* **1985**, *26*, 2341–2342.
- (7) Rodphaya, D., Sekiguchi, J., Yamada, Y. *J. Antibiot.* **1986**, 629–635.
- (8) Michel, K. H., DeMarco, P. V., Nagarajan, R. *J. Antibiot.* **1977**, *30*, 571–575.
- (9) Tatsuta, K., Nakagawa, A., Maniwa, S., Kinoshita, M. *Tetrahedron Lett.* **1980**, *21*, 1479–1482.
- (10) Gurusiddaiah, S., Ronald, R. C., Magnuson, J. A., McFadden, B. A., Washington State University Research Foundation, I. P., WA, US 4,220,718, September 2, 1980.
- (11) Gurusiddaiah, S., Ronald, R. C., Magnuson, J. A., McFadden, B. A. *Antimicrob. Agents Chemother.* **1981**, *19*, 153–165.
- (12) Alderidge, D. C., Armstrong, J. J., Speaks, R. N., Turner, W. B., *J. Chem. Soc. C* **1967**, 1667–1676.
- (13) Fex, T. *Tetrahedron Lett.* **1981**, *22*, 2703–2706.
- (14) Krishan, A. *J. Cell Biol.* **1972**, *54*, 657–664.
- (15) Kletzien, R. F., Perdue, J. F., Springer, A. *J. Biol. Chem.* **1972**, *247*, 2964–2966.
- (16) Kuo, S.-C., Lampen, J. O. *Ann. N. Y. Acad. Sci.* **1974**, *235*, 137.
- (17) Goto, S., Chen, K.-X., Oda, S., Hori, H., Terada, H. *J. Am. Chem. Soc.* **1998**, *120*, 2457–2463.

- (18) Hayashi, M., Kim, Y., Hiraoka, H., Natori, M., Takamatsu, S., Kawakubo, T., Masuma, R., Komiyama, K., Omura, S. *J. Antibiot.* **1995**, *48*, 1435–1439.
- (19) Takamatsu, S., Kim, Y., Hayashi, M., Hiraoka, H., Natori, M., Ko, I. K., Omura, S. *J. Antibiot.* **1996**, *49*, 95–98.
- (20) Dal Pozzo, A., Acquasaliente, M., Donzelli, G., DeMaria, P., Nicoli, M. C. *J. Med. Chem.* **1987**, *30*, 1674–1677.
- (21) Bartlett, P. A. *J. Am. Chem. Soc.* **1976**, *98*, 3305–3312.
- (22) Perriot, P., Petit, Y., Larcheveque, M. *Synthesis* **1983**, 297–300.
- (23) Bestmann, H.-J., Seng, F., Schultz, H. *Chem. Ber.* **1963**, *96*, 465–469.
- (24) Lerche, H., Konig, D., Severin, T. *Chem. Ber.* **1974**, *107*, 1509–1517.
- (25) Lutz, R. E., Scott, G. W. **1948**, 284–296.
- (26) Buback, M., Heiner, T., Hermans, B., Kowollik, C., Kozhuchkov, S. I., de Meijere, A. *Eur. J. Org. Chem.* **1998**, 107–112.
- (27) Iesce, M. R., Cermola, F., Piazza, A., Scarpati, R., Graziano, M. L. *Synthesis* **1995**, 439–443.
- (28) Midland, M. M., Tramontano, A. J. *J. Org. Chem.* **1980**, *45*, 28–29.
- (29) Shahi, S. P., Koide, K. *Angew. Chem., Int. Ed.* **2004**, *43*, 2525–2527.
- (30) Nineham, A. W., Raphael, R. A. *Chem. Commun.* **1949**, 118–121.
- (31) Vaitiekunas, A., Nord, F. F. **1953**, *76*, 2737–2740.
- (32) Coelho, A., Sotelo, E., Ravina, E. *Tetrahedron* **2003**, *59*, 2477–2484.
- (33) Kundu, N. G., Das, P. *J. Chem. Soc., Chem. Commun.* **1995**, 99–100.
- (34) Kundu, N. G., Das, P. *J. Chem. Res. (S)* **1996**, 298–299.
- (35) Kundu, N. G., Das, P., Balzarini, J., De Clereq, E. *Biorg. Med. Chem.* **1997**, *5*, 2011–2018.
- (36) Minn, K. *Synlett* **1991**, 115–116.
- (37) Müller, T., Ansorge, M., Aktah, D. *Angew. Chem. Int. Ed.* **2000**, *39*, 1253–1256.
- (38) Müller, T. B., R.; Ansorge, M. *Org. Lett.* **2000**, *2*, 1967–1970.
- (39) Bernotas, R. C. *Synlett* **2004**, 2165–2166.
- (40) Arcadi, A., Cacchi, S., Marinelli, F., Misiti, D. *Tetrahedron Lett.* **1988**, *29*, 1457–1460.
- (41) Saiah, M. K. E., Pellicciari, R. *Tetrahedron Lett.* **1995**, *36*, 4497–4500.

- (42) Zimmerman, H. E. *J. Org. Chem.* **1955**, *20*, 549–557.
- (43) Iorga, B., Eymery, F., Carmichael, D., Savignac, P. *Eur. J. Org. Chem.* **2000**, 3103–3115.
- (44) Bader, F. E., Dickel, D. F., Schlittler, E. *J. Am. Chem. Soc.* **1954**, *76*, 1695–1696.
- (45) Bader, F. E., Dickel, D. F., Huebner, C. F., Lucas, R. A., Schlittler, E. *J. Am. Chem. Soc.* **1955**, *77*, 3547–3550.
- (46) Feng, X., Fandrick, K., Johnson, R., Janowsky, A., Cashman, J. R. *Bioorg. Med. Chem.* **2003**, *11*, 775–780.
- (47) Friess, S. L., Farnham, N. *J. Am. Chem. Soc.* **1950**, *72*, 5518–5521.
- (48) Ogata, Y., Sawaki, Y. *J. Org. Chem.* **1972**, *37*, 2953–2957.
- (49) Smissman, E. E., Li, J. P., Israili, Z. H. *J. Org. Chem.* **1968**, *33*, 4231–4235.
- (50) Schreiber, S. L. *Science* **2000**, *287*, 1964–1969.
- (51) Burke, M. D., Berger, E. M., Schreiber, S. L. *Science* **2003**, *302*, 613–618.
- (52) Brummond, K. M., Mitasev, B. *Org. Lett.* **2004**, *6*, 2245–2248.
- (53) Oguri, H., Schreiber, S. L. *Org. Lett.* **2005**, *7*, 47–50.
- (54) Zon, L. I., Peterson, R. T. *Nat. Drug Disc.* **2005**, *4*, 35–44.
- (55) Stuckenholtz, C., Ulanich, P. E., Bahary, N. *Curr. Top. Dev. Biol.* **2004**, *65*, 47–82.
- (56) Bahary, N., Zon, L. I. *Stem Cells* **1998**, *16*, 89–98.
- (57) Meta, C. T., Sonye, J. P., Bahary, N., Koide, K. *Unpublished results.* **2006**.
- (58) Sonye, J. P., Koide, K. *Synth. Commun.* **2006**, *36*, 599–602.
- (59) Sonye, J. P., Koide, K. *Submitted* **2006**.
- (60) Sonye, J. P., Bahary, N., Koide, K. *Manuscript in preparation* **2006**.
- (61) Schwab, P., Grubbs, R. H., Ziller, J. W. *J. Am. Chem. Soc.* **1996**, *118*, 100–110.
- (62) Scholl, M., Ding, S., Lee, C. W., Grubbs, R. H. *Org. Lett.* **1999**, *1*, 953–956.
- (63) Garber, S. B., Kingsbury, J. S., Gray, B. L., Hoyveda, A. H. *J. Am. Chem. Soc.* **2000**, *122*, 8168–8179.
- (64) Michrowska, A., Bujok, R., Harutyunyan, S., Sashuk, V., Dolgonos, G., Grela, K. *J. Am. Chem. Soc.* **2004**, *126*, 9318–9325.
- (65) Deiters, A., Martin, S. F. *Chem. Rev.* **2004**, *104*, 2199–2238.

- (66) Albert, B. J., Sivaramakrishnan, A., Naka, T., Koide, K. *J. Am. Chem. Soc.* **2006**, *128*, 2792–2793.
- (67) Dewi, P., Randl, S., Blechert, S. *Tetrahedron Lett.* **2005**, *46*, 577–580.
- (68) Funk, T. W., Efskind, J., Grubbs, R. H. *Org. Lett.* **2005**, *7*, 187–190.
- (69) Chatterjee, A. K., Choi, T. L., Sanders, D. P., Grubbs, R. H. *J. Am. Chem. Soc.* **2003**, *125*, 11360–11370.
- (70) Hong, S. H., Sanders, D. P., Lee, C. W., Grubbs, R. H. *J. Am. Chem. Soc.* **2005**, *127*, 17160–17161.
- (71) Ulman, M., Grubbs, R. H. *J. Org. Chem.* **1999**, *64*, 7202–7207.
- (72) Hong, S. H., Day, M. W., Grubbs, R. H. *J. Am. Chem. Soc.* **2004**, *126*, 7414–7415.
- (73) van Rensburg, W. J., Steynberg, P. J., Meyer, W. H., Kirk, M. M., Forman, G. S. *J. Am. Chem. Soc.* **2004**, *126*, 14332–14333.